DOCTOR OF PHILOSOPHY

The development of a novel system to assess the effect of sudden foot and ankle inversion/supination on the musculoskeletal system

Dahrouj, Ahmad Sami

Award date:
2011

DOCTOR OF PHILOSOPHY

The development of a novel system to assess the effect of sudden foot and ankle inversion/supination on the musculoskeletal system

Ahmad Sami Dahrouj

2011

University of Dundee

The development of a novel system to assess the effect of sudden foot and ankle inversion/supination on the musculoskeletal system

by

Ahmad Sami Dahrouj

A thesis submitted in fulfilment of the requirements

for the degree of Doctor of Philosophy (PhD)

University of Dundee

2011

Contents

List of Figures

List of Tables

List of Algorithms

List of Abbreviations

aft after, page 179

Ank flex Ankle plantar-flexion angle, page 169

Ank inv Ankle inversion angle, page 169

Avg Gspeed Average gait speed, page 183

COM drop COM drop due to the rotation of the platform, page 183

ComX X component of the COM relative to the left ankle, page 150

ComYL Y component of the COM relative to the left ankle, page 150

ComYR Y component of the COM relative to the left ankle, page 150

FIA Foot inversion angle, page 149

FPfA Foot plantar-flexion angle, page 149

L Stance T The duration of the stance phase for the left step at foot strike to the platform, page 169

land rot The orientation (in the XY plane) of the foot when it lands on the foot-plate, page 184

LAnk drop Left ankle drop due to the rotation of the platform, page 183

LHSaft Left heel strike after platform, page 149

LTOprev Left toe-off before platform step, page 149

Max Maximum, page 180

PAA Platform adduction angle, page 149

PARB Platform adduction rotation begins, page 149

PARE Platform adduction rotation ends, page 149

PIA Platform inversion angle, page 149

PIAc Platform inversion acceleration, page 149

plat platform, page 179

PLHS Platform left heel strike, page 149

PLTO Platform left toe-off, page 149

PMAA Platform maximum adduction angle, page 183

PMAV Platform maximum adduction velocity, page 183

PMIA Platform maximum inversion angle, page 183

PMIV Platform maximum inversion velocity, page 183

PMPfA Platform maximum plantar-flexion angle, page 183

PMPfV Platform maximum plantar-flexion velocity, page 183

PPfA Platform plantar-flexion angle, page 149

PPfAx Platform plantar-flexion acceleration, page 149

PRB Platform rotation begins, page 149

prev previous, page 179

PRHS Platform right heel strike, page 149

PRTO Platform right toe-off, page 149

PSAA Platform stop adduction angle, page 183

PSG Platform strain gauge, page 149

PSIA Platform stop inversion angle, page 183

PSPfA Platform stop plantar-flexion angle, page 183

PWM Pulse-width modulation, page 64

R Stance T The duration of the stance phase for the right step just before the platform, page 169

RHSaft Right heel strike after platform rotates, page 149

RTOtoROT The time between toe off of the right step just before the platform and the begining of rotation of the platform, page 169

TibX Tibia rotation around laboratory x-axis, page 150

X land Pos The x-axis component of the landing position of the left foot on the platform, page 169

Y land Pos The y-axis component of the landing position of the left foot on the platform, page 169

To Mum & Dad...

Acknowledgements

My earnest thanks go to my supervisor Professor Rami Abboud for providing me with this valuable opportunity and for his continuous support and enthusiastic encouragement during the duration of this research project. Professor Abboud was an excellent mentor, his input, advice, and guidance over the course of this study was of great value for this research project.

Many thanks also go to my co-supervisor Dr. Tim Drew, who has provided me with much valuable input regarding the design and manufacturing of the robotic platform presented in this thesis. Dr. Drew was always available to give advice and help me throughout the duration of my research.

Special thanks also go to Dr. Weijie Wang for his advice regarding the statistical analysis aspect of this project, Dr. Graham Arnold for his great help with the electrical engineering aspect of this project, Mrs. Sheila Gibbs for her help with the EMG and Vicon® systems, Mr. Ian Christie for his help with the illustrations and his valuable comments on this document, Mr. Sadiq Nassir for his IT support, and Mr. Duncan Kirkcaldy and the staff at Medical Physics Department, Ninewells Hospital and Medical School, for their help with the manufacturing of the robotic platform.

A big thanks goes to all the staff and my friends at IMAR for their continued support and encouragement and for making my stay at the department enjoyable.

Last but not least, a massive thanks to my parents and family without whom none of this would have been possible.

Declaration

I hereby declare that this thesis has been compiled by me, that it is a record of work completed by myself, and that it has not previously been accepted for a higher degree at this university or any other institution of learning.

.....

Ahmad S Dahrouj

Abstract

Background Ankle sprains are one of the most common type of sports injury. They occur most frequently when the foot is in a supine or inverted position. Recovery from an ankle sprain can take from one and up to 26 weeks depending on the severity of the injury. During that period the individual will be unable to participate in any meaningful sports activity and as such it is important to be able to prevent the occurrence of such injuries. Prevention of ankle sprain injuries would require a better understanding of the risk factors of this injury. Several studies attempted to assess such risk actors by inducing foot inversion or supination however the platforms used in these studies were shown to be limited, mostly because they rotated the foot of static subjects while ankle injury occurs when subjects are active and moving. Hence this project is addressing this issue by developing a new more advanced system that can be used to assess the effect of sudden foot and ankle inversion/supination on the musculoskeletal system of dynamic subjects (e.g. walking, running, jumping, etc...).

Aims The primary aim of this research is to develop a system that can be used to assess the effect of sudden foot and ankle inversion/supination on the musculoskeletal system of dynamic subjects. The second aim of this project is to assess the role of shoes in ankle sprains.

System development A three degrees of freedom (DOF) rotating platform has

been designed, manufactured and installed in the Institute of Motion Analysis and Research (IMAR) Sports Laboratory. The platform rotates around 3 different axes allowing inversion or supination of the foot and ankle of dynamic subjects. The degree of rotation around each axis can easily be set by the researcher/operator. A strain gauge was used to detect foot strike to the platform. As a safety measure laser emitter/receivers check that the entire foot is on the footplate before the platform rotates. Optical encoders provide essential feedback of rotation angles, speed and acceleration. The necessary software and user interface for controlling the platform were also written and tested. The platform was synchronised with a bilateral four-channel EMG (electromyography) system and a 12 camera Vicon® MX-13 system thus allowing us to measure muscle activity and kinematic data during the supination of the foot. A set of software modules were written to allow automated management and processing of the data generated by the new system.

Validation study The new system was implemented in a study to validate it and to assess the role of shoes in ankle sprains. In this study, subjects would walk in three different foot conditions: barefoot, and with two different types of sports shoes, along the walkway of the Sports Laboratory where the platform was fitted. When a subject steps on the embedded platform, it rotates causing the subject's foot to supinate. At the same time, the EMG data from the peroneus longus, tibialis anterior, and lateral gastrocnemius muscles are recorded, along with the kinematics of the subject's whole body.

Results A new system that allows assessing the effect of sudden foot and ankle inversion/supination on the musculoskeletal system of dynamic subjects was successfully developed and validated. Data from the validation study

revealed increased muscle activity following induced foot supination in shod conditions compared to barefoot. Muscle activity of the rotating platform step was found to be significantly higher than the steps before and after. The platform rotation was also found to have an observable effect on body kinematics.

Conclusion A platform that allows supination of the foot of dynamic subjects was designed and manufactured. The platform was synchronised and used with a Vicon® motion capture system and an EMG capture system. The system has the capabilities to also be synchronised with other systems like the Pedar® foot pressure systems. The new system proved to be accurate and reliable. Its flexibility and novelty provides opportunities for further studies and the outcome of these is hoped to help unveil unknown and hidden information that may prove helpful in preventing ankle injury. The conducted experimental study whilst supporting the reported findings in the literature, it also reveals new findings.

1 Introduction and aims and objectives

1.1 Background to the Thesis

Ankle sprains are one of the most common types of sports injury. They occur mostly when the foot is in a supinated or inverted position. Recovery from an ankle sprain can take anything from one to 26 weeks, depending upon the severity of the injury. During this recovery period the individual will be unable to participate in any sports activity. The risk factors for ankle sprains are still being investigated. The role of many of these risk factors, however, is still unclear, and there is a lack of consensus between existing studies that investigated these risk factors. People who have suffered a previous ankle injury have been shown to be highly susceptible to re-injury. This highlights the importance of preventing ankle sprain injury in the first place, and the first step in this prevention is to better understand the risk factors of injury.

Several studies attempted to assess such risk actors by inducing foot inversion or supination however the platforms used in these studies were shown to be limited mostly because they rotated the foot of static subjects while ankle injury occurs when subjects are active and moving.

1.2 Aims and Objectives

The primary aim of this project was to develop a system that can be used to assess the effect of sudden foot and ankle inversion/supination on the musculoskeletal system of dynamic subjects (e.g. walking, running, jumping, etc...). The secondary aim of this project was to assess the role of shoes in ankle sprains.

The primary objectives of this project were to:

1. Design and build a robotic manipulator with three degrees of freedom (DOF) in rotation that can safely invert or supinate the foot of a dynamic subject.
2. Design and build the electronic and pneumatic circuits necessary to allow control over the robotic platform.
3. Write a control algorithm and a user interface for controlling the robotic platform.
4. Test and validate the newly designed platform.
5. Synchronise the robotic platform with a bilateral four-channel EMG system and a 12 camera Vicon® MX-13 system.
6. Write software for automated management and processing of the recorded data from the robotic platform, Vicon® and EMG capture systems.
7. Validate the newly developed system.

The developed system would as such consist of a newly designed robotic platform (the main component of the system), a Vicon® motion capture system, a bilateral four-channel EMG system, and the software that would be specifically written to automatically extract, manage and process all captured data.

The secondary objective of this project was to:

- Conduct an experimental study using the newly developed system to assess the role of shoes in ankle sprain injury.

1.3 Rationale for the Study

Many of the platforms presented in the literature which attempt to safely simulate an ankle sprain injury in a laboratory environment do so while subjects stand statically on them. Ankle sprain injuries however usually occur while subjects are moving and participating in some sort of activity rather than just standing still. This limits the ability of the platforms in such studies to simulate a realistic ankle sprain injury and ultimately their use in understanding the risk factors of such injury and as such how to protect against it. The few platforms presented in the literature that could rotate the foot of a moving subject consisted of a simple trapdoor mechanism and were found to be limited. The newly developed system that is presented in this thesis provides an advanced robotic platform that can better simulate a controlled ankle sprain injury.

Footwear has been suggested to play a negative role in ankle sprains. Several studies have already been conducted and the results showed that shoes are indeed a risk factor for ankle sprains. These previous studies, nonetheless, were performed with subjects standing stationary on an inverting platform. Ankle sprains however usually occur when subjects are active and moving. The experimental study presented in this thesis fills this gap in the literature by assessing the role of shoes on ankle sprains of walking subjects.

1.4 Scope and Boundaries of this Project

The project presented in this thesis covers the design, manufacturing, assembly, testing and optimisation of a novel functional robotic platform that can be easily used by researchers and clinicians to impart sudden inversion or supination of the foot and ankle of a dynamic subject. The project also covers the development of a method to synchronise the robotic platform to work with a bilateral four-channel EMG system and a Vicon® motion capture system. Also included in this project is the development of software modules that allow fast and automated management and processing of all the data recorded by the robotic platform, EMG system, and Vicon® system.

An element of this project utilises the newly developed system to assess the role of shoes in ankle sprain injury. The experimental study also serves to validate the developed system.The use of the developed system in further experiments that would provide a better understating of the risk factors of ankle sprain injuries and how to protect against such injuries is outside the scope of this current project.

This project requires an understanding in the fields of mechanical engineering, electrical engineering, software programming, anatomy of the lower limb, biomechanics of the human body, and the scientific research method. The thesis was written so that readers who are familiar with only some of the required fields can still obtain a general understanding of the research project. A complete and detailed presentation of the background information required by this project however remains outside the scope of this thesis.

1.5 Ethical Approval

Ethical approval for the experimental study presented in this thesis was granted by the University of Dundee Research Ethics Committee.

1.6 Structure of this Thesis

This thesis is divided into 11 chapters:

Chapter 1 provides an introduction to the thesis.

Chapter 2 contains a review of the literature that focuses on the different foot rotating platforms available in the existing literature. The advantages and limitations of these platforms are discussed and the need for a new more advanced platform is highlighted. This chapter also contains background information about ankle sprain injury covering the frequency, mechanism and risk factors of injury. This background information was used as the basis for the requirements of the robotic platform that was designed.

Chapter 3 highlights the requirements and technical challenges for the design of the new platform. Some concept designs of the platform are also presented here (primary objective one).

Chapter 4 contains the detailed mechanical design of the robotic platform (primary objective one).

Chapter 5 presents the electronics, control algorithm and user interface that were used to control the operation of the robotic platform. This chapter also presents the work that was done in testing, optimising and validating the robotic platform (primary objectives two, three and four).

Chapter 6 presents the work that was undertaken to integrate and synchronise the platform with the Vicon® and EMG systems (primary objective 5).

Chapter 7 presents the experimental study that was conducted to validate the system and investigate the role of shoes in ankle sprain injury (primary objective 7 and secondary objective).

Chapter 8 presents the software that was specifically written to automatically extract, manage and process all the captured data (primary objective 6).

Chapter 9 presents the results of the experimental study.

Chapter 10 discusses the findings of the experimental study in relation to the performance of the robotic platform and the role of shoes on ankle sprain injury. This chapter also discusses some of the possible applications of the newly developed system.

Chapter 11 is a summary and conclusion to this thesis. This chapter also highlights several recommendations that would expand the functionality of the new system. Several studies that can be conducted using the new system that would provide a better understanding of the ankle sprain injury and how to prevent it are also suggested.

2 Review of the Literature

2.1 The foot and ankle

2.1.1 Anatomy of the foot

The foot is a complex and important part of the human body; it allows us to stand, walk and run smoothly on different types of terrain. It consists of 26 bones (28 including the sesamoids) which are divided into seven tarsals, five metatarsals, and 14 phalanges (Figure 2.1). The joints of the foot allow for closely interrelated motion between these bones, thus, giving the foot the flexibility needed to tackle different terrain and surfaces (Nordin and Frankel 2001b). Intrinsic and extrinsic muscles of the lower limb attach to the bones of the foot via tendons and act to provide control over the movement of the joints. Ligaments connect the bones together and provide guidance to their motion; they also act passively to limit any excessive movement (Nordin and Frankel 2001b). The foot, however, must also possess the rigidity and strength necessary to support the body weight and provide locomotion. This is achieved by a number of longitudinal and transverse arches (Figure 2.2), formed by the way the foot bones interlock, and upheld by the ligaments and muscles (Abboud 2002).

The foot can be divided into four major segments: the hind-foot, the mid-foot, the fore-foot, and the phalanges (Figure 2.1). The hind-foot is made up of the

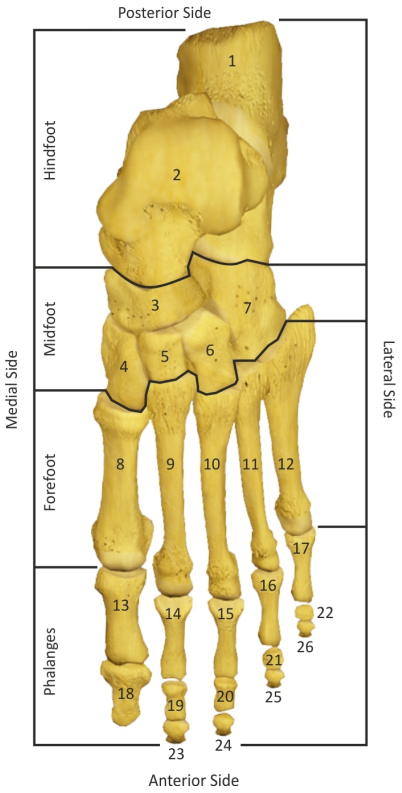

1	Calcaneus	14	2nd Proximal Phalange
2	Talus	15	3rd Proximal Phalange
3	Navicular	16	4th Proximal Phalange
4	Medial Cuneiform	17	5th Proximal Phalange
5	Intermediate Cuneiform	18	1st Distal Phalange
6	Lateral Cuneiform	19	2nd Intermediate Phalange
7	Cuboid	20	3rd Intermediate Phalange
8	1st Metatarsal	21	4th Intermediate Phalange
9	2nd Metatarsal	22	5th Intermediate Phalange
10	3rd Metatarsal	23	2nd Distal Phalange
11	4th Metatarsal	24	3rd Distal Phalange
12	5th Metatarsal	25	4th Distal Phalange
13	1st Proximal Phalange	26	5th Distal Phalange

Figure 2.1: Bones of the foot (IMAR, University of Dundee)

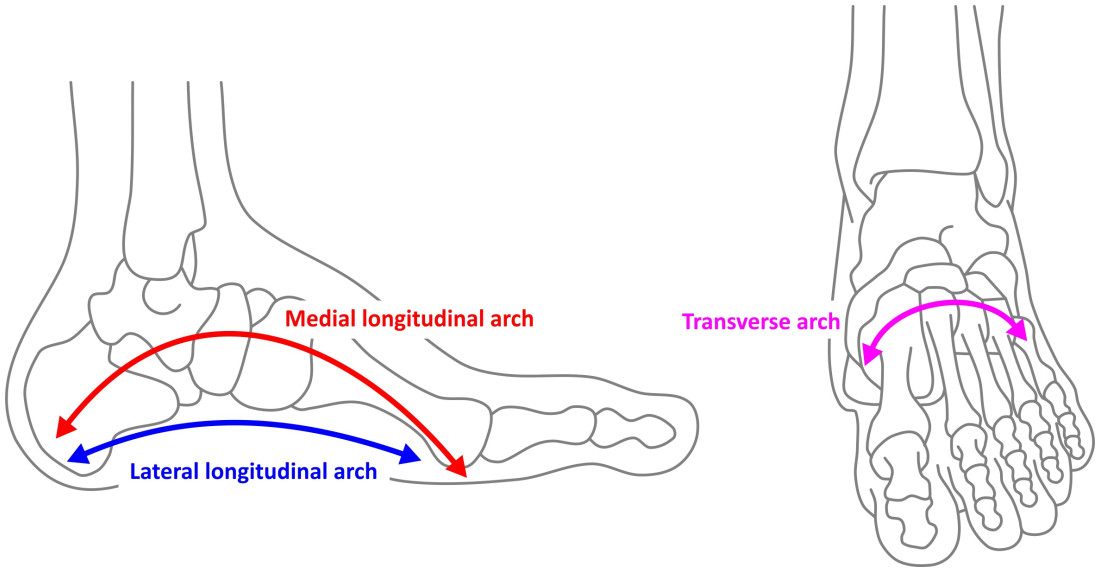

Figure 2.2: Arches of the foot (IMAR, University of Dundee)

talus and calcaneus. The talus, being a part of the ankle joint, transmits forces between the foot and the leg. The mid-foot consists of the navicular, the cuboid, and three cuneiforms. The five metatarsals form the forefoot and they articulate with the phalanges. All digits except for the hallux, which is made up of two phalanges, consist of three phalanges.

2.1.2 Foot Kinematics

Motion is usually described relative to a reference frame. Clinically, the most used reference frame is that described by the anatomical planes of the body: the frontal plane, the sagittal plane, and the transverse plane (Figure 2.3). Inversion/eversion (Figure 2.4a) is the rotation of the foot within the frontal plane, plantar-flexion/dorsi-flexion (Figure 2.4b) is that in the sagittal plane, while rotation in the transverse plane is termed abduction/adduction (Figure 2.4c) (Nordin and Frankel 2001b; Abboud 2002).

Supination and pronation (Figure 2.4d) are terms also used in describing foot movement. Supination is a combination of adduction, inversion, and plantar-flexion while pronation combines abduction, eversion and dorsi-flexion (Abboud 2002).

There are also translational and rotational motion within the foot, enabled by the various joints within it and allowing it to deform and adapt to different surfaces. This current study, however, will only investigate the kinematics of the foot as a rigid body (refer to Section 8.2.2).

2.1.3 Joints of the foot and ankle

A joint, in medical terms, refers to the location where different bones meet. Generally, a joint will allow motion between the connected bones. This motion

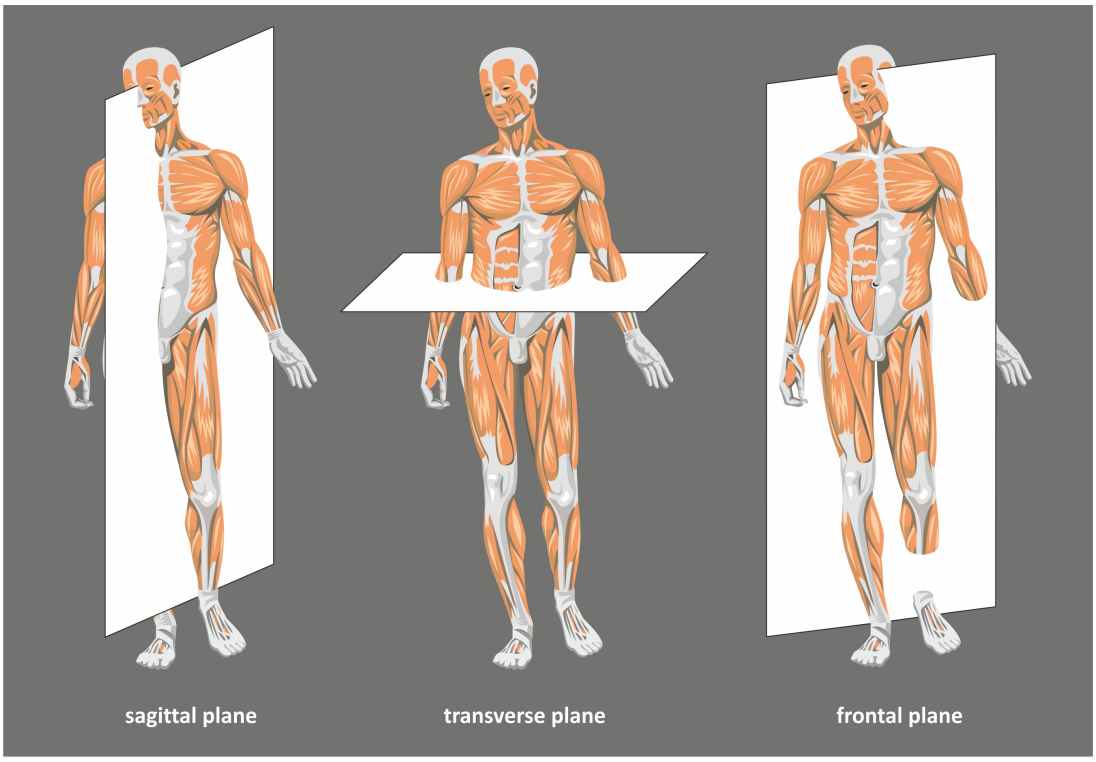

Figure 2.3: Anatomical planes of the body (IMAR, University of Dundee)

can be translational (e.g. gliding), rotational (e.g. rolling and spinning), or a combination of both depending upon the shape of the articulating bones and the ligaments connecting them (Riegger 1988). A joint can also be described by the degrees of freedom (DOF) it provides, depending on how many independent movements it allows. Zero DOF means no motion is possible. A rigid body can have up to a maximum 6-DOF, i.e. it can rotate independently around any of the three axes defining its reference frame, as well as translate independently within any of those three planes (Figure 2.5). I

The passive stability of a joint is determined by the shape of the articulating surfaces and their congruency, as well as by the ligaments surrounding it (Nordin and Frankel 2001b). Dynamic stability on the other hand is provided by the muscles and tendons, which are also the actuators of the joint.

The two joint complexes in the foot that are of interest for this research are the ankle and subtalar joints. The midtarsal, tarsometatarsal, metatarsophalangeal,

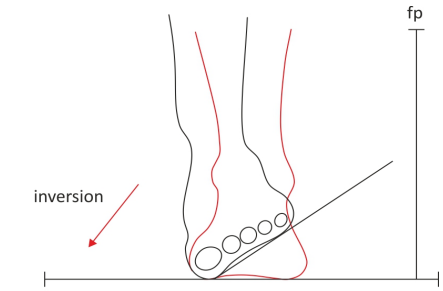

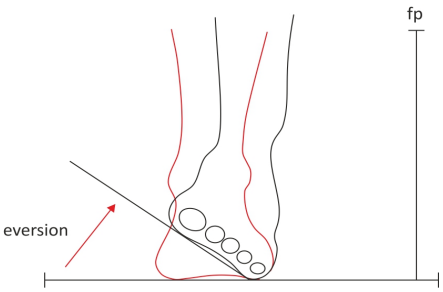

(a) Inversion and eversion

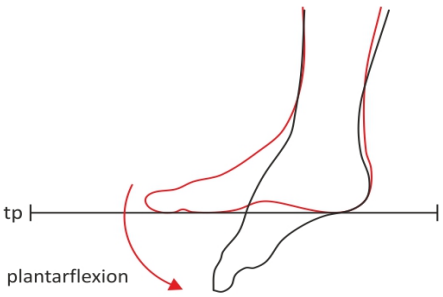

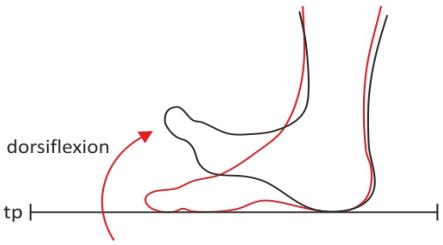

(b) Plantar-flexion and dorsi-flexion

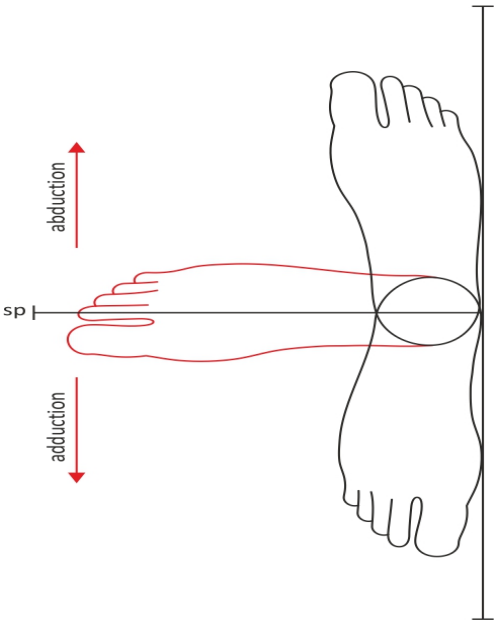

(c) Adduction and Abduction

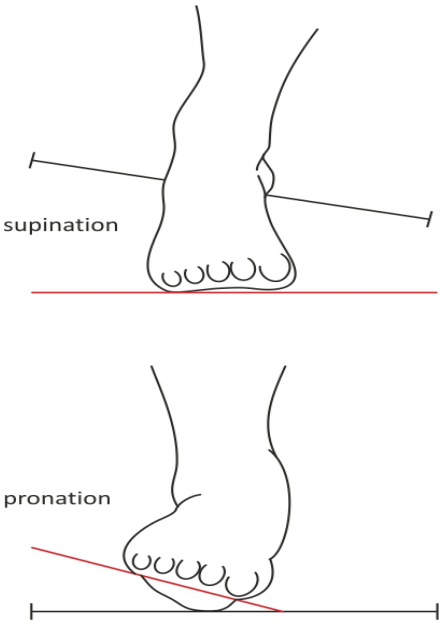

(d) Supination and pronation

Figure 2.4: Motion of the foot (IMAR, University of Dundee)

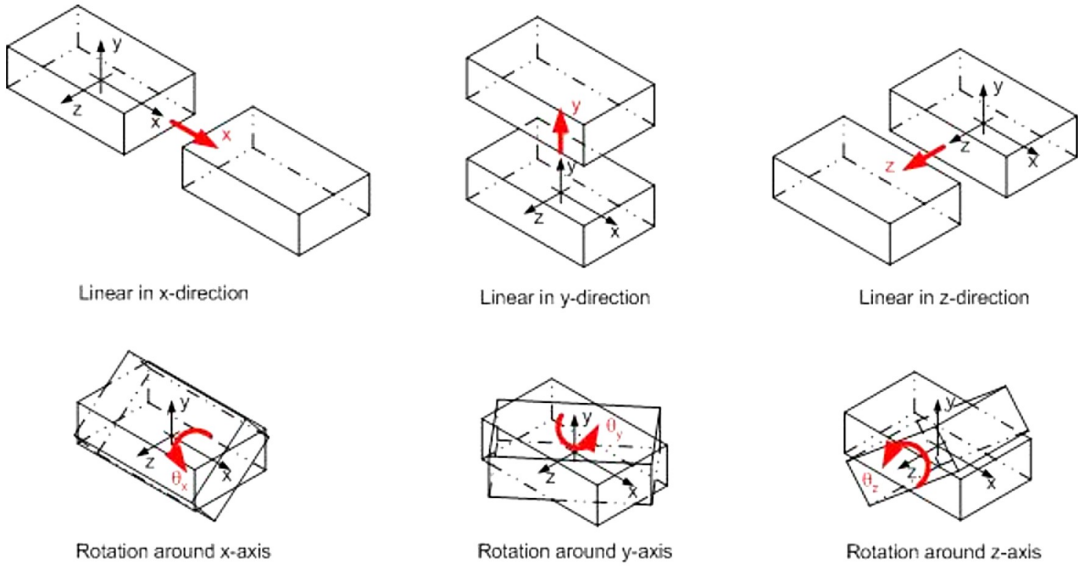

Figure 2.5: Degrees of freedom for a rigid body (adapted from Bamberg (2002))

and interphalangeal joints will not be discussed here as they are not directly involved in ankle sprains.

The ankle joint can be simplified as a 1-DOF hinge joint, permitting rotation around one axis only. The orientation of this axis however, is rather oblique and does not lie completely in the frontal plane. As such, and even though the primary motion of the ankle is plantar-flexion and dorsi-flexion, there is some abduction/adduction movement present (Riegger 1988; Nordin and Frankel 2001b; Kerr *et al.* 2009). The ankle joint itself is formed by the articulation of the tibia and fibula with the talus. The nature of this bony structure is one that exhibits greater stability in dorsi-flexion than plantar-flexion (Nordin and Frankel 2001b; Abboud 2002). The lateral ligamentous complex (LLC) provides resistance to ankle inversion while the medial ligamentous complex provide resistance to eversion motion; the former being mostly injured in ankle sprains (refer to Section 2.2).

The articulation between the talus and calcaneus forms the subtalar joint (Figure 2.6). The resultant axis of rotation forms an angle of 16° and 42°with the sagittal

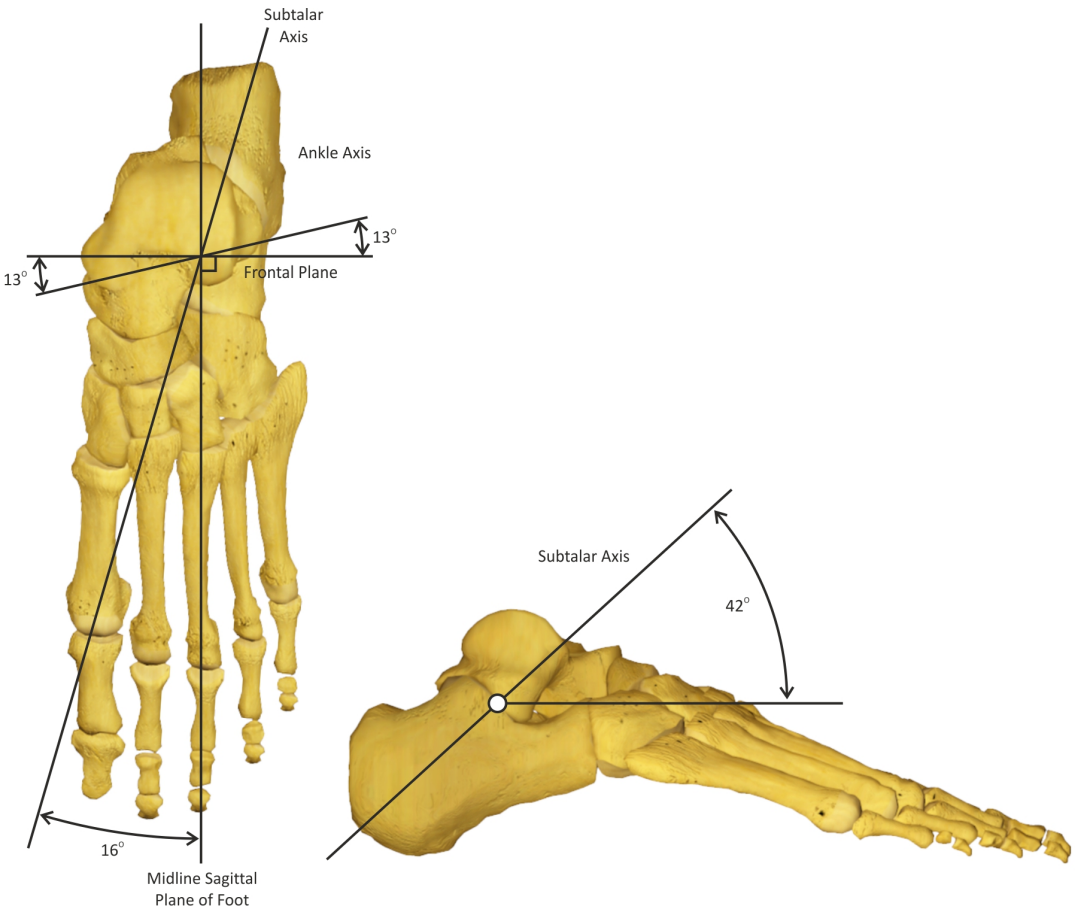

Figure 2.6: Subtalar joint (IMAR, University of Dundee)

and transverse planes respectively. This implies that the motion provided by this joint is supination and pronation (Nordin and Frankel 2001b).

The ankle and subtalar joints are actuated mainly by extrinsic muscles. The tibialis anterior (TA) acts to dorsi-flex the foot while the gastrocnemius and soleus muscles provide plantar-flexion. Inversion, along with adduction, are produced by the tibialis posterior muscle. The peroneus longus (PL) and peroneus brevis muscles combine to produce eversion and abduction.

2.2 Ankle sprains

2.2.1 Frequency of injury

Under normal walking conditions the foot is subjected to vertical forces as great as 120% of a person's body weight. During running theses forces will reach an enormous 275% of that person's body weight (Nordin and Frankel 2001b). It is little wonder that the foot and ankle are the most commonly injured parts of the body in most sports.

In their study that spanned eight years and included 15,093 sports injuries, Garrick and Requa (1988) reported that 25.2% of sports injuries were related to the foot and ankle. Ankle injuries were highest in sports such as basketball, volleyball and football; constituting approximately 20% of all injuries in those sports. Ankle sprains are the most common and account for roughly 70% of ankle injuries in those sports.

2.2.2 Mechanism of injury

The anterior talo-fibular ligament (ATFL), being the weakest of the LLC (Figure 2.7), is usually the first and most commonly injured ligament (Attarian *et al.* 1985; Puffer 2001). As the load on the ankle becomes more extreme, failure of the calcaneo-fibular ligament (CFL) and the posterior talo-fibular ligament (PTFL) will also occur leading to a more severe injury.

Ankle sprains occur mostly when the foot is being loaded while in a supinated or inverted position (Safran *et al.* 1999; Puffer 2001). McKay *et al.* (2001) found that most ankle injuries were occurring during foot strike. Based on that and in order to mimic real life ankle injury situations in a laboratory environment one must be able to induce inversion and supination of the foot while it is being

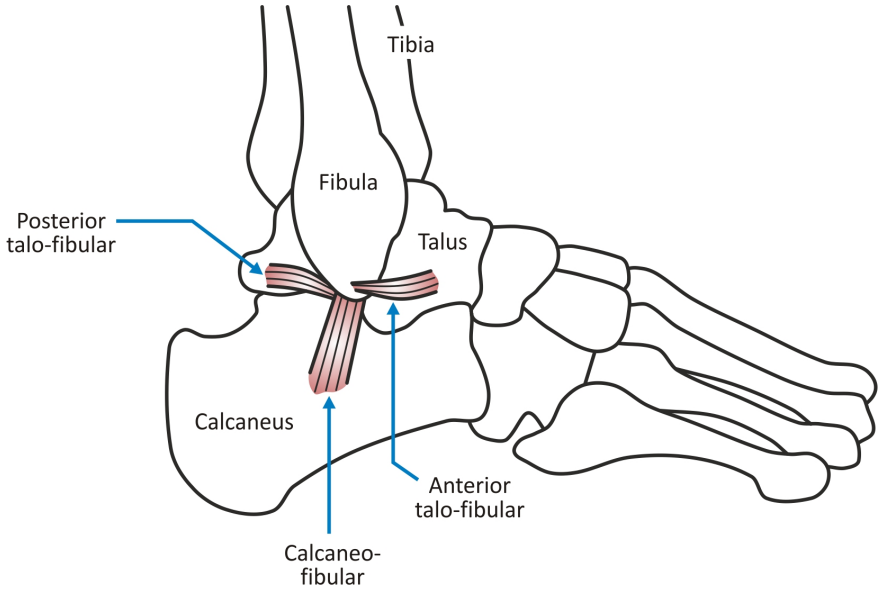

Figure 2.7: Lateral ligamentous complex (IMAR, University of Dundee)

loaded. Wright *et al.* (2000) demonstrated how increased plantar-flexion at foot strike raises the risk of ankle sprain. Proper positioning of the foot at foot strike is, therefore, essential to avoid ankle injury.

2.2.3 Risk factors

Risk factors for ankle sprains have been investigated and reported in the literature. The role of many of those factors, however, is still unclear, and there is a lack of consensus between the studies that investigated these risk factors. Gender, age, isokinetic strength of the lower leg muscles, joint laxity, ankle alignment and body size have all been investigated but whether these factors contribute to ankle injury is still being debated (Baumhauer *et al.* 1995; Beynnon *et al.* (2002); Murphy *et al.* 2003; Willems *et al.* 2005b; Willems *et al.* 2005a).

According to McKay *et al.* (2001) the existence of a previous ankle sprain will increase the chances of an ankle injury by five times. The evidence against previous injury as a risk factor, especially when the subject did not undergo any proper physiotherapy, is strong and well documented (Milgrom *et al.* 1991;

Yeung *et al.* 1994; Hawkins *et al.* 2001; Bahr and Bahr 2007). Prevention of ankle injuries in the first place, as such, is vitally important if we want to reduce the number of ankle sprain incidents.

The use of footwear has also been suggested as a risk factor for ankle sprains. They have been shown to decrease foot proprioception (Robbins *et al.* 1995; Waddington and Adams 2000; Sekizawa *et al.* 2001), as well as, increase the external moments acting on the ankle joint, thus predisposing the ankle for injury (Kerr *et al.* (2009); Ramanathan *et al.* 2011a; Ramanathan *et al.* 2011b).

2.2.4 Consequences

The consequences of ankle sprains can be severe and chronic. People who have sustained an ankle sprain previously have a higher probability of sustaining another (Safran *et al.* 1999; McKay *et al.* 2001; Murphy *et al.* 2003). In their study involving 380 athletes from 19 different sports, Yeung *et al.* (1994) found that 73% of subjects had recurrent ankle sprains, and 59% of which suffered residual symptoms impeding their athletic performance. It is evident that people with previous ankle sprains may continue to suffer residual pain for a long time after injury (Puffer 2001; Anandacoomarasamy and Barnsley 2005).

Ankle sprains require time to heal during which subjects will be unable to participate in any sporting activities. In a study involving approximately 10,000 basketball players, almost half the athletes who suffered an ankle injury during a game had to miss at least one week of competition time (McKay *et al.* 2001).

The recovery time of an ankle sprain depends on the severity of the injury. A Grade 1 injury, which involves the ATFL being stretched, requires between a one to two weeks of rest. Partial tear of the ATFL and injury to the CFL is classified as a Grade 2 ankle sprain and requires between two and six weeks

of rest. Recovery from a Grade 3 injury, where there is complete tear of the ligament and tenderness at the ATFL, CFL, and PTFL, may require anything up to 26 weeks of rest time (Puffer 2001).

2.2.5 How to reduce ankle sprains

The consequences of ankle sprains are severe and the high re-injury rates makes it important to investigate prevention methods. Special training and conditioning programs have been devised and shown to reduce the risk of ankle sprains. Bahr *et al.* (2007) investigated the effects of a special training program on volleyball players with a history of ankle sprain injury. The program involved educating the players and coaches regarding the injury's risk factors, as well as special training targeting mostly proper pushoff and landing techniques during special game manoeuvres, in addition to proprioceptive enhancing exercises. The authors highlighted a two-fold decrease in ankle sprain incidents. In addition, McKay *et al.* (2001) highlighted that proper stretching and warming up of muscles before participating in activity was shown to reduce the risk of ankle sprains.

Ankle taping is also used as a method to reduce the risk of ankle sprains among athletes. Taping's ability to resist inverting moment, however, is very limited (Ashton-Miller *et al.* 1996) and reduces by 50% after $15\,min$ of exercise (Frankeny *et al.* 1993). Taping techniques seem to reduce injury by increasing the proprioception of the foot (Callaghan 1997). Athletes who suffered a previous ankle sprain injury tend to benefit best with this method (Thacker *et al.* 1999). Even though they are popular among athletes, ankle tapes are usually applied by trained personnel and lack adjustability thereafter.

Ankle braces on the other hand can easily be applied and readjusted by untrained users (Callaghan 1997). They protect the ankle by restricting its motion

and preventing excessive rotations. Ubell *et al.* (2003) demonstrated that ankle braces offer higher resistance to forced inversion when compared to unbraced ankles. While they seem to reduce the risk of ankle sprains, some researchers have highlighted that ankle braces may in fact interfere negatively with athletic performance.

Finally, ankle sprains can be reduced by improving the design of current footwear which have been implicated as a risk factors for ankle sprains (refer to Section 2.2.3). For that to be achieved a clear understanding of the mechanism through which shoes contribute to ankle sprains must be realised. A method to easily and effectively test and assess the protective features of footwear, as well as to test the effectiveness of future designs must be devised and implemented.

2.2.6 Footwear

Most people around the world wear shoes on a daily basis. They provide comfort and protect the feet from cuts, abrasion, and some traumatic injury. Footwear is also viewed by many as a fashion item, where looks and brand matter most, which ultimately dictates the price tag. Sports footwear on the other hand, is designed to improve performance as well as better protect the athlete's foot (Lake 2000). Given the various benefits of wearing shoes, several studies have demonstrated that footwear is not only failing to protect the foot from ankle sprain injury but may also be contributing towards it.

Kerr *et al.* (2009) compared the EMG signal of the PL muscle between shod and unshod conditions upon sudden inversion of the foot. They found increased PL muscle activity in the shod condition which they explained was due to the increased external inversion moment caused by the shoe sole. As such, they highlighted the negative role of footwear in ankle sprain occurrence. Similar finding have also been reported elsewhere in the literature (Ramanathan *et al.*

2011a; Ramanathan *et al.* 2011b).

Shoes have also been shown to affect foot proprioception and impede the position sense of the ankle and subtalar joints (Robbins *et al.* 1995; Waddington and Adams 2000; Sekizawa *et al.* 2001). Sekizawa *et al.* (2001) highlighted that shoes caused subjects to underestimate the rotation of their foot during both plantar-flexion and inversion. This led them to suggest that the wearing of shoes increased the risk of sustaining an ankle sprain.

Robbins and Waked (1997) suggested that falsely advertising the protective characteristics of shoes predisposes users to ankle sprains. To prove this, they covered a force-plate with an EVA layer which is usually used in the production of shoe soles. Even though the EVA layer remained the same during all trials, they 'tricked' their subjects by incorrectly advertising the EVA used as either superior, neutral, or inferior. They found after repetitive trials that forces measured by the force plate were significantly higher when the superior message was relayed as compared to the inferior one. Clinghan *et al.* (2008) also found that more expensive sports shoes provided neither better comfort nor cushioning then their less expensive counterparts within the same brand.

2.3 Foot rotating platforms

Ankle sprains usually occur when the foot is being loaded in an inverted or supinated position as highlighted previously. Based on this, several methods were devised to induce sudden inversion/supination of the foot in a safe laboratory environment, allowing researchers to better understand the risk factors of ankle sprain injury and how to prevent it. These methods can be classified into two groups: static subject induced rotation (SSIR) and dynamic subject induced rotation (DSIR).

2.3.1 Static subject induced rotation

Experiments where induced rotation of the foot was imparted while subjects were motionless were categorised as SSIR. These form the majority in the literature but they also showed different distinguishing features that separates them from each other:

- The maximum rotational speed and degree of rotation of the platform.
- The DOF of the platform and how it rotates the foot; supination or inversion.
- The actuating method of the foot-plate; gravity actuated or externally actuated.
- The foot was secured/unsecured to the rotating foot-plate.
- The body load on the foot was controlled/uncontrolled.

All SSIR experiments consisted of a subject standing statically on a rotating platform (Figure 2.8); a comparison between them is summarised in Table 2.1. All used platforms, except for one, had only 1-DOF, thus permitting rotation around one axis only. The angle between that axis and the longitudinal axis of the foot dictates the nature of the foot rotation. When those axes are parallel, as most researchers had them aligned, the foot would be inverted. Chan *et al.* (2008) on the other hand, designed their platform in such a way that they could vary that angle, permitting simultaneous but dependent inversion and plantar-flexion of the foot. The fact that the imparted inversion and plantar-flexion motion are dependent means that for a given inversion and flexion angle there will be only one possible path of rotation. Being able to simultaneously and independently rotate the foot around different axes could reveal new information regrading the mechanism of ankle sprain injury. Is the ankle more likely to get injured if it were already being plantar-flexed when inversion motion is

imparted or is it more vulnerable if both inversion and plantar-flexion motions are occurring at the same time? Lynch *et al.* (1996) pre plantar-flexed the foot by means of a wedge on the platform where subjects stood. Vaes *et al.* (2002) did something similar by pre plantar-flexing and adducting the foot (Figure 2.9). The induced motion imparted by the platform in such setups, however, remains purely of inversion nature. Additionally the fact the foot was pre-rotated could have caused the protective muscles of the lower leg to pre-contract before the imparting of motion and before the measurement of muscle activity began. This highlights the importance of being able to rotate the foot around more than one axis simultaneously. Kernozek *et al.* (2008) were the only investigators to use a 2-DOF platform, which allowed control of the tilting angle in inversion and plantar-flexion independently. As their platform was a trapdoor mechanism actuated by the weight of each subject, the researchers had no control over the path it took to reach the target angles. This would make it difficult to compare data between different subjects as the platform rotation path would not necessarily be the same. Alternatively it would be interesting to investigate for any significant differences in the path of rotation for the foot between active subjects with no history of ankle sprain injury and those with a history of recurrent injuries.

The platforms can be divided into two categories based on the driving force that actuates them: gravity driven or externally driven. In gravity driven platforms, the trapdoor like foot-plate is rotated by its weight and/or that of the subject standing upon it. The researcher controls the start of rotation and the final tilt angle only; they have no control over the platform once rotation is initiated. These platforms are thus, cheaper and simpler to design and build, but also provide less control. Externally driven platforms on the other hand, provide greater control during the rotation phase of the foot-plate, at the expense of cost and complexity. Lynch *et al.* (1996) for example, employed hydraulic power

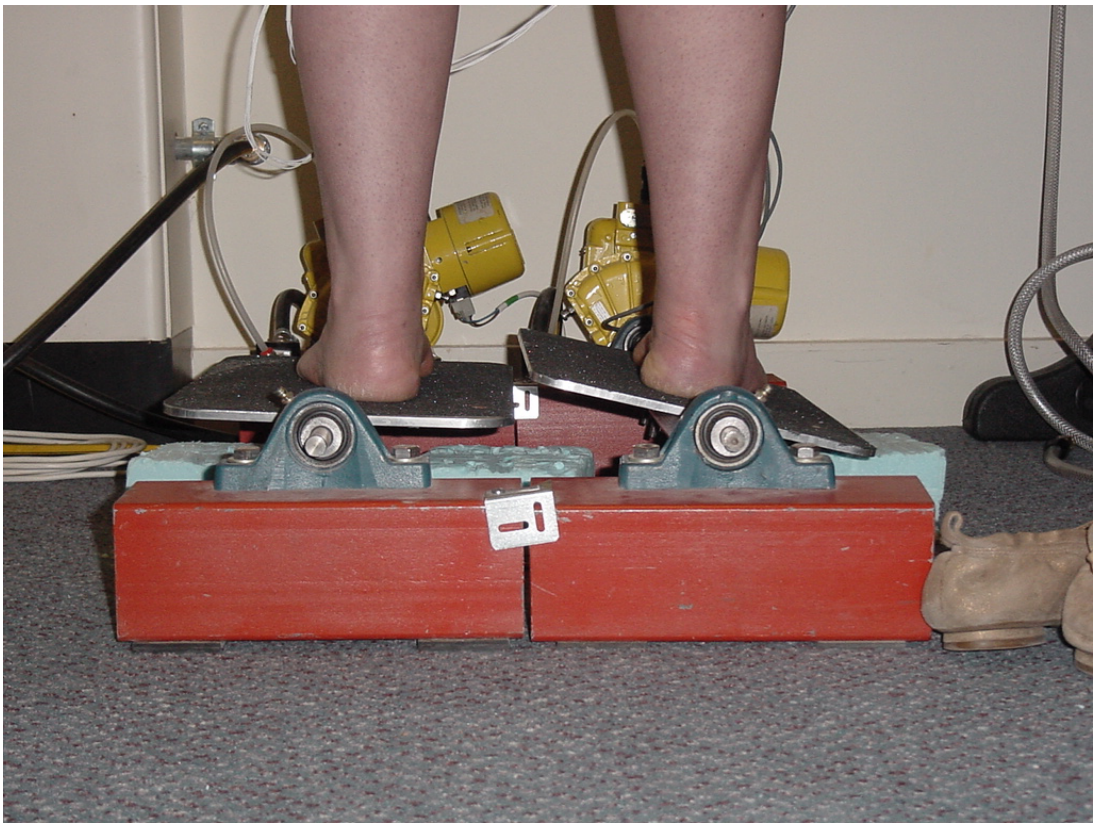

Figure 2.8: Subject standing still on an inverting platform (IMAR, University of Dundee)

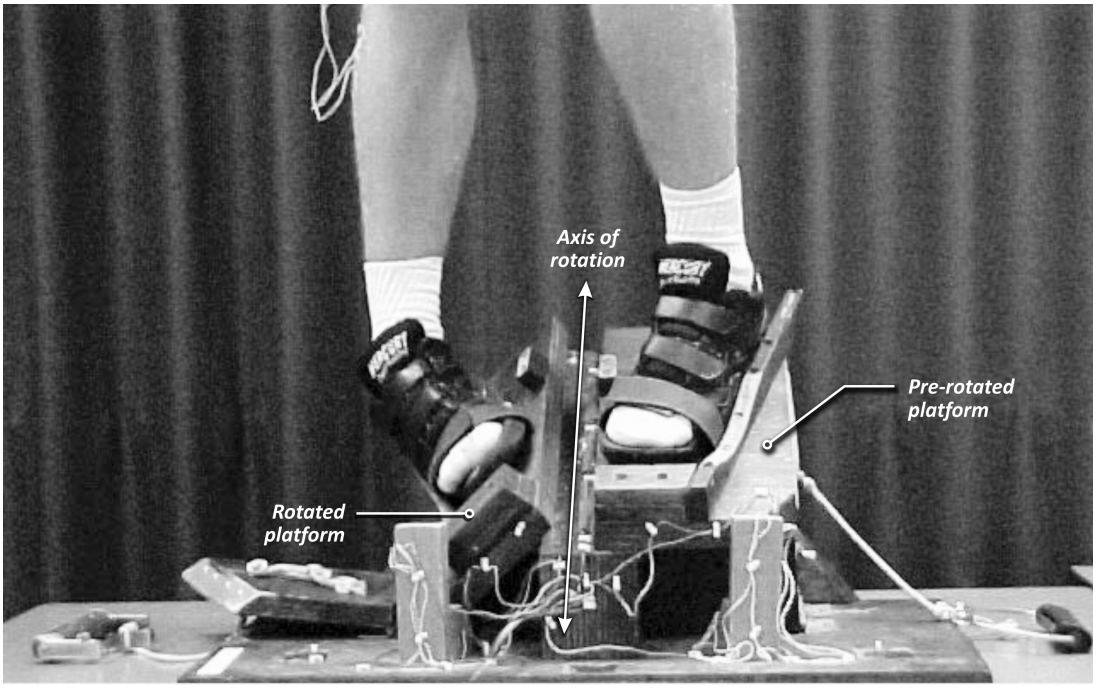

Figure 2.9: Pre-rotated foot (adapted from Vaes *et al.* 2002)

Table 2.1: A comparison between the different SSIR experiments in the literature (G is for gravity, H is for Hydraulic, P is for pneumatic and S is for spring)

Source	DOF	Foot Rotation	Rotation Angle	Speed(max) or Duration	Actuation method	Foot straps
Isakov *et al.* (1986)	1	Inversion	20°	60 ms to 80 ms	S	No
Ramot (1990)	1	Inversion	35°	40 ms	S	Yes
Lynch *et al.* (1996)	1	Inversion Plantar-flexion	18° 10°, 20°	50°/S and 200°/S 0	H	NA
Ricard *et al.* (2000)	1	Inversion	35°	60 ms	G	No
Benesch *et al.* (2000)	1	Inversion	30°	430°/S	G	No
Vaes *et al.* (2002)	1	Inversion Plantar-flexion Adduction	50° 40° 15°	106 ms 0 0	NA	Yes
Konradsen *et al.* (2005)	1	Inversion	30°	150 ms	H	Both
Wilson and Madigan (2007)		Inversion	22°	60 ms	G	No
Eechaute *et al.* (2007)	1	Inversion Plantar-flexion Adduction	50° 40° 15°	383°/S to 680°/S 0 0	NA	Yes
Chan *et al.* (2008)	1	Adjustable	30°	NA	G	No
Kernozek *et al.* (2008)	2	Inversion Plantar-flexion	30° 10°, 20° , 30°	91 ms (at 30° Plantar-flexion)	G	NO
Kerr *et al.* (2009)	1	Inversion	10°, 20°	100°/S	P	No
Ramanathan *et al.* 2011a and Ramanathan *et al.* 2011b	1	Inversion	20°	100°/S	P	No

to actively control the rotational speed of their platform, setting it to $50°/s$ in some trials and to $200°/s$ in others. Lynch *et al.* (1996) found that higher rotation speeds resulted in significantly shorter reaction times for for both the PL and TA muscles. They also found that having the foot plantar-flexed resulted in significantly longer reaction times in the PL muscle suggesting a higher risk to sustaining an ankle sprain. This highlights the importance of being able to control the rotation speed of the platform and the type of foot rotation. Kerr *et al.* (2009) used pneumatic actuators to randomise the movement of their platform, as well as to create a 'test sequence' where the foot-plate rotated continuously to a set of predefined angles of different magnitudes.

The tilt angle of the platforms in the studied literature ranged from 10° to a surprisingly high 50°. The majority of the researchers, however, chose an angle of approximately 20°or 30°. The rotation speed varied between $100°/s$ and $680°/s$. The duration of rotation was between $40\,ms$ and $150\,ms$ (Table 2.1).

Some researchers chose to strap the subject's foot to the platform, possibly to avoid slipping and to force the foot to rotate exactly with the foot-plate. Others decided to leave the foot free on the platform (Table 2.1). It is also worth noting that some researchers used a scale under the opposite foot and asked subjects to control the support provided by that leg themselves (Lynch *et al.* 1996; Konradsen *et al.* 2005). Others rotated the platform after they asked the subjects to unload the opposite foot (Vaes *et al.* 2002; Eechaute *et al.* 2007). Having subjects keep their opposite foot on the ground for support allows them to use that foot to protect and remove the load from the foot being rotated; this could alter the measured response of the muscles protecting the rotated foot. Having subjects unload the opposite foot means that the lower leg muscles of the foot being rotated would have to actively support and provide balance for the subject; this could also affect the measured response from those muscles.

2.3.2 Dynamic subject induced rotation

Experiments where induced rotation of the foot is imparted while subjects are moving are categorised as DSIR. Such experiments are sparse in the literature compared to SSIR and the methods used vary considerably.

Hopkins *et al.* (2007) fitted a 1-DOF trapdoor-like mechanism similar to the gravity actuated SSIR platforms described in Section 2.3.1, into a $6.1\,m$ walkway. The trapdoor was held in position by a spring ball plunger that supported up to $45\,N$ of force. The researchers had their subjects walk with the medial side of the foot, $6\,cm$ away from the axis of rotation of the trapdoor. When the walking subject stepped on the platform it dropped rotating to an angle of 30°. This setup had the same advantages and disadvantages of the gravity actuated SSIR platforms, i.e. relatively inexpensive and less complex but with no control over the platform during its rotation. Also, due to the fixed $45\,N$ release force of the trapdoor, the researchers would have been unable to control the timing of the release. Figure 2.10 shows the normal component of the GRF averaged from 100 healthy subjects and normalised to the body weight of the subjects. A value of approximately 15% body weight can be seen at foot strike. This means that a subject weighting more than $30.5\,Kg$ will cause the platform used by Hopkins *et al.* to rotate at foot strike[1]. The subjects in this experiment were asked to walk to the cadence of a metronome at a speed of 90 steps/minute. This means that on average the duration of each step would be approximately $667\,ms$ (60/90 = 0.667 seconds/step). The initial double limb stance for normal generic gait during which the subject would have both of their feet on the ground constitutes the first 10% of the gait cycle (Perry and Burnfield 2010); this would be $66.7\,ms$ for a cadence of $90\,steps/minute$. Hopkins *et al.* (2007) measured the PL and PB muscle reaction times and found that they were $56.9\,ms$ and $60.1\,ms$

[1] $30.5\,Kg = \frac{45 \times 15}{9.81 \times 100}$ where 9.81 is gravitational acceleration

respectively which is less than $66.7\,ms$. This means that at those times the subject was still able to support themselves and could protect the inverted foot with their opposite foot that was still planted on the ground (assuming subjects weighed more than $30.5\,Kg$ so that the platform began rotating at footstrike). The fact that subjects were now moving, and in such a setup, implies that the researchers would not be able to align the longitudinal axis of the foot to the rotational axis of the platform. Landing with the foot externally rotated on the trapdoor will result in less inversion of the foot and the presence of some plantar-flexion. Asking subjects to walk with the longitudinal axis of their feet parallel to the axis of rotation of the trapdoor, so as to control the nature of foot rotation, means interfering with the subject's normal gait. Linford *et al.* (2006) used a similar setup, but used four trapdoors on each side of an $8.5\,m$ walkway. This had the benefit of preventing subjects from anticipating where or when the trapdoor would be released. The length of the trapdoor (as shown in Figure 2.11) is relatively long. This may cause subjects to modify their gait in order to avoid stepping on the end edge of the trapdoor with their next step.

Nieuwenhuijzen *et al.* (2002) also used a trapdoor mechanism to induce inversion of the foot during walking. Their device consisted of a portable box with a trapdoor supported by a spring, which offered $23\,N$ of resistance when the trapdoor was fully rotated to 25°. The box was dropped on to a treadmill where a subject was walking in a timed manner such that the subject would step on it with their left foot (Figure 2.12). The advantage of using a treadmill is the ability to control the walking speed of subjects. On the other hand, the dropped box can not be made flush with the walking surface. It would also be difficult to have subjects do any sports activity such as dribbling a basketball for example, whilst walking. The fact that the platform began rotating from a load as low as $200\,g$, suggests that the opposite foot would be bearing most of the load during

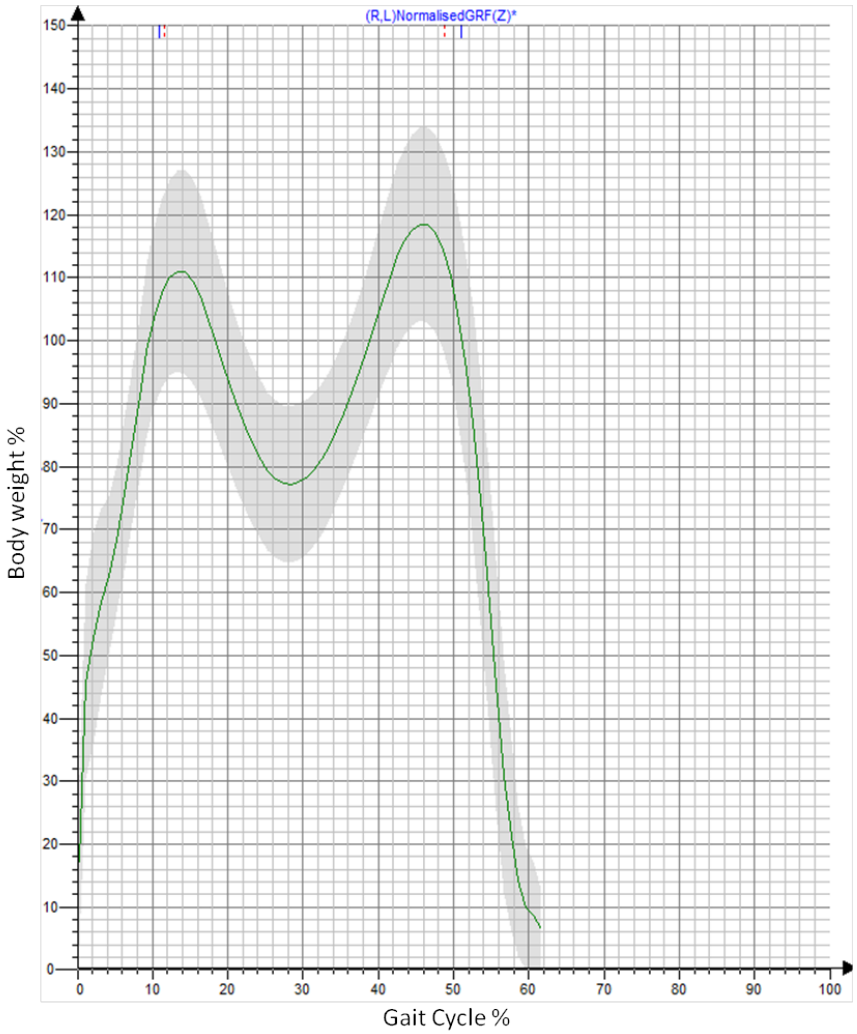

Figure 2.10: Average normalised GRF from a 100 healthy subjects plotted against the normalised gait cycle

rotation. Proper loading of the foot being rotated would occur at the instant the platform hits the wedge and stops rotating (the same is true for the previously described trapdoor mechanisms where the platform could rotate freely). The average duration time for full rotation of the platform was $62\,ms$ which (assuming a cadence of 90 steps/minute) would mean that when the rotated foot was loaded the opposite foot was still on the ground and could provide support and protection. Ankle sprain injuries however occur when the foot is being loaded in an inverted or supinated position which limits the use of this setup in simulating a realistic ankle sprain injury.

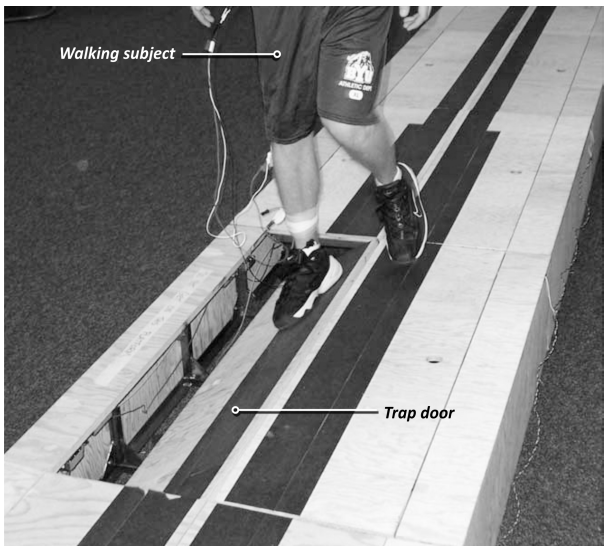

Figure 2.11: Ankle inverting platform (adapted from Linford *et al.* (2006))

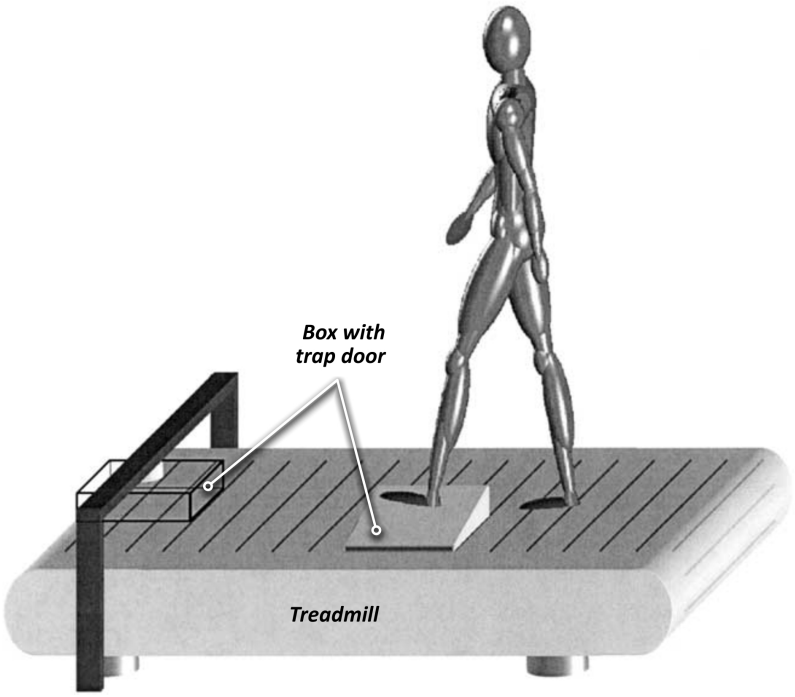

Figure 2.12: Ankle inverting platform (adapted from Nieuwenhuijzen *et al.* (2002))

The final method found in the literature that was employed in DSIR was jumping on either a trapdoor mechanism platform or an inclined surface. Grüneberg *et al.* (2003) had their subjects jump in a controlled manner from a height of 30 cm onto a trapdoor mechanism.

2.3.3 Need for a new foot rotating platform

Most of the studies reported in the literature rotated the foot of subjects who were standing still on a rotating platform. Ankle sprain injuries however do not usually occur when subjects are standing still, but rather when they are active and moving. Only a few studies in the literature reported rotating the foot of a moving subject. Those studies however were limited, mainly due to the rotating platform they utilised:

- The rotating platform in all these studies could only impart inversion motion to the foot; ankle sprain injuries also occur when the foot is being supinated. For a more inclusive study investigating ankle sprain injuries a researcher must be able to impart both foot inversion and foot supination.
- The platforms in all the DSIR studies were designed similar to a trapdoor mechanism where control over the degree of rotation is limited. This limits the use of such platforms in studies that aim to assess the effect of different rotation angles. When utilising a platform to impart foot rotation the degree of rotation must be set to a safe value lower then that which causes ankle injury. Based on such it is important to understand the relationship between the imparted degree of rotation and the measured outcomes.
- The platforms in these studies were actuated by weight of the subject with no control over the speed of actuation. Lynch *et al.* (1996) demonstrated that rotating the foot at higher speeds resulted in significantly lower

reaction times from the PL and TA muscles. Their study was however conducted on standing subjects.

- The platforms used in the DSIR studies provided limited control over the timing of the platform rotation following subject's foot strike on the platform. In fact in all the studies that involved a walking subject, the platform initiated rotation while the opposite foot was still in contact with the ground thus permitting the subject to protect their rotated foot by shifting the load onto the opposite foot.
- None of the platforms in the DSIR studies were synchronised to work with a motion capture system that allowed measurement of the lower body kinematics. Hopkins *et al.* (2007) and Linford *et al.* (2006) utilised a goniometer that measured the degree of foot inversion only. These researchers could not measure the effect of the platform rotation on the body kinematics nor could they record the instances of foot-strike to the platform and toe-off.

3 Technical considerations

3.1 Requirements and limitations

The robotic platform needed to replicate real life foot supination conditions as accurate as possible, yet at the same time give researchers and clinicians all the control and flexibility required to conduct their research and assessments. To achieve this the platform had to meet certain requirements:

- Ankle injury usually occurs when the foot is being loaded in an inverted or supinated position. In order for the platform to be able to invert and supinate the foot it must have a minimum of 3-DOF in rotation.
- Support subjects weighing up to $120\,kg$ to accommodate the larger population.
- Rotate to the required angles accurately and consistently.
- Rotate with an angular velocity higher than $100°/s$ which is the minimum rotational speed reported in the available literature. There are no studies in the literature (at the time of this writing and to the knowledge of this author) highlighting the inversion/supination velocities at which ankle sprains occur. As such, it is important that the platform is able to rotate at a wide range of angular velocities to allow investigating the relation between ankle and foot inversion/supination velocity and ankle sprain injury.

- Have a foot-plate with a surface area large enough to accommodate different foot sizes, as well as, be easily struck during walking.
- Be embedded flush with the Sports Laboratory floor to keep the walking area flat and allow subjects to walk normally.
- Hidden and not obvious to subjects, so as not to affect the psyche of subjects during tests.
- Allow control over the time the platform waits before beginning of rotation following foot strike to the platform.
- Safe mechanically and functionally:
  - the platform must not fail mechanically, and all its parts must withstand the operational stresses.
  - the subject's foot must not get stuck between the rotating foot-plate and the surrounding floor.
  - the foot-plate must rotate only when the foot has landed on it fully, and when no parts of the foot lay outside the foot-plate.
  - the foot-plate must have enough traction to prevent the foot slipping while it rotates.
- Be easy to operate by any researcher/clinician who will:
  - Set the degree and speed of rotation
  - Start/stop its operation
  - Save the rotation and strain gauge data
- Be clean and not make a mess in the clean laboratory/clinic environment.

The Sports Laboratory, which was chosen to house the robotic platform, was not designed to house a 3-DOF rotating platform. This, along with other factors, imposed certain limitations and constraints on the design of the platform, mainly:

- The pit where the platform was to be fitted was too shallow. The free and available space of the pit measured $275\,cm \times 80\,cm \times 23\,cm$ in length, width, and depth respectively. The $23\,cm$ depth was the most critical factor as this was too shallow and did not allow for linear actuators to be mounted vertically, thus limiting the design choices dramatically. Additionally, and depending upon the position of the centre of rotation of the platform, the depth constraint also limited the size of the foot-plate that could be used; the larger the foot-plate, the less platform rotation can be achieved before the foot-plate hits the ground. This was in fact, one of the biggest challenges that this project faced.
- No drilling was allowed in the pit concrete base, since this may damage and compromise its water-tight treatment.
- Hydraulic actuators were not encouraged as they could leak and compromise the clean environment of the laboratory/clinic. There was also no infrastructure available at the Sports Laboratory to support them.
- The cost of the platform must be reasonable for commercial purposes.

3.2 Type of Actuators to be used

The platform must have 3-DOF and thus there needs to be at least three actuators driving it. There are different types of actuators that can be used; we classify them based on their power source:

Electricity: Electric actuators (Figure 3.1a) are fast acting, clean, simple, precise and easy to control. They, however, lack the power required to drive the platform and as such were not a suitable option.

Compressed air: Pneumatic actuators (Figure 3.1b) are more powerful than the electric ones and are fast acting, clean, and not very expensive. Their

(a) Electric linear actuators (adapted from D'souza (2011))

(b) Pneumatic actuators (adapted from ALLAIR 2008)

Figure 3.1: Different types of actuators

downside is that they are not as precise, hard to control, and cannot hold a load steadily. That is due mostly to the compressible nature of air.

Liquid: Hydraulic actuators are the most powerful. They are fast acting, relatively simple to control (as liquid is incompressible) and can hold loads more steadily than their pneumatic and electric counterparts. Their disadvantage lies in the fact that they are messy, complex and more expensive.

IMAR is already equipped with an air compressor and a compressed air storage tank. This and the fact that hydraulic systems are complex and messy and unsuitable for the current laboratory environment, made the pneumatic actuators the preferred choice.

4 Robotic platform design

4.1 Ideas and Concept Designs

> "Virtually nothing comes out right the first time. Failures, repeated failures, are finger posts on the road to achievement. The only time you don't want to fail is the last time you try something.... One fails forward toward success." — Charles F. Kettering, engineer and inventor.

In any design process an engineer will usually come up with several ideas and concept designs before realising the final product. In designing the current robotic manipulator, several design ideas were considered, two of which had the potential of being the final product.

The first concept design depicted a parallel manipulator with all its three actuators in a closed loop chain and acting directly on the foot-plate (Figure 4.1). Parallel manipulators (Figure 4.2a) usually have better stiffness and operating speeds than their counterparts (Figure 4.2b), the serial manipulators, while serial ones are usually less complex.

In this concept design, the foot-plate's geometric centre coincided with all three axes of rotation. This allowed the same platform to act on both left and right feet, simply by having the platform rotate in the opposite direction and having

the subject walk the opposite way. This positioning of the geometric centre permits the use of a larger foot-plate and/or increases the platform's range of motion.

While this concept design offered some attractive advantages it nonetheless had some flaws and disadvantages that would deem it unfeasible. The first concern was the parallel design nature of the platform, which would require a complicated control algorithm, especiallythat pneumatic actuators were to be used (refer to Section 4.2.5).

The alignment of the geometric centre of the foot-plate with the axes of rotations implies that upon rotation, half of the plate will shift downwards while the other half will shift upwards. If a subject steps on the upward moving side the actuators must act against the entire body weight, thus, requiring the use of powerful actuators. The shallow depth of the pit, however, limits the bore size of actuators that could be used, and ultimately the available actuation force. According to simulation performed using Autodesk® inventor, the maximum bore size of $63\,mm$ that could fit in the pit, will not allow the platform to rotate at the required speed.

Subject safety, however, was the main problem facing this design. If a subject stepped on the falling edge of the foot-plate, their opposite foot would be in a collision course with the rising edge, with the possibility of causing injury.

The second concept design addressed the drawbacks of the first design. The axis of rotation around the x-axis was shifted to the edge of the foot-plate which eliminated the risk of foot injury, and at the same time, reduced the load put on the actuators. The axis of rotation around the y-axis was shifted to 1/3 of the foot-plate; any further and the platform's range of motion would become very limited. These changes, however, meant that two platforms would be needed, one to supinate each foot.

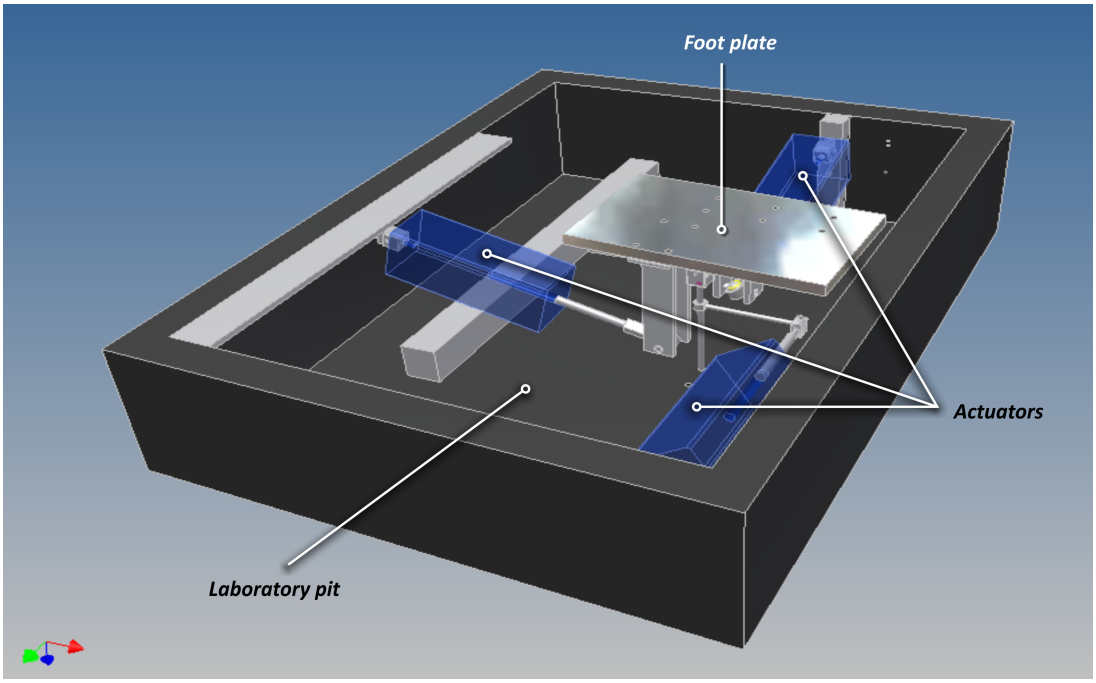

Figure 4.1: First concept design of the platform (Red arrow on the bottom left of the figure indicates the direction of the x-axis, the green arrow is for the y-axis and the blue is for the z-axis)

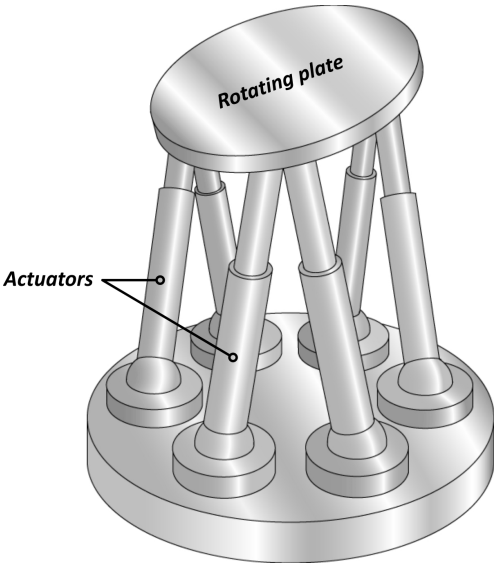

(a) Parallel manipulator (adapted from Taghirad (2007))

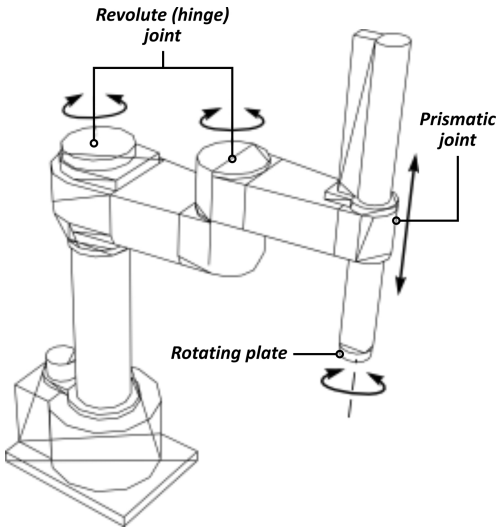

(b) Serial manipulator (adapted from Chopra (2007))

Figure 4.2: Parallel versus serial manipulators

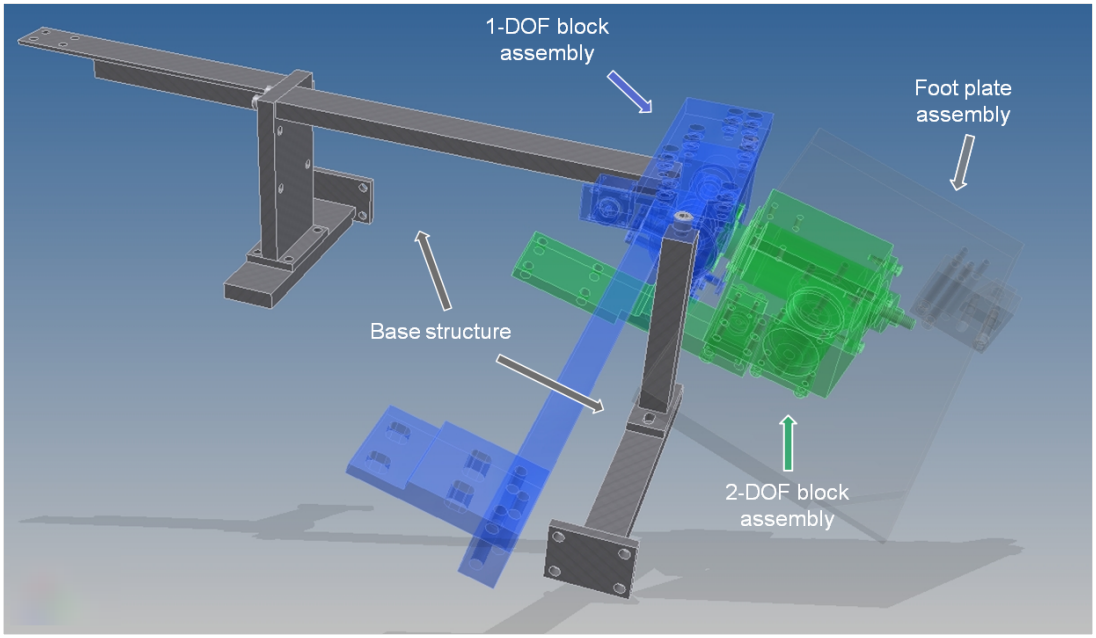

Figure 4.3: The robotic platform consists of four different assemblies

To reduce the complexity of the control algorithm, the design was changed from a parallel manipulator configuration into a serial manipulator configuration.

4.2 Detailed Design

The second concept design was deemed feasible and was found to meet all the necessary requirements. A detailed design was produced for the manufacturing company to build.

The final design of the platform consisted of many parts, each serving a different role. Due to the large number of parts designed, not all of them will be covered in the discussion below; their detailed drawings are available in Appendix A. To make the design choices and the function of the parts clearer the platform design has been divided into four different assemblies (Figure 4.3).

4.2.1 Footplate assembly

The foot-plate is the main part of the assembly (Figure 4.4). Its main purpose is to support and rotate the subject's foot. In order to prevent the foot from slipping while the foot-plate rotates, an anti-slip mat was glued to its surface. For safety reasons the platform must never rotate unless the entire foot was contained within its boundaries. Based on that, and in order to increase the chances of a correct foot strike (FS), the foot-plate had to be as large as possible. Unfortunately the shallow depth of the pit dictated the size of the foot-plate. The bigger the foot-plate the smaller the angle of rotation before it hits the ground. A compromise was made and the foot-plate was sized to $450\,mm \times 250\,mm$, which allowed 25° rotation around the x-axis (platform inversion), with 20° rotation around the y-axis (platform flexion), while still accommodating large foot sizes.

The foot-plate must also be level with the laboratory floor to keep the walkway flat allowing subjects to walk naturally (refer to Section 3.1). The depth of the foot-plate was set to $23.5\,mm$. This gives the platform greater versatility by allowing the attachment of different foot-plates with uneven surfaces while keeping them level with the floor.

There is a custom-designed hinge joint bolted to the corner of the foot-plate that links it to a rod of one of the three pneumatic actuators. The base of that cylinder attaches to the 2-DOF block assembly. This allows the cylinder to act directly on the foot-plate and rotate it around the z-axis (platform adduction).

4.2.2 2-DOF block assembly

The foot-plate assembly attaches directly to Shaft 1 of the 2-DOF block assembly (Figure 4.5). The 2-DOF block (Figure 4.6) consists of a $160\,mm \times 140\,mm \times 90\,mm$ aluminium block with two pre-drilled holes (Figure 4.7), with each hole

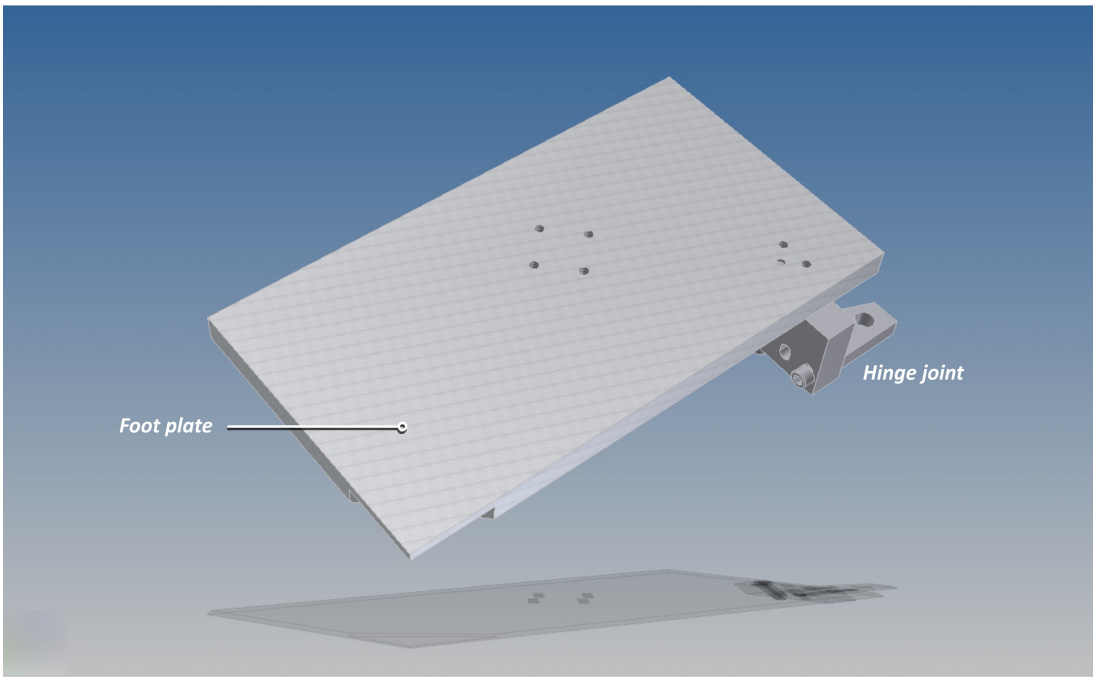

Figure 4.4: Foot plate assembly

having a small shoulder at only one end. In each of these holes two sealed roller bearings are fitted, one at each end and separated by a hollow cylindrical spacer. An aluminium plate is bolted to the block at the end opposite the shoulder of each hole; the plate in combination with the shoulder keeps the bearings from falling out. The bearings allow a shaft to rotate freely through each hole thus giving the platform 2-DOF. Shaft 1 allows the foot-plate to rotate around the z-axis; this shaft also features an integrated pulley at one end. The pulley rotates the input shaft of one of three optical encoders installed on the platform via an elastic belt. A custom frame with four slots was designed to hold the optical encoders while allowing fine tuning of their positions so as to keep the belts tight. Another pulley was bolted directly on the block encircling hole 2. Shaft 2 permits the aluminium block, and along with it the foot-plate to rotate around the y-axis. The end of each shaft was threaded so that a nut and a custom washer can hold each of the shafts in place.

Attached to the aluminium block is a steel arm that connects to one of the

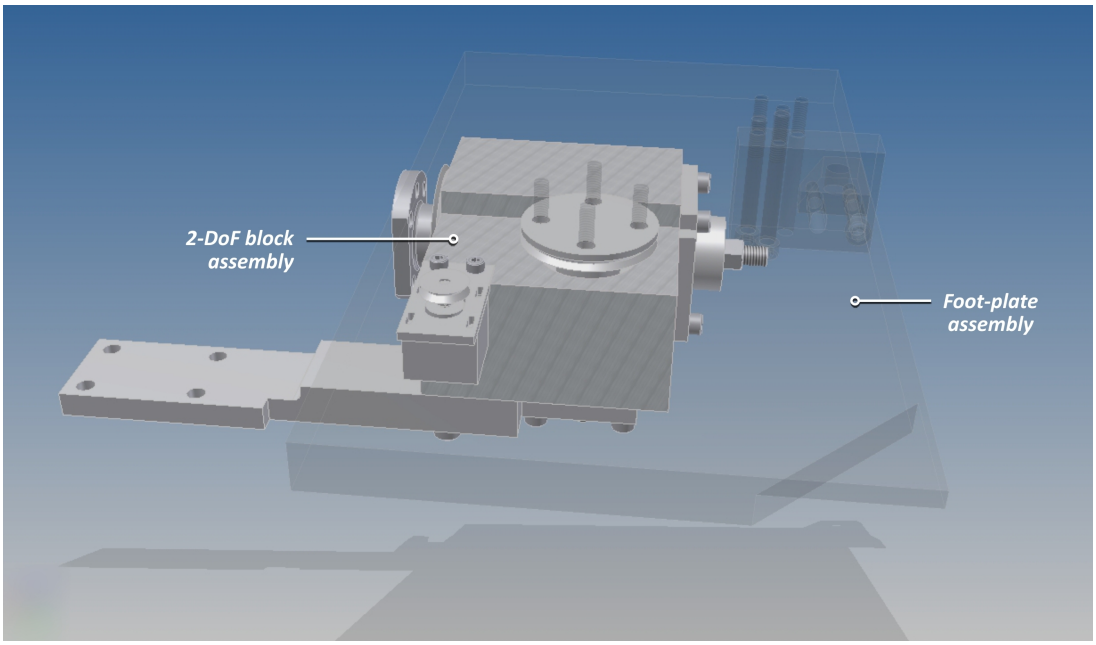

Figure 4.5: Foot plate attached to 2-DOF block assembly

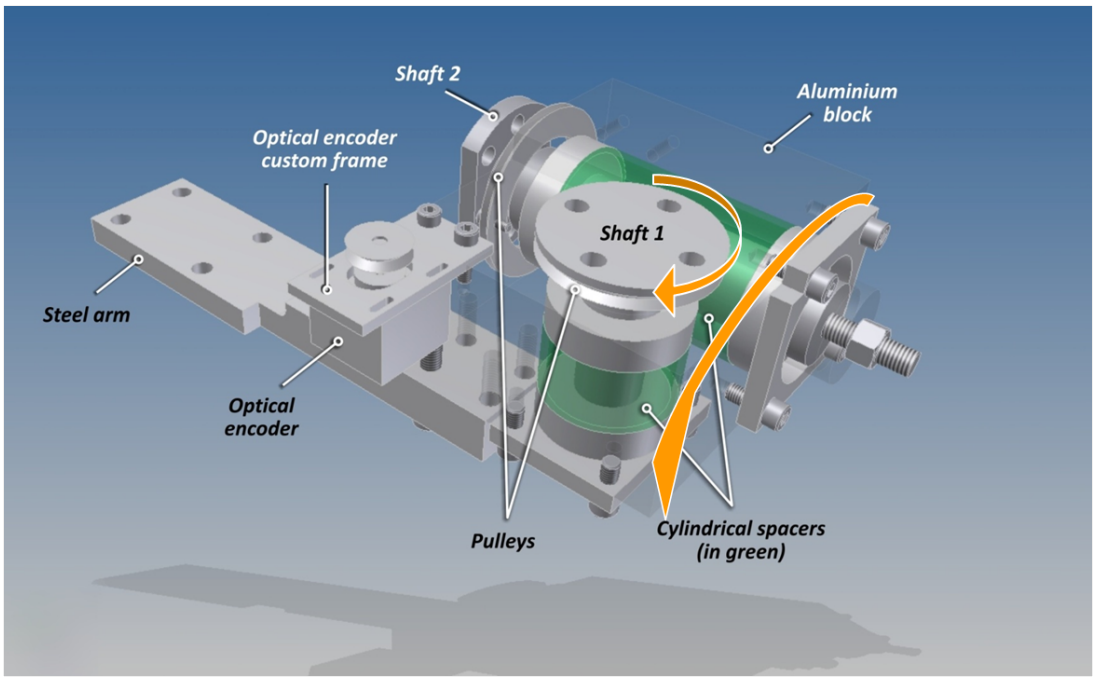

Figure 4.6: 2-DOF block assembly. The orange arrows indicate the direction of rotation provided by shaft 1 and shaft 2

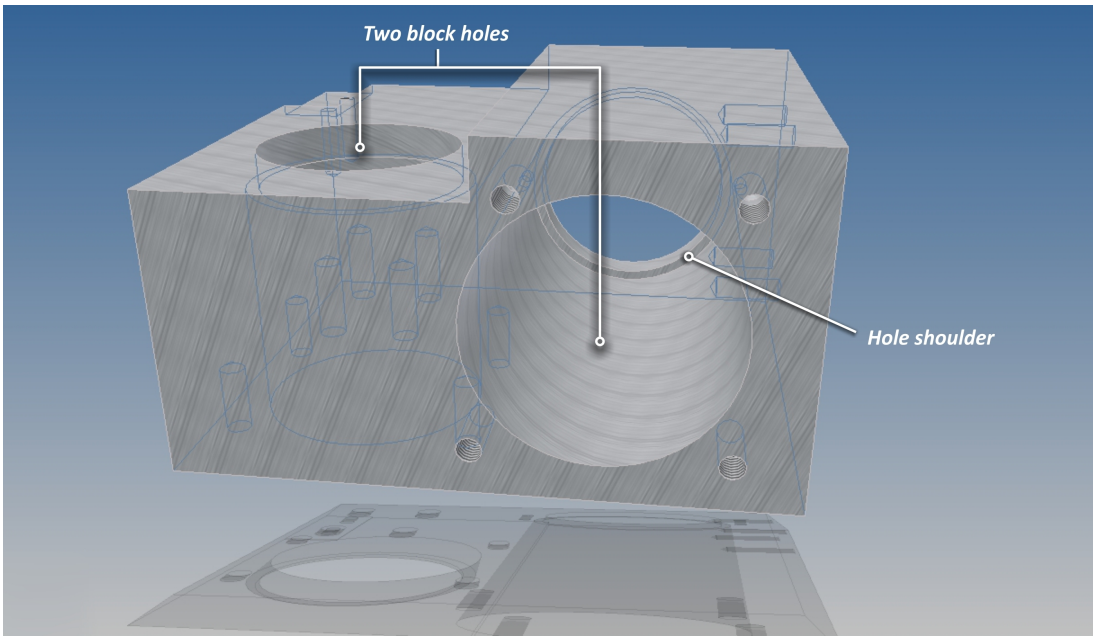

Figure 4.7: 2-DOF aluminium block

pneumatic cylinders, providing the actuating force that rotates the platform around the y-axis.

4.2.3 1-DOF block assembly

Shaft 2 of the 2-DOF block assembly is bolted to a rectangular steel bar that is part of the 1-DOF block assembly (Figure 4.8) .

The 1-DOF block assembly (Figure 4.9) consists of a rectangular steel plate that fastens to the metallic chassis of the pit securing the entire platform in place. Two custom designed house bearings were bolted to the rectangular steel plate. The first house bearing is rectangular in shape, while the second has one of its ends rounded to avoid collision with the moving foot-plate. Within each of these house bearings is a 1-row angular contact ball bearing; together they allow a steel shaft (shaft 3) to rotate freely around the x-axis giving the platform its third DOF. The bearings were chosen because of their ability to withstand the high axial and normal loads generated by the pneumatic actuators.

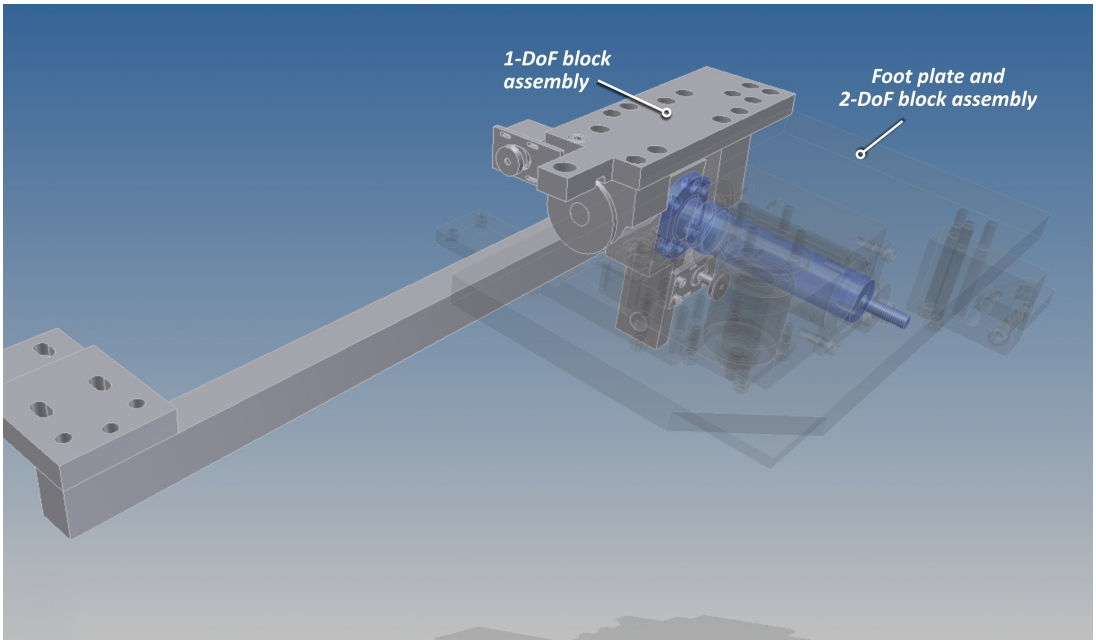

Figure 4.8: 2-DOF block and foot-plate attached to 1-DOF block assembly

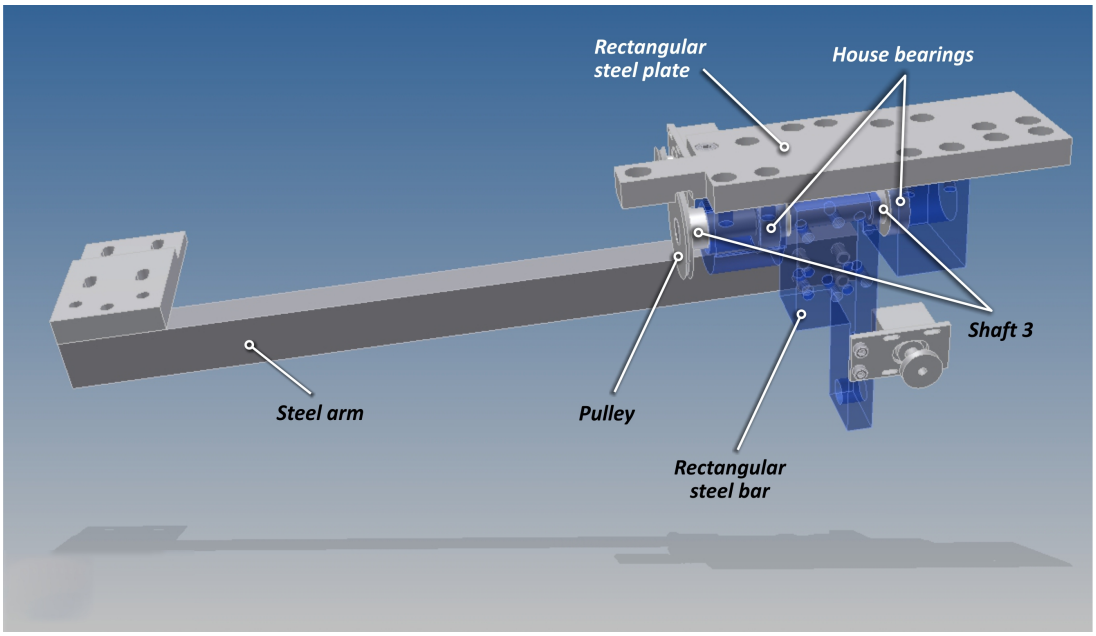

Figure 4.9: 1-DOF block assembly

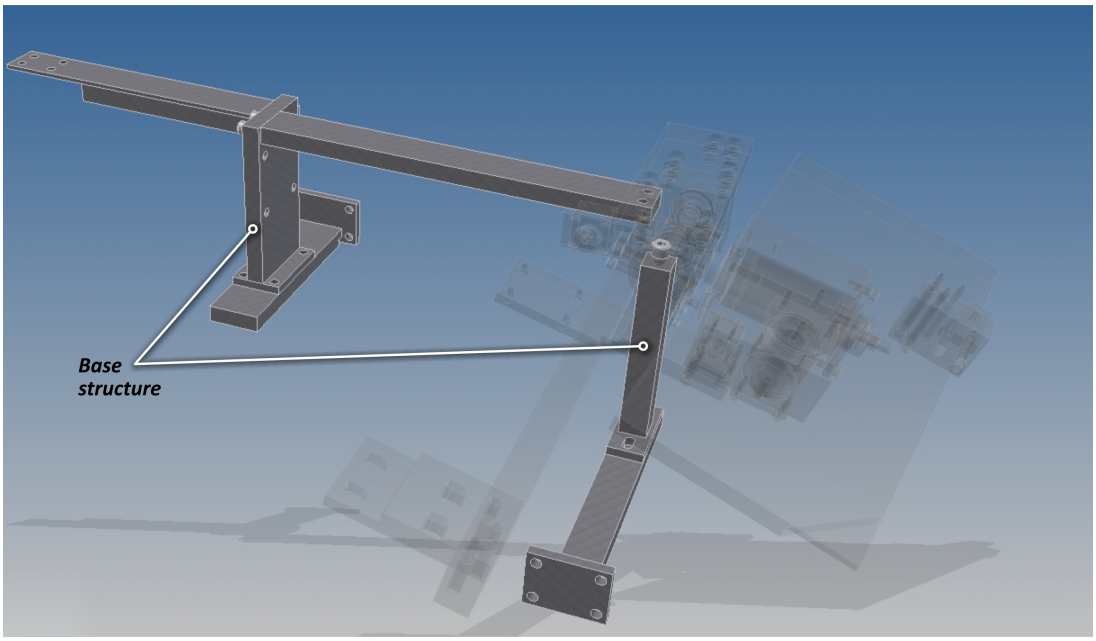

Figure 4.10: Base Structure supports the entire platform

Shaft 3 passes through and supports the rectangular steel bar. Secured to the end of the steel shaft is the third pulley. This pulley rotates with the shaft and the rectangular steel bar, allowing us to measure the rotation of the platform around the x-axis.

Attached to the rectangular bar is a steel arm that supports the last of the pneumatic actuators. A sizeable part of material was also extruded out of the end of the steel bar to prevent any collision with the rod of the flexing cylinder. The 1-DOF block assembly also hosts the remaining two optical encoders.

4.2.4 Base structure

The base structure, along with the rectangular steel plate of the 1-DOF block assembly, support the platform and hold it securely in place (Figure 4.10). Since drilling in the pit floor was not possible (refer to Section 3.1), the base components had to be connected to the metallic chassis of the pit (Figure 4.11).

The base structure consists of two block assemblies. Block 1 of the base structure

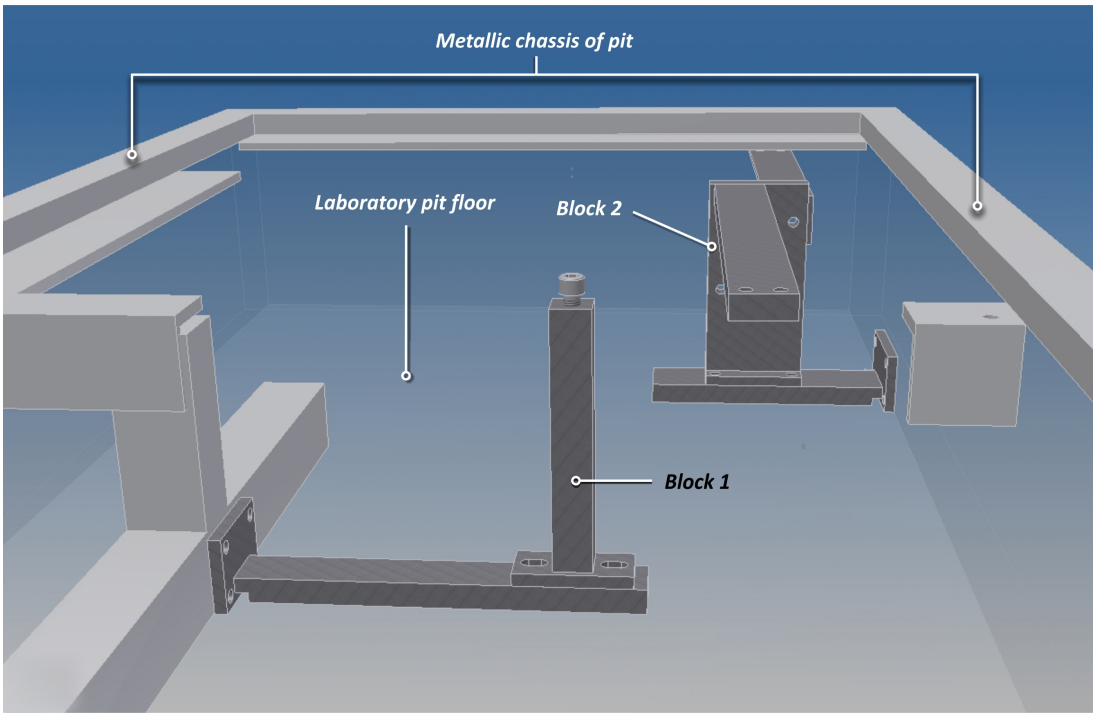

Figure 4.11: Base structure connected to the pit's chassis

is bolted to the free end of the rectangular steel plate, providing support in the vertical direction. Most of the load carried by block 1 is transferred through a vertical steel bar, and, via a horizontal steel bar, to the ground. The horizontal steel bar is welded to a small rectangular steel plate which is bolted to the metal chassis of the pit; this secures block 1 in place.

Block 2 consists of a vertical rectangular steel plate that holds the third pneumatic actuator. A rectangular steel bar, connecting block 2 and the 1-DOF block assembly, acts to counteract the forces generated by this actuator. A rectangular steel bar on the ground is bolted to and supports the vertical steel plate. The ground steel bar is welded to a small rectangular plate which is bolted to the metallic chassis of the pit, securing block 2 in place.

4.2.5 Actuators

Three pneumatic actuators/cylinders were used to drive the platform. The actuators length and bore diameter were chosen based on geometric constraints and the required output force calculated using computer simulation. The first cylinder has its main body connected to the vertical plate of block 2 of the base structure via an off-the-shelf joint (Figure 4.12a). Its acting rod is connected to the steel bar of the 1-DOF block assembly thus rotating the foot-plate around the x-axis (Figure 4.12b). This allows the platform to impart foot inversion. The second cylinder has its main body connected to the steel arm of the 1-DOF block assembly (Figure 4.13a). Its acting rod is jointed to the steel arm of the 2-DOF block assembly allowing rotation of the foot-plate around the y-axis (Figure 4.13b) which allows the platform to plantar-flex the foot. The third cylinder is compact and has its main body connected to the aluminium block of the 2-DOF assembly (Figure 4.14a). Its acting rod is jointed to the foot-plate via the custom-made hinge, this actuator rotates the foot-plate around the z-axis (Figure 4.14b). This actuator thus allows the platform to adduct the foot of a subject.

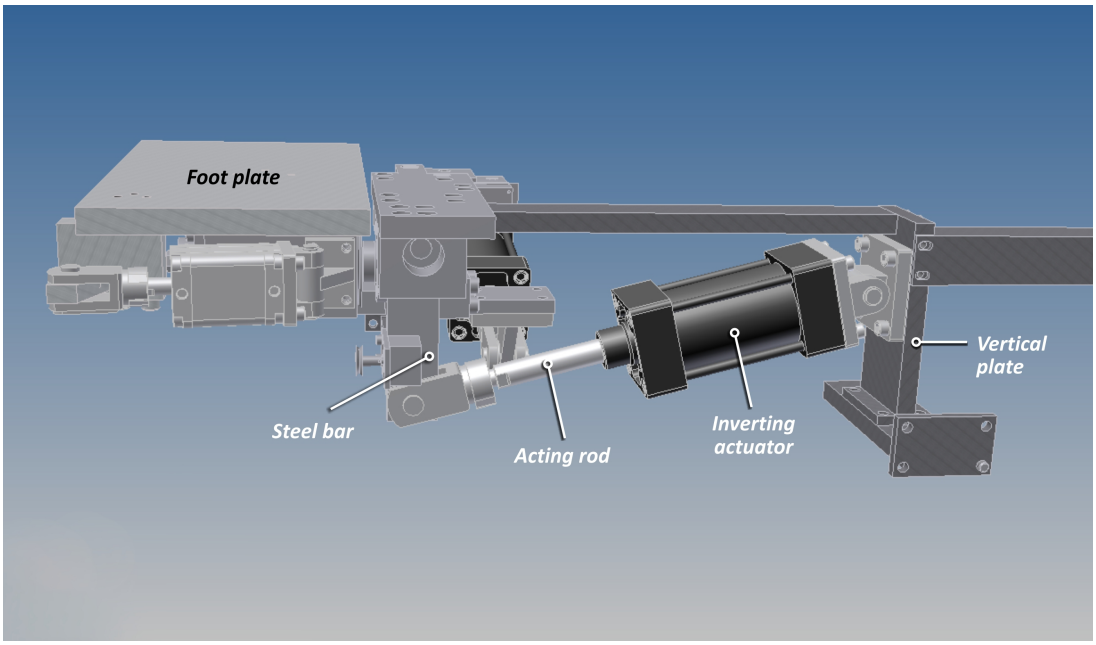

(a) Platform neutral

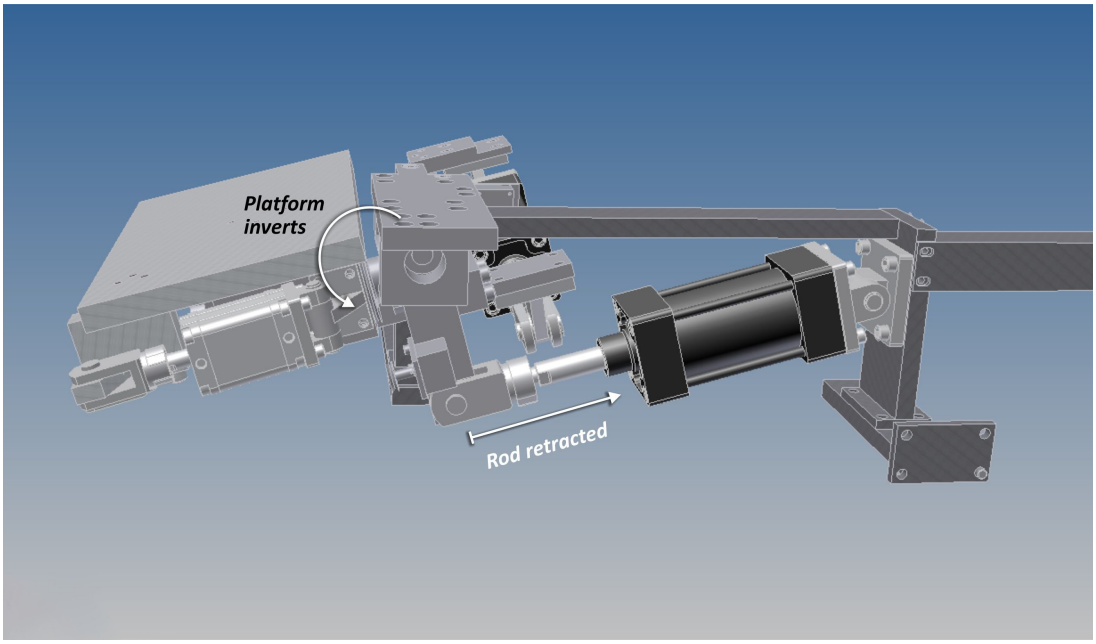

(b) Platform inverted

Figure 4.12: Inverting actuator

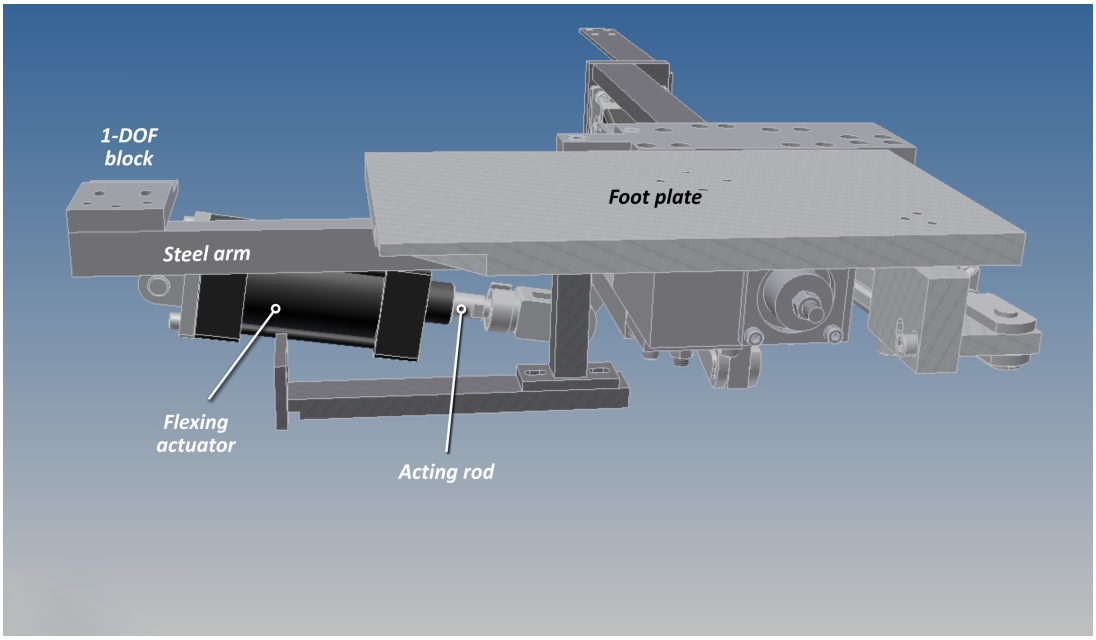

(a) Platform neutral

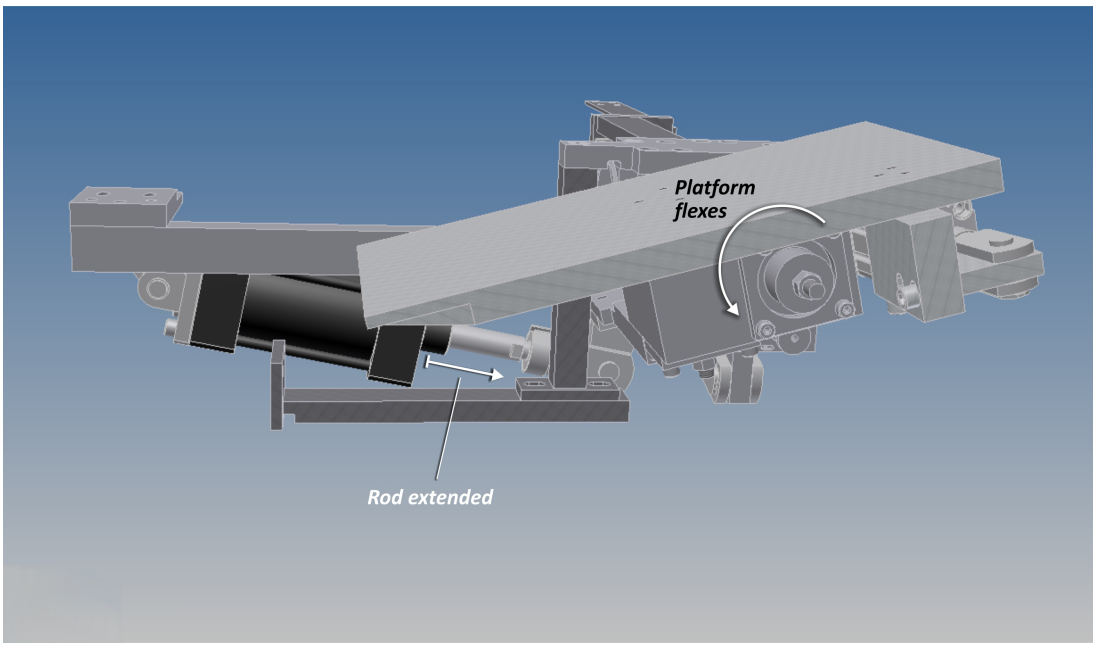

(b) Platform flexed

Figure 4.13: Flexing actuator

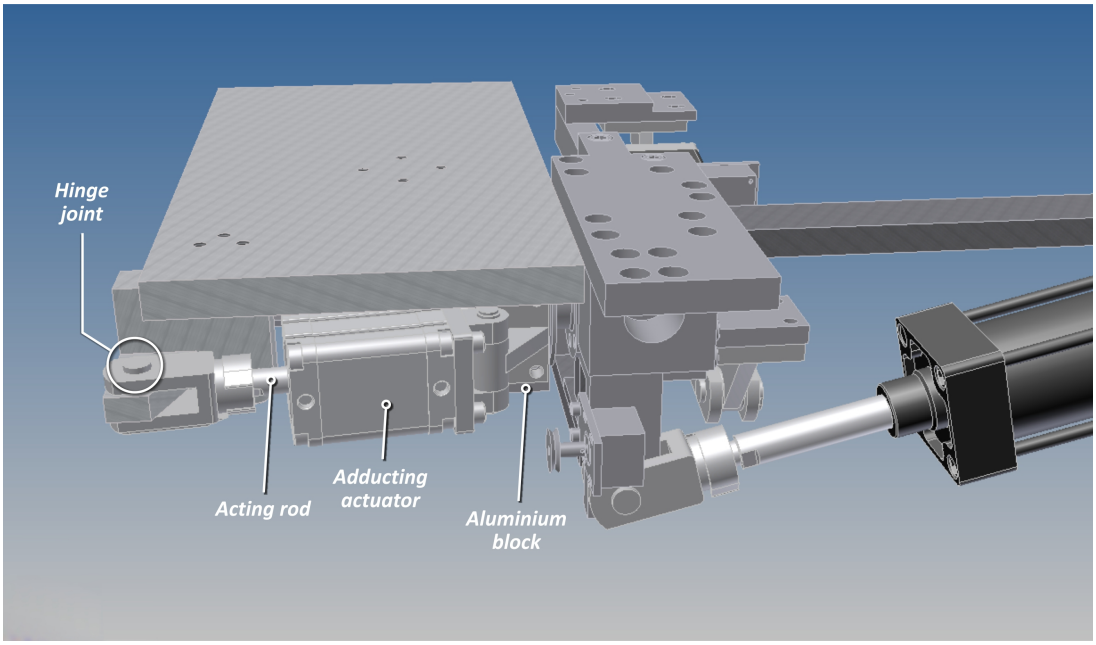

(a) Platform neutral

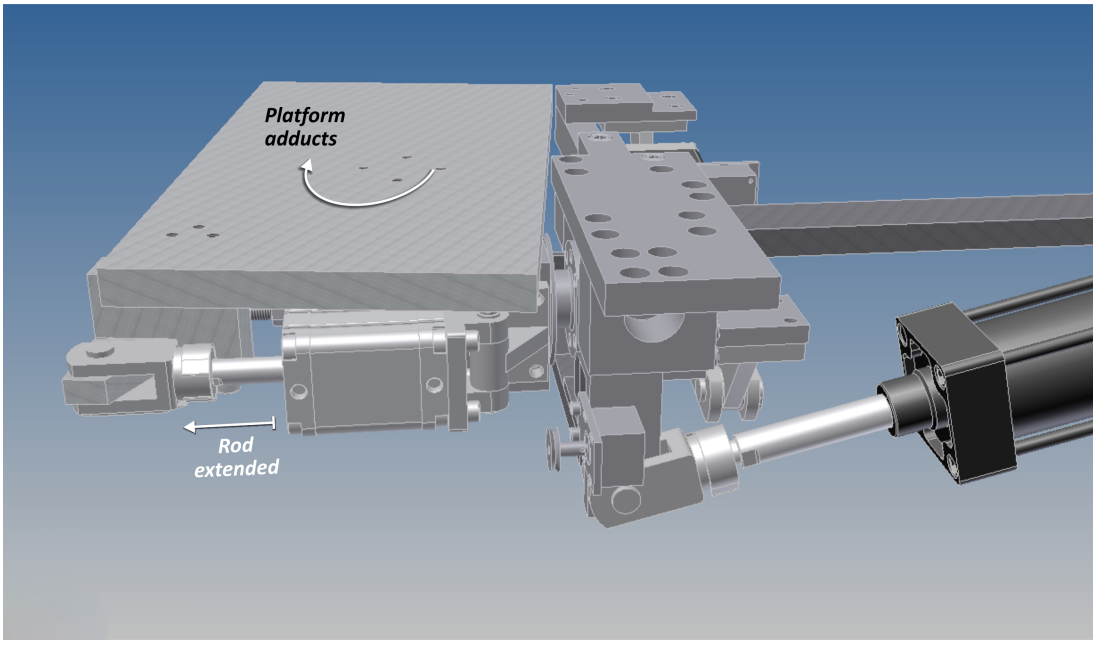

(b) Platform adducted

Figure 4.14: Adducting actuator

4.3 Pneumatic circuit

In order to power and actuate the robotic manipulator, pneumatic circuitry was designed and implemented. The main components of which are described below:

Air compressor was used to compress air up to a pressure of 10 bar.

Air storage tank was used to store the compressed air generated by the compressor. It allowed a steady and consistent supply of compressed air.

Pressure regulator was used to regulate and control the pressure from the air storage tank. This was used to reduce the pressure from 10 to 8 bar, a more suitable amount for the valves used.

Pneumatic cylinders provided the force necessary to actuate the platform. They can be divided into two types; single acting and double acting. Single acting cylinders provide actuation force in one direction only with their return stroke is achieved by means of a spring. The double acting cylinders used for this research provided actuation force in both inward and outward directions.

Directional control valves were used to control the actuation direction of the cylinders. Initially, 5/2 directional control valves were used as they contain five ports and two functional positions. They supply air to either the left or right chambers of the cylinder but cannot cut off the air supply from both at the same time. They were later substituted with 5/3 directional control valves (refer to Section 5.4.2), which have a third functional position where air supply is cut from both ports of the cylinder (Figure 4.15).

Proportional control valves or choke valves were used to control the speed of actuation of the cylinders.

Silencers were connected to the output ports of the other valves to suppress their noise.

Figure 4.15: Electropneumatic valves

All the valves used contained solenoids which allow control of their orifice openings using an electric signal. They are referred to as electropneumatic valves.

4.4 Manufacturing

After the design was finalised, the left foot platform was sent for manufacturing at the Medical Physics Department at Ninewells Hospital and Medical School. The manufacturers requested that we supply them with step files (.stp) of our design as they did not have the software necessary to open native Autodesk® inventor files. As such, files of every part and assembly of the platform were converted into this required format. Some of the design features, however, were lost during this conversion; mainly welding and thread data. To address this problem a meeting was organised with the manufacturers where we reviewed all the files together and added any missing elements. Agreement on the material to be used, mainly aluminium, stainless steel, and mild steel was also finalised.

Figure 4.16: Manufactured parts of the platform

The material was chosen based upon cost and to satisfy the required mechanical properties. The meeting also provided an opportunity for the manufacturers to give their feedback on the design and advise on some minor changes that would reduce the cost of manufacturing. Manufacturing of the platform was then completed after four months (Figure 4.16).

The right-foot platform was manufactured at Diemax Engineering, Dundee. The main reason being lower production cost. The same steps were taken, where we had a meeting with Diemax Engineering and supplied them with .stp files of our design. A few minor adjustments of the design were made to further facilitate the assembly process (refer to Section 4.2.1).

It is worth noting that the right-foot platform was sent for manufacturing after testing of the left-foot platform ensuring that it was working as intended. This platform took around two years to complete and as such was not available for the experiments. It will however be used for future studies to provide more comprehensive information. The right-foot platform will therefore be excluded from any discussion throughout the remainder of this thesis.

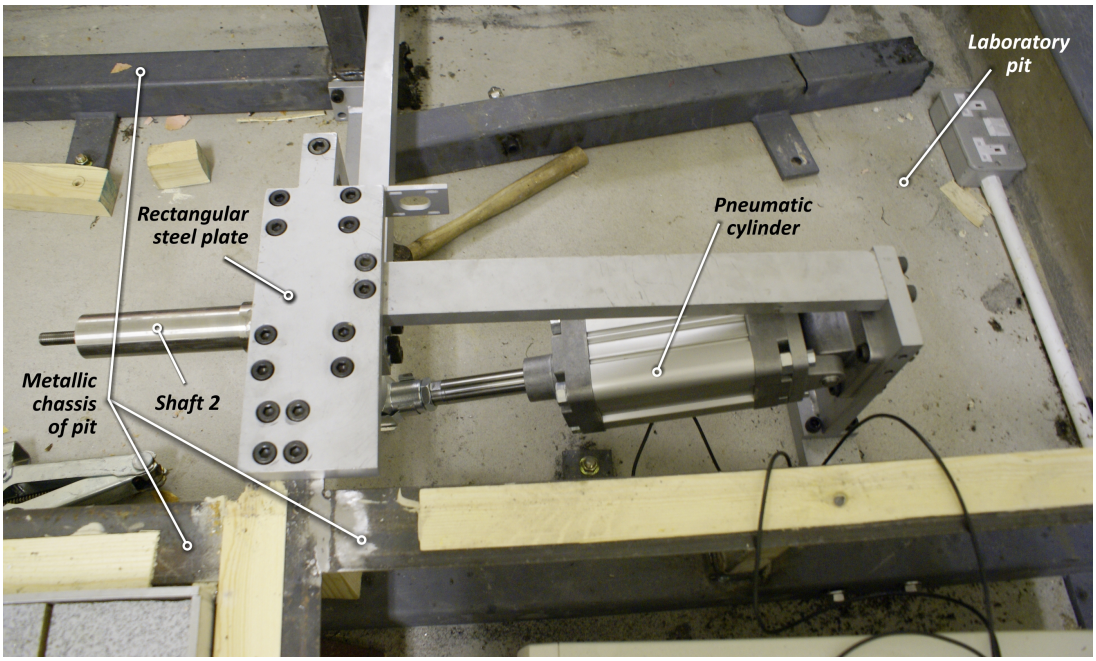

Figure 4.17: Platform being assembled in the pit

4.5 Assembly and Fitting

The manufactured platform was now ready to be assembled and incorporated into the Sport Laboratory. As the pit was not originally designed to host a rotating platform few adjustments had to be made, which included some cutting and drilling of the metallic chassis. The assembly process went relatively smoothly, with only few minor issues caused by some unevenness in the pit floor that was unaccounted for.

The base structure and 1-DOF block assemblies were bolted to the pit chassis (Figure 4.17). The strain gauge was then attached to shaft 2 and the optical encoders were bolted in place (Figure 4.18). The 2-DOF block assembly was then assembled and the foot-plate connected (Figure 4.19). Finally, the remaining cylinders were bolted in place and the 2-DOF assembly was joined with the 1-DOF block assembly (Figures 4.20 and 4.21).

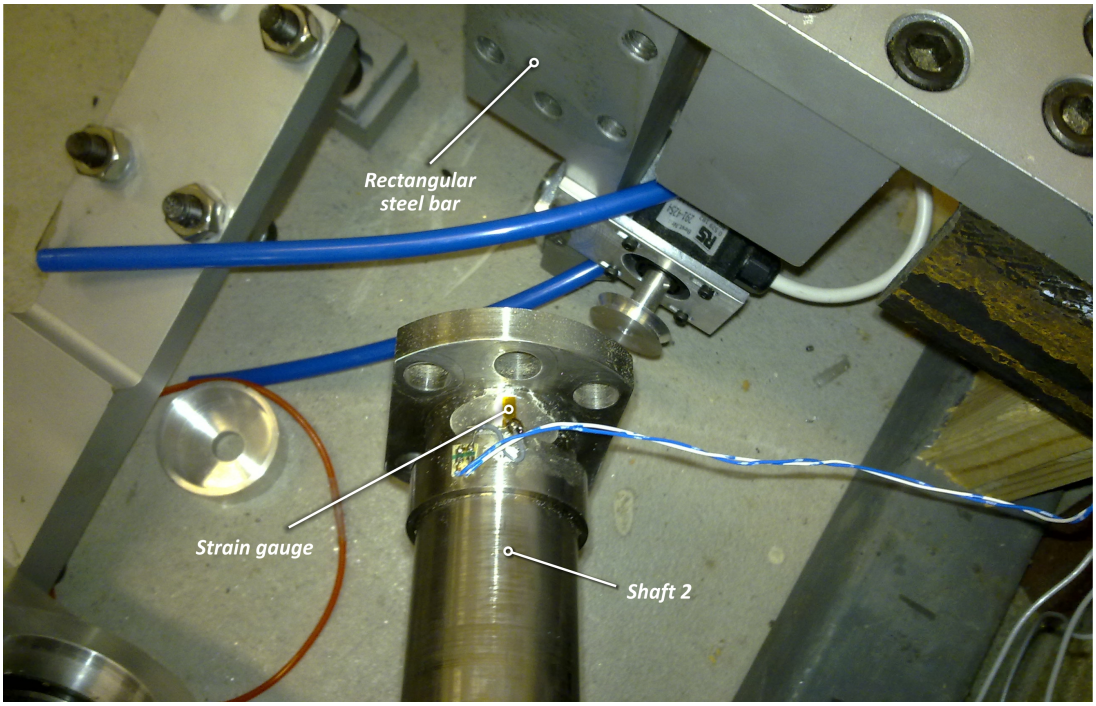

Figure 4.18: Strain gauge and optical encoders fixed in place

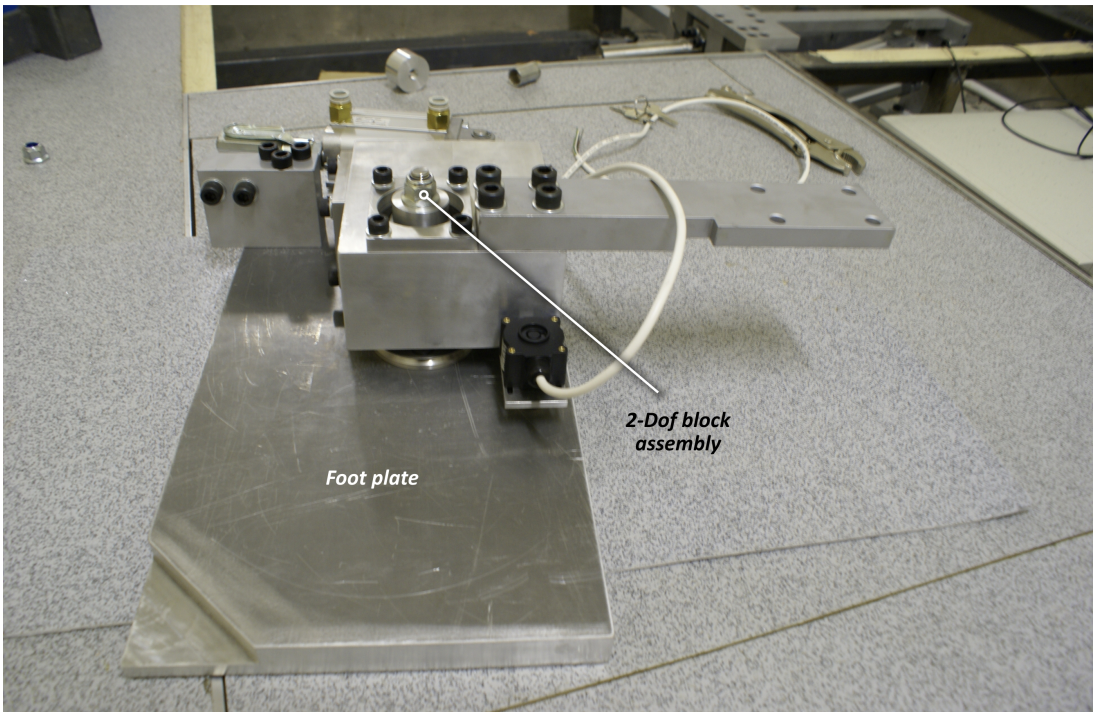

Figure 4.19: 2-DOF block being assembled

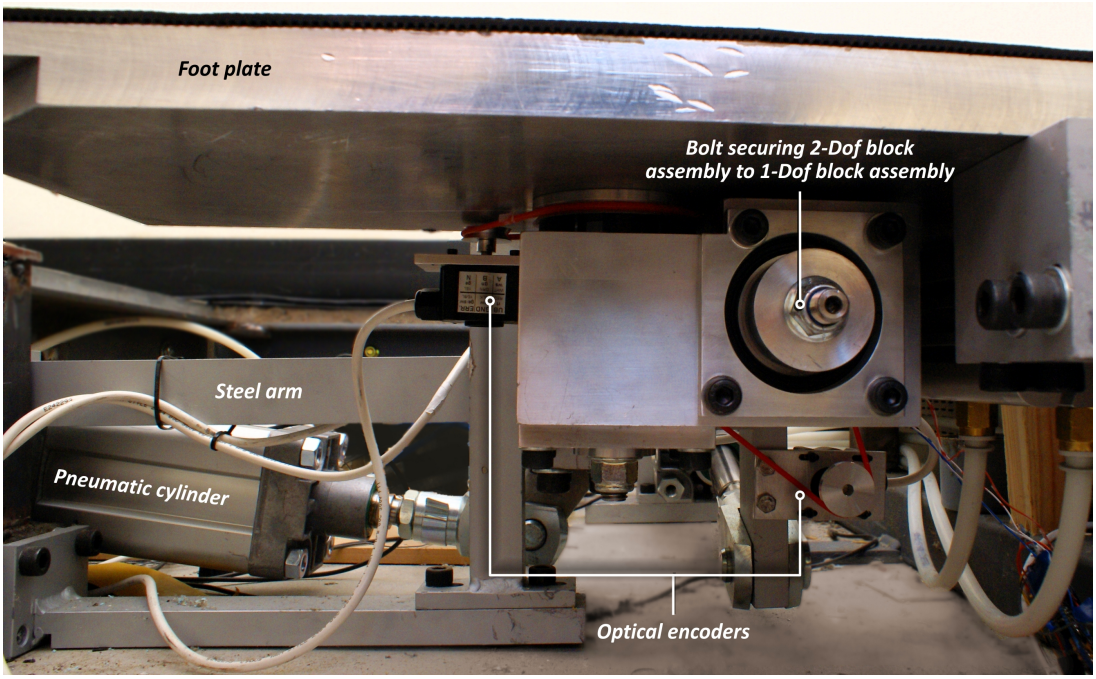

Figure 4.20: 2-DOF block joined with the 1-DOF assembly

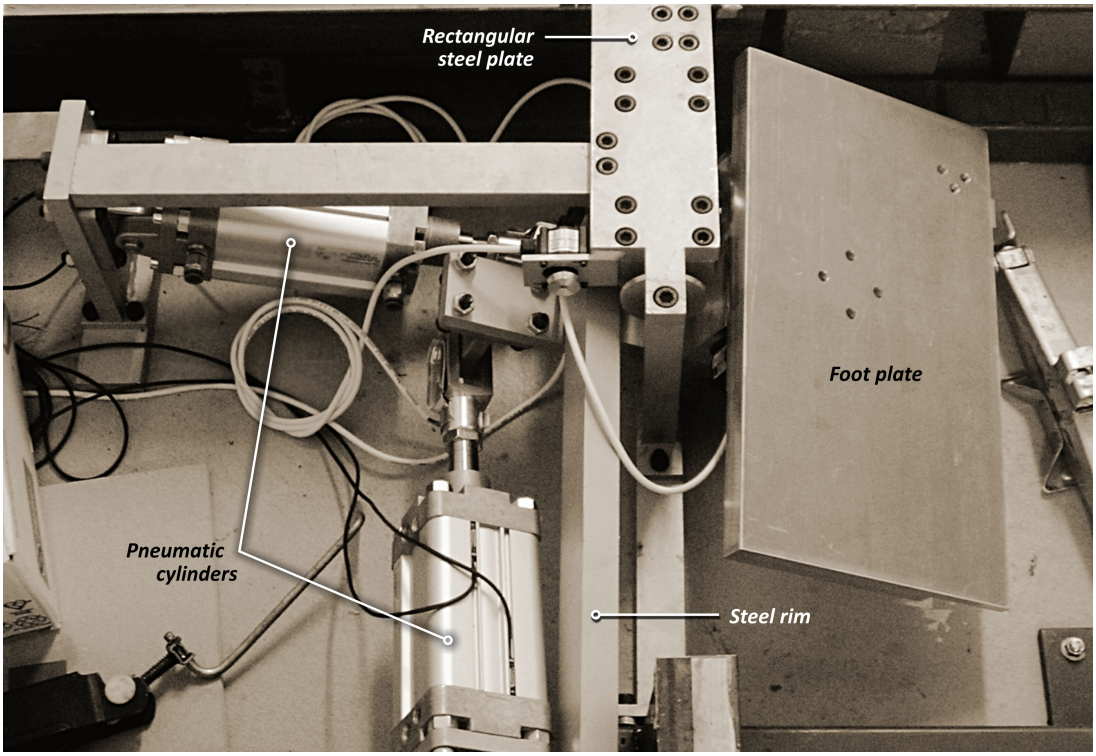

Figure 4.21: Assembled platform

5 Electronics, control and user interface

5.1 Electronics

In order to precisely control the platform and be able to monitor its functions, an electronic circuit was designed (Appendix B) and a prototype was assembled (Figure 5.1). Using electronics to control the robotic manipulator gave greater flexibility and functionality as opposed to relying on a totally pneumatic control circuit. The major components of the electronic circuit were:

- PIC® micro-controller
- Strain gauges
- Optical laser detectors
- Optical encoders
- Reed switches
- Electropneumatic valves (refer to Section 4.3)

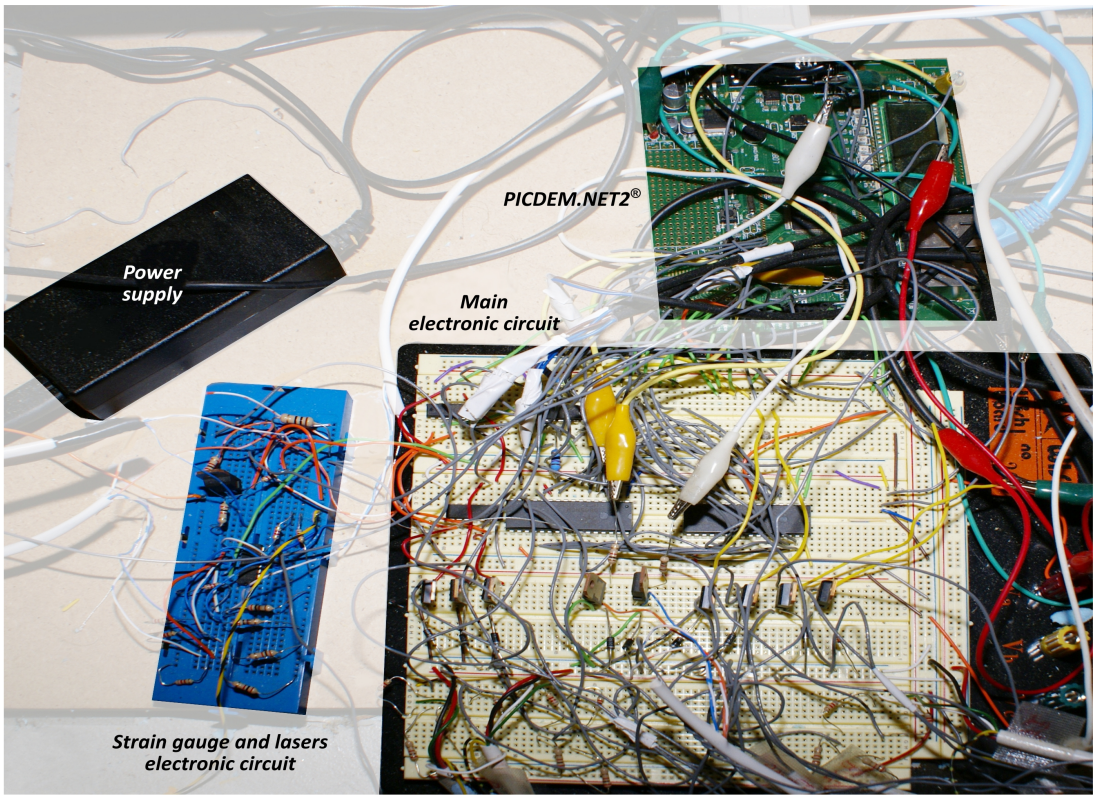

Figure 5.1: Built electronic circuit prototype

5.1.1 The processing unit

The PIC® is the processing unit and main component of the electronic circuit-the brain of the system so to speak. It takes orders from the researcher and interacts with all the electronics and electropneumatic valves of the platform. The PIC® reads the output from all the different sensors, processes that data and then issues orders to the electropneumatic valves, thus controlling the rotation of the platform based upon researcher instructions.

For the PIC® to function properly it must be placed in the pit near the platform making it difficult for researcher interaction. After some investigations, it was decided to use the PIC18F97J60 PIC® model since it had a built-in Ethernet module, which allows a researcher to interact with the PIC® through any computer via the network. The chosen chip had 128 Kb of built-in memory and a CPU that ran at a clock speed of 41.667 MHz, enough to provide smooth operation

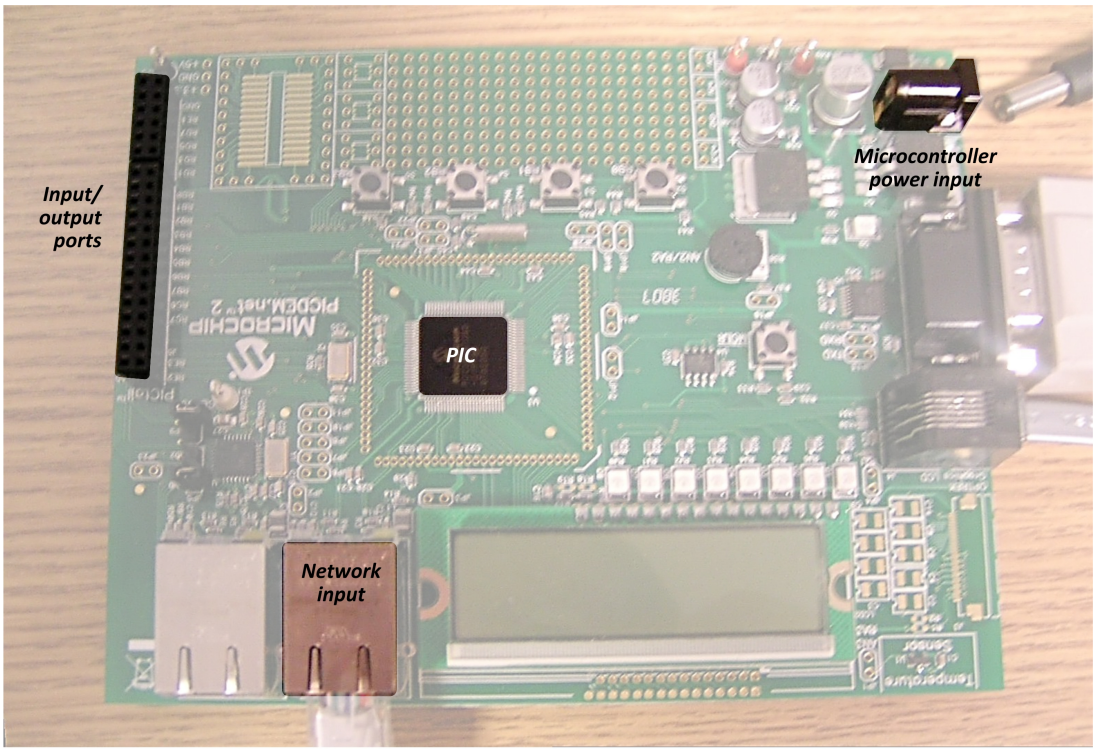

Figure 5.2: PICDEM.NET® 2 development board

of the robotic platform. This PIC® also features 100 pins used to connect to the electronic components. This number of pins was sufficient for the current design and also allows room for future expandability with minimal cost and effort.

The PIC18F97J60 contained all the features necessary to run the platform, however, by itself it was not the most efficient for development purposes. The PICDEM.NET® 2 (Figure 5.2) is a development board with a PIC18F97J60 chip and contained a pre-built electronic circuit and functionality that allows faster and easier development. It was, as such, chosen for the current project.

5.1.2 Strain gauges

The platform was to be used to induce foot rotation of moving subjects. It must be able to accurately detect the exact moment a subject steps on it. To achieve this, a strain gauge (SG) was attached to shaft 2 of the platform (Figure 5.3).

This sensor measures strain, i.e. changes in length of the shaft caused by the weight of subjects. As the main purpose of the SG was to detect the foot strike the output of the SG was not calibrated to allow exact measurement of forces on the foot-plate. In order to be able to accurately measure the forces on the foot-plate more SGs would need to be added. The output from the SG, nonetheless, still offers an indication of the normal force acting on the foot-plate, the higher the output value the higher the normal force on the foot-plate.

Upon testing, the output of the strain gauge was found to drift considerably over time, decreasing its reliability in detecting foot strikes. The reason for those deviations was heat generated by the electric current passing through the sensor, where the output of a strain gauge increases with increasing temperature. To address this problem another strain gauge was attached to the shaft and connected to the first one in a bridge circuit. Such a circuit allowed the output of one sensor to be subtracted from the other. This method works since the same current passes through both gauges, and as such, their temperature increases by the same amount and the resultant increase in the strain gauges' outputs gets cancelled out. To avoid the useful output of the sensors being cancelled out the new sensor was placed on shaft 2 opposite to the first sensor. This means that at foot strike, the output of the first will increase while that of the second will decrease by the same amount, and the resulting output from the bridge circuit will be twice the amount of each sensor.

5.1.3 Optical lasers

One of the main advantages of this new system was that it allowed induced supination of the foot during walking or running. This, however, also raised a safety issue in case the subject stepped partially on the foot-plate where any rotation of the platform may cause injury. To overcome this safety issue, it was

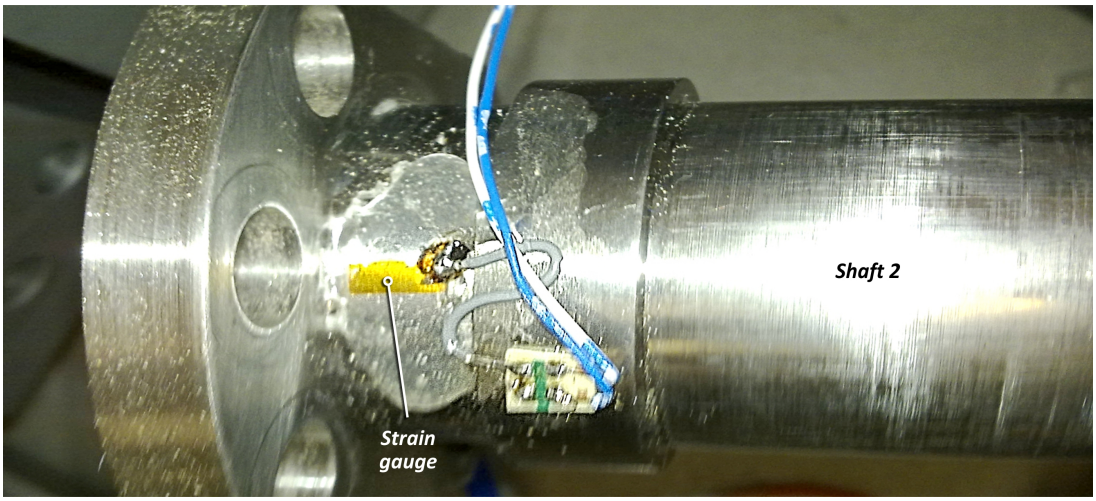

Figure 5.3: Strain gauge

essential to devise a method to prevent the platform from rotating when the subject's foot was not completely on the foot-plate.

Several possible solutions were considered. The first attempt at solving the aforementioned problem was to utilise the Vicon® motion capture system. The idea was that markers could be put on the edges of the subjects' feet, while at the same time, the size and position coordinates of the foot-plate in the laboratory would be fed into Vicon®. Vicon® could then detect if the markers fell outside the area of the foot-plate indicating an improper landing and signalling a command to the PIC® to prevent the platform from rotating. This method, however, could not work as there was no way to acquire the required data from Vicon® in real time; trials needed to be processed first thus making this possible idea unrealistic.

Another method was to employ the FASTRAK® system, which is an electromagnetic motion tracking system already used at IMAR. This solution also failed due to the metallic nature of the platform which interfered with the readings from the FASTRAK® (it utilises electromagnetic field and is susceptible to metal objects).

Finally, a suitable method was found which employed four optical emitter/recei-

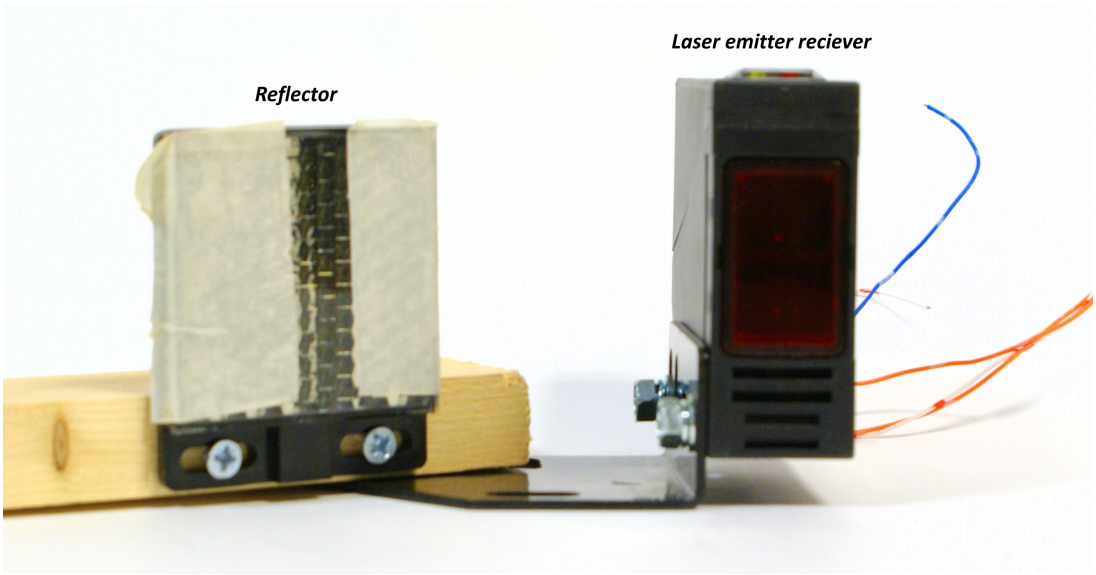

Figure 5.4: Laser emitter/receiver

vers to check the validity of the foot strike. The optical emitter/receiver consisted of a laser emitter and receiver built into a combined unit (Figure 5.4). Those were placed on the sides of the walkway such that their beams passed over the four edges of the foot-plate. On the opposite side of each laser was a reflector that reflected the light back, where it's picked up by the built-in receiver (Figure 5.5). A subject's foot that lay partially on the foot-plate cut the laser beam preventing it from reaching the receiver. This caused the laser device to emit a signal to the PIC® informing it of an invalid foot strike. The PIC® responded and informed the system of this condition keeping the platform stationary.

5.1.4 Optical Encoders

Three identical optical encoders were used to monitor the rotation of the foot-plate around all three axes of the platform. They are rotated by the pulleys attached to the three shafts of the platform (refer to Section 4.2) via elastic belts (Figure 5.6). The sensors used emit 1000 pulses every 360° of rotation which corresponds to a resolution of 2.78 pulses/deg. The pulleys attached to the platform

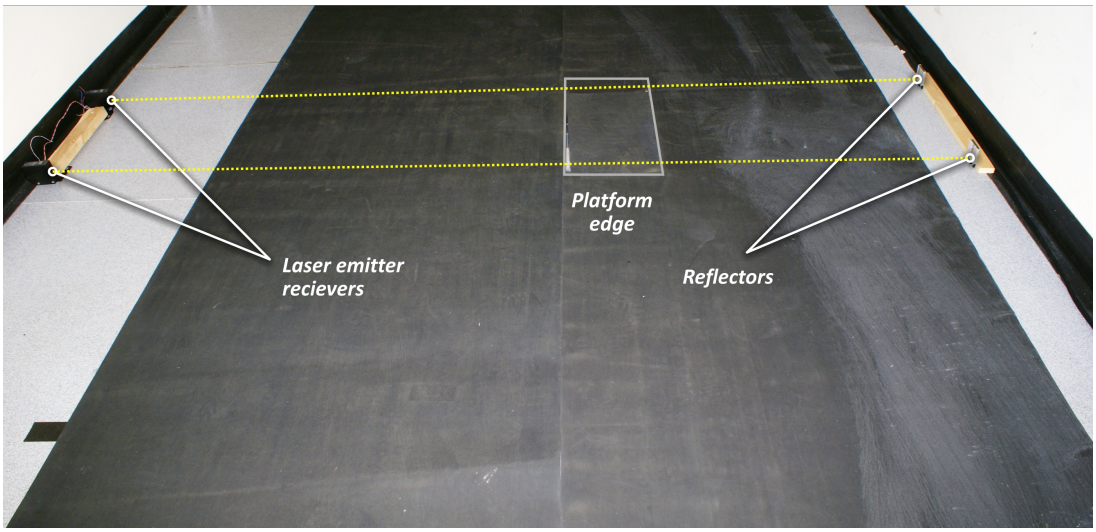

Figure 5.5: Laser emitters/receivers covering the horizontal edges of the foot-plate

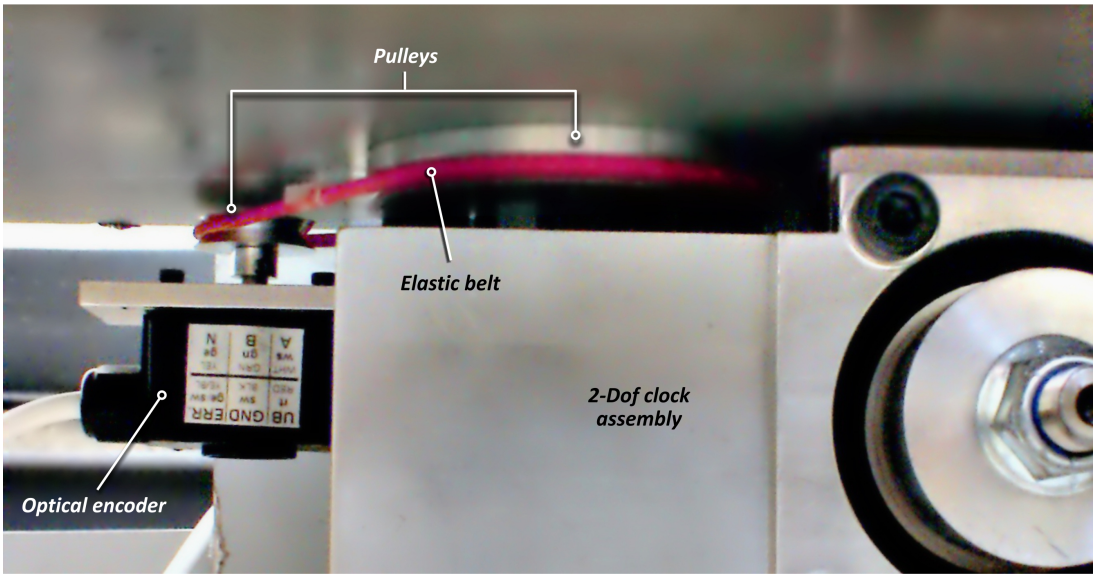

Figure 5.6: Optical encoder

shafts were larger than those attached to the encoder shafts which meant that the sensor shaft will turn several times for each turn of the corresponding platform shaft. This increased the resolution of the sensors to 8.00 pulses/deg, 9.75 pulses/deg, and 8.25 pulses/deg in inversion, flexion, and adduction respectively.

The nature of the output from the encoders, however, required additional coding to reliably read the corresponding angle and reduced the performance of the

Table 5.1: Optical encoder validation results

	Optical encoder (deg)	AAF (deg)	DAF (deg)	Tractograph (deg)
Inversion	14.8	15	15	NA
	21.4	21.5	21	NA
	24.9	25	25	NA
Flexion	10.1	10	10	NA
	13.3	13	13	NA
	15.7	16	16	NA
Adduction	8.1	NA	NA	8
	8.4	NA	NA	8
	8.8	NA	NA	9

PIC®. For this reason off-the-shelf counters designed to take the load off the PIC® were employed. These also had the benefit of electronically increasing the sensitivity of the encoders by a factor of four. The final resolutions of the encoders were 32, 39, and 33 pulses/deg in inversion, flexion, and adduction respectively. To confirm that these calculated resolutions resulted in correct measurements the output of the optical encoders was validated using analogue and a digital angle finders and a tractograph. Rotation around each axis was measured independently where the platform rotated around that axis only. The analogue and digital angle finders (AAF and DAF) with an accuracy of 0.5° and 1° were used to validate inversion and flexion rotations while the tractograph was used to validate adduction rotation. Measurements were conducted once the platform stopped rotating and readings from the external measures and those from the optical encoders were compared. Three measurements were taken for each axis of rotation and the obtained results presented in Table 5.1 demonstrate the validity of the optical encoders.

The optical encoders allowed the researcher to check the performance of the platform. They also provided feedback to the control algorithm (refer to Section

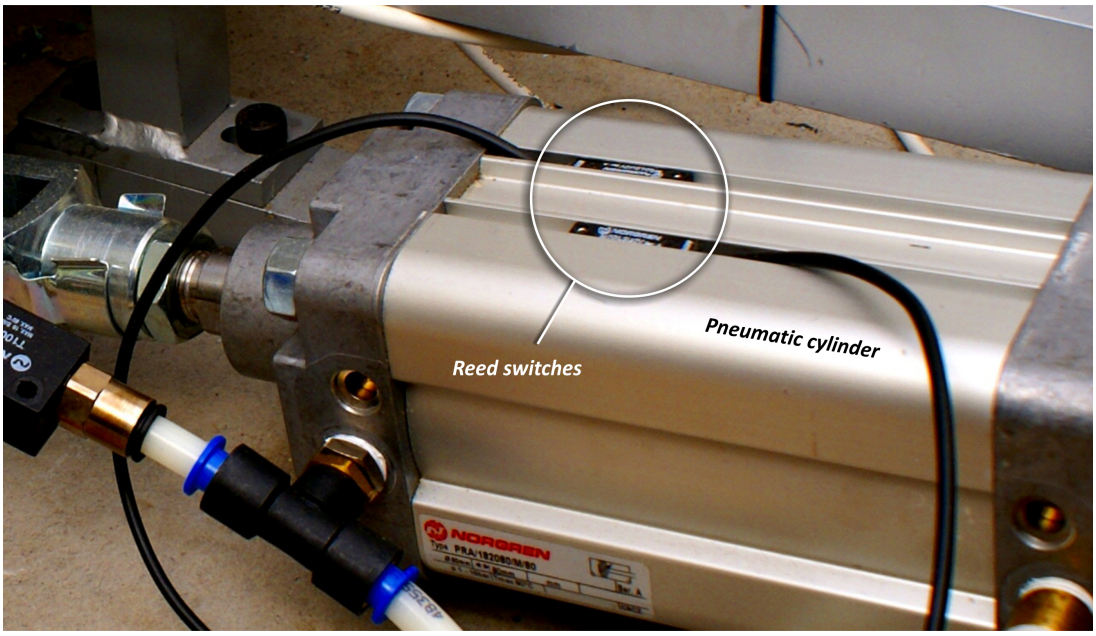

Figure 5.7: Reed Switches

5.3.1) increasing its accuracy and performance.

5.1.5 Reed switches

The PIC® relies on the optical encoders to control the rotation of the platform and prevent excessive rotations. Reed switches were employed as a safety backup measure in case of a failure in the PIC® or control algorithm. Reed switches were attached directly to the body of the pneumatic cylinders (Figure 5.7), and connected directly to the power source of the electropneumatic valves. The pneumatic cylinders used contained a magnetised piston which activated the reed switches when it passed by it. This caused the switches to cut the power from the valves, closing them and preventing the platform from further rotation.

5.2 Controlling the proportional valves

The proportional valves used were designed to be controlled by a pulse-width modulation (PWM) signal. The operating manual however, did not supply any information regarding the properties of the signal, but rather recommended the use of a separate controller offered by that same company. This controller allows control of the valve opening, however, it requires an analogue input rather then a PWM signal. This was problematic since the PIC® does not have an analogue output, and thus, cannot interact directly with the controller. Another issue was the cost of the controller which raised the total cost of the system by £600 due to the fact that six would be required. For this reason it was decided to purchase one controller and reverse engineer its output signal. This was achieved using a data acquisition card (DAQ) and Labview® software. The frequency of the required PWM signal was found to be $170\,Hz$.

5.3 The PIC® control software

The PIC® itself, has the processing power necessary to control the platform, however, it can only do so with the proper software installed on it. Such code was to be written in C18 programming language, a PIC® specific version of the C language. The purpose of the software was to instruct the PIC® on how to control the platform. This code was written in-house specifically for the control of the robotic manipulator and builds on the PIC® pre-installed software and libraries. What follows is a description of the function of the software.

The code is divided into different modules and sections, each with a specific function. This allows faster development, easier debugging as well as making the code more understandable by others who may wish to expand the platform's

functionality. The software also contains comments[1] that explain vague parts of the code. The different sections of the code are described below:

Variables section contains a list of all the variables used by the software. Variables are defined and set in this section.

PIC initialization section is where the PIC® hardware and functions are set and initialised (Algorithm 5.1).

Interrupt section is where the PIC® waits for foot strike. If detected, the PIC® then checks the validity of the landing. If no part of the foot was outside the foot-plate, the CONTROL module is called, the synchronisation signal is sent, and the platform rotation is recorded at an $11.8\,ms$ interval (Algorithm 5.2 and Figure 5.8).

Pulse width modulation is the method used to control the orifice opening of the proportional valves. The frequency input of those valves was found to be $170\,Hz$ (refer to Section 5.2), which is lower then the smallest PWM frequency the PIC® can output based on its internal dedicated timer. For this reason a software PWM generator with the required frequency was written and incorporated into the code; it is a subsection of the Interrupt section.

Read angle module reads the angle of the platform around a specified axis from the counters (refer to Section 5.1.4).

Zero plate module (Figure 5.9) rotates the platform and levels it back with the laboratory floor. It then resets the counter angles back to zero.

Valve control section contains several modules that operate on the directional control valves so as to control the direction of rotation of the platform (Algorithm 5.3).

[1]Comments are stated after the double back slash characters (//)

Algorithm 5.1 Extract from the PIC® initialization section

```
// setting PWM software method
// conf timer 3 for operation with compare mode and 16bit
// read-write
T3CON = 0b01100001;
// disable timer over flow interrupt flag
PIE2bits.TMR3IE = 0;
// set ccp4 to compare mode in software interrupt mode
CCP4CON = 0b00001010;
// enable comparator interrupt
PIE3bits.CCP4IE = 1;
```

Fuzzy logic control module is an algorithm that was specially written to control the rotation of the platform. The valves, however, have a slow response time of $50\,ms$, which would necessitate a lot of optimisation to the algorithm to allow the desired operation. This approach was discarded in favour of a more straight forward and less complicated method.

Control module was used to reliably and accurately rotate the platform to the specific target angles.

Interface section contained the necessary code that allowed the PIC® to communicate and understand the graphical user interface, which was run on the researchers networked computer (refer to Section 5.5).

For a more technical description of the program and for the code itself please refer to Appendix C.

5.3.1 The Control module

The CONTROL module (Algorithm 5.4 and Figure 5.10) was used to reliably and accurately rotate the platform to the target angles. It is called in the INTERRUPT section after a successful foot strike. It utilises the PWM, READ ANGLE, and VALVE CONTROL modules to achieve its purpose. For the current research this module can be divided into two parts: start and stop.

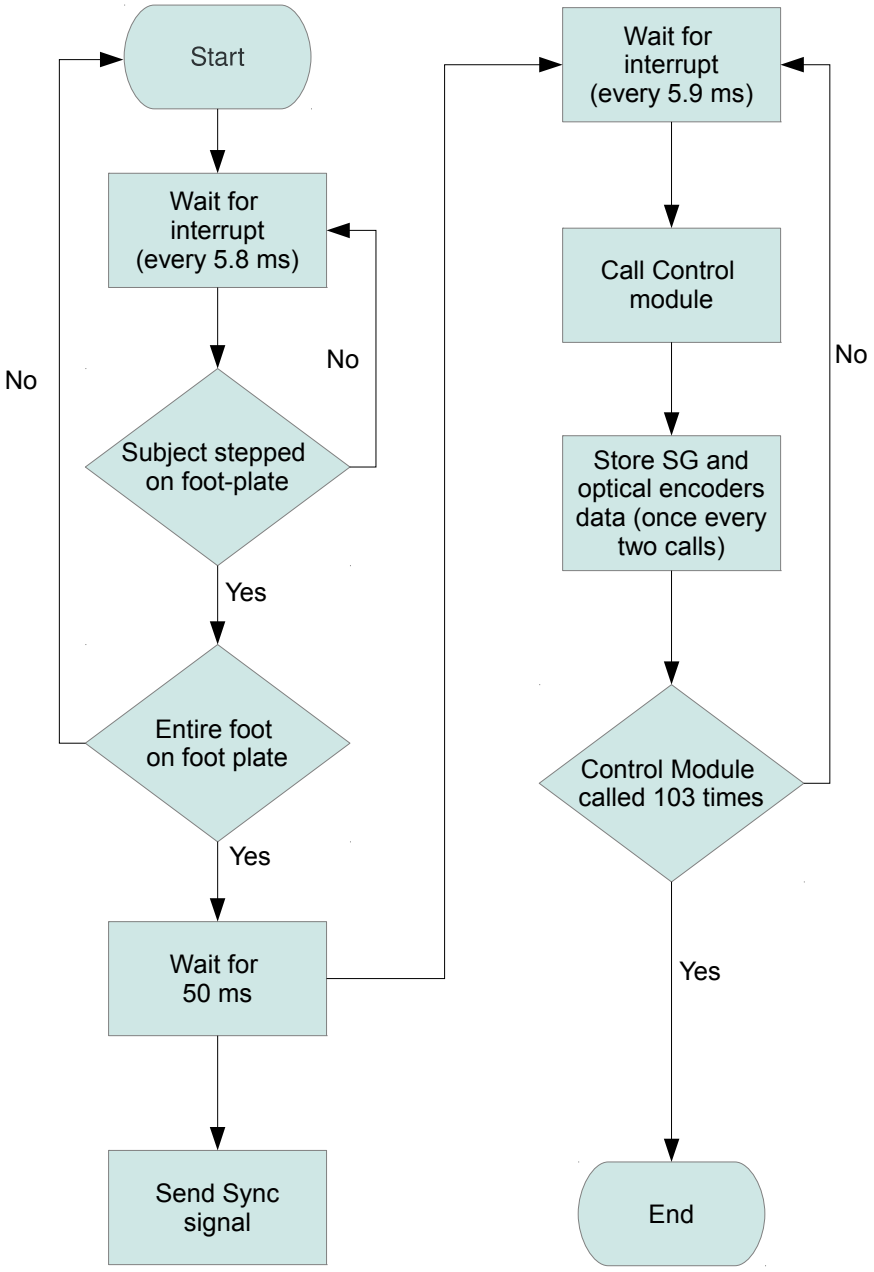

Figure 5.8: Flow chart for part of the Interrupt module

Algorithm 5.2 Extract from the Interrupt section

```
// read strain gauge value
ProcessIO();
// check that the user has issued the start command and that a
// subject has stepped on the footplate.
if (start && (on_off==0) && check_foot){
strain[0]=ADRES/31 - strain[1];
if (strain[0] > 4)
check_step = 1;

// check that all foot is on the foot-plate
if (check_foot==0)
// call control module
{ control(tangle_inv,tangle_flex,tangle_rot);
// send synchronisation signal
VSYNC = 0;
// record rotation data
position_inv[n/2] = read_angle(1);
position_flex[n/2] = read_angle(2);
position_rot[n/2] = read_angle(3);
```

Algorithm 5.3 Extract from the Valve control section.

```
// set inversion directional control valve to rotate the platform
// upwards
void inv_up (void){
LATEbits.LATE4 = 0;
LATEbits.LATE7 = 1;
}
// set inversion directional control valve to rotate the platform
// downwards
void inv_down (void){
LATEbits.LATE7 = 0;
LATEbits.LATE4 = 1;
}
// set inversion directional control valve to stop rotation the
// platform
void inv_stop (void){
LATEbits.LATE4 = 0;
LATEbits.LATE7 = 0;
}
```

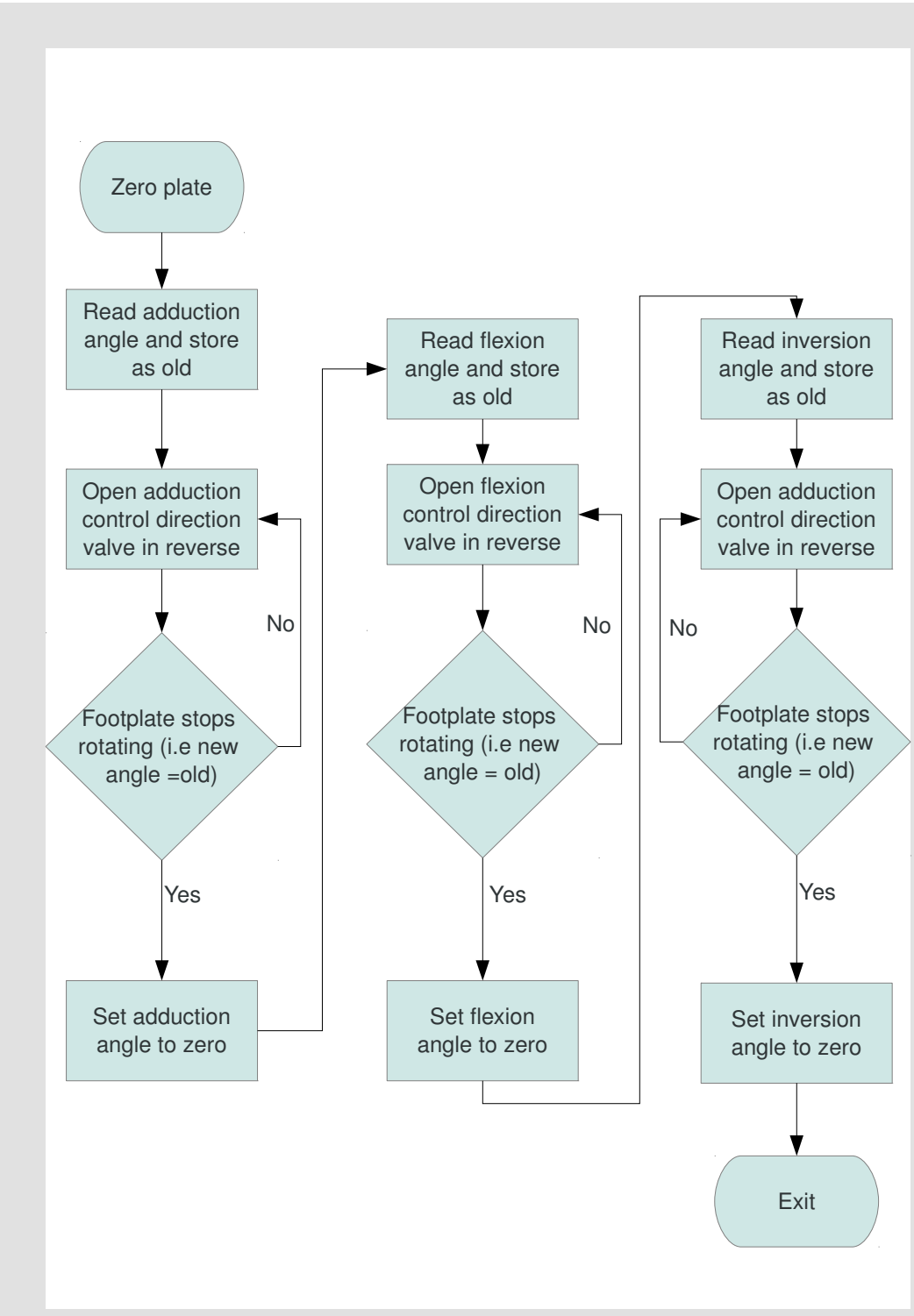

Figure 5.9: Flow chart of the Zero plate module

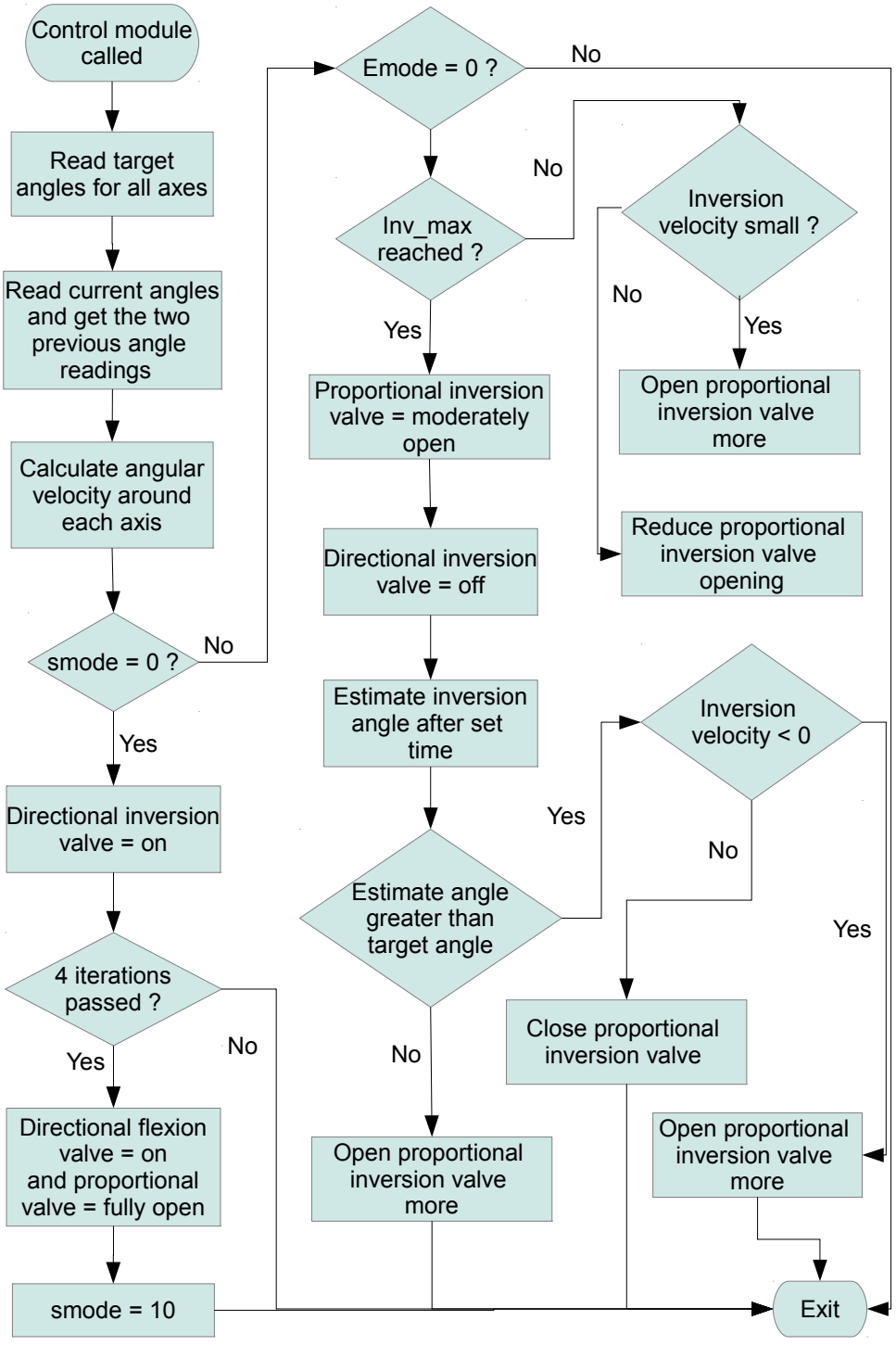

Figure 5.10: Flow chart for the control of inversion rotation in the Control module

Algorithm 5.4 Extract from the control algorithm for inversion

```
// limit the rotational velocity of the platform
// 30 corresponds to 150 degrees/second
if(velo_inv<30)
dcycle_inv=85;
else dcycle_inv=85 - (velo_inv-30)*8;

// testcontrol[0] is the inversion flag to identify the current
// stage of the control procedure
// if *_max is reached and testcontrol[0] is set to 0
if ((n==inv_max)&&(testcontrol[0]==0)){
// keep proportional valve open
dcycle_inv = 75;
// close inversion valves
inv_stop();
// set inversion testcontrol flag to 1
testcontrol[0]=1;
}
// estimate position of platform after inv_time amount of time,
// in relation to the target angle
//notice that testcontrol[0] is set to two once flex_max is reached
if (testcontrol[0]>1)
calc_angle_inv = (velo_inv*inv_time + new_angle_inv)-Tangle_inv;

// if inversion flag is set and platform will exceed its
// target angle
if(testcontrol[0]>1 && calc_angle_inv>0){
// if platform is rebounding
if(velo_inv<0)
// open valve to counteract rebounding
dcycle_inv= 40 - velo_inv*10;
else dcycle_inv=0 ;
}
// if inversion flag is set and platform will not reach its
// target angle
if(calc_angle_inv<0 && testcontrol[0]>1 )
// open valve more based on estimate
dcycle_inv= 50 - calc_angle_inv/2;
```

The start section was applied first and it opened the inversion and flexion valves to their full capacity, so as to achieve maximum rotation speed.

In the stop section, the CONTROL module waited a pre-specified amount of time (*_max) before closing the inversion and flexion valves, except for the proportional valves. The wait time was determined during testing and optimisation of the control algorithm (refer to Section 5.4.2); it allows the platform to rotate close to a value that is slightly less than the target angle. Final position fine tuning was then achieved using the proportional control valves which were kept open. Based on the velocity and position of the platform, the CONTROL module determined an estimated position of the platform after a given amount of time, also derived from optimisation and its relation to the target angle. The proportional valve opening was then closed by an amount based upon that estimation.

The CONTROL module also tries to control and restrict the rotational velocity range of the platform. In inversion, for example, if the rotational velocity was below $150^{\circ}/s$ the proportional valve was kept fully open. Once the velocity exceeded that value, however, that valve will be partially closed; the higher the velocity the more it closes.

Air, the power source for the actuators, is a compressible fluid; its volume can decrease as it is pressurised. This occurs when the valves controlling the loaded rotating platform are suddenly closed. Part of the kinetic energy of the loaded platform will be stored as potential energy by the air in the actuators. This air becomes like a spring that will push back against the platform causing it to rebound. While this may be desired in some experiments it was required to be negated for the present study. To achieve this, the control algorithm used the proportional valve as a relief valve, opening it when it sensed any rebound from the foot-plate.

The platform was not to commence adduction while it was still inverting or

flexing, as this would cause the foot-plate to slip underneath the foot without adducting the foot. To avoid this, the platform initiated adduction once the foot-plate stopped inverting and flexing; this assured there was enough friction between the foot and the foot-plate.

5.4 Testing and optimisation

The pneumatic cylinders actuate the foot-plate rotating it to a preset position. The cylinders are powered by compressed air and controlled by electropneumatic valves. The valves are controlled by the control algorithm via the PIC® micro-controller, which sends control signals to the valves. For the whole system to function properly and reliably, the behaviour and reaction of the valves, cylinders and the foot-plate to such a signal must first be examined and understood.

5.4.1 Pneumatic valves function

Three different types of valves were used: directional, proportional, and on/off valves (refer to Section 4.3). Several tests were conducted to understand how these valves integrated and interacted with the system. Trying to find ways to increase the rotational velocity of the platform, for example, we compared the performance of the proportional valve to that of the on/off valve. Such a test revealed that the proportional valve allows for increased rotational speeds (Figure 5.11a and 5.11b).

To try and understand the combined response of all the valves when working in unison, the PIC® was set to send a signal to all valves turning them fully open, for a fixed specified duration of time when a subject stepped onto the foot-plate. The time it took the platform to start rotating, the rotation speed, and how many degrees it rotated for were all recorded. These tests revealed a delay of

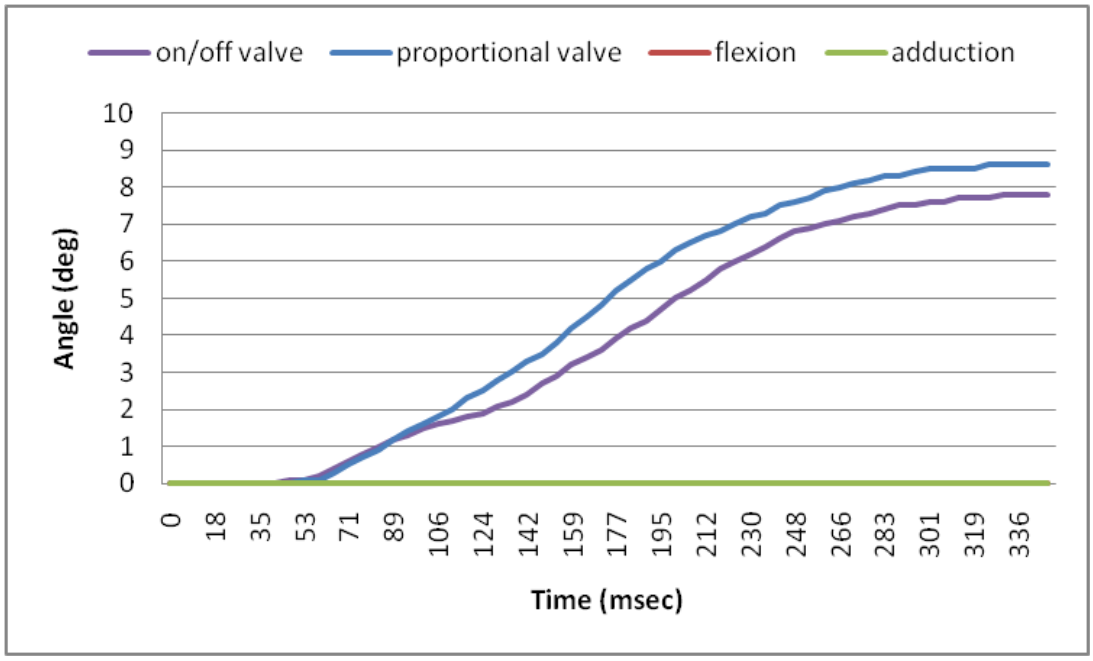

(a) Platform degree of rotation in inversion

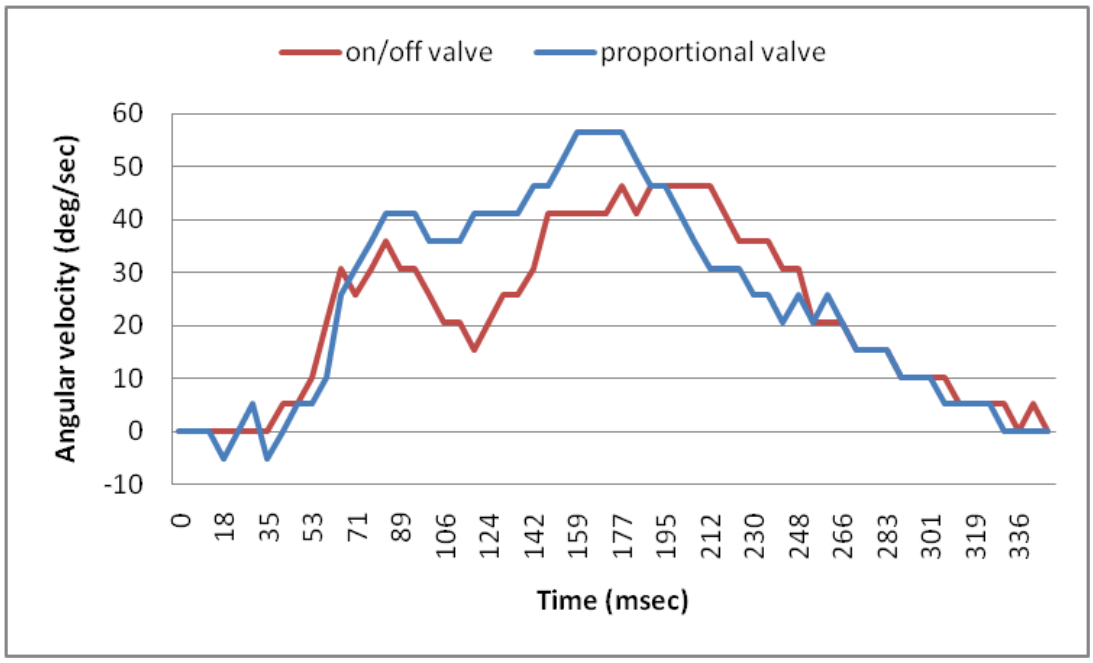

(b) Platform rotational velocity in inversion

Figure 5.11: The effect of using the proportional valves on platform performance as compared to using the on/off valves

approximately 60 ms between the instant the signal was sent to the valves and the time the platform started moving (Figure 5.12a). Further testing of each valve separately revealed that they all had similar such delay. This delay had a negative effect on the responsiveness of the platform and provided a challenge for the control algorithm (refer to Section 5.3.1). It was also observed that the platform kept rotating after the flow valves were closed (Figure 5.12a and 5.12b). While it was expected that the platform would not stop instantly after the closure of the valves, due to the compressible nature of the powering fluid, the observed delay in stopping was greater than anticipated.

The conducted tests also demonstrated the ability of the platform to rotate further and faster in flexion than in inversion (Figure 5.12a and 5.12b). This was due to the fact that the flexing cylinder actuated the foot-plate by extending its rod while that of inversion acts by retracting its rod(refer to Section 4.2.5); double acting pneumatic cylinders actuate faster and with more force in the extension stroke as compared to the retraction one. This led to the introduction of a delay in the activation of the flexing cylinder so as to keep both rotations synchronous.

In an attempt to increase the response time of the platform an attempt to pre-switch the directional valves before the subject stepped on the platform was investigated. Tests revealed a large loss in the stiffness of the platform when the directional valves were pre-switched. Figure 5.13 indicates a rotation of approximately 4° even though the flow control valves connected to the exhaust of the directional valves remained closed.

5.4.2 Control optimisation

After experimenting on the pneumatic valves and studying how they reacted and affected the behaviour of the platform, it was time to use that knowledge

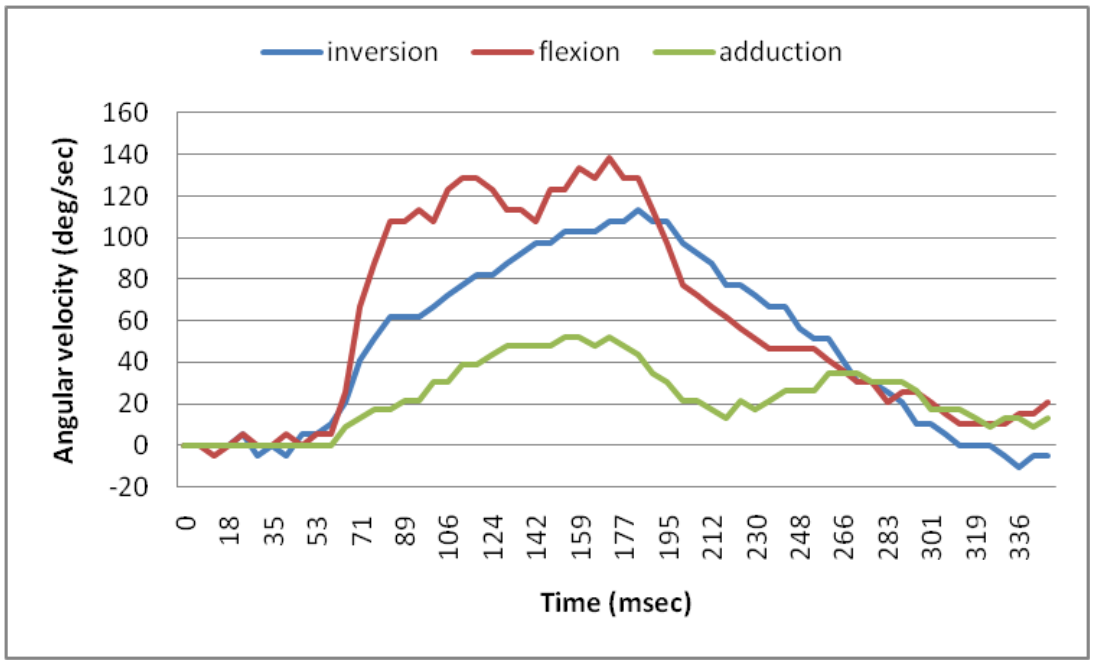

(a) Platform rotational velocity when all valves were turned fully open

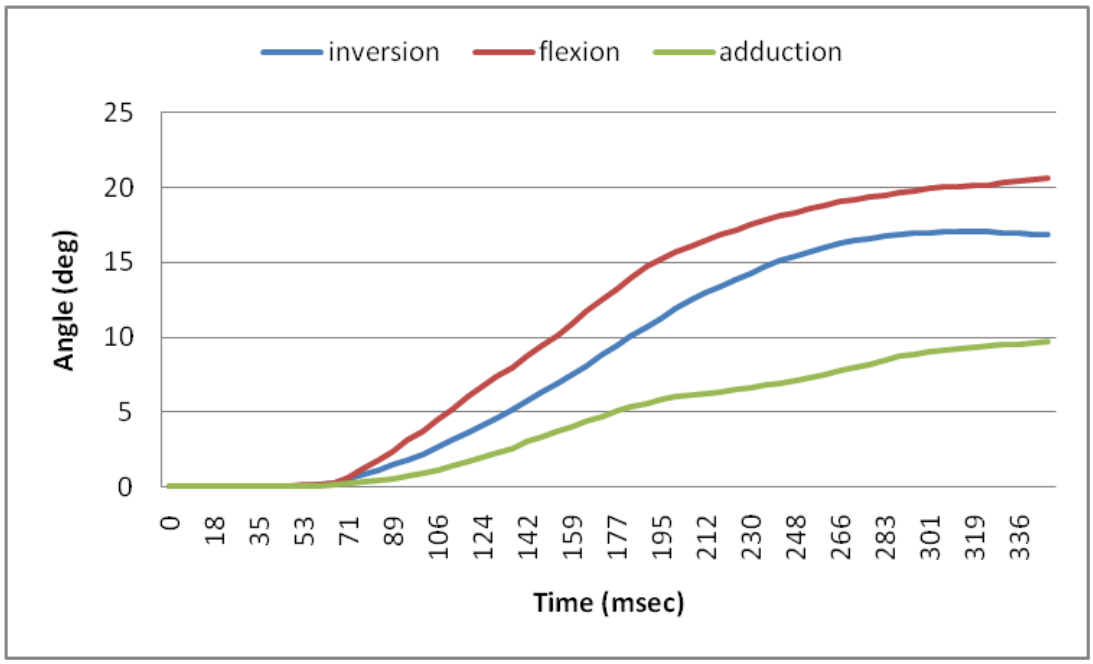

(b) Platform rotation angle when all valves were turned fully open

Figure 5.12: All valves turned fully open

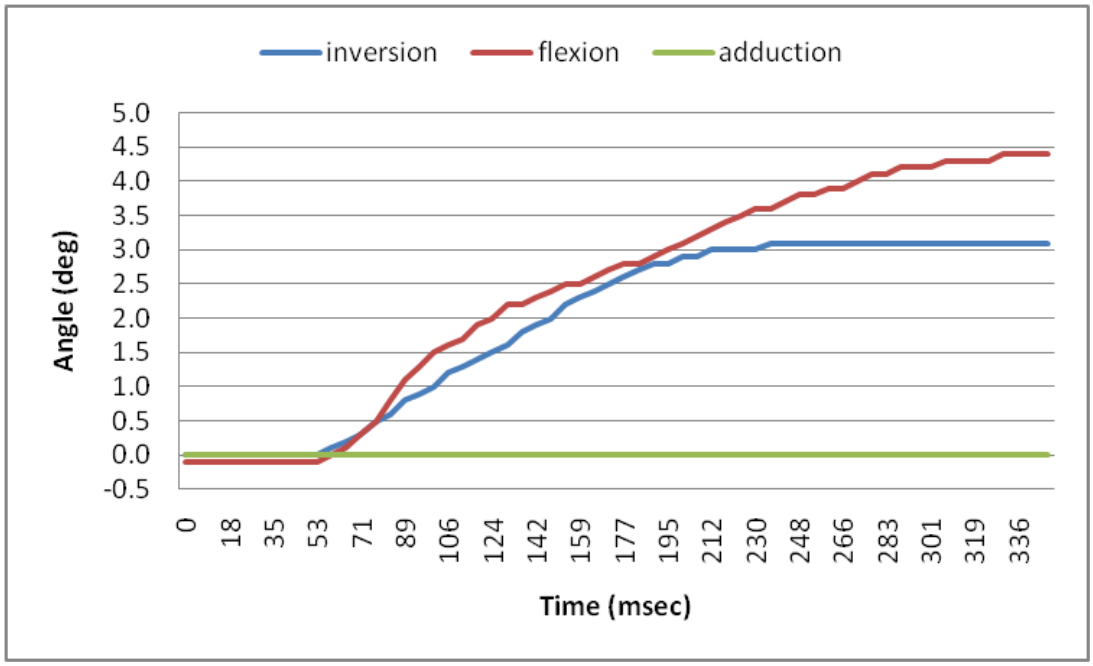

Figure 5.13: Pre-switched directional valves

to create a functional control algorithm to control the platform (refer to Section 5.3.1). Different control methods were tried and tested. The best performing methods were then refined and enhanced following rigorous testing.

One of the problems encountered, which was highlighted earlier, was the inability of the flow valves to stop the rotation of the platform quickly enough. If the control algorithm was to rely only on the flow valves the platform would exceed the target angle (Figure 5.14). The reasonable thing to do was to try to employ the directional valves to decrease the stopping time. Reversing the directional valve, however, caused the platform to rebound and bounce back in the opposite direction (Figure 5.15). Closing the flow valves before reversing the directional valves did not help reduce the platform rebound either.

In the first pneumatic circuit configuration, 5/2 directional valves were used. These valves allowed the cylinder to either retract or extend, they do not however, provide a way of stopping the cylinder rod from moving (refer to Section 4.3). The proportional control valves were connected to the exit ports of the directional

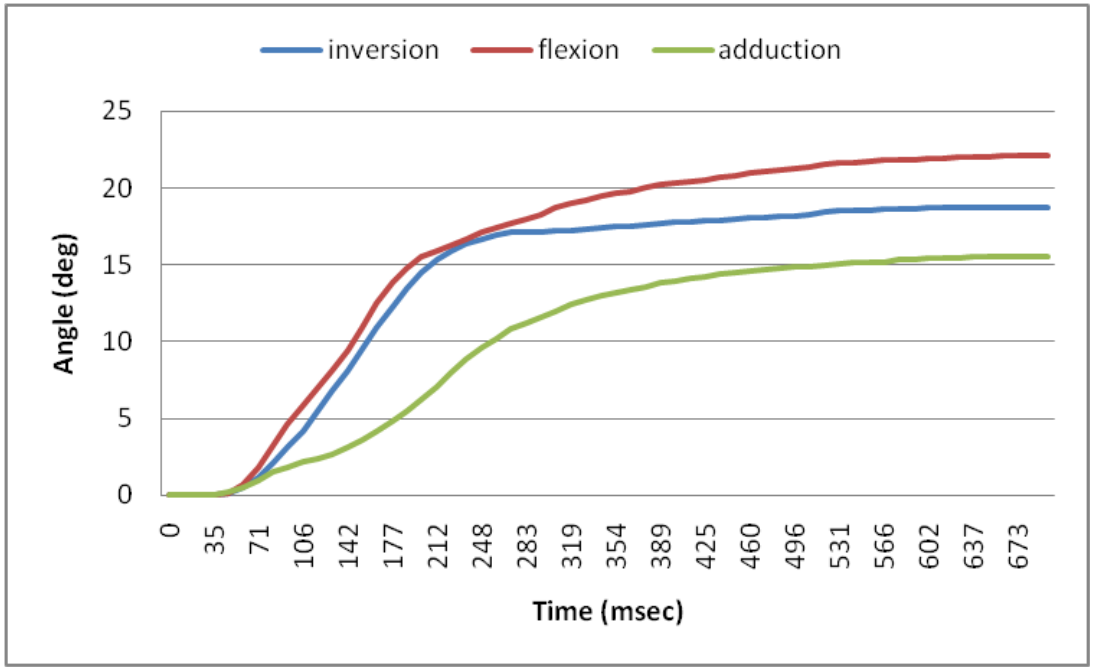

Figure 5.14: Movement continues after valves are closed

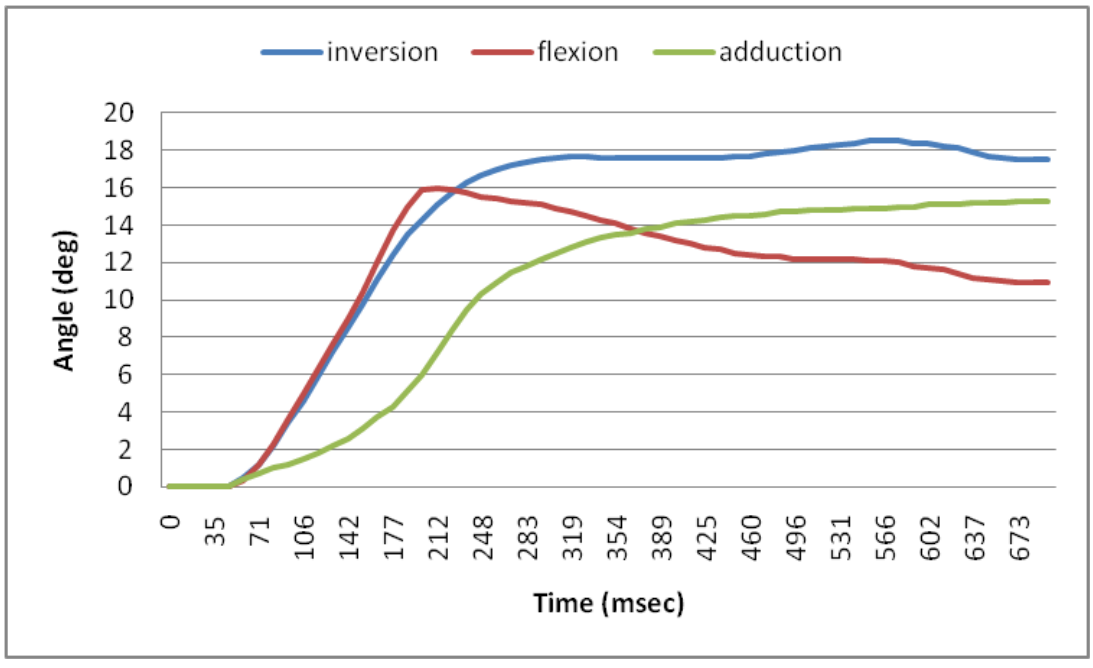

Figure 5.15: Directional valve switches direction in flexion

valves allowing control over speed of actuation, and providing a means of stopping the cylinder. On/off two ports 2/2 valves were connected to the cylinders exit ports directly in such a way so as to increase air flow and ultimately increase the speed of actuation. Since the flow valves were failing to stop the platform rotation timely, and switching the 5/2 directional vales resulted in bouncing back of the foot-plate, it was decided to opt for 5/3 directional valves. These valves can be used to cut the air supply from the cylinders whilst at the same time closing the exhaust ports; they do not require flow valves at their exhaust. The proportional control valves were moved to replace the now redundant 2/2 valves.

The initial control algorithm used the feedback from the optical encoders to monitor the position and velocity of the platform. Using those two variables, an estimate of the platform's position after a specified amount of time, called prediction time, was calculated. The PIC® was programmed so that the moment the estimated position exceeded the set target angle, the directional valve closed. The proportional valves remained open and employed a similar algorithm (refer to Section 5.3.1) to fine tune the final position of the foot-plate. Figure 5.16 demonstrates the effect of the value of prediction time on the performance of the platform. A long prediction time will cause the valves to close too early (Figure 5.16a), while reducing the prediction time will delay the valve closure (Figure 5.16b). Setting the prediction time too short, however, caused the platform to overshoot the target angle.

Using the previous method to determine the closing time of the main valves had some limitations. The algorithm relies on the velocity data in its calculations and assumes it increases linearly with time. When a subject stepped on the rising edge (beginning) of the platform the rotation speed in flexion is reduced and loses its linearity. This caused the valves to close too late and ultimately the platform to overshoot its target angle (Figure 5.17).

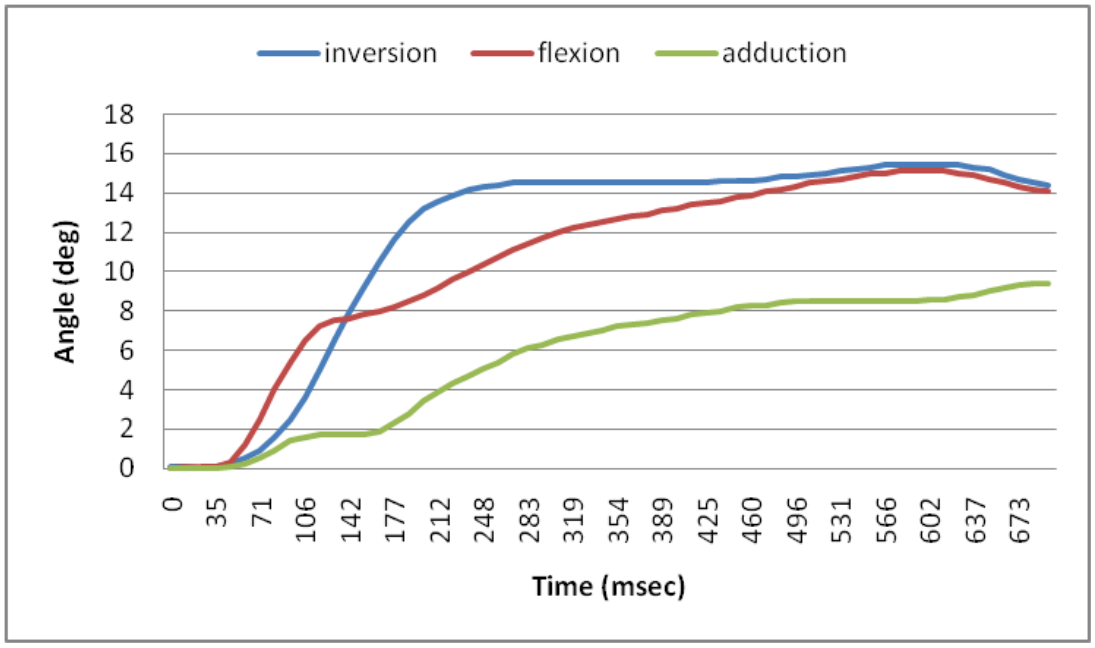

(a) Long prediction time

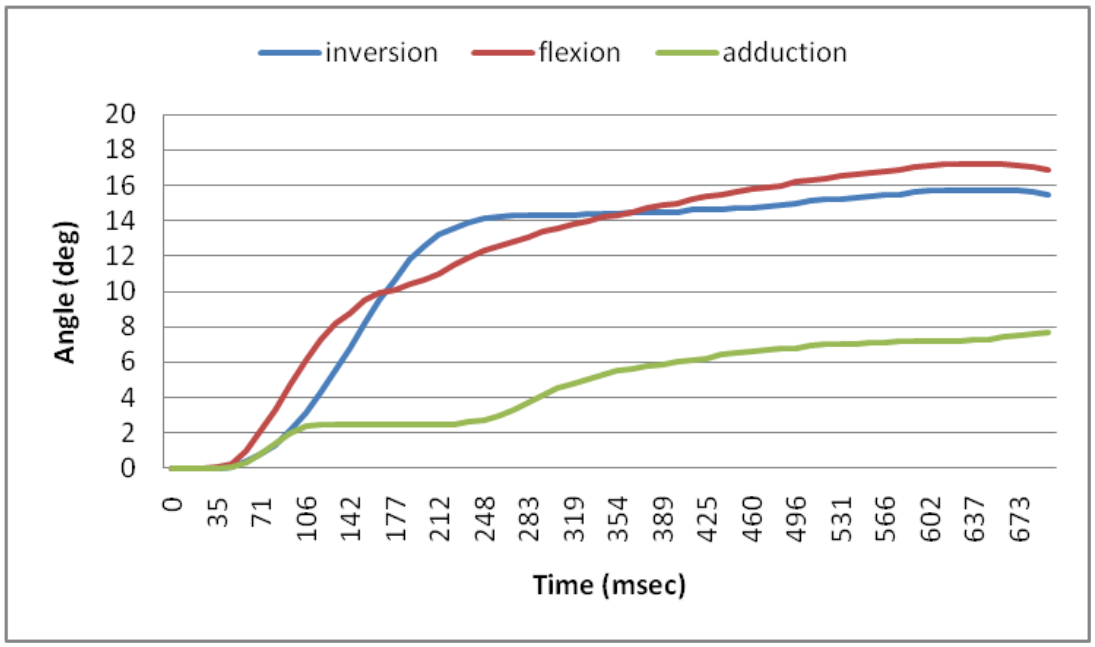

(b) Short prediction time

Figure 5.16: Effect of varying the prediction time

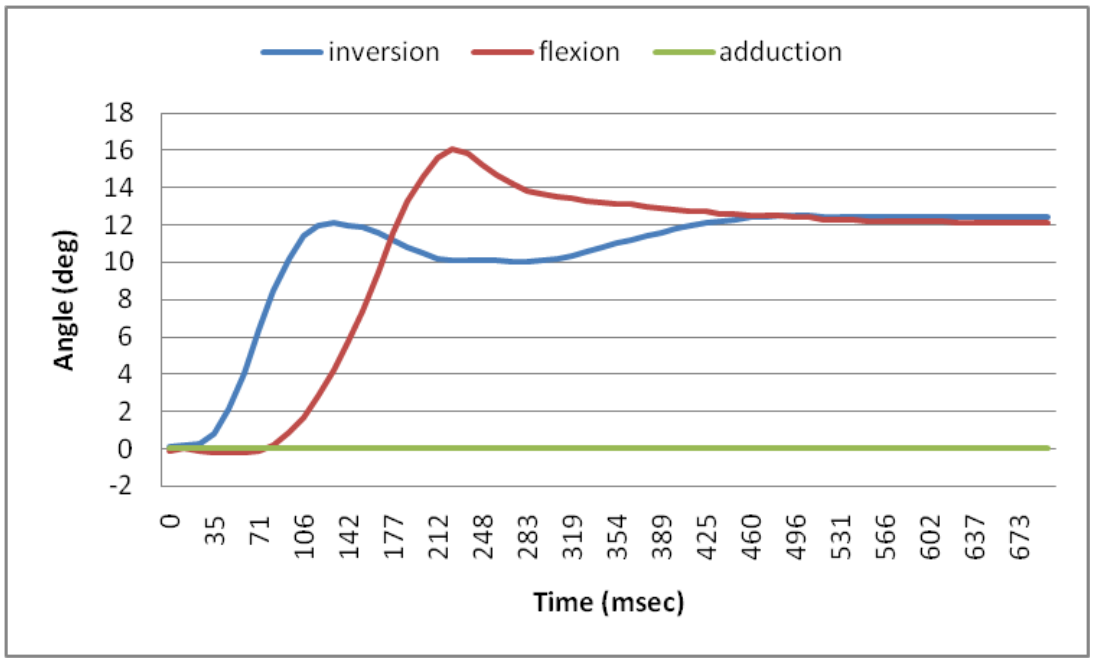

Figure 5.17: Stepping on the platform edge (flexion and inversion set to 12°)

The use of a prediction time was thus stopped[2] and as an alternative a fixed closure time of the direction valves was used. That value, however, was different for each target angle. After conducting several experiments the fixed time necessary to achieve 15°, 15°, and 8° in inversion, flexion and rotation respectively, was determined. The experiments also allowed determining the variables used in fine tuning position, controlling velocity, and preventing rebound (refer to Section 5.3.1). The result of the platform performance using the final algorithm is shown in Figures (5.18a) and (5.18b) (note the reduced rebound as compared to Figure 5.17).

5.5 Interface

The robotic platform was designed to be used by non-engineering researchers whose field of expertise does not normally involve programming nor micro-

[2]The prediction time method for the proportional valves used for fine tuning position remains to be used

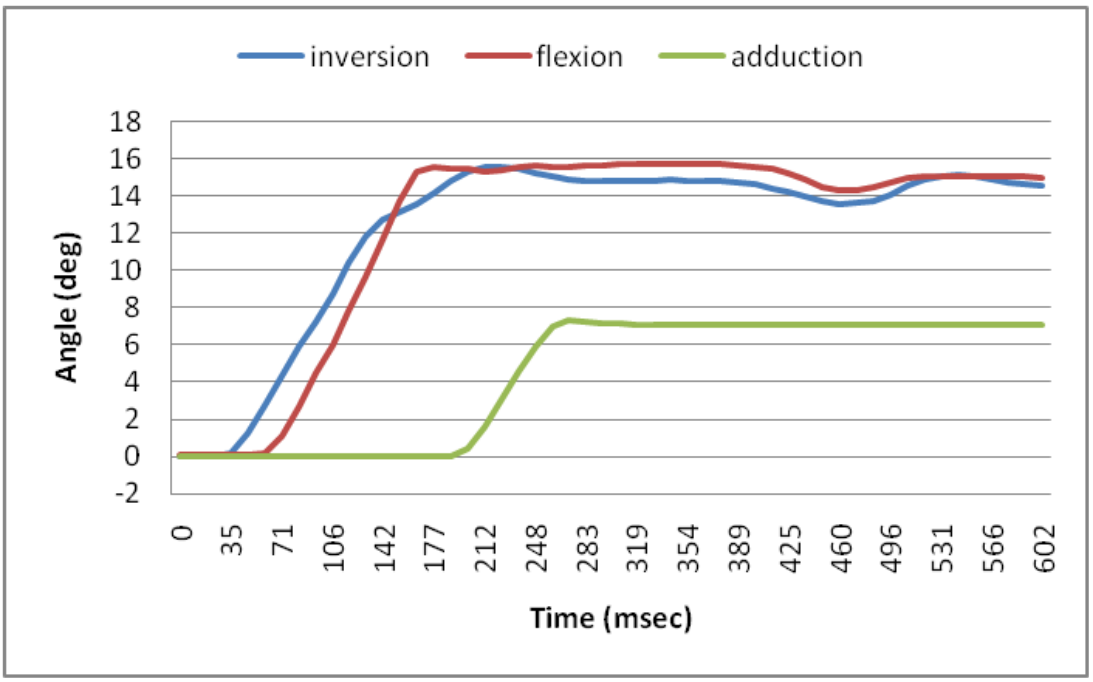

(a) Platform rotation angle using the optimised control algorithm

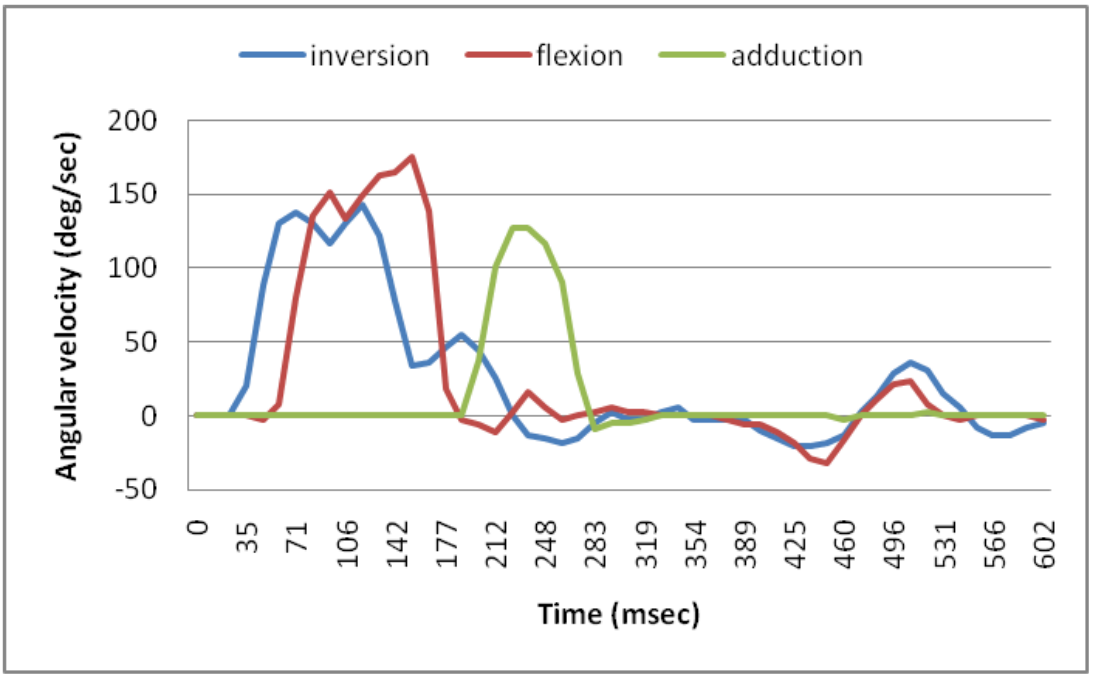

(b) Platform rotational velocity using the optimised control algorithm

Figure 5.18: Platform rotation using optimised control algorithm

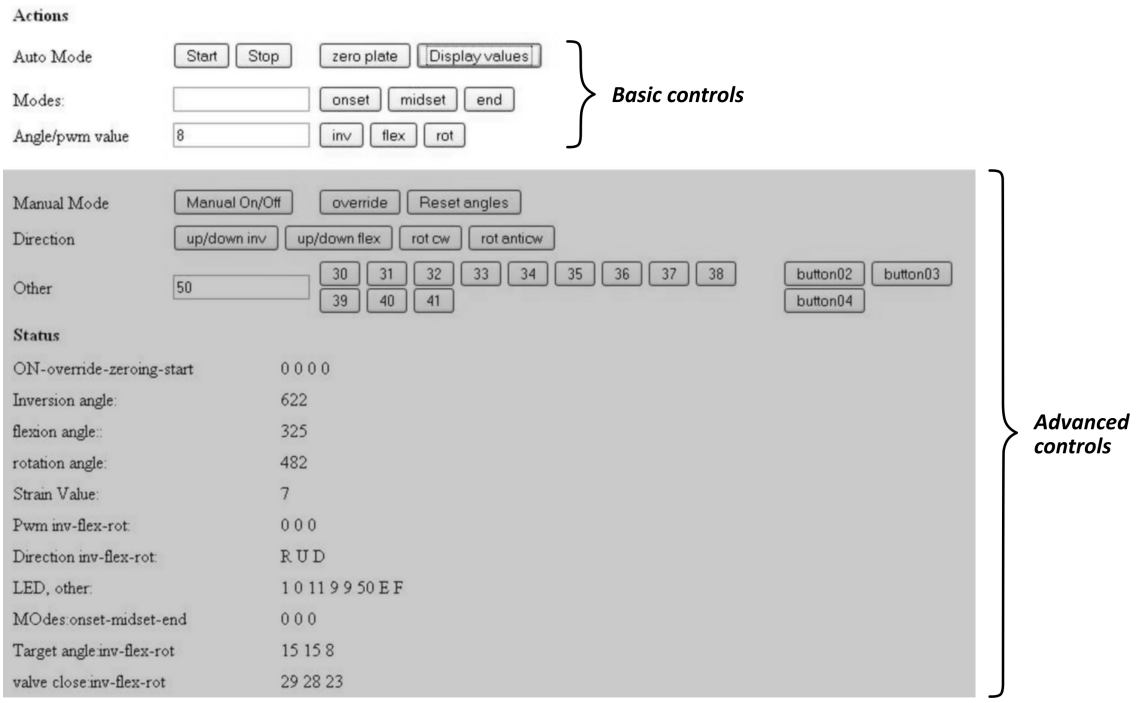

Figure 5.19: Platform control interface

controllers. For this reason an intuitive and easy to use web interface was designed and written in HTML language (Figure 5.19).[3] The interface can be accessed through any networked computer in the laboratory and can run on any web browsing software. It gives the researcher total control over the robotic platform.

To control the platform, the researcher first presses the *zero plate* button, which levels the foot-plate with ground and calibrates the output value of the optical encoders. The *start* button informs the platform to rotate once proper foot strike on the foot-plate is confirmed. The *stop* button cancels the *start* condition bringing the platform back to *standby* mode. The *Modes* section allows the researcher to specify the rotation profile/mode, while the angles section lets them specify the target angles of rotation around all three axes. After a successful trial the researcher would press the *Display values* button which displays the output data of the platform during the whole trial. The researcher can then save these

[3]The interface builds on the microchip web server supplied with the PIC®

values and press *zero plate* in preparation for the next trial.

The platform was designed with flexibility and expandability in mind to allow further research development. To make it easier for the engineer/researcher to tune and test any added features, the interface incorporated extra control buttons and functions (Figure 5.19). When the researcher presses the *manual* button they are given total access over the platform's valves and sensors as well as the various parameters of the control software. These advanced features in the interface were used in tuning and calibrating the robotic manipulator for the current project (refer to Section 5.4.2).

6 Vicon® and EMG integration

6.1 Introduction

The robotic platform allows inducing foot inversion and supination of dynamic subjects. That by itself is of little use if researchers were unable to record useful data from the subjects during the platform rotation. This chapter presents the work carried out to synchronise the robotic platform with external systems. For this project, the robotic platform was synchronised with a bilateral four-channel EMG system and a Vicon® MX-13 system which allows assessing the effect of induced foot inversion and supination on the musculoskeletal system.

6.2 Motion capture systems

Our current understanding of the Gait cycle (GC) was made possible by the help of motion capture systems. They reveal details that otherwise could not be noticed with the naked eye, and thus, allow for a better understanding of body kinematics. Motion capture systems are employed in research as well as for clinical purposes.

Motion capture systems can be classified into two major categories: optical based and non-optical based. Non-optical systems include goniometers placed directly at the joints and magnetic based systems such as FASTRAK®.

Optical based systems rely on optical sensors such as video cameras to capture movement. They can be categorised into three groups based on the body marking method they employ. passive-marker systems rely on reflective markers attached to specific anatomical positions of the body; the markers are termed passive since they do not emit light on their own but can only reflect it. They are the oldest among modern optical systems and are therefore well tested and widely used in research. The passive markers, however, need to be externally labelled, which can be time-consuming if no auto-labelling algorithm is used, or if such an algorithm is unreliable. Active-marker systems, on the other hand, rely on light-emitting markers. The unique lighting pattern of each marker act as its ID tag, thus, eliminating the need for external labelling. Finally, there are the markerless systems, which require no markers and rely solely on computer vision algorithms to identify motion. The latter are the most recent systems but are still in their infancy and are not as accurate as the passive and active marker systems.

6.3 Vicon®

Vicon® is an optical passive-marker 3D motion capture system. Retro-reflective markers, which reflect light back in the same direction it strikes them, are placed on specific anatomical positions on the body. Vicon® cameras (Figure 6.1), surrounded by infrared emitting LED capture and track the positions of these markers. Nexus®, the software supplied with Vicon® systems, reconstructs the position of the markers in three-dimensional (3D) space and allows the user to label each marker. Nexus® then utilises a biomechanical model of the human body, for example Plug-in Gait®, to calculate the kinematic data of different body segments (Ebbutt *et al.* 2005).

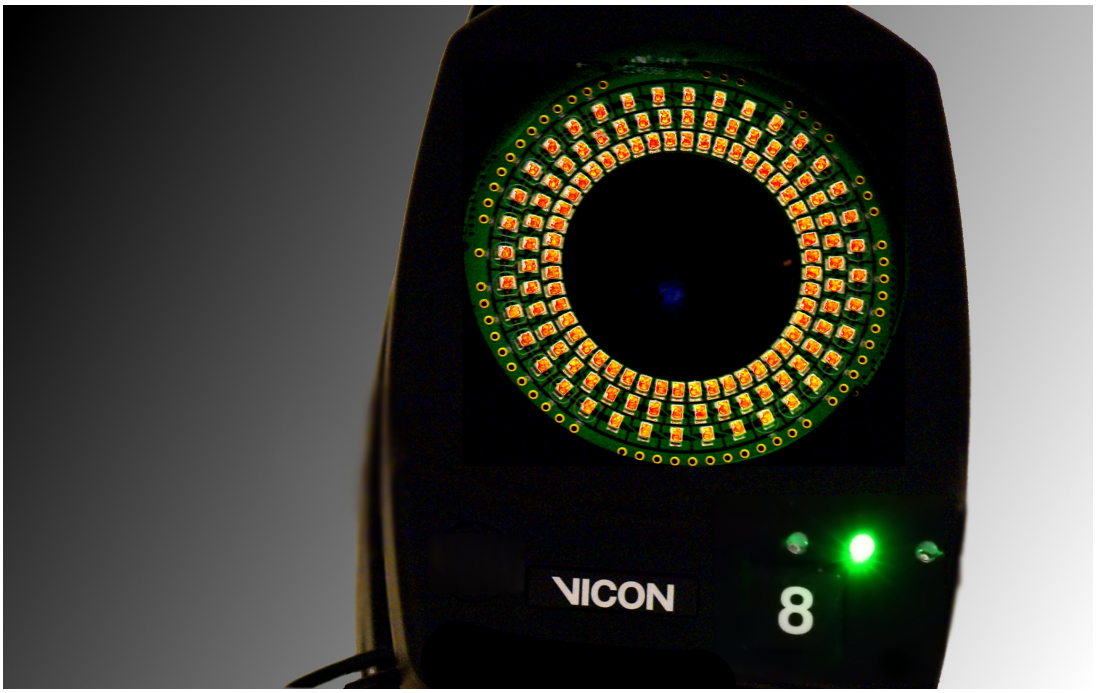

Figure 6.1: Vicon® Cameras

6.3.1 System specifications

The Sports Laboratory where the platform was fitted is equipped with a 12-camera Vicon® MX13 system. The cameras have a resolution of 1.3 megapixels and can capture video frames at a rate of up to 484 Hz. Higher resolutions allow for a larger capture volume, and/or smaller and more closely placed markers. The capture rate is usually set based on the speed of the subject's motion. The system also contains an analogue box which provides connectivity to external devices.

6.4 The EMG system

The EMG capture device used for this project is the Mobi8 from TMS® International (Figure 6.2). Mobi8 has four channels allowing capture from four different muscles, as well as, bluetooth connectivity providing greater freedom of move-

Figure 6.2: The EMG system used at IMAR

ment for subjects. It has also other channels, which can be used to record the synchronisation signal that is essential for the current project.

Mobi8 has a sampling frequency of up to 2048 Hz and has a 24-bit analog-to-digital A/D converter with a resolution of 12.2 nV per bit. The amplifier gain is 19.5x while its input impedance is $10^{12}\Omega$. These specifications make it well suited for EMG capture.

6.5 Synchronisation

A wireless synchroniser (Figure 6.3) with a fixed delay, developed in-house at IMAR, was used to synchronise the Vicon®, Mobi8 and robotic platform systems together. It consisted of an emitter device and a receiver antenna. The synchroniser, however, was designed to be triggered manually by the researcher via a push button; there was no input port to attach the synchronisation cable from the platform. Building a new synchroniser would have been a lengthy process so it was decided that the current device had to be modified to comply with the

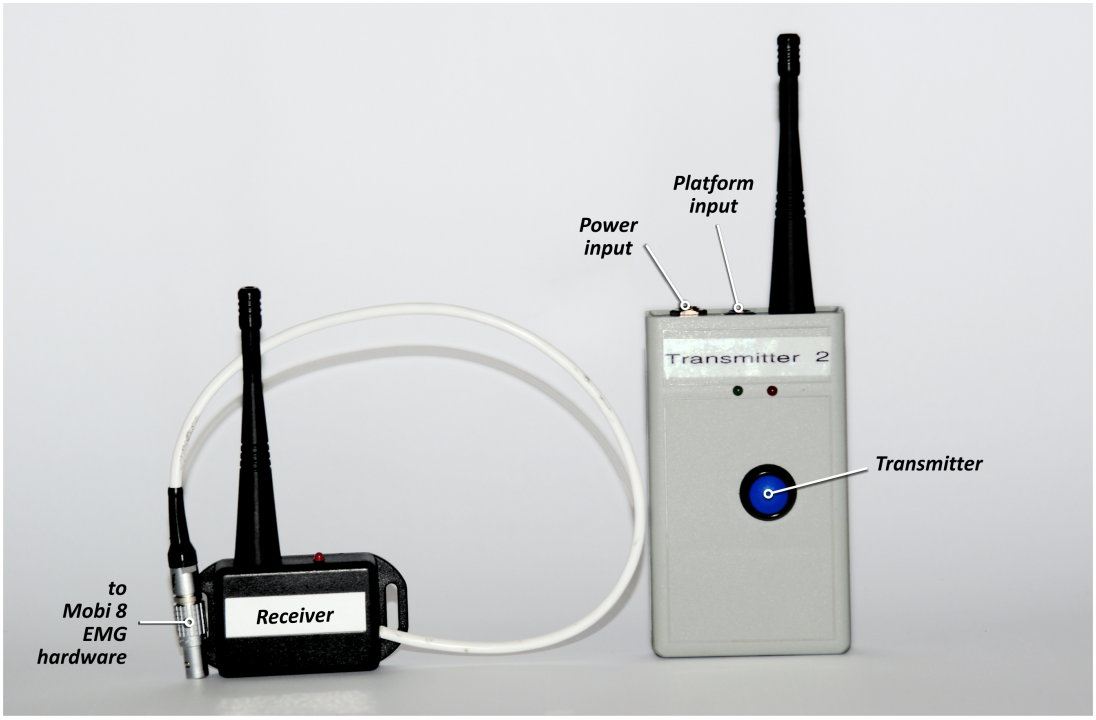

Figure 6.3: Synchroniser

platform's output.

The transmitter device connects to Vicon® through analogue input channel 13, of the input/output Vicon® board. The receiver antenna connects to the Mobi8 EMG system via channel E analogue input. When a subject steps correctly on the foot-plate, pin RA2 of the PIC® changes its state into a high, $3.3\,V$, sending a signal through the synchronisation cable triggering the synchroniser. The synchroniser then emits a signal with a $50\,ms$ fixed delay that is received and recorded by both the Mobi8 channel E and Vicon® analogue input. The data from the three systems can now be synchronised and aligned using the common signal.

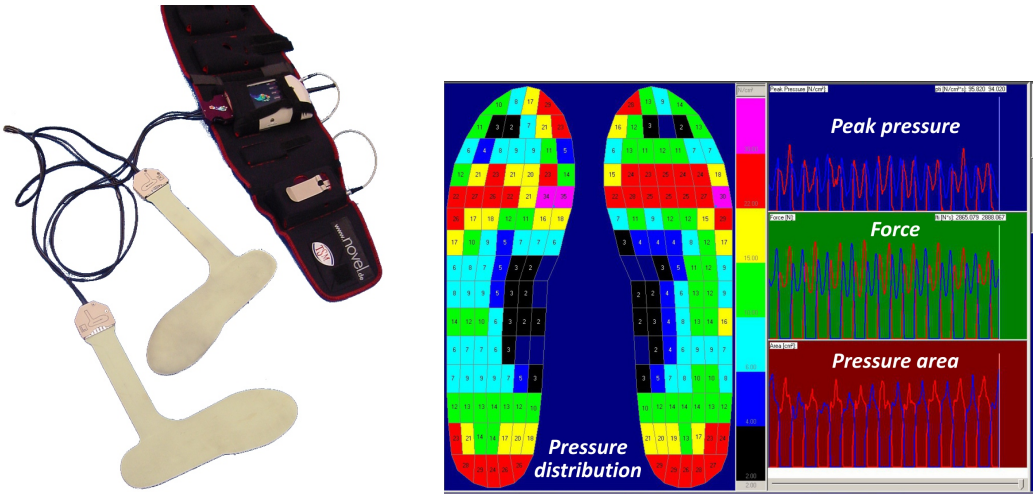

(a) Pedar® hardware **(b)** Output (IMAR, University of Dundee)

Figure 6.4: Pedar® insole pressure measurement System

6.6 Expandability and further recommendations

The robotic platform is capable of transmitting a synchronisation signal allowing it to be used with other devices. It was successfully implemented with both the EMG and Vicon® systems but is not limited to them. Other systems that could be used with the platform include the Pedar® in-shoe pressure measurement system (Figures 6.4a and 6.4b) for example. Synchronising with Pedar® allows to study the pressure distribution under the plantar surface of the foot, during the rotation of the platform. Another option would be to attach a pressure mat directly to the surface of the foot plate, thus allowing pressure measurements to be recorded when subjects are barefoot.

7 Validation study

7.1 Introduction

After fully testing the new system it was time to validate it by utilising the new system in an experimental study that investigated the role of shoes in ankle sprain injury. The experiment would also provide an opportunity to assess the potential and capabilities of the system and to investigate wider possible uses for it.

An ethics approval form (Appendix E) was filled and submitted to the University of Dundee Research Ethics Committee which granted ethical approval of this experimental study allowing recruitment of healthy human subjects.

Subject recruitment posters (Appendix F) were displayed around the University of Dundee campus, Ninewells Hospital and around Dundee. The research was advertised in Hermes II (a weekly email sent by the University of Dundee to all staff and student members); emails regarding the project were also specifically sent to the University of Dundee students and staff at the College of Medicine, Dentistry and Nursing.

7.2 Power analysis

In order to decide on the number of subjects required for this study and to ensure that statistical significance is not missed due to a Type II error, a power analysis was conducted. The method used for this analysis is based on the description provided by Armitage *et al.* (2002) where the estimate of the sample size n is governed by the following equation:

$$n > 2\left[\frac{(z_{2\alpha} + z_{2\beta})\sigma}{\delta}\right]^2$$

Where z refers to the standardised normal deviate, 2α is the two-sided significance level, β is the Type II error rate, σ is the standard deviation (SD), and δ is the true difference. For this study the two-sided significance level was set to 0.05 and the power of the analysis $(1-\beta)$ set to 80% or 0.8. An estimate for the SD (the sample SD) was calculated from the maximum standard error (for the peak and average of the EMG data) reported by Kerr *et al.* (2009):

$$s = 0.06 \times \sqrt{62} = 0.47$$

To detect for 20% differences and using the maximum peak EMG value reported by Kerr *et al.* (2009):

$$\delta = 0.2 \times 2.33 = 0.47$$

Hence:

$$n > 2\left[\frac{(1.96 + 0.842)0.47}{0.47}\right]^2$$

As such, the required number of subjects is 16.

7.3 Subjects

Fifty-one subjects responded showing an interest to participate in the study; two of which had recent ankle injuries and were therefore excluded. All interested subjects were emailed an information sheet (Appendix G) explaining the aims of the project and what to expect regarding experiments. Of the 49 responses, 36 people volunteered and participated in the study, seven of which were removed from the database due to the following:

- Two subjects were excluded due to noisy signal caused by a faulty power connection that affected the synchronisation unit.
- One subject due to missing/falling Vicon® markers.
- One subject due to the platform failing to rotate accurately. This problem was not obvious when the platform was initially checked. As the experiment progressed, however, the performance of the platform began deteriorating such that it could no longer rotate accurately forcing us to abort the experiment. This was the only occasion that the platform caused any problems. The cause was found to be compressed air leaking at one of the valves.
- One subject due to Vicon® data containing a huge amount of ghost markers which are non-existent markers that are reported by the cameras as real. The main culprit was the heating system in the laboratory, which was turned on just at the beginning of the experiment. A change in temperature was found to affect camera calibration.
- One subject had a recent injury to their right ankle but were permitted to participate as a simple case study.
- One subject continually failed to strike the platform properly so were excluded from the study.

Figure 7.1: Two shoes used in this study

7.4 Materials and Methods

7.4.1 Footwear

Two sets of different sport shoes were purchased for this study (Figure 7.1). The first were running shoes from a famous brand and the second were flat soled sport shoes from a different well known brand. Both sets included sizes 4 to 11 UK, with one size increment, to cover as many subjects as possible. Criteria for choosing the shoes were as follows:

- Sport shoes were chosen since previous research shows most ankle sprains occur while participating in a sport's activity (refer to Section 2.2.1).
- Mid range priced as the cost of shoes is not related to performance (refer to Section 2.2.6).
- Sold in Sport shops where any person can buy them.
- Available in sizes 4 to 11 UK to cover most shoe sizes.

Vicon® markers were placed on top of the shoes as shown in Figure 8.6. No matter how good the fit between the shoes and foot, the foot cannot be guaranteed to be rotating exactly the same as the outside of the shoe. This implies that the captured inversion and plantar-flexion angles of the foot when wearing one of the shoes may be slightly inaccurate. To avoid this inaccuracy it was suggested to cut the shoes where the markers were to be placed, so as to allow attachment directly to the foot, thus faithfully capturing its movement. This however could effect the integrity of the shoes and thus the validity of the study. It was as such decided to leave the footwear as they were bearing in mind that the obtained foot rotation data when wearing shoes may contain some inaccuracy. A study to investigate the effect of introducing cuts to the shoes is, however, recommended.

7.4.2 Clothing

Male participants were required to wear shorts and no shirt, while females were asked to wear shorts and a sports Bra. This was necessary to allow proper attachment of the EMG electrodes and reflective markers to the upper and lower body. Participants were informed about this before attending. They were also given the choice to bring their own clothing or use the ones available in the department.

7.4.3 Camera aiming

The Sports Laboratory Vicon® system where the platform is fitted is usually set to be used with two force-plates placed in the middle of the walkway. The robotic manipulator, however, was placed further away from the force-plates, which required moving the cameras from their original position and setting a new capture volume encompassing the robotic platform. Ideally, kinematic data for at

least one stride before the platform and one stride after FS to the platform must be captured. This allows investigation of the effect of induced foot supination on the GC.

Of more importance, however, was the ability to track the movement of the foot and ankle as the platform rotated, especially when dropped below floor level. In order to represent a marker in 3D, a minimum of two cameras must be able to see the marker at the same time. Three cameras were needed to entirely track the motion of the foot during the rotation event. Unfortunately this meant that the remaining cameras were only able to capture one step before and one step after FS the platform. The future addition of further cameras in the Sports Laboratory for a more complete picture is recommended.

7.4.4 Laboratory environment

As participants were not warmly clothed it was important to heat the laboratory to a comfortable temperature of $24°C$. The heating in the laboratory was turned on two hours before subjects arrived. This is to ensure that the temperature has stabilised by the time the experiment began and prevent the presence of ghost markers in the captured data. The cameras were then calibrated as suggested by the Vicon® manual and the Lab's reference frame was set with its origin at the top right edge of the footplate. The capture rate of the cameras was set to $100\,Hz$, to capture adequate gait kinematics.

7.4.5 System preparation

Before the arrival of each subject the system was tested and set. This was important to avoid any problems during data capture and to reduce the time of the already lengthy experiment which lasted around an hour and forty-five

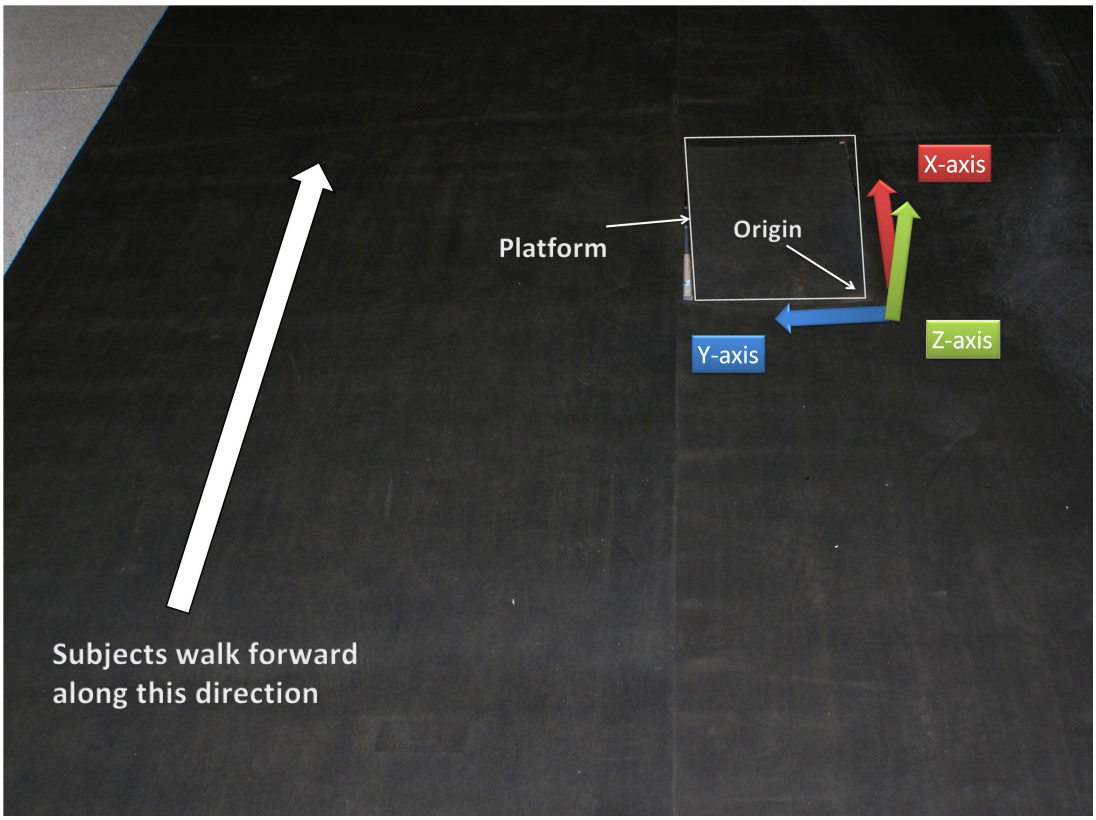

Figure 7.2: Laboratory reference frame

minutes.

Fifty-one reflective markers with diameter of 14.5 mm were used for the experiment. Thirty-eight were normal markers and four were wand markers. Before each experiment the normal markers were prepared and attached to a double-sided adhesive tape and porous tape was cut and attached to the wand markers. The Vicon® cameras were then calibrated using the supplied five markers wand. The wand was then placed at the edge of the foot-plate to set the reference frame of the laboratory (Figure 7.2). Vicon® was now ready for data capture.

The platform was then prepared. First, the main compressed air supply valve was opened and the PIC® controller was switched on. The rotation angles were set to 15° in inversion and flexion, and to 8° in adduction. The optical emitters/receivers were then tested to ensure they were correctly aligned and were properly detecting partial foot landings. Finally the *Zero* command was sent to

the platform, rising and levelling the foot-plate with the laboratory floor.

New batteries were placed in the EMG system, and new electrodes were placed on the working table ready for when the subject arrives. The synchroniser's wireless receiver was connected to channel E of the EMG system. The main synchroniser box was also connected to the Vicon® system input board.

7.4.6 Subject preparation

When participants first arrived for the study, they were taken to the IMAR changing room where they were informed of the objectives of the study and the experiment procedure. They were then given the chance to raise any questions they had. Subjects were also informed of their right to stop participation at any time without the need to provide any explanation. They were asked to confirm that they had no recent ankle injuries, nor any other existing health problems. They were also asked about their activity levels and which, if any, sports they participated in.

Subjects were then shown the platform in operation, with the researcher stepping on it. This was to ensure they understood, approved and were aware of what they would be doing. They were then asked to sign and date the consent form (Appendix H).

Anthropological measurements of participants were taken and recorded by the researcher. These measurements are required by the Vicon® Plug-in Gait® model and include:

- Weight and height measurements.
- Hand and wrist thickness.
- Distance between the two anterior superior illiac spines (ASIS).

- Leg length, measured from the centre of the ASIS to the centre of the lateral malleoli while subjects are lying on their back.
- Tibial torsion which is the internal rotation of the tibia and measured as the angle between the proximal and distal articular surfaces of the tibia (Figure 7.3).
- Elbow, knee, and ankle widths.

The normal markers were then fixed onto the participant's body and the wand markers secured to their legs with the porous tape prepared earlier (Figure 7.4). Four markers were also attached on a Velcro® headband which was then fitted on the subject's head. EMG electrodes were attached to the subjects' left tibialis anterior, peroneus longus and gastrocnemius muscle bellies (Figure 7.5). The ground electrode was placed on the illiac crest. The EMG system was secured around the subject's waist via a Velcro® strap (Figure 7.6).

Subjects were then taken from the changing room to the Sport Laboratory. The first thing was to check the quality of the EMG signal which was judged visually by the researcher. To align the wand markers, participants were first given a walker crutch to hold onto and were asked to slightly bend both knees while they facing forward. The participants' feet position was then adjusted so that their knee motion lied in the sagittal plane. They were asked to straighten one knee and keep the other slightly flexed. The wand markers on the flexed knee were aligned by pointing a laser line perpendicular to the plane of the subject's knee; the thigh wand marker was moved until the laser line passed through it, the greater trochantar and the knee marker. The tibia marker was adjusted so that the laser passed through it, the knee marker and the ankle marker (lateral malleoli) (Figure 7.7). The same was done for the opposite leg. Now the subject was ready for the experiment.

Figure 7.3: Measurement of tibial torsion

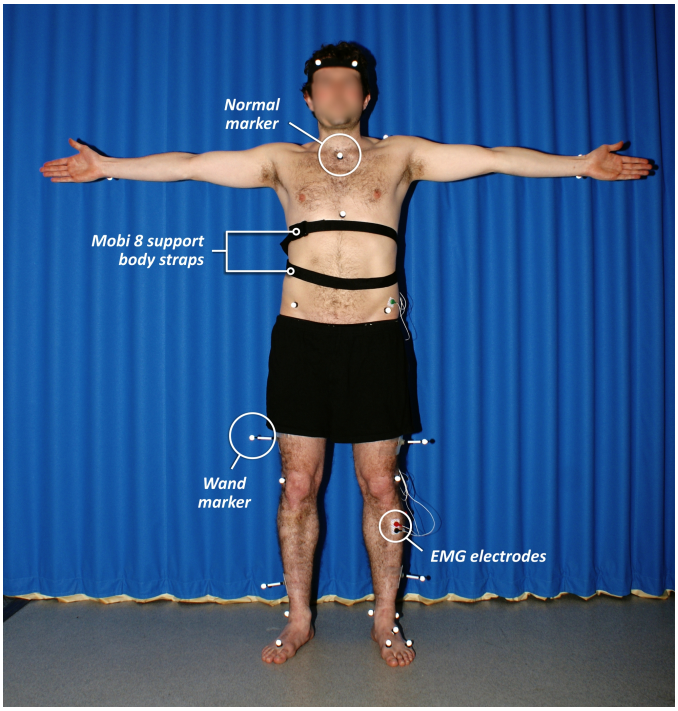

Figure 7.4: Markers attached to subject

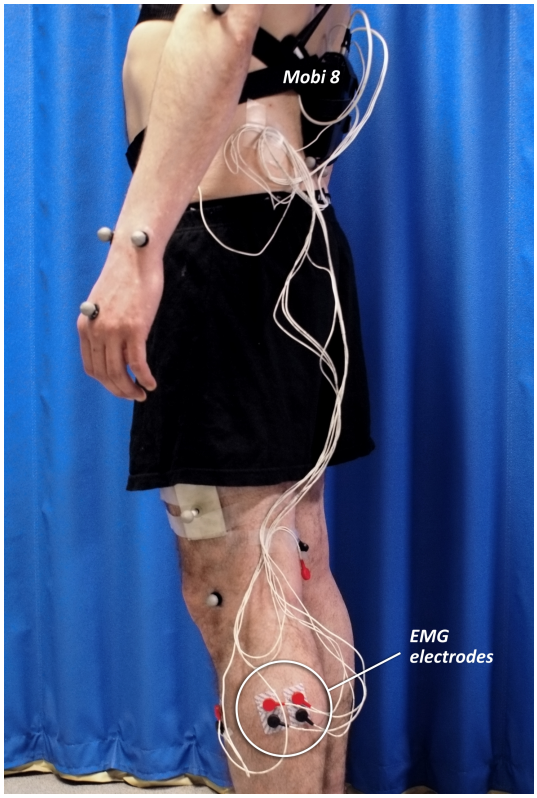

Figure 7.5: Electrodes attached to subject

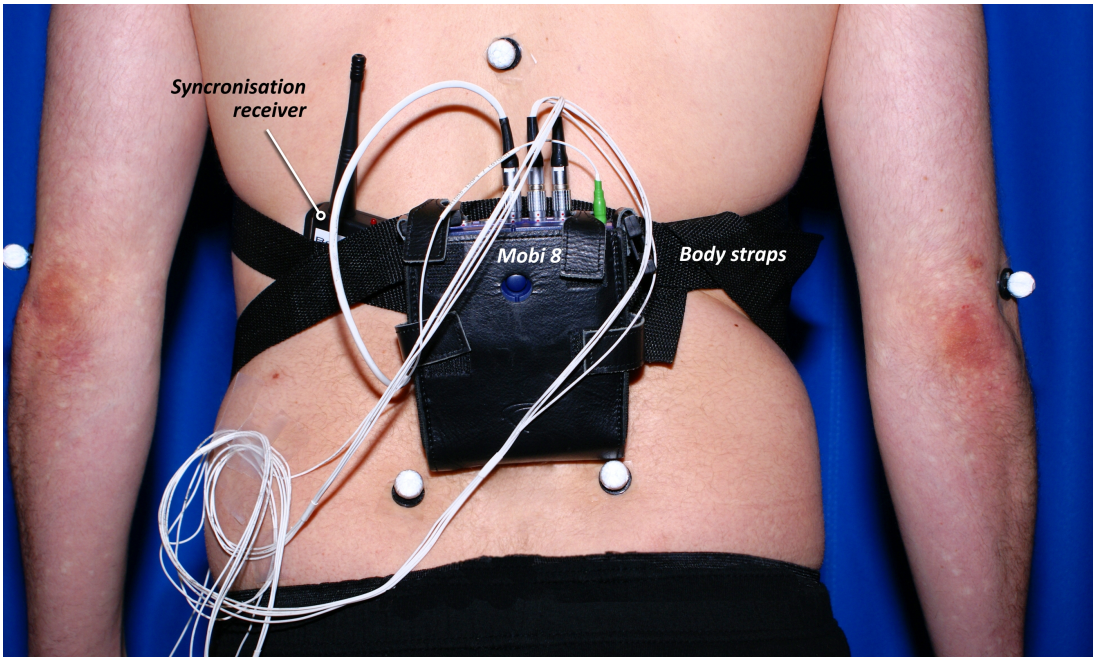

Figure 7.6: EMG system secured around the subject's body

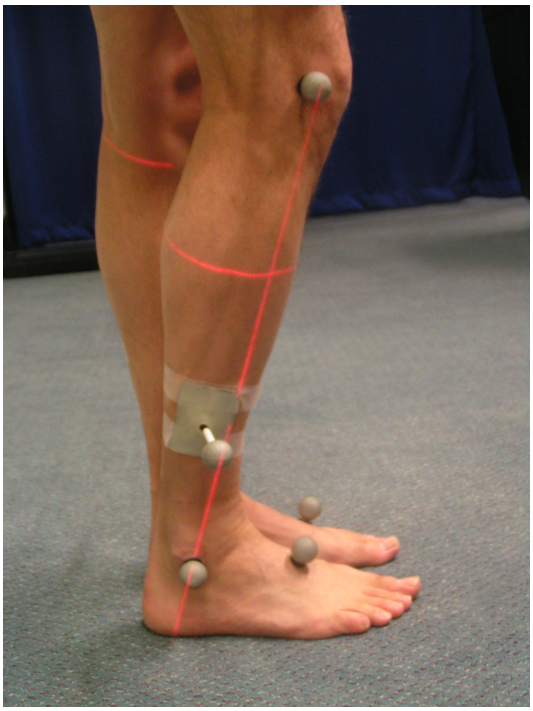

Figure 7.7: Alignment of the tibia wand marker (IMAR, University of Dundee)

7.4.7 Data collection

Participants needed to strike the foot-plate correctly (i.e. with no part of their foot lying outside the surface of the foot-plate), otherwise the platform would not rotate to avoid causing possible injury (refer to Section 5.1.3). Such faulty trials extend the time of the experiment, exhaust the subject, and do not offer any value for the current research. It was therefore essential to decrease the chances of incorrect foot landing. This was achieved by adjusting and tuning the starting position of participants. First, subjects were asked to walk normally without looking at the ground or aiming to hit the foot-plate; they were instructed to begin walking with the same leg for every trial. Their starting position was marked by a training cone. If they over reached the foot-plate, landing in front of it, the cone was moved slightly backward. If they fell short of the foot-plate the cone was moved slightly forward. This was repeated until subjects were landing correctly on the foot plate (Figure 7.8). During this calibration procedure, the

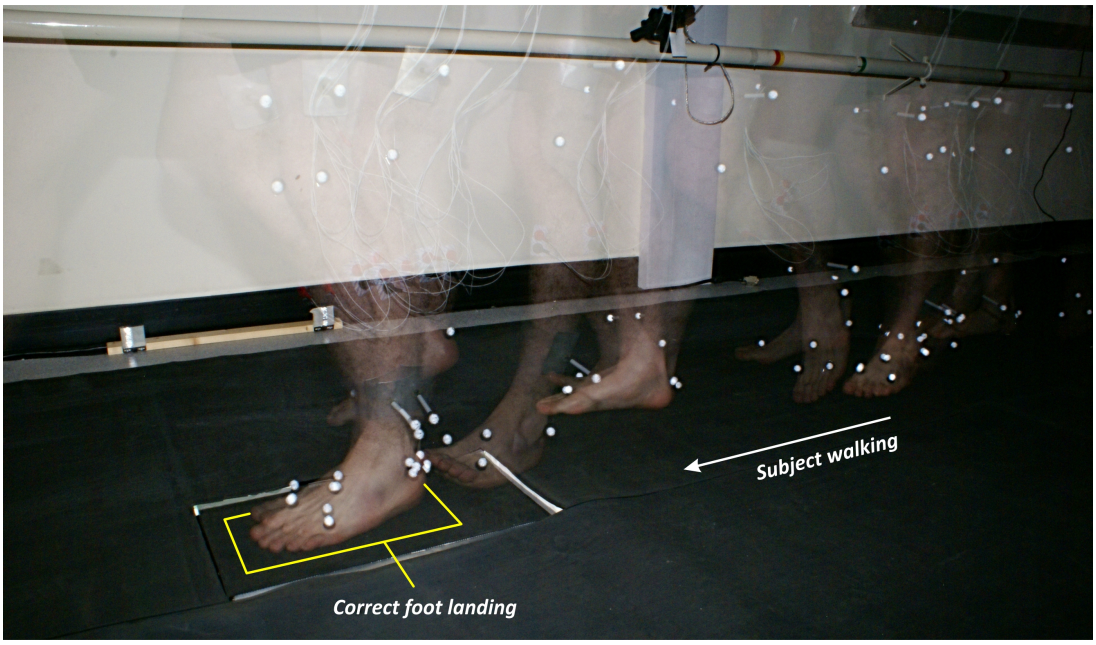

Figure 7.8: Correct landing on foot-plate

foot-plate was fixed in its position, level with the laboratory floor. Following that, participants were informed about how they should walk during data capture:

- walk at their normal speed.
- look straight forward, not at the ground.
- try not to adjust their gait in order to hit the foot-plate.

Now that a starting position was set and participants understood what they had to do, it was time for data collection. The first step was to capture a static trial. Participants were instructed to stand on the foot-plate facing the researcher and looking straight ahead, with their hands at shoulder level. A trial was recorded in Vicon® and named static#, where # is 0 if subjects were barefoot, 1 when wearing running shoes, and 2 when wearing the flat sole sports shoes. The sequence through which each foot condition was tested for was varied between subjects. There were three different testing sequences:

Sequence 1 Subjects in sequence 1 were first barefoot and then they changed into shoes1 followed by shoes2.

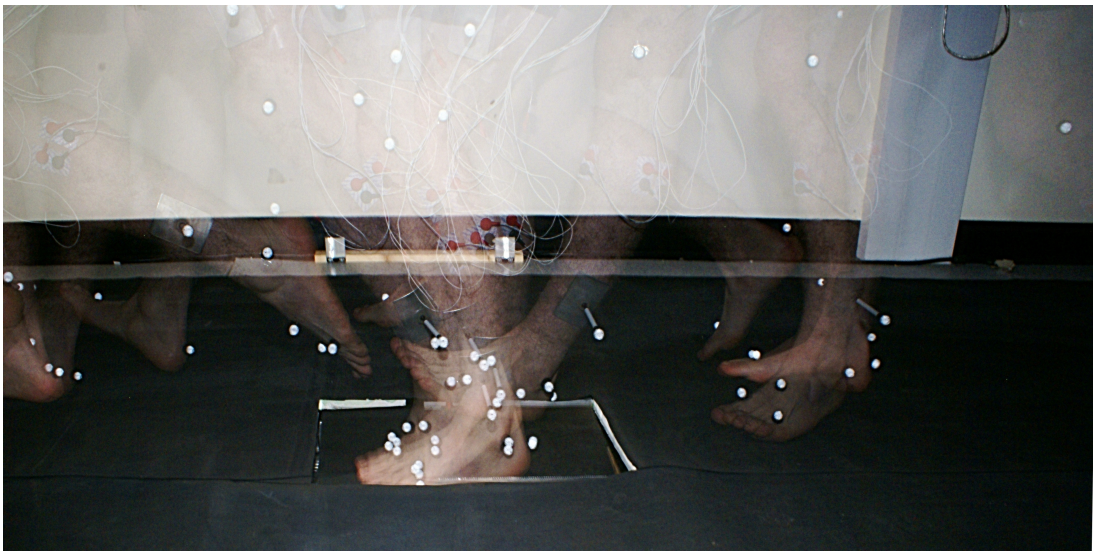

Figure 7.9: Successful platform rotation

Sequence 2 Subjects in sequence 2 had shoes1 on first and then barefoot followed by shoes2.

Sequence 3 Subjects in sequence 3 had shoes1 on first and then they changed into shoes2 followed by barefoot.

After the static trial, participants were asked to return to their original starting position for the dynamic trials. The *start* button on the platform's user interface was pressed, readying it for rotation. Vicon® and EMG capture were initiated, and only after that the subject was asked to start walking. The researcher observed their walking to ensure they were walking as instructed. After they passed the platform the capturing of motion and EMG data was stopped. Both software, Nexus® and Portilab®, automatically save the data in new files with incrementing file names. If the trial was successful and the foot-plate rotated (Figure 7.9), the researcher saved the platform data naming the file with the same number as that of Vicon® and Portilab®. A "-#" was added to the end of the file name pointing out the foot condition (refer to Section 7.4.7). If the trial was unsuccessful the data was not saved.

For each foot condition five successful and usable trials were recorded before moving to the next foot condition. A successful trial was when the platform rotated, a usable trial, however, needed to meet several further conditions:

1. The platform rotated to 15° (±1.5°) around both the X and Y axes.
2. Subjects did not alter their walking pattern to land on the platform. This judgement was decided by the monitoring researcher.
3. Subjects foot did not catch the safety foam at the end of rotation.

The first three successful trials of the first foot condition and the first trial of the consequent conditions were not counted. This was to reduce the "surprise" element which may have biased the first trials.

After the required number of usable trials was achieved, the participant was asked to return to the changing room where they changed into the next scenario as per their allocated sequence. Ankle markers were left in place and care was taken in not touching the calibrated wand markers. New markers were put on the shoes/feet for the next trial. A new static trial was taken to account for the different geometry of the new conditions, and trials proceeded as described previously.

During the trials subjects were asked if they experienced any pain or discomfort from the induced supination and were also reminded that they could stop taking part at any time. It is worth noting that no subjects reported any pain or discomfort, and all completed the full set of trials.

7.4.8 Post data collection

After completing successful data collection, subjects were taken back to the changing room where all electrodes were removed and the Mobi8 was detached from the subjects to avoid any damage. The reflective markers were then removed; a

special tape removal spray for hairy subjects was used. To conclude the trial, subjects were asked for their opinions about the experiment. All participants indicated that they found the project interesting with some requesting to be informed of the results and others offering to return for future research.

7.5 Vicon® Processing

Motion data captured using Vicon® were saved in raw format and require processing to be of any use (refer to Section 8.2.2). Supplied Nexus® software was used to systematically process the raw data and generate ASCII (a character-encoding scheme) files. Data processing was extremely time-consuming and was based on the instructions from the Vicon® manual. This involved the following:

1. Insert measured anthropological data of the subject.
2. Reconstruct marker trajectories.
3. Specify region of interest of the trial.
4. Label the markers.
5. Apply a Woltring filter to smooth the otherwise noisy position data of the markers (for dynamic trials only).
6. Fill in gaps of missing markers (for dynamic trials only).
7. Apply the dynamic or static models.
8. Export data into ASCII format (dynamic trials only).

Firstly the static trials were processed, as their output was required by Nexus® to handle the dynamic trials and allow auto labelling. Anthropological data of the relevant subject was first typed into Nexus® and only needed to be done once for each subject. The next step was to reconstruct the marker positions, thus,

allowing them to be visualised. The researcher then had to manually label each marker with its correct name. Finally the researcher would run the static Plug-in Gait® pipeline (a list of Nexus® modules) which consisted of two modules:

Static gait model: calculates the offset angles which is used to readjust the dynamic data.

Static subject calibration module: associates the anthropological data with marker locations to calibrate the locations of the subject's joints .

Following the static trials, the next stage of the study was processing the dynamic trials. The first step was to reconstruct the marker trajectories (Figure 7.10) which tracks and displays all the markers during the trial. Since recording of the trials was initiated before subjects began walking, part of the trial involved the subject being outside the capture volume of the cameras. So the next step was to define the region of interest for each trial; this was achieved by visual inspection by the researcher. As the *auto-labelling* in Nexus® was not reliable, it was necessary to ensure that most markers were visible in the region of interest, otherwise auto-labelling would not work properly. Once the region of interest was defined all remaining data in the trial were automatically deleted by Nexus®. For this reason, and to avoid having to reprocess trials, it was essential to ensure that all necessary information were contained in that region of interest.

Markers were then labelled partly achieved using Nexus's® *auto-labelling* function. This function was unfortunately very susceptible to errors and although Vicon® manual instructions were properly followed, *Auto-label* kept mislabelling markers. These error were sometime easily spotted (Figure 7.11a), however, in other situations the only way to spot these errors was to hover the mouse over each labelled marker to see its name (Figure 7.11b). This proved to be even more time-consuming then manually labelling the markers. To overcome this problem it was decided to allocate a different colour to each marker which proved helpful

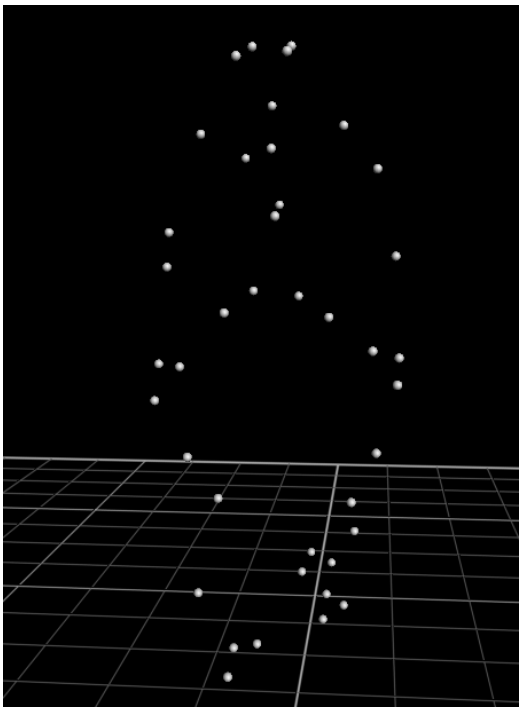

Figure 7.10: Reconstructed and unlabelled markers

in revealing mislabelled markers. Unfortunately, Nexus® did not allow re-saving of the model when the only changes made to it were the colouring of the labels. For this reason the model would have to be re-modified for each subject and foot condition, which would also be time-consuming. It was decided to leave the labelling errors and write a Matlab® module that would detect and point the mislabelled markers out (refer to Section 8.7.3).

Following that, a custom pipeline was applied to the trial. The first operation in the pipeline was a Woltring filter used to smooth the markers position data. Another Woltring filter was applied afterwards to fill gaps of missing markers that were smaller than five frames. Gaps occur when the cameras fail to capture a marker for any part during the trial. Next, a dynamic body language model was applied to reconstruct the positions of any missing markers in a four marker segment, where 3 markers were present. This model is based on parts of the *Golem* model code supplied by Vicon®. Following that, Vicon®'s own dynamic

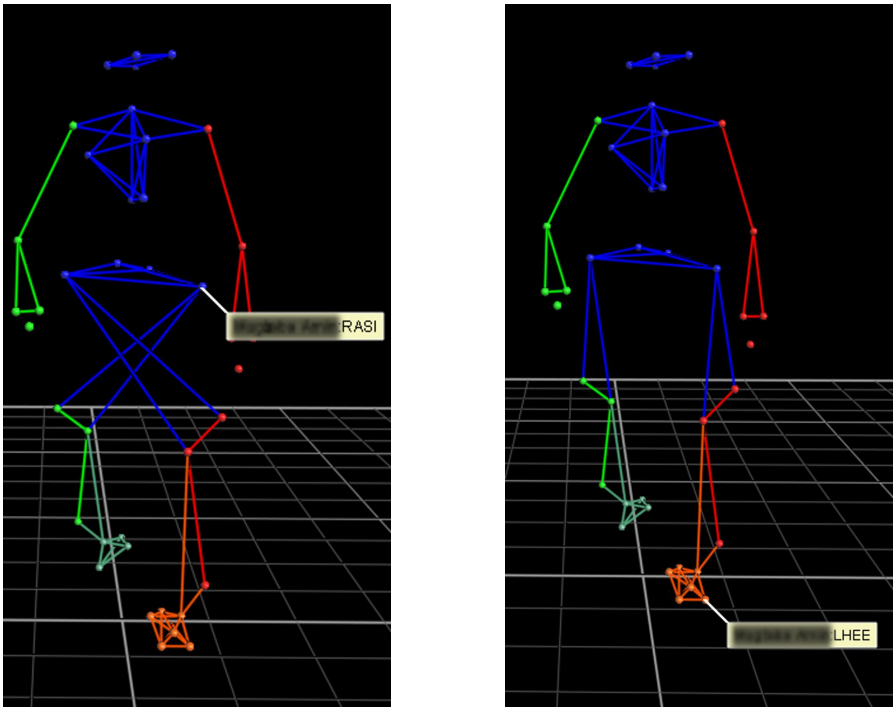

(a) Easy to spot error **(b)** Difficult to spot error

Figure 7.11: Mislabelled markers

Plug-in Gait® model was applied; this generated all the kinematic data to be used except those of the left foot. Then, our own dynamic model was applied to generate the left foot and ankle kinematic data (refer to Section 8.5). Finally, the advanced version of *Export data to ASCII file* was used to write an ASCII file with all the generated data, which can be easily accessed by Matlab® for post-processing.

7.6 EMG data file processing

EMG data were saved in a poly sample file (.s00) format, accessible only using the supplied Portilab® ReView® software. ReView® can visualise and export the captured data but has no functionality whatsoever to further process the data. For this reason it was necessary to export the data files into a format readable by Matlab®, the chosen processing software. ReView® had no batch option, therefore

EMG files of every successful trial had to be opened separately and exported to the usable ASCII format. This also served as an opportunity to visually check the quality of the captured data. Exported files were also renamed to make them easier to identify and index by Matlab®.

8 Data management and processing software

8.1 Introduction

The newly developed system was designed to be versatile to be used in future studies and by other researchers. As such an easy to use software for automatically extracting and processing the data was written (mostly using Matlab®). This software consisted of more than 3500 lines of code part of the new system. It serves to reduce the work load on the researcher and will greatly decrease the time required to process and handle the vast amounts of data generated by the system.

In this chapter the main modules of the software are listed and their function is explained. It is worth noting that the modules were written to process the data from the experimental study presented earlier and are presented below as such. The code can however be easily adapted to suit other future projects since the main core of the software does not need to be changed.

8.2 Background

In order to understand the reasoning behind some of the software functions the following background information are presented.

8.2.1 Human Gait

Gait or walking is a repetitive task and can be described by the gait cycle (GC, Figure 8.1). The main characteristic of gait that differentiates it from running is the presence of double limb support (DLS) which is when both feet are in contact with the ground simultaneously (Perry and Burnfield 2010). A stride, which describes one GC, begins when one foot hits the ground and ends the next time that same foot forms ground contact. The stance phase constitutes 60% of the GC and begins at initial foot contact (IFC), or heel strike (HS) in normal gait, passes through foot-flat (FF) and terminates with toe-off (TO). It is the weight bearing portion of the GC that provides support, stability, and propulsive force. The stance phase contains two DLS events, initial DLS and terminal DLS, during which weight is transferred from one foot to the other. The end of the terminal DLS marks the beginning of the swing phase, which accounts for 40% of the GC. During this swing phase the foot is swung forwards through the air from behind the person's centre of mass (COM) landing in front of the COM. This marks the end of the swing phase and the beginning of a new GC (Perry and Burnfield 2010).

The distance one limb covers from the beginning of the GC until its end is termed stride length. The distance between the HS of one limb and that of the opposite is called step length. The speed at which the COM of the person travels at is refereed to as gait speed (GS).

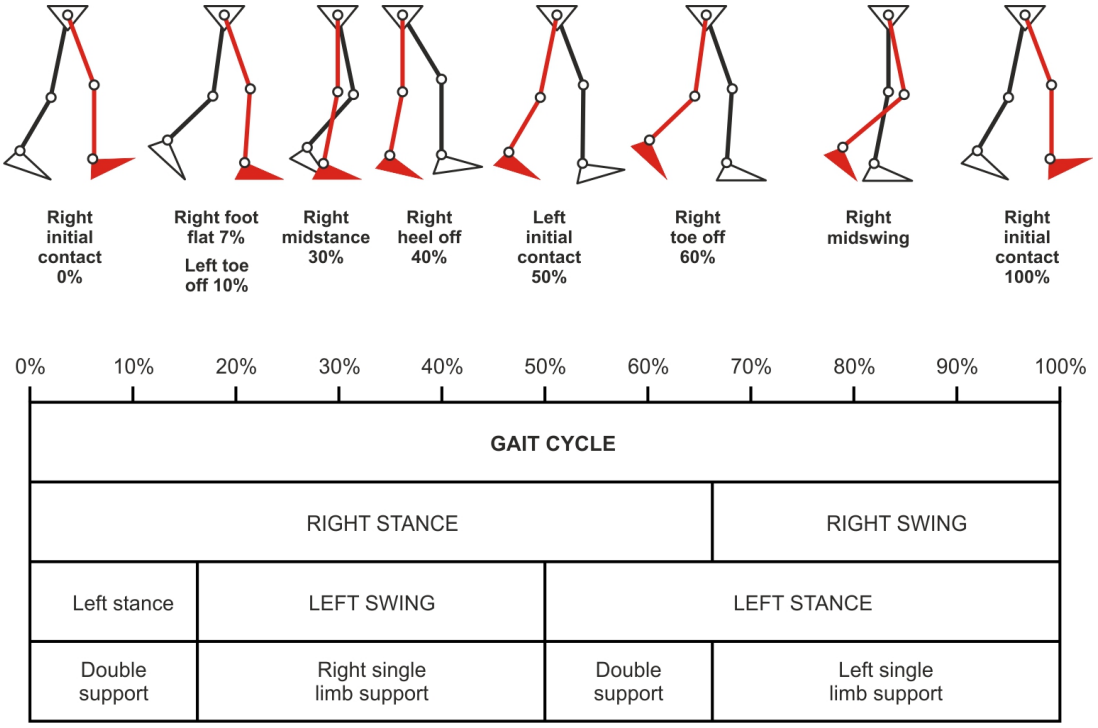

Figure 8.1: Gait cycle (IMAR, University of Dundee)

8.2.2 Biomechanical Model of the human body

Motion of the human body is complex and involves movement of many different parts. To capture every single and slightest movement of every segment is not feasible with the current technology. Vicon® cameras only capture the movement of markers placed on a subject, but the captured data does not yet describe the kinematics of the human body. That is where a biomechanical model of the human body comes into play as it allows calculation of the joint angles and body kinetics (assuming force-plates were used) based on the captured data.

A biomechanical model of the human body divides the body into different rigid bodies (or segments in Vicon® terms) and defines the nature of their movements. The model is based on the anatomy of the human body but involves several assumptions and simplifications depending on the motion that is being studied. To examine the role that foot positioning before foot strike has on ankle sprains the foot would be modelled as a single segment, linked to the lower leg by a

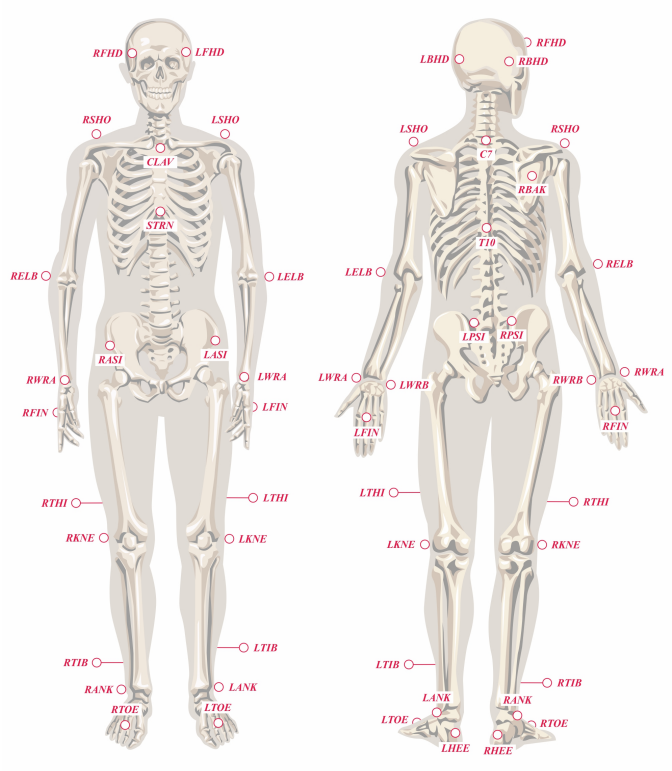

Figure 8.2: PiG® marker set (IMAR, University of Dundee)

hinge joint; we are only interested in plantar-flexion and dorsi-flexion movements. If, on the other hand, we want to study the way the foot adapts and provides stability on uneven surfaces, we would model the foot as a group of interconnected segments and define a more complex joint connection between them.

8.2.3 Plug-in Gait®

Plug-in Gait® (PiG®) is the body model provided by Vicon® (Figure 8.2). It is a combination of two models, one describing the upper body kinetics and the other describing that of the lower body; this research is only interested in the kinematics. PiG® has been shown to produce repeatable results and its sagittal plane kinematics correlate well with the other major models (Ferrari *et al.* 2008). It is also widely used in research and clinical applications.

PiG® divides the upper body into 12 segments: head, thorax, two clavicles (left

and right), two humeri, two radii, two wrists, and two hands. The kinematic data of the upper body, however, is of little interest for this study; it was used only to allow calculation of the subject's centre of mass (COM).

The lower body model is based on a model suggested by Kadaba *et al.* (1990). It divides into seven segments: pelvis, two femurs, two tibiae, and two feet. This allows Plug-in Gait® to calculate the hip, knee, and ankle rotational kinematics, as well as the progression of the pelvis relative to the lab's reference frame (refer to Section 7.4.4). In dynamic trials, the foot segment is defined only by two real markers and as such, is not reliable in measuring inversion/eversion of the foot. For this reason there is a need to create a better model of the foot and ankle that allows measurement of ankle inversion and ankle eversion.

When both upper and lower body markers are present, PiG® allows calculation of the position of the COM of a subject. It has been shown to give good results compared to COM calculations based on the ground reaction force (Gutierrez-Farewik *et al.* 2006).

8.2.4 The Muscle

Muscles are the force generators of the human body; they generate and control movement in our joints. While the muscle fibre is the structural unit of a muscle the sarcomere is the basic unit for muscle contraction. Each muscle fibre consists of several strands of myofibril, which in turn, is formed by serially repeating patterns of sarcomeres. The longer a muscle the more serially arranged sarcomeres it has and the higher its velocity of contraction. The more sarcomeres in parallel the thicker the muscle is and the higher the force it can generate (Nordin and Frankel 2001a).

8.2.5 Muscle activation

Motor neurons of the nervous system act to control muscle activation. A motor neuron connects to several muscle fibres via its end-plates to form one motor unit (MU), which implies that all muscle fibres of a MU will contract simultaneously. The firing of a neuron generates an electrical signal that propagates along the length of the muscle fibres of the MU. This signal is termed muscle unit action potential (MUAP). Usually, several MUs need to be active in order to generate a noticeable contraction in the muscle. The magnitude of the generated force, thus, depends on the firing rate of the motor neuron as well as the number of employed MUs.

Electromyography (EMG) is the study of the muscle's electric signal, which can be detected using special electrodes. While there are two types of electrodes (surface and indwelling) this study opted for the first type as they are non-invasive, easier to use and have an acceptable signal detection. The detected electric signal is a summation of the MUAPs generated by all the MUs in a muscle. The amplitude of the detected signal from a muscle depends on the following factors:

- The diameter of the muscle fibre; the larger the fibre the bigger the amplitude.
- The distance between the MUAP and the electrodes; the larger the distance the smaller the amplitude.
- The tissue and skin separating the electrodes from the active muscle fibres. The skin acts as a low pass filter for the signal.
- The properties of the electrodes and electrolyte used for detection.

Due to the many different factors affecting the amplitude of the EMG signal, it is difficult to directly compare the recorded EMG signals between different

subjects (Basmajian and De Luca 1985).

8.2.6 EMG signal processing methods

The EMG signal recorded by the electrodes is first amplified and digitised before it is sent to the computer for analysis. Due to the nature of the amplifiers used, the resulting signal was randomly distributed between the negative and positive side of the scale; its average was therefore zero (Basmajian and De Luca 1985). While the unprocessed signal provides qualitative information when visually inspected by the trained eye, motion artefacts and the random nature of the signal make it difficult to perform any quantitative analysis without processing.

The first step of processing is to filter the digitised signal to remove noise and motion artefacts. For general applications, it is recommended to apply a $10\,Hz$ to $20\,Hz$ high pass filter and $500\,Hz$ low pass filter. This is a bandwidth filter that removes elements of the signal that has a frequency outside the $20\,Hz$-$500\,Hz$ range.

The next step is to fully rectify the signal by inverting all negative elements of the signal to give an absolute positive value. This permits calculating the Average Rectified Value (ARV) of the signal over a specified time interval. Root Mean Square (RMS) is another method used for amplitude estimation of EMG signals over a specific time interval and is recommended over the previous method (Basmajian and De Luca 1985). RMS can be applied to both rectified and unrectified signals, yielding the same result.

Spectral analysis techniques are also used in the analysis of EMG signals and can reveal further information regarding the contraction of muscle such as muscle fatigue (Basmajian and De Luca 1985). Fast Fourier transform (FFT) is a commonly used method for estimating the frequency content of a signal. Of interest

in the obtained power density spectrum, are the mean frequency, the median frequency and the bandwidth of the spectrum (Basmajian and De Luca 1985).

8.3 Platform data extractor

The researcher interacted with the platform via a web browser. The platform data were recorded using the *save* function of the web browser. Unfortunately the output file is not easily processed using Excel® and Matlab® as data are not arranged in columns (Figure 8.3). As a result the researcher has to copy and paste each set of values and arrange them into columns manually. This is a time-consuming task considering the number of files to be processed. For this reason a program (Figure 8.4) was specifically written in-house that automatically rearranges the data in a suitable format. This program is also capable of batch processing data. The researcher needs to only point the program at the folder containing the data files and hit the *Extract Data* button and the program automatically processes all the files in that folder saving a new properly formatted copy of each file. These new files are saved with the same name as the previous ones, with the addition of "E" added at the beginning of each file name to differentiate the two.

8.4 Data management

8.4.1 Trials indexing

In order to simplify the task of automated data indexing and processing, the researcher must create an Excel file for each of their subjects. These files should contain the name of the useful trials in one column. Each Excel® file should be named as the name of the subject this file refers to. When collecting data

```
Microchip TCP/IP Stack Home Mr. Robot
      Home Features Architecture Stack Footprint

      Welcome!
      Stack version: v3.75
      Build date: Aug 27 2009 14:58:24This site is powered by a Microchip PIC
      microcontroller running a Microchip TCP/IP Stack. Everything you see is
      served through a Microchip PIC18F97J60 family Ethernet module.

      Actions
      Auto Mode
      Modes:
      Angle/pwm value

      Manual Mode
      Direction
      Other
      Status
      ON-override-zeroing-start233 92 239 40
      Inversion angle:-1
      flexion angle::0
      rotation angle:0
      Strain value:7
      Pwm inv-flex-rot:0 0 0
      Direction inv-flex-rot:171 55 138
      LED, other:36 170 10 10 20 50 13 19
      MOdes:onset-midset-end0 0 0
      Target angle:inv-flex-rot15 15 8
      valve close:inv-flex-rot13 20 36
      Inversion angle values:
      -1 -2 -2 2 26 70 117 170 222 278 342 400 436 460 482 501 516 529
      534 530 523 512 499 484 478 482 488 494 498 502 504 505 505 505 506 507
      514 516 518 521 524 527 530 531 531 530 527 522 513 501 485 468
      flexion angle values:
      1 1 1 1 1 2 19 65 119 176 242 309 367 428 475 479 473 466
      459 459 469 478 479 478 478 477 477 477 477 476 476 476 477 478 479 481
      513 536 552 558 560 561 565 571 574 573 571 568 564 557 545 530
      rotation angle values:
      1 1 1 1 2 1 0 1 1 1 0 0 1 2 2 3 4 34
      95 165 233 298 352 375 370 354 335 322 321 324 327 329 329 329 329 329
      329 329 328 328 326 322 315 309 306 306 306 306 306 306 306 307
      Strain gage values:
      14 14 14 9 5 9 10 8 9 9 12 18 20 21 23 26 19 25
      27 25 24 22 21 19 17 16 16 16 17 18 18 18 18 18 19 19
      20 21 21 22 22 22 22 23 22 21 20 19 17 16 13 10
```

Figure 8.3: Platform raw data

the researcher must add "-#" at the end of the name of each platform file; "#" would be a number corresponding to the foot condition of that trial. This would allow Matlab to automatically identify the foot condition of each trial.

The Excel file can also be used to document issues relating to the trials (e.g. missing synchronisation signal for a certain trial). Such notes should be inserted in a column with the headline "general notes"; the current Matlab modules will ignore this section.

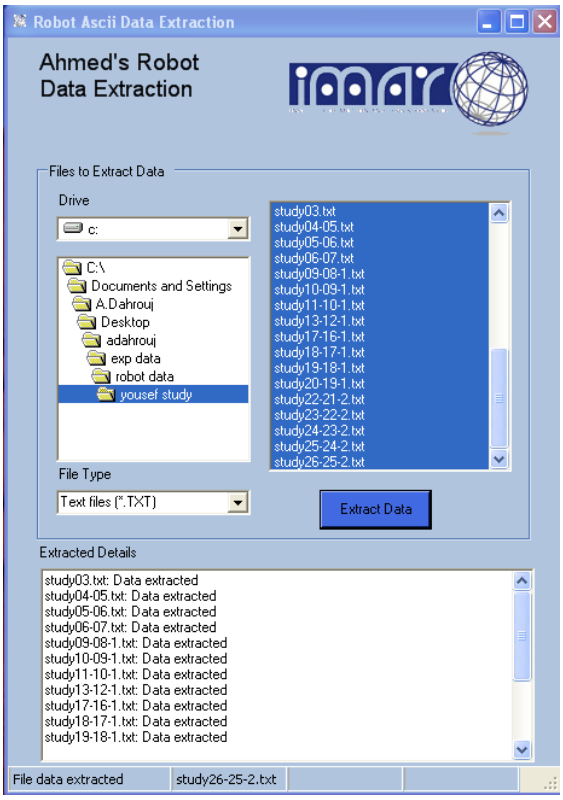

Figure 8.4: Robot Data Extraction software

8.4.2 Files agreement check

The experimental study generated a huge number of files; for the 29 subjects studied, there were approximately 8000 files. These files, however, were not readily usable, with Vicon® having up to five files per trial. Files of successful trials were thus processed reducing the number into 2835 useful ASCII files. The ASCII files were then categorised into three main folders: Vicon®, EMG, and Platform. Inside each of these folders, is a folder for each subject named as the subject's name; ASCII files of successful trials for that subject were copied into it. The entire procedure of processing and organising the files was manually conducted by the researcher. As a consequence errors were unavoidable even though great care was taken to ensure the data were organised correctly.

Double checking that large number of files visually would have been very time-consuming and not 100% accurate. Knowing that one wrong file could distort

the entire database of a subject; a Matlab® script was written to check for any possible errors.

Each subject had one folder with their name allocated, in each of the three main folders. The script compared the names of the files for each subject between the three folders and tabulated all differences found in a clear form. The researcher could then easily correct errors.

8.4.3 Data indexing

The ASCII files contained all the captured data but unfortunately not in a properly formatted and organised form. The data files were spread across different folders, making access ambiguous. Moreover, the ASCII format is not a native file format for Matlab®. Reading ASCII files, therefore, takes time and hinders the development of the processing software. To overcome these problems, a Matlab® script, *index data*, was written.

Index data (Figure 8.5) uses the Excel® files (refer to Section 8.4.1) to decide which subject and trial to act on. This means if the researcher needed to exclude a trial that was missing, for example the synchronisation signal, they only need to delete the trial number from the Excel sheet and rerun the script.

Index data first creates a five-column cell[1] matrix. It then reads the names of the Excel files and stores them in the first column as subject names. After that, it imports each Excel file and reads it, ignoring the *General notes* section of the file. *Index data* now has the successful trial numbers for each subject and their corresponding foot condition. In the second column the script writes a number that describes the order of footwear used in the experiment for each subject:

[1] A cell in Matlab® can contain any type of data like integers, floats, characters...It can also contain a matrix of cells making it the choice for storing complex data.

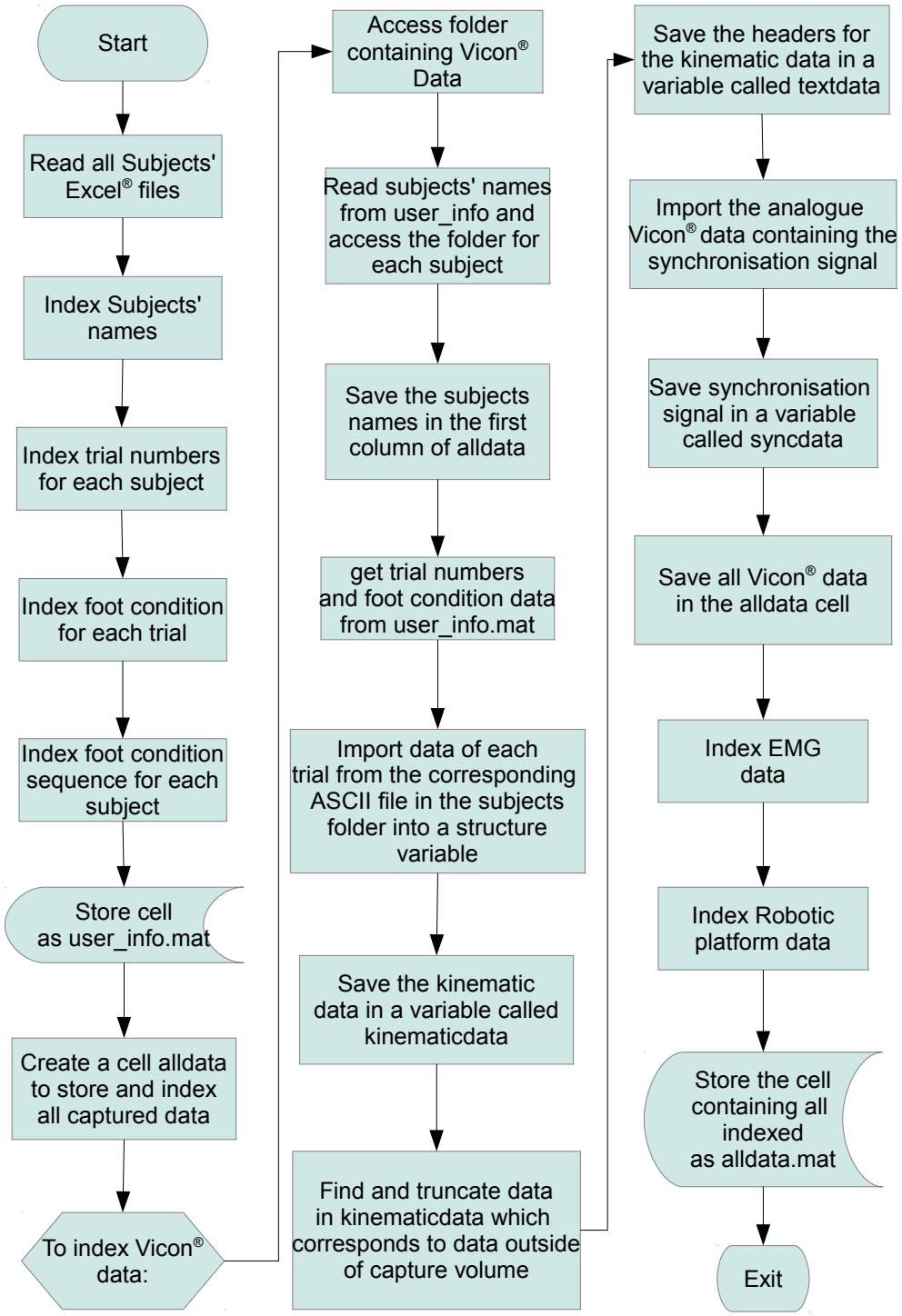

Figure 8.5: Flow chart of the *Index data* module

One means a subject did the barefoot trials first, followed by shoes1 trials and ending with shoes2 trials.

Two means a subject did the shoes1 trials first, followed by barefoot trials, and ending with shoes2 trials.

Three means a subject did the shoes1 trials first, followed by shoes2 trials, and ending with barefoot trials.

The script infers this by comparing the numbers of the first trial in each condition. Take for example this scenario:

1. The first trial of the barefoot condition is trial number 5.
2. The first trial of the shoe1 condition is trial number 20.
3. The first trial of the shoe2 condition is trial number 28.

The barefoot trial has the lowest number, meaning it was first in order. Shoes2 has the biggest trial number meaning it was the last in order, and shoes1 condition was second in order. In this case, *Index data* writes *1* in column two for this subject.

In column three, the script writes the trial numbers of the barefoot condition. Column four contains those of shoes1 condition and column five those of shoes2 condition. The resulting 4×30 cell matrix is saved in Matlab®'s native format, *.mat,* under the name *user_info* for later ease of access.

Index data then creates another 4×30 cell matrix where all data is saved. The first row is the header of the matrix containing the titles of the columns. The first column contains the names of the subjects acquired from *user_info*. The second column contains the Vicon® data for each subject. The third contains the EMG data, and the fourth contains the platform data. Each cell in these three columns is further divided into three cells labelled according to the foot condition; it contains the data of only that foot condition.

The script first processes files in the Vicon® folder, accessing each subject's folder separately, based on the information from *user_info.* It then processes only the trials whose numbers are indicated in *user_info*, the same also being done for the EMG and Platform data.

Vicon®'s ASCII files contain kinematic data as well as data from the synchronisation signal. The data are, however, captured at different frequencies and thus have different time scales. *Index data* divides the file into two different matrices, kinematic data and synchronisation data, and stores each in a different cell within the same row. The kinematic data contained a lot of zero filled rows at the beginning of the file. These rows correspond to the time in which the subject was outside the capture volume. *Index data* detects those rows and truncates them, leaving only the useful data, saving memory space and increasing performance. The script also generates a text matrix, textdata, referencing the columns in *kinematicdata;* for example column three in *kinematicdata* was referenced as the x-axis component of the left front head marker, *LFHD(X)*. These three cells were all saved in a single row whose first column contained the trial number.

The EMG ASCII file contained six columns:

- The first contained the time data.
- The middle four contained the EMG data, three of which correspond to the captured muscles and one zero filled (with some spikes) column; this was due to the fact that the Portilab has pairs of channels. This column was detected by the script and truncated accordingly.
- The last column contained the synchronisation signal data.

The end of the EMG file contains lots of zero filled rows. This is caused by the Portilab® software and these rows are also truncated. The data are saved in one cell, *emgdata*, and the trial number in another.

Platform data contains lots of different information, some of which (such as the valves' closing times) are used to help advance the development of the platform. *Index data* reads only the angles and strain gauge data. It saves them in a cell, *robotdata*, and the trial number in another cell.

8.5 A custom model for the foot and ankle

The PiG® body model does not provide accurate foot inversion/eversion data since it models the foot using two markers only (refer to Section 8.2.3). For this reason a custom model for the foot was specifically written in-house using Bodylanguage, the programming language used for writing body models in Vicon®. The complete code of this model is presented in Appendix D.

The model was designed to allow measurement of foot inversion and plantar-flexion. Since part of the study in which this model will be used involves subjects wearing shoes, which are more rigid and not as flexible as the foot; it adds little benefit to model the many different segments of the foot. Instead the foot is modelled as one rigid segment.

To fully describe a rigid body in 3D space would require at least three non-collinear markers attached to it. The custom foot model, thus, requires five markers to be attached to the foot (Figure 8.6). These extra markers are required because the model defines the foot differently when calculating foot inversion than when calculating foot plantar-flexion; this was to simplify the design and allow better control over axis definition. The five markers are attached to the following parts of the left foot:

- Right medial malleolus (RMMAL).
- Left medial malleolus (LMMAL) .
- Left distal 1st metatarsal (LD1MT) .

(a) Barefoot **(b)** Shoes 2

Figure 8.6: Marker placement using the custom foot model

- Left distal 5th metatarsal (LD5MT) .
- Left proximal 3rd metatarsal (LP3MT).

The model first calculates the ankle joint centre (LAJC2) as the midpoint of the segment defined by the RMMAL and LMMAL points. The left foot centre (LFC) is similarly calculated using the LD1MT and LD5MT points.

Foot inversion is defined as the rotation of the foot segment relative to the tibia segment around the axis defined by the line joining LP3MT to LAJC2, where the foot is defined as:

FOOTi = [LAJC2,LP3MT-LAJC2,LD1MT-LTOE,xzy]

and tibia is defined as:

LTIBIAi = [LAJC2,LP3MT-LAJC2,LMANK-LANK,xzy]

In Bodylanguage, this implies that the foot is modelled as a plane defined by a three dimensional Cartesian coordinate system which centre is LAJC2. The x-axis of this system is defined by the line joining LP3MT and LAJC2. The z-axis is defined by the line perpendicular to both the x-axis and the line joining

LD1MT and LTOE (notice the xzy at the end of the defining statement which dictates the order of axis definition). Finally the z-axis is defined by the line perpendicular to both the X and Y axes. The same can be applied to the tibia. Since the foot and tibia, as defined here, share the same x-axis, the motion between the two is limited to 1-DOF with the axis of rotation being the line joining LP3MT and LAJC2.

For plantar-flexion the foot is defined as:

FOOTf = [LFC,LANK-LMANK,LP3MT-LAJC2,yzx]

and tibia is defined as:

LTIBIAf = [LAJC2,LANK-LMANK,LANK-LKNE,yxz]

This means that foot plantar-flexion is the rotation of the foot relative to the tibia around axis defined by LANK and LMANK.

Tibia progression is defined as the rotation of LTIBIAf relative to the laboratory reference plane.

8.6 Platform data processing

Platform data were processed using the *PROBOT.m* script. *PROBOT* generates a matrix cell variable, p_robot_data, that contains the following information[2] (Figure 8.7):

- The degree of rotation of the foot-plate around all three axes versus time. These are acquired from *alldata.mat*.
- The angular velocity of the foot-plate around all three axes versus time. These are calculated by differentiating the angle data over time.

[2]Some of these information will only be used for optimising the performance of the platform

- The angular acceleration of the foot-plate around all three axes versus time. These are calculated by differentiating the angular velocity data over time.
- Maximum degree of rotation around each of the three axes.
- Maximum angular velocity around each of the three axes.
- The strain gauge values versus time. These are acquired from *alldata.mat*. These data describe the bearing load on the left foot. When the platform starts rotating, it was expected that the bearing load would decrease then increase when the platform started decelerating (refer to Section 10.2.1).
- The time instants at which the foot-plate starts rotating around each of the three axes. For a given axis of rotation, this instant is defined as the moment when angular velocity exceeds a certain threshold of $10^{\circ}/sec$. This eliminated false detection due to movement of the foot-plate caused by the weight of the subject when they first stepped on the foot-plate.
- The time instants at which the foot-plate "stops" rotating around each of the three axes. For a given axis of rotation, this instant is defined as the moment when angular velocity axis drops below $0^{\circ}/s$. This was not necessarily the same instant at which maximum rotation was reached.
- The degree of rotation around each axis when the foot-plate "stops" rotating around it.

The robotic manipulator sampled data at a frequency of $85\,HZ$, while Vicon® data were sampled at a rate of $100\,HZ$. Since the platform data was used alongside Vicon® data, and to avoid having to deal with a different timescale, *PROBOT* automatically up-sampled the frequency of the platform data to $100\,HZ$.

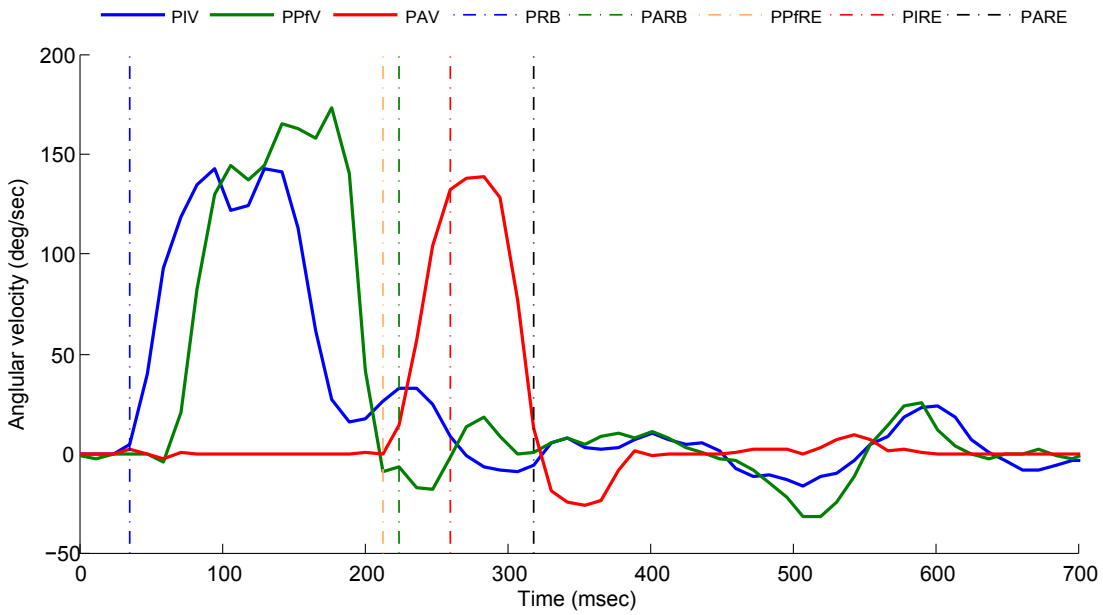

Figure 8.7: Platform events detection based on rotational velocity (PIV = Platform inversion velocity; PPfV = Platform plantar-flexion velocity; PAV = Platform adduction velocity; PRB = Platform rotation begins; PARB = Platform adduction rotation begins; PPfRE = Platform plantar-flexion rotation ends; PIRE = Platform inversion rotation ends; PARE = Platform adduction rotation ends)

8.7 Kinematic data processing

8.7.1 Markers check

Vicon®'s *auto-label* function, used in labelling the markers, was unreliable (refer to Section 7.5).

Check_markers automatically checked for incorrectly labelled markers in all Vicon® trials. It was designed to examine the labelling of the head markers, the thorax markers, and the feet markers, where mistakes were visually difficult to see (refer to Section 7.5).

Check_markers employs a simple yet robust and reliable algorithm. It works by comparing the position of the markers of one body segment together, at the instant when the subject steps on the foot-plate. That instant is easily identi-

fiable by the presence of the synchronisation signal. To check the thorax markers, for example, check_label first acquires their coordinates from *alldata.mat* at the instance where synchronisation signal is found. The position of those markers relative to each other is known and remains the same as the thorax is a rigid body. This script thus checks that:

- The STRN and T10 markers are both below the CLAV and C7 markers.
- The STRN and CLAV markers are both in front of the C7 and T10 markers.
- The RBAK is to the right, when looking at subject from behind, of all the other four markers. In other words, the value of the y-axis component of RBAK is smaller then that of the other markers.

If any of these conditions was not met, the thorax segment was flagged as mislabelled for that specific trial and subject. The same thing was performed for the other three segments[3]. After the script had checked all trials for all subjects, it generated a table highlighting all the mislabelled segments and in which trials and subjects they were found.

8.7.2 Gait parameters detection

There are several ways of capturing gait parameters. Force plates embedded in walkways, and synchronised with Vicon®, allows detection of such parameters. Vicon® then extrapolates for steps outside the force plate. The robotic manipulator and force-plates present in the Sports Laboratory, however, were fixed to the ground and could not be aligned in a straight line. The force-plates are also positioned more than one stride away from the platform and lay outside the capture volume of the Vicon® cameras, making it difficult to take advantage of the force-plates for gait events detection. In addition, Vicon® does not perform well

[3]There are 2 foot segments, left and right.

in detecting gait events when subjects are not on the force plate. Foot switches that could be connected to the EMG acquisition device are also used for this purpose but they would necessitate the use of socks when subjects are barefoot, which may negatively affect the proprioception of the foot. For this reason it was necessary to devise a reliable way of detecting those parameters, hence the *gait_parameters* Matlab® module was developed.

Gait_parameters requires two input arguments; the kinematic data of the ankle and toe. It is called in the *PVICON* (refer to Section 8.7.3) module when processing each trial. The kinematic data of the ankle and toe markers supplied to this function are position data, so *gait_parameters* differentiate these data twice to obtain velocity and acceleration data.

Subjects in the laboratory walk forward along the x-axis. At foot strike, and during the stance phase, the foot ceases to move along that axis. Hence, ankle velocity data in the x-axis are first used by *gait_parameters* to identify the total number of heel strikes, and approximate their occurrence. Following that, *gait_parameters* analyses each step alone and identifies the precise occurrence of HS, FF, and TO events. It also indicates whether a subject landed with their heel first, or if it was a foot flat or toe strike (these are currently categorised together).

When a subject's foot lands with the heel first, and assuming they are not just walking on their heels, the front of the foot will rotate forward around an axis passing approximately through the point of contact between the heel and the ground. In other words, just before HS, both the heel and toe markers are moving downwards in the Z direction at a relatively similar speed. Once the heel hits the ground, its vertical speed will be almost zero, while that of the toe will continue unhindered. Thus *gait_parameters,* analyses this velocity difference to detect HS. When it cannot detect such an instant, the assumption of landing

with heel first is discounted, and an alternative method is used to detect foot strike.

This method examines the acceleration of the ankle in the vertical direction. While a subject is moving their foot towards the ground, the foot is gradually decelerating in the vertical direction until foot contact, where the deceleration increases dramatically and is almost at its maximum. This instant is defined by *gait_parameters* as foot strike.

Foot flat is identified as the moment when the toe marker almost stops moving in the vertical direction. Sometimes however, this condition is not met, and ball strike is then reported as the instant when the toe marker is greatly decelerating.

Toe off is the most difficult to identify and least accurately which is due to the absence of a marker on the distal end of the toe. The way *gait_parameters* identifies TO is by first checking for a movement of the toe marker in the Z and X axes of the laboratory. This, however, is not the instant of TO due to the location of the toe marker on the proximal end. This implies that when this marker starts moving, the distal end of the toe may still be on the ground. TO is, as such, identified as the instant when the entire foot is moving at relatively the same speed in either the X or Z axis. The reasoning behind this, and assuming subjects are walking normally with the heel rotating around the toe before TO, is:

1. Before TO, the heel is moving upwards much faster than the toe marker, since it is farther away from the axis of rotation located at the front foot.
2. At TO, the rotation of the foot around an axis passing through the contact area between toe and ground ceases to exist, and the whole foot is moving at relatively the same speed.

In order to test and validate the performance of the *gait_parameters* module, its results were compared to those obtained using the force plate. Existing data

consisting of trials from seven different normal subjects were used for the validation test. Table 8.1 highlights the differences between results obtained using the *gait_parameters* module and those obtained using the force plate data. In HS, the differences between the two methods are minimal with a maximum of only one frame difference between the two. TO data showed similar results, except for one subject, where the module detected TO four frames earlier. Further investigation revealed that the toe markers for that subject were placed higher up the foot.

8.7.3 Vicon® data processing

PVICON is used to process Vicon® data files. As all other modules, *PVICON* automatically loops through all the trials of a subject and through all the subjects found in *all_data.mat*. For each trial, *PVICON* generates and records the following data:

- Time at which the synchronisation signal was detected by Vicon®. This is an important instance and serves as the reference point for all three systems.
- Time, relative to the synchronisation signal, at which special relevant events occur.
  - Left foot heel strike on the foot-plate.
  - Left foot foot flat on the foot-plate.
  - Left foot toe off on the foot-plate.
  - Left toe off strike of the step previous to the foot-plate one.
  - Left heel strike of the step following the foot-plate one.
  - Right heel strike before the platform.

Table 8.1: Differences in gait events detection between the *gait_parameters* and the force plates detection methods

Subject	Trial	HS difference	TO difference
1	1	-1	1
2	1	-1	1
2	2	0	0
2	3	0	0
3	1	0	-4
3	2	-1	-4
4	1	0	0
4	2	1	0
5	1	0	-1
5	2	0	0
6	1	0	-1
6	2	0	1
6	3	0	0
7	1	-1	0
7	2	-1	0
7	3	-1	0
7	4	0	0

  - Right toe off just before the platform starts rotating.
  - Right heel strike following the platform rotation.
  - Maximum inversion of the left foot between FS and TO.
  - Maximum plantar-flexion of the left foot during platform rotation.
- Duration of right foot stance just before the platform rotates.
- The degree of flexion and rotation of the left foot when it lands on the foot-plate. This is important since foot position at foot strike has been shown to be a risk factor for ankle sprains (refer to Section 2.2.2).
- The landing position of the foot on the foot-plate. This data provides two important elements:
  - The first is related to the robotic manipulator and could allow improving the control algorithm resulting in better rotational accuracy at faster speed. This could only be usable, however, if the subjects landing position was detected in real time, and available to the microcontroller.
  - The landing position could also have an effect on the muscles and body reaction. The further the foot from the axis of rotation, the bigger the vertical distance it will travel and the more linear momentum it will have before the platform stops rotating. Our hypothesis is that this may generate bigger reactions due to the increased resultant forces on the foot required to negate that extra momentum.
- Maximum inversion of the left foot due to foot-plate rotation.
- Maximum plantar-flexion of the left foot due to foot-plate rotation.
- Distance between the right and left foot (in the x-axis), the moment the left foot strikes the platform.

- Data describing the behaviour of the right foot, during induced supination of the left foot:
  - Its stride length.
  - How far the right foot has landed in front of the left foot.
  - Its average speed in the x-axis during the platform's rotation.
  - Its maximum speed in the x-axis.
- Left foot stride length starting with the platform foot strike.
- The distance the left ankle drops due to the rotation of the platform.
- The distance the COM drops due to the rotation of the platform.
- Average gait speed of the subject.
- The time between right toe off just before the platform and the beginning of platform rotation.
- Continuous kinematic data that describes the effect of induced foot supination on the body movement.
  - COM of the subject in the y-axis relative to the position of the left and right feet in the y-axis.
  - COM of the subject in the x-axis, relative to the position of the left foot in the x-axis.
  - Hip flexion/extension and adduction/abduction.
  - Knee flexion/extension.
  - Tibia progression around the X and Y axes.
  - Left foot flexion and inversion.
  - Gait speed of the subject.

PVICON first reads the Vicon® data consisting of *kinematicdata*, *syncdata*, and *textdata*, which are now stored in *all_data.mat* (refer to Section 8.4.1). After that it searches for the synchronisation signal in *syncdata* and detects the time of its occurrence. The synchronisation signal however, has a different timescale than that of the kinematic data, as it was sampled at $500\,Hz$ while the Vicon® cameras were capturing at a rate of $100\,frames/sec$. For this reason the time of the synchronisation signal was rescaled by dividing its value by five. The detected synchronisation signal, nonetheless, was not the real signal as the synchroniser had an inherent fixed delay of $50\,ms$ (refer to Section 6.5). To account for this, *PVICON* subtracts $50\,ms$ of the synchronisation signal recorded time.

Next, *PVICON* uses the *gait_parameters* module (refer to Section 8.7.2) to acquire the gait parameters of the trial. The synchronisation signal was generated by the platform when the subject stepped on the foot-plate, for this reason the left stride with the heel strike time closest to that of the synchronisation signal was considered as the stride on the foot-plate. *PVICON* also looks at the right foot strides just before and after the foot-plate.

The kinematic data of the foot calculated using our foot Vicon® module were not calibrated; *PVICON* automatically handled this task. The markers on the tibia and ankle were not moved for the duration of the experiment. For this reason, the tibia can be used to calibrate foot flexion. Foot flexion is the rotation of the foot around the y-axis relative to the tibia; as such, it is set to zero when the foot is flat on the ground and the tibia is in a vertical position. Foot inversion is set to zero at foot flat.

The position of the COM is defined using the laboratory reference frame. This representation is, however, of very little significance since the subject does not walk the same way during each trial. Any differences in the values of the COM between different trials could as such be due to this difference in walking; it

will be impossible to check for changes induced by the platform rotation. To address this issue, *PVICON* was written to calculate the position of the COM relative to the left foot position in the X and Y directions. The value of the COM in the z-axis was also modified to account for the effect of the different sole thicknesses in the shoes. *PVICON* then subtracts a fixed value equal to the shoes sole thickness used from the z-axis value of the COM.

People walk differently, and even though the gait cycle for each person is similar, a subject does not walk in exactly the same way nor with the same speed for each trial. The platform was designed and programmed to allow control over the delay between when the subject first steps on it and when it rotates. For this specific research the delay was set to $50\,ms$ (that does not include the delay from the valves (refer to Section 5.4.1)), so as the subject will be in single limb support when it starts rotating. In some rare cases, nonetheless, subjects would walk slower resulting in premature rotation. *PVICON* intelligently checks for those trials and flags them, so they may be excluded from the main analysis. Another issue is marker tracking loss, usually because the marker was knocked out of position by the rotation of the platform; these trials had missing data and were as such also flagged.

8.8 EMG data processing

PEMG was written to process EMG data. It reads the raw EMG data from the *all_data* variable. The raw data for each trial were divided into a five-column matrix, the first containing the time signal, the middle three containing the muscle activity data for the three captured muscles, and the last containing the synchronisation signal.

PEMG first checks for the synchronisation signal and acquires the time of its

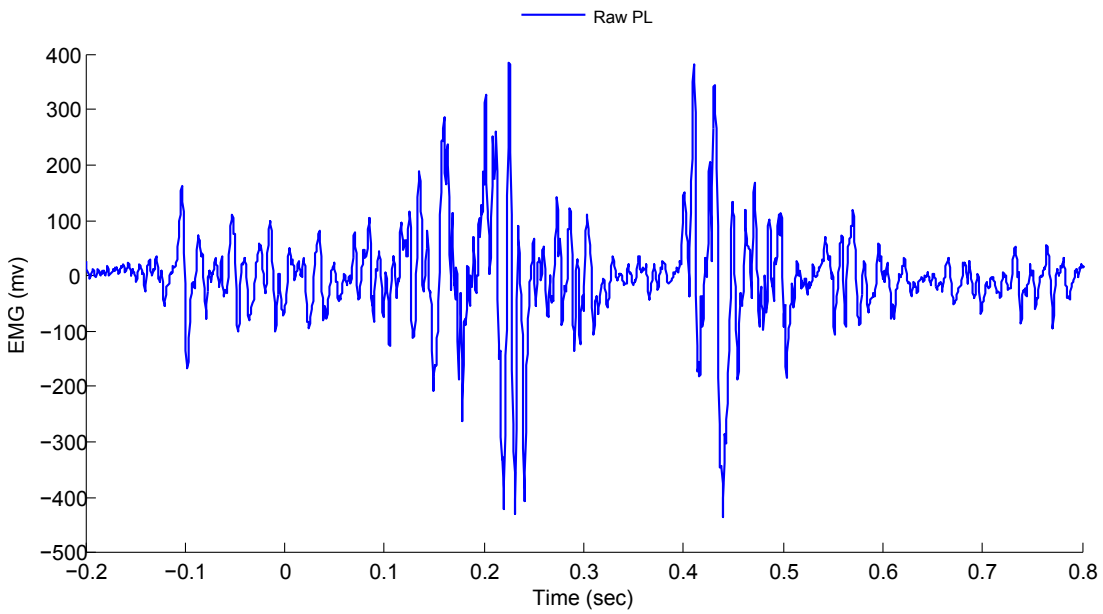

Figure 8.8: Raw EMG signal

occurrence. It then generates a band pass Butterworth filter of the 6th order with acting frequencies of $20\,Hz$ and $500\,Hz$. The filter is then applied on raw EMG signals (Figure 8.8) using Matlab®'s *filtfilt* function; *filtfilt* apply the filter forwards then backwards thus avoiding the time shift which usually occurs when filtering a signal. Following that, *PEMG* rectifies the filtered signals and then applies an envelop low-pass filter with an acting frequency of $10\,Hz$ (Figure 8.9).

PEMG then acquires specific events time data calculated previously using *PROBOT* and *PVICON* modules (refer to Section 8.6 and 8.7.3). These values are then scaled to be compatible with the $2048\,Hz$ sampling frequency of the EMG data. *PEMG* uses these data to create 11 time intervals of specific interest. *PEMG* calculates the mean, RMS, integral, and maximum values of the EMG signals in those intervals. These are as follows:

1. Stance phase of the left foot step at LFS to the platform (i.e. LFS until LTO).

2. From LFS to the platform until the beginning of foot-plate rotation.

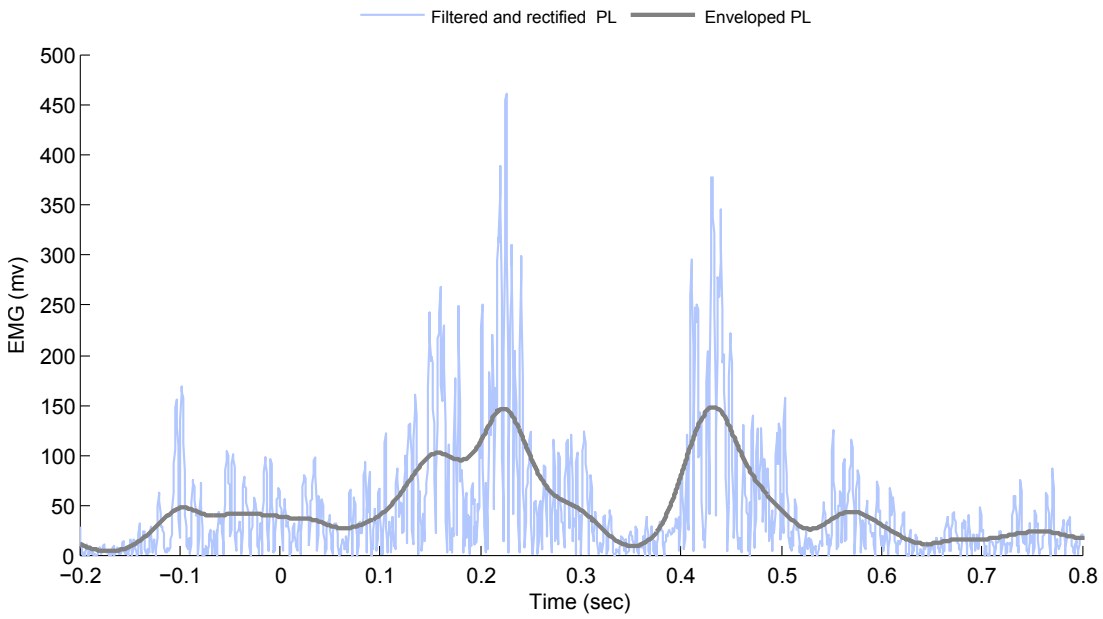

Figure 8.9: Filtered and enveloped EMG signal

3. From the beginning of foot-plate rotation until LTO.
4. From the beginning of footplate rotation until it stops rotating in flexion and inversion.
5. From the beginning of foot-plate rotation until it stops rotating in adduction.
6. From the moment the platform stops adducting until LTO.
7. From LTO until LHS of the step after the platform.
8. The stance phase of the left step prior to the platform (estimated using the stance time of the left step on the platform).
9. The stance phase of the left step prior to the platform (estimated using the stance time of the right step just before the platform).
10. The stance phase of the left step following FS to the platform (estimated using the stance time of the left step on the platform).
11. The stance phase of the left step following FS to the platform (estimated using the stance time of the right step just before the platform).

The limited number of Vicon® cameras that were available at the time of the current study meant that the LHS of the step prior to the platform, and the LTO of the step after the platform were not captured (refer to Section 7.4.3). For this reason the interval time for those steps was estimated using the stance time of the left step on the platform and the right step just before the platform.

Finally, *PEMG* performs a frequency analysis using the *freq_ana* function (refer to Section 8.10) of the EMG signals. This analysis is applied over the three step intervals: the step prior to the platform, the step on the platform, and the step after the platform. *Freq_ana* generates two statistics for each muscle, the mean frequency and the median frequency.

8.9 Data output

8.9.1 Allplots

Allplots was created to generate all the graphs needed to inspect and visually analyse the data. *Allplots* can batch process data and automatically generate graphs for multiple trials and different subjects, allowing for easy comparison. As in all other Matlab® modules, it was designed to be used by non-technical researchers who may have only basic or no knowledge of Matlab®. *Allplots* can automatically generate the following:

- Plots of Vicon® and robotic platform data combined on the same graph. Robotic platform data are automatically up-sampled to the same frequency as Vicon data.
- Plots of EMG, Vicon® and robotic platform data combined on the same graph. Both Vicon and robotic platform data are up-sampled to the same frequency as EMG data.

- Plots with double y-axis which facilitates plotting different sets of data that has a different y-axis range.

Allplots can also plot graphs with the x-axis normalised to one complete gait cycle. This facilitates comparing left and right body kinematics on the same graph. This module will also automatically generate the necessary legend for the graph. Many of the plots in this thesis (mainly the ones in Chapter 9) were generated by this module.

8.9.2 Stat_export:

Stat_export (Figure 8.10) exports the results of the processed data to a format suitable for use with SPSS® (version 17.0), the statistical analysis program used throughout this study. This module also randomly selects trials from each subject in order to obtain an equal number between the three foot conditions. All data normalisation was also performed using this module.

8.10 Other modules

There are several more modules that have been developed for the purpose of this study, but are not presented here as they have a minor complementary role. For a complete list of modules, please refer to Appendix I.

Emgfreq*:*

Emgfreq applies frequency analysis on an EMG signal. It transforms the signal into frequency domain using discrete fast Fourier transform (FFT). The power of the transformed signal is then calculated to obtain the power density spectrum of the signal. Finally, the mean and median frequency of the power density spectrum are calculated.

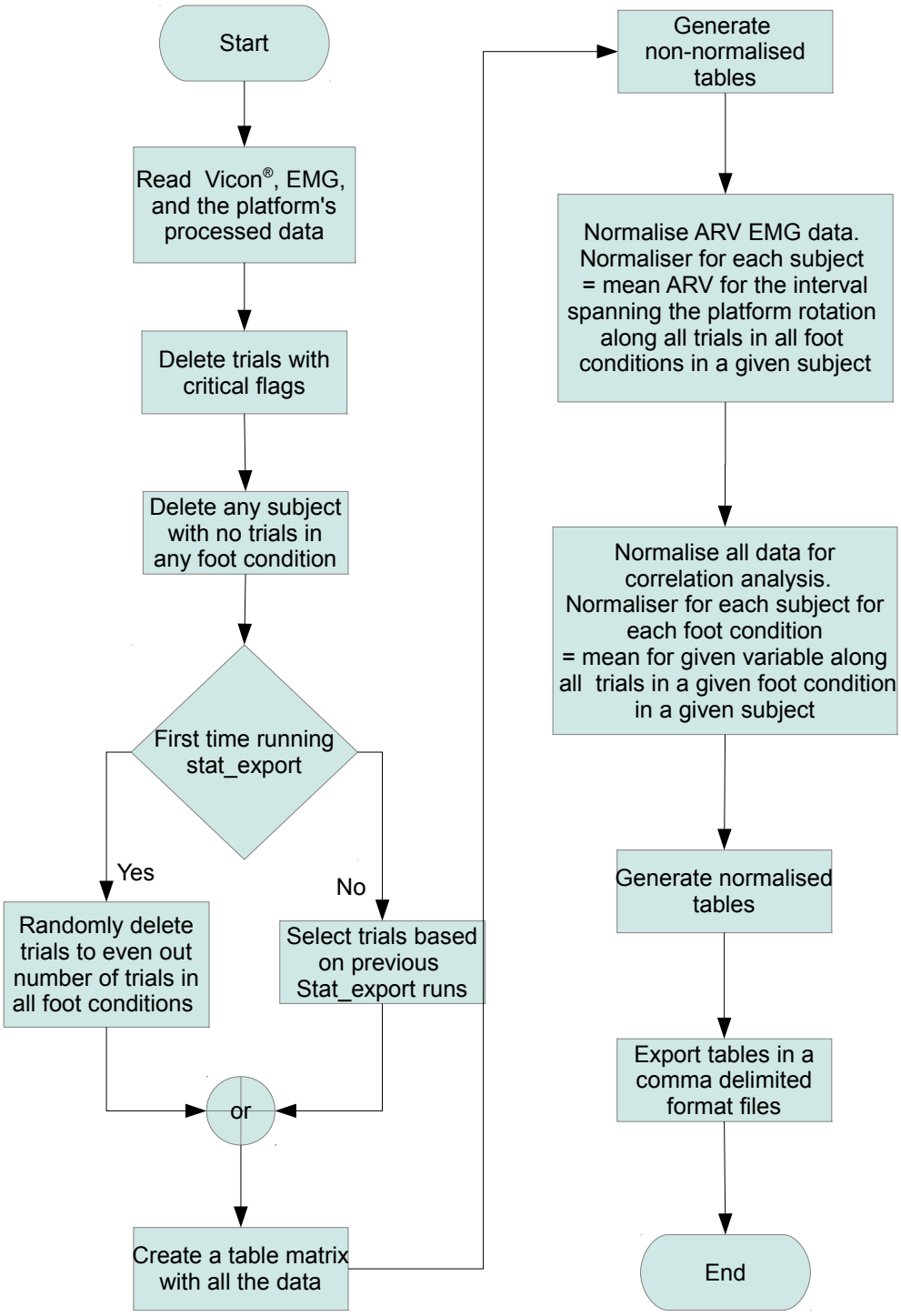

Figure 8.10: Flow chart of the *Stat_export* module

EMG_activity:

EMG_activity was an attempt to automatically detect EMG activity interval corresponding to a GC when kinematic data were missing. Mainly for the steps before and after the platform. The basic idea of how the module works and the obtained results are summarised below.

In normal gait, the PL, LG, and TA are not active for the entire GC, but only for a part of it (usually less then 60% of the GC). The noise threshold of the EMG signal is thus calculated as the mean of all 30% lowest values of EMG signal. All parts of the signal with a value higher than the threshold are considered to correspond to muscle activity. Activities that are shorter than a certain time are filtered out to remove random spikes (usually motion artefacts) in the signal.

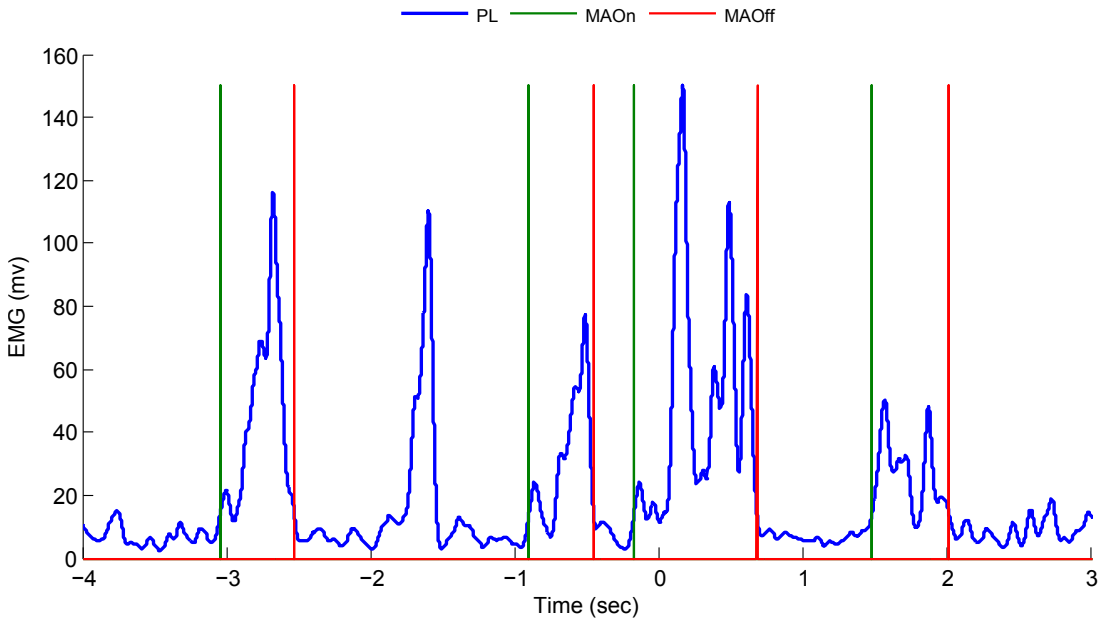

Figure 8.11: EMG activity automatic detection with error due to a short activity interval (PL = PL muscle activity, MAOn = beginning of muscle activity, MAOff = End of muscle activity)

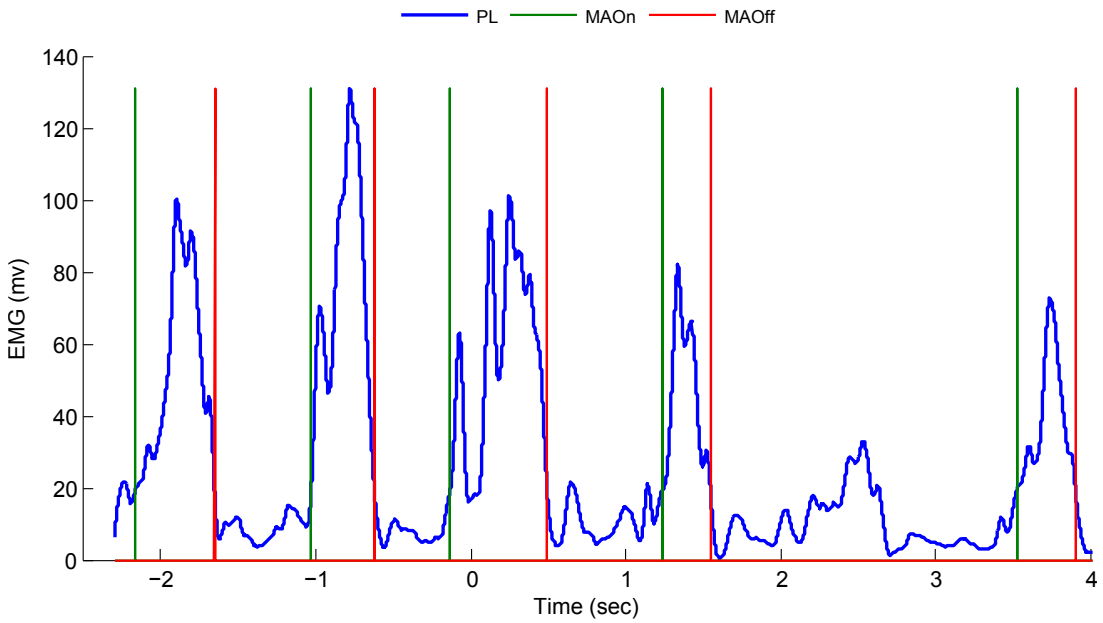

Figure 8.12: EMG activity automatic detection error due to small signal amplitude

Activities separated by a a short interval of time, less than that between two consecutive stance phases are merged.

The module managed to correctly identify muscle activity intervals for a good number of trials. In some trials, however, the module would fail to indicate an activity interval that was either too short (Figure 8.11) or where the amplitude of the signal was too small (Figure 8.12). Eventually development of this module was halted since it still required a great deal of time for further optimisation and validation.

9 Results and statistical analysis of the validation study

Data collected from volunteers were processed using the custom written Matlab® modules. This is the first study that incorporated three different systems (Vicon®, EMG, and the new robotic manipulator) to assess the effect of shoes on lower limb muscle activity and body kinematics, due to sudden supination of the foot during walking. In order to investigate the various effects induced by platform rotation on the lower limb muscle activity and body kinematics of the subjects, graphs of the captured and calculated variables were generated and analysed. This study also allowed assessment of the performance of the platform, since this was the first time it was used.

9.1 Platform performance

Platform data of all successful trials from 29 subjects were analysed in order to assess the performance of the platform. A total of exactly 600 trials were included. For each rotation axis, two variables were investigated: the maximum angle and the "stop" angle (refer to Section 8.6). Together these measurements gave a good representation of the accuracy and consistency of the robotic manipulator.

The target angle of the platform for inversion was set to 15°. The maximum

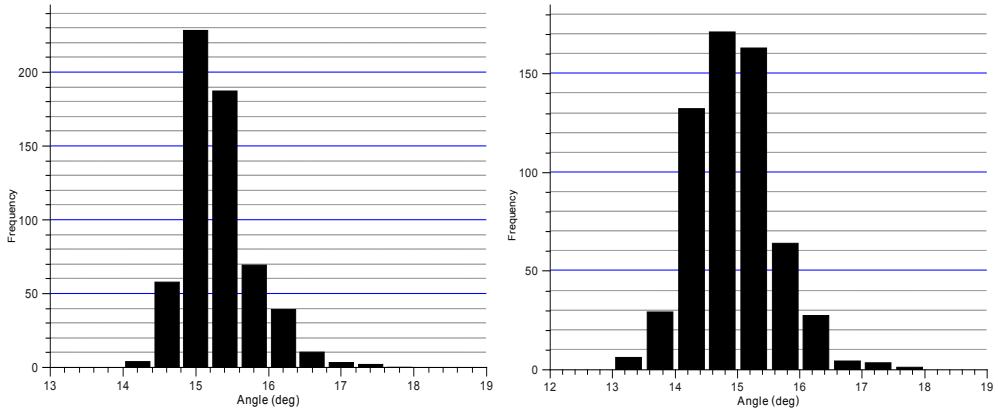

(a) Histogram of maximum inversion angles **(b)** Histogram of stop inversion angles

Figure 9.1: Platform Inversion angles

inversion angle achieved by the platform was centred around 15.3° with the majority (99%) of trials laying between 14° and 17° (Figure 9.1a). The achieved stop angle in inversion was centred around 14.9° with the majority (98%) of trials laying between 13.5° and 16.5° (Figure 9.1b).

The target angle of the platform for flexion was set to 15°. The maximum flexion angle achieved by the platform was centred around 15.9° with the majority (99%) of trials laying between 14° and 18° (Figure 9.2a). The achieved stop angle in flexion was centred around 15.1° with the majority (97%) of trials laying between 13° and 18° (Figure 9.2b).

The target angle of the platform for adduction was set to 8°. The maximum adduction angle achieved by the platform was centred around 7.9° with the majority (97%) of trials laying between 6.5° and 9.5° (Figure 9.3a). The achieved stop angle in adduction was centred around 7.7° with the majority (91%) of trials laying between 6.5° and 9.5° (Figure 9.3b).

This is the first study involving the newly designed system, and as such, the effect of deviations in the degree of rotation of the platform on the lower limb muscle activity and body kinematics is to be explored. For this reason, trials

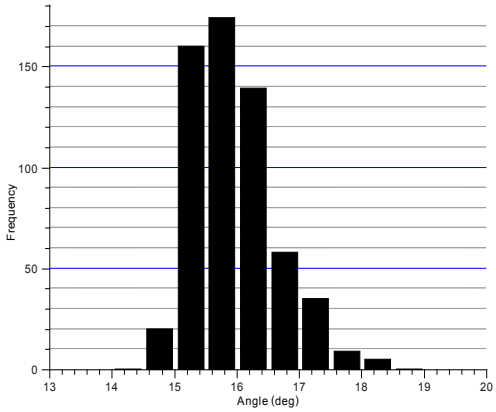

(a) Histogram of maximum flexion angles

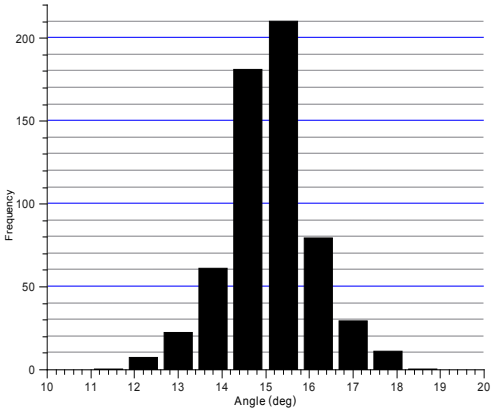

(b) Histogram of stop flexion angles

Figure 9.2: Platform flexion angles

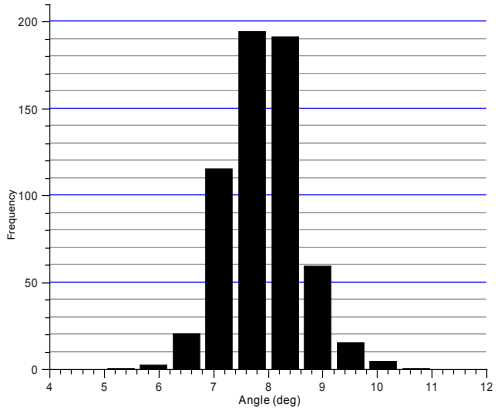

(a) Histogram of maximum adduction angles

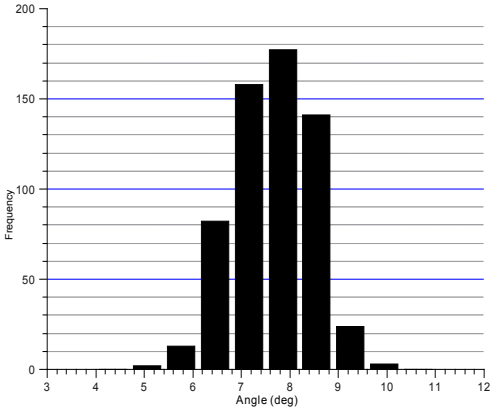

(b) Histogram of stop adduction angles

Figure 9.3: Platform adduction angles

with large rotation deviations were excluded from the statistical analysis. The exclusion criteria were as follows:

- Platform inversion stop angle less then 13.5° or greater then 16.5°.
- Platform inversion maximum angle less then 14° or greater then 17°.
- Platform flexion stop angle less then 13° or greater then 17°.
- Platform flexion maximum angle less then 14° or greater then 18°.

9.2 Graphical visual analysis of the data

Presented below are graphs that demonstrate some of the relevant effects on lower limb muscle activity and body kinematics, due to induced supination of the foot, imparted by the newly developed robotic manipulator.

Abbreviations used in the following graphs:

PIA Platform inversion angle

PPfA Platform plantar-flexion angle

PAA Platform adduction angle

PIAc Platform inversion acceleration

PSG Platform strain gauge

PPfAc Platform plantar-flexion acceleration

PRHS Platform right heel strike

PLHS Platform left heel strike

PLTO Platform left toe-off

PRTO Platform right toe-off

LTOprev Left toe-off before platform step

PRB Platform rotation begins

PARB Platform adduction rotation begins

PARE Platform adduction rotation ends

RHSaft Right heel strike after platform rotates

LHSaft Left heel strike after platform

FIA Foot inversion angle

FPfA Foot plantar-flexion angle

TibX Tibia rotation around laboratory x-axis

ComX X component of the COM relative to the X component of the left ankle

ComYL Y component of the COM relative to the Y component of the left ankle

ComYR Y component of the COM relative to the Y component of the right ankle

9.2.1 The relationship between the load on the foot plate and the platform's acceleration

The strain gauge attached to the main shaft of the platform gives an indication of the normal force on the foot-plate (refer to Section 5.1.2). In Figure 9.4, the value of the SG increases after initial foot strike, and continues to do so until the platform starts accelerating downwards, at that instant the gauges' output starts to decrease indicating a decrease of the load on the foot-plate. When the platform starts decelerating, on the other hand, the load on the foot-plate increases again. The values of the SG then stabilise until RFS where it begins to decrease again, and continues to decrease after PLTO .

9.2.2 The relationship between platform rotation and body kinematics

The relationship between platform rotation and foot inversion is illustrated in Figure 9.5. As the platform starts inverting, the foot also inverts but at a slower rate. Rotation of both continues until the platform stops inverting, where the rate of foot inversion has been greatly reduced. When the platform starts adduction movement, the foot begins to invert again, until the end of the platform adduction.

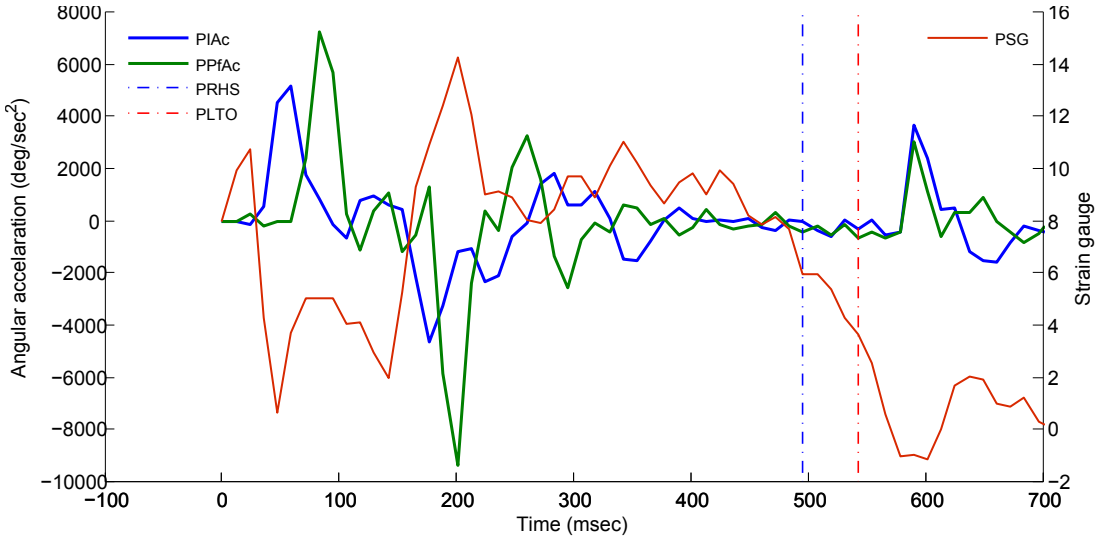

Figure 9.4: Platform angular acceleration and strain gauge output (Time = 0 refers to when the synchronisation signal was sent)

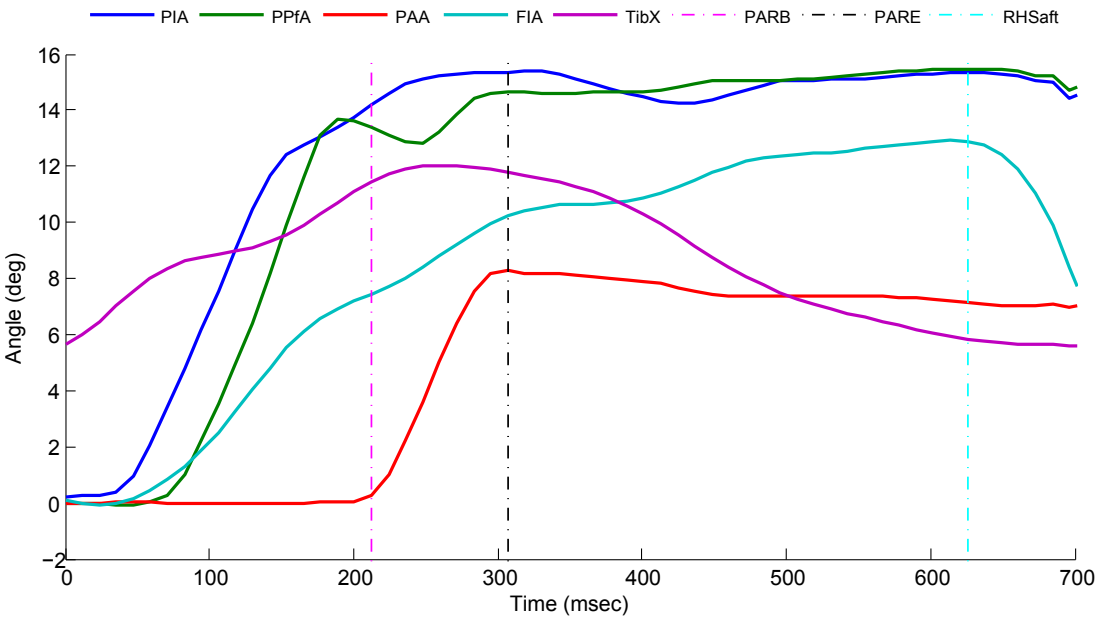

Figure 9.5: Platform inversion versus Foot inversion

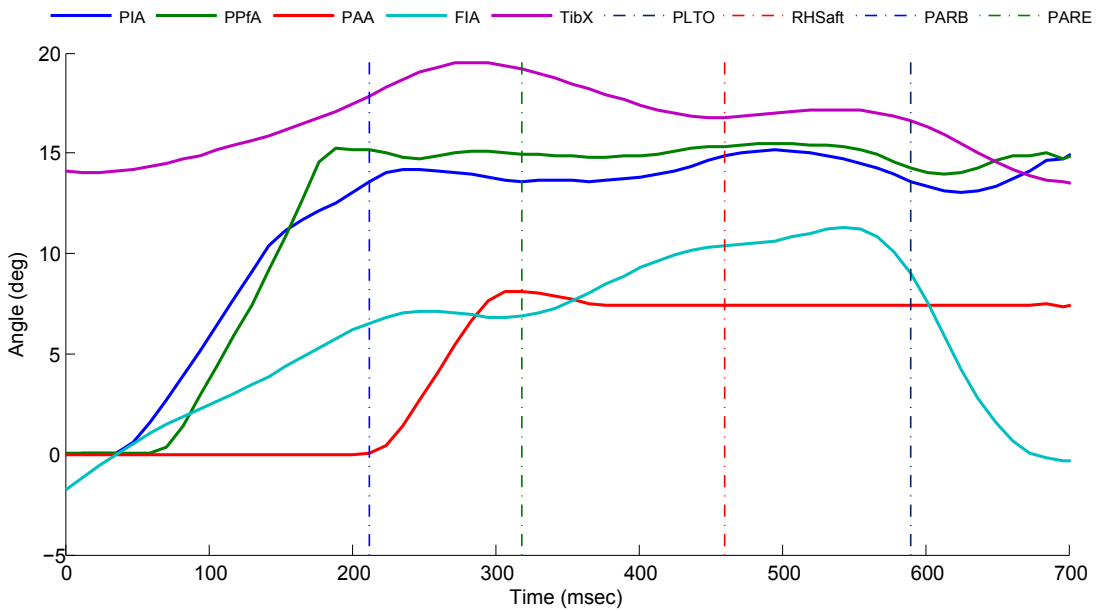

Figure 9.6: Foot inversion and Tibia progression

Inversion is the rotation of the foot around the x-axis relative to the lower leg. As such the orientation of the tibia has a direct effect upon foot inversion. This is demonstrated in Figures 9.6 and 9.7. In Figure 9.6, the platform starts inverting with the foot inverting at a slower rate, at the same time the tibia angle is increasing. The platform stops inverting and begins to adduct, the tibia rotation rate, on the other hand, has increased. The foot then, stops inverting and reverses rotation direction towards eversion. The adduction rotation of the platform stops and the tibia is now rotating in the opposite direction while the foot starts to invert again.

Figure 9.7 shows a similar effect at the beginning of platform rotation. When the platform starts adducting however, foot inversion continues and tibial rotation is at a lower rate than shown in Figure 9.6. After the platform has stopped rotating the tibia's rotation decreases at a high rate while the rate of inversion increases significantly.

In Figure 9.8, the platform starts inverting and the SG value starts decreasing reaching below zero. The foot, however, remains unaffected until the platform

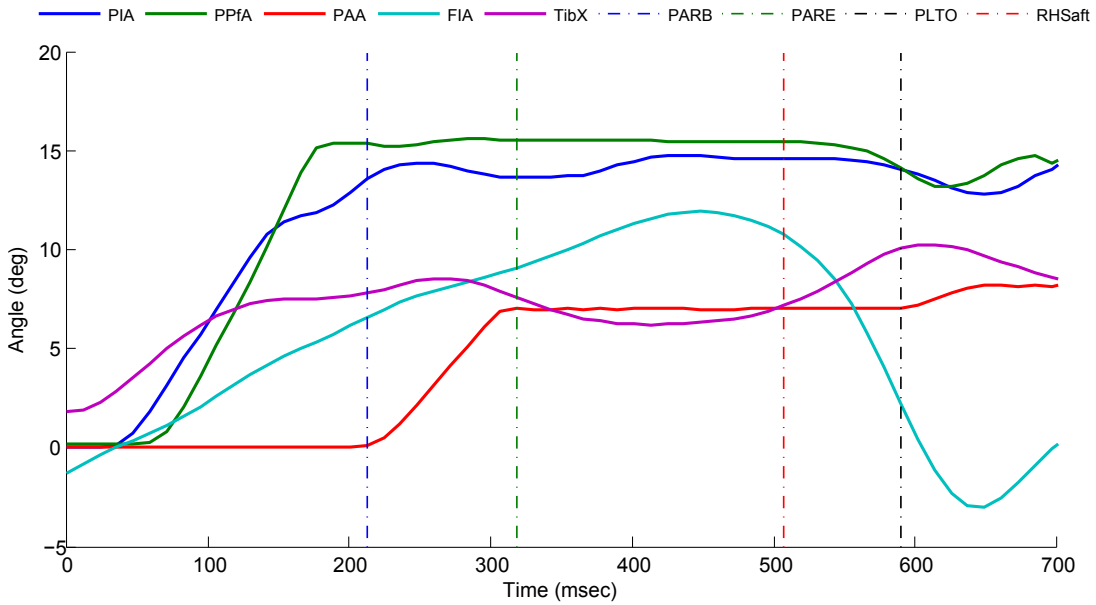

Figure 9.7: Foot inversion and Tibia progression 2

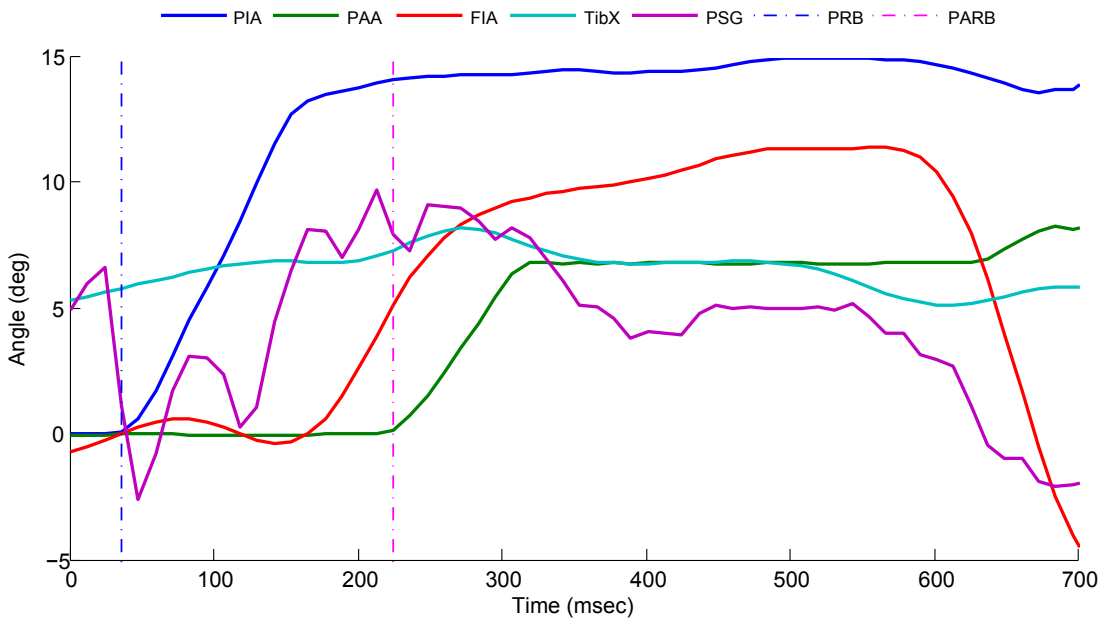

Figure 9.8: Platform rotating faster then foot drop

stops rotating and the SG value increases again. At that moment the foot starts inverting at a much faster rate than shown in the previous graphs. The tibia rotation in this graph is similar to that of Figure 9.6 suggesting that the tibia played no role in this observed behaviour of the foot.

The relation between platform flexion and foot plantar-flexion is depicted in Fi-

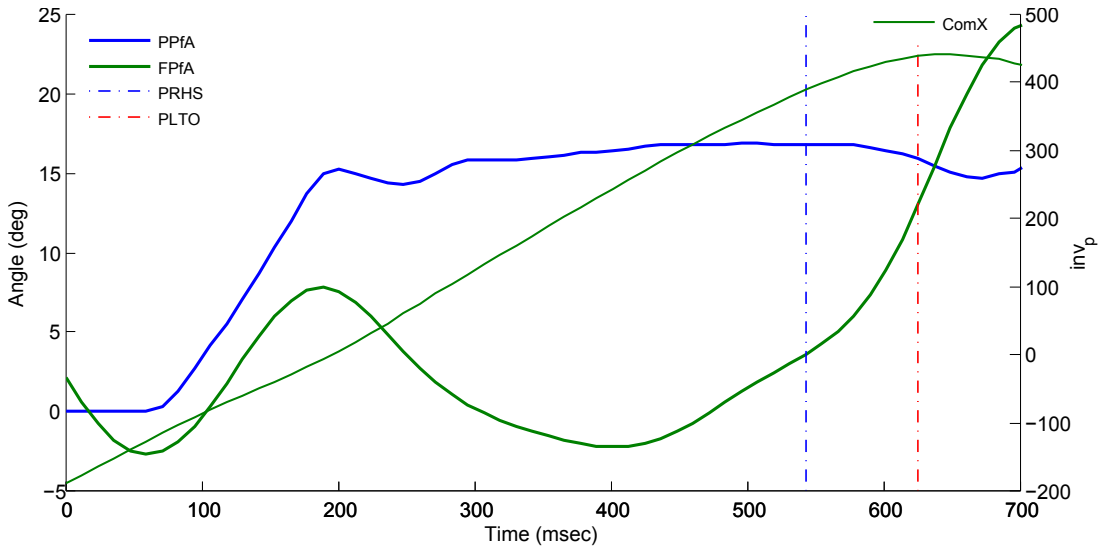

Figure 9.9: Platform plantar-flexion versus foot plantar-flexion

gure 9.9. In the first stage of stance and after heel strike, the foot is rotating towards dorsi-flexion. The platform then starts rotating in flexion and the rotation of the foot starts shifting towards plantar-flexion. When the platform stops rotating the foot rotation switches direction again towards dorsi-flexion. ComX represents the position of the COM relative to the ankle centre of the left foot in the X direction.

9.2.3 Plug-in Gait® and our foot model

The newly developed custom foot model generated (after being processed in Matlab® using *PVICON)* similar results to that of the PiG® model when comparing between foot plantar-flexion data (Figure 9.10). While the curves from both models had a similar shape there was an offset difference between the two.

9.2.4 Left side and right side body kinematics

The left side and right side body kinematics are compared in the following graphs. The time axes of these graphs were normalised for both sides of the body to

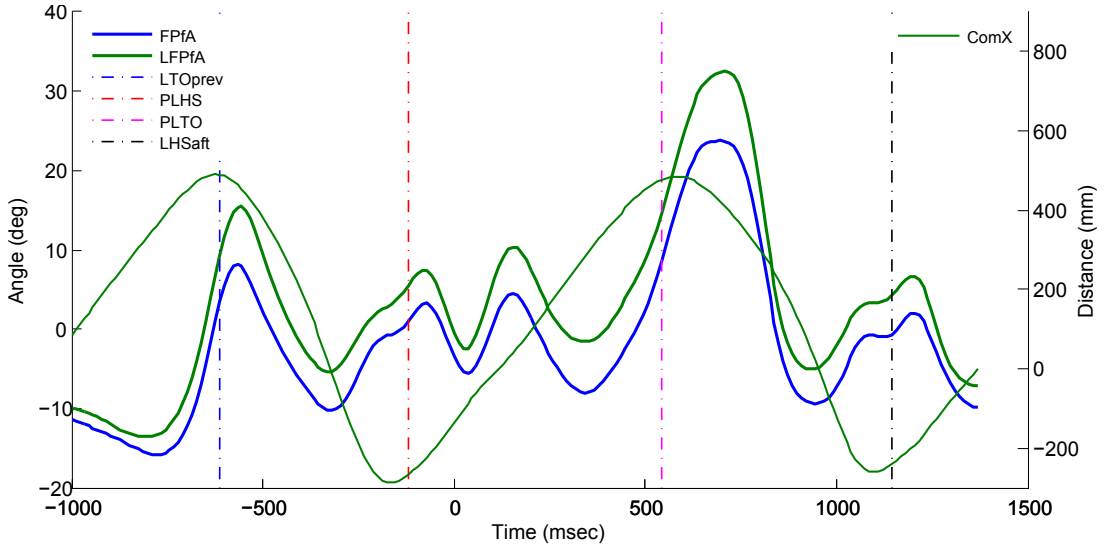

Figure 9.10: PiG® versus the newly developed custom foot model

represent one GC. Body kinematics of the right side correspond to the GC of the right step just before left FS to the platform, while the left side body kinematics correspond to the GC of the left step on the platform. The stance phase of the right GC terminated before the platform started rotating and body kinematics during this phase were not affected by platform. The swing phase of the right GC (the part of the graph after PRTO) however occurred during the platform rotation and body kinematics corresponding to this phase could have been altered by this rotation.

Figure 9.11 compares the COM position in the y-axis relative to the left and right foot y-axis positions. At right foot strike (RFS) the COM is approximately 98 mm from the right foot malleoli. The distance between the two then starts to decrease and continues to do so until it peaks slightly before RTO where the distance starts to increase again.

At LFS the COM is 82 mm from the left malleoli. Similar to the right side, this distance begins to decrease until the platform starts rotating. At that moment the distance between the COM and the left foot begins to increase until just before the platform stops rotating. The COM then follows a path similar to that

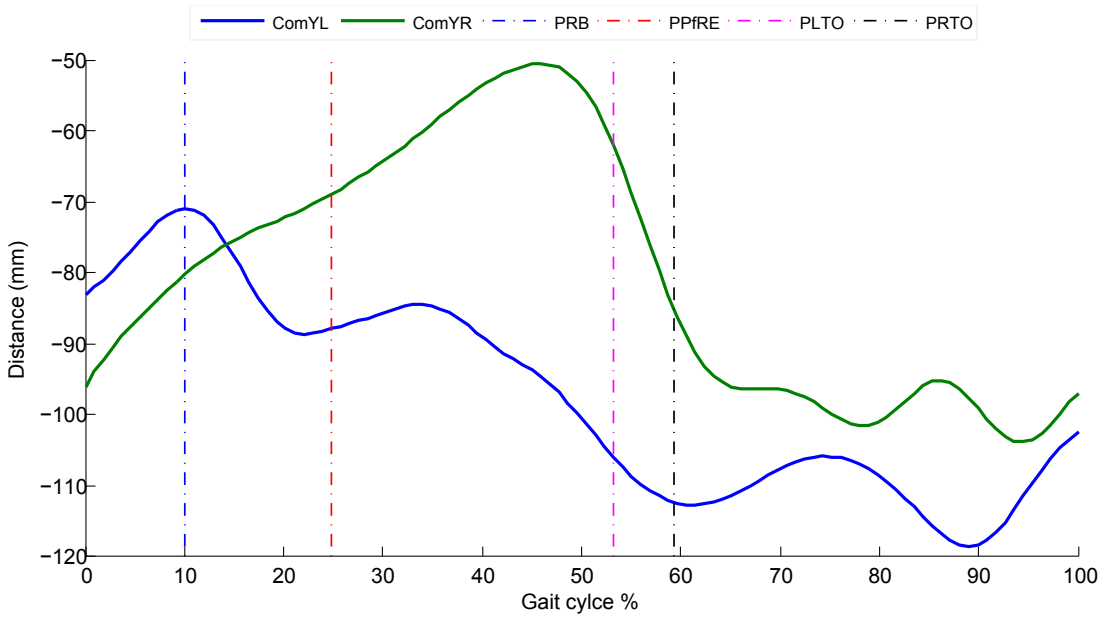

Figure 9.11: COM displacement comparison between left and right stride

of the right side.

Significant differences are also evident when comparing the left and right hip flexion/extension movement (Figure 9.12). At RHS the hip is in flexion but is starting to rotate towards extension until slightly before RTO, where it reaches maximum extension of almost 10°. The right hip then starts to flex smoothly, and at the next RHS, the flexion of the hip is significantly higher than at the initial RHS.

The left hip movement, on the other hand, exhibits some differences. Just before the platform stops rotating, the hip also stops rotating for approximately 10% of the GC, it then starts extending again but does not reach the same angle as the right hip. At the next LFS the rotation of the left hip is similar to that at the initial LFS.

The adduction/abduction movement of the hip also shows some differences between the left and the right sides (Figure 9.13). At FS, both sides are almost in a neutral position, with the right side at 0° and the left at -2.5° adduction. Progressing further into the stance phase, the right hip moves into adduction

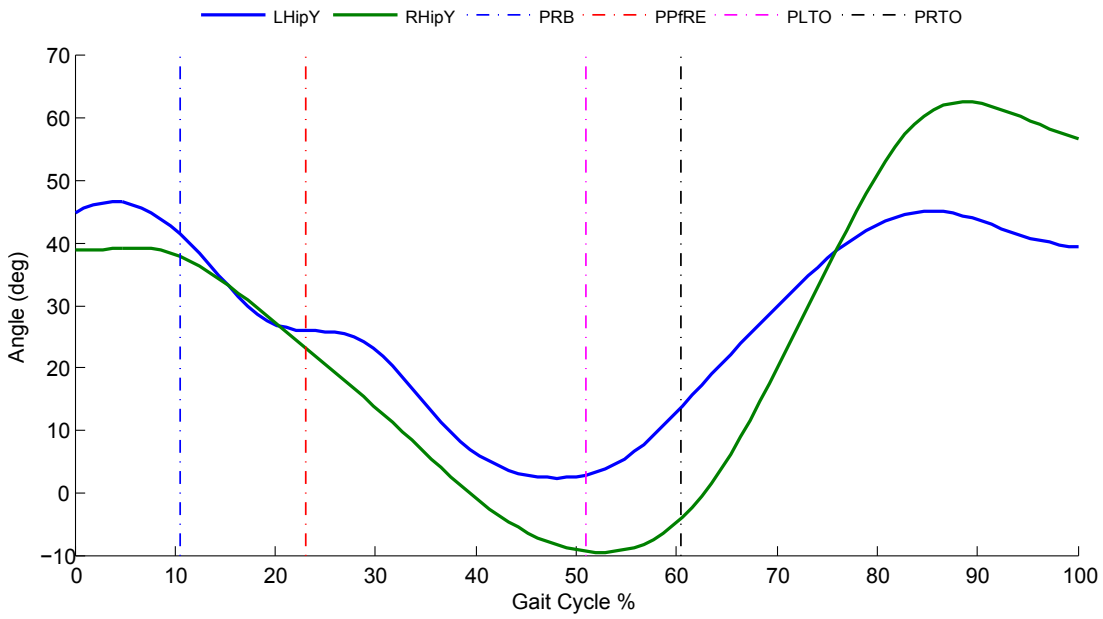

Figure 9.12: Hip flexion/extension comparison between left and right stride

peaking at 11°, where it reverses and starts moving towards abduction. The right hip continues abducting until slightly after RTO, where it switches direction again and oscillates towards adduction. The adduction angle at the next RHS is approximately 5°.

After LFS, the left hip adducts peaking twice in the stance phase of the GC. The first peak, at 4°, occurs slightly after platform rotation begins. Just before the platform starts its adduction rotation, the hip is at a local minimum of -4° adduction. At that point the left hip starts adducting again, peaking at the end of the platform rotation at value of 3°. It then abducts sharply reaching -12° adduction slightly after LTO, where the hip starts to adduct again until the next LHS.

The effect of the platform induced rotation on the sagittal plane knee kinematics is highlighted in Figure 9.14. The motion of the right knee can be described by two parabolas. The first parabola starts with 10° flexion at RFS, peaks at approximately 13% of the GC, and extends back again to 10° flexion at 40% of the GC. The second parabola peaks at 80% of the GC with a value of 90° flexion.

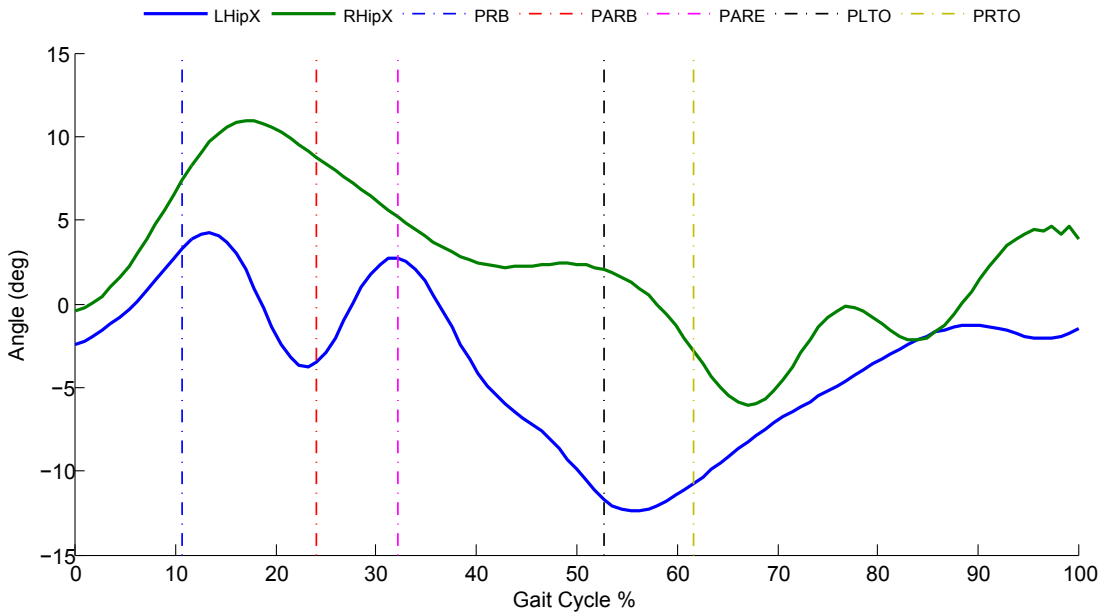

Figure 9.13: Hip adduction/abduction comparison between left and right stride

At the next RFS the knee is 10° more flexed than the previous RFS.

The left knee motion, on the other hand, consists of three parabolas. The first starts at LFS with the left knee flexed at 10° similarly to the right knee. This parabola peaks at approximately 32° flexion at the beginning of platform movement. The end of the first parabola and beginning of the second is at 22% of the GC, slightly before the platform stops its inversion and flexion movement. The peak knee flexion of the second parabola is slightly less than the first parabola, approximately 28°. The third and final parabola is similar in shape and value to that of the right knee, the only difference being the knee flexion value at the end of the current GC, where the left knee goes back to the original degree of flexion it started at.

The motion of the right foot in the sagittal plane begins with 5° plantar-flexion at RFS (Figure 9.15). The foot continues plantar-flexing until 10° at 10% of the GC, where it begins dorsi-flexing. The right foot continues to dorsi-flex until approximately 52% of the GC where it reaches -9° plantar-flexion. At this point it returns to plantar-flexing again to peak just after RTO at 15°. It then dorsi-

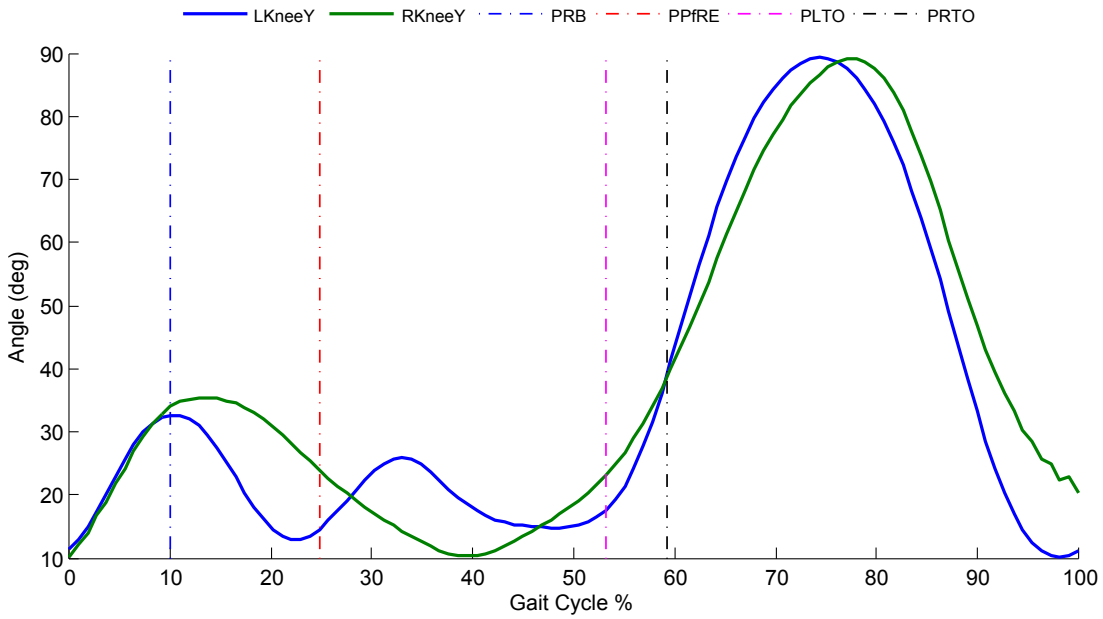

Figure 9.14: Knee flexion/extension comparison between left and right stride

flexes again to -10° at 80% GC, and then ends the GC with a similar angle as it started.

The left foot, alternatively, follows a different path. At LFS the foot is slightly more plantar-flexed then peaks earlier at 5% of the GC. When the platform starts rotating the foot reverses its motion from dorsi-flexion back to plantar-flexion. The foot's plantar-flexion reaches its local maximum at the end of the platform rotation at an angle of approximately 16°. It then begins to dorsi-flex to reach its minimum of 10° at 35% of the GC. The foot then starts to plantar-flex slowly until just before LTO where its rotation speed increases. The left foot reaches maximum plantar-flexion just after LTO at an angle of 40°. At the end of the GC the left foot is at a similar angle to the right one, unlike its orientation at the beginning of the GC.

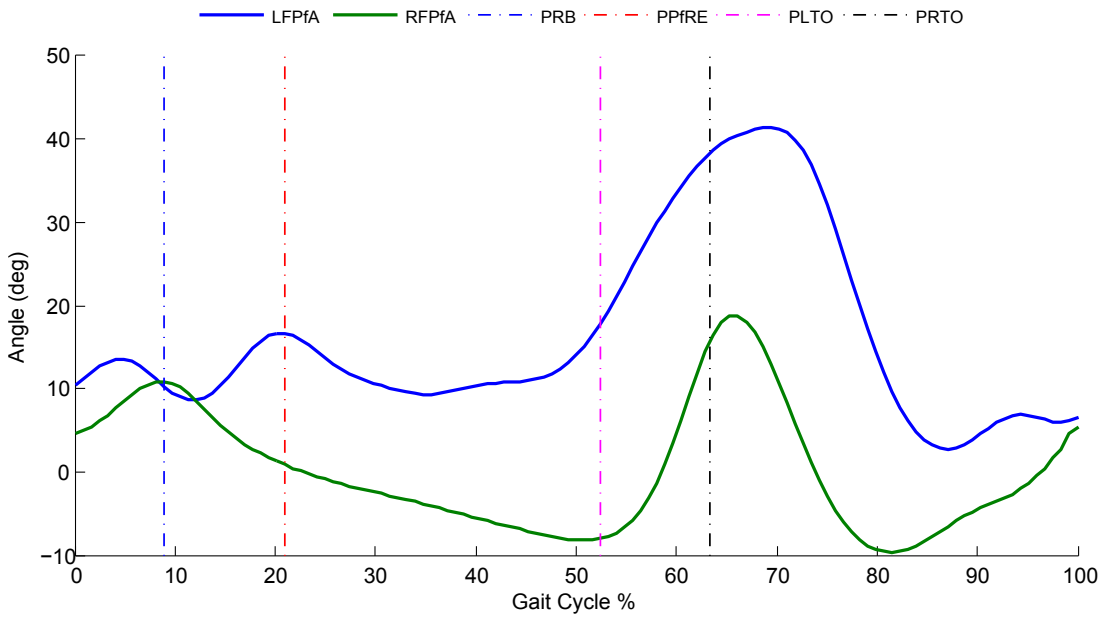

Figure 9.15: Foot plantar-flexion comparison between left and right stride

9.2.5 The effect of foot Supination on lower limb muscle activity

The EMG of the PL muscle is plotted against the platform inversion and adduction angles as well as that of foot inversion (Figure 9.16). Two major parabolas appear in the EMG signal, the first starting slightly after the platform and foot starts inverting and peaks just before the platform stops inverting. The second parabola begins after the platform starts adduction movement and has a higher peak then its predecessor.

The FS of the left foot for the step preceding the platform was not recorded as it was outside the capture volume (refer to Section 7.4.3); only the TO of that step was captured. To compare the PL activity of that step to the platform one (Figure 9.17), an estimated FS time was used based on the stance time of the platform step (refer to Section 8.7.3). The most apparent difference between the two plots is the first parabola in the platform step, which is not present in the PL activity of the previous one.

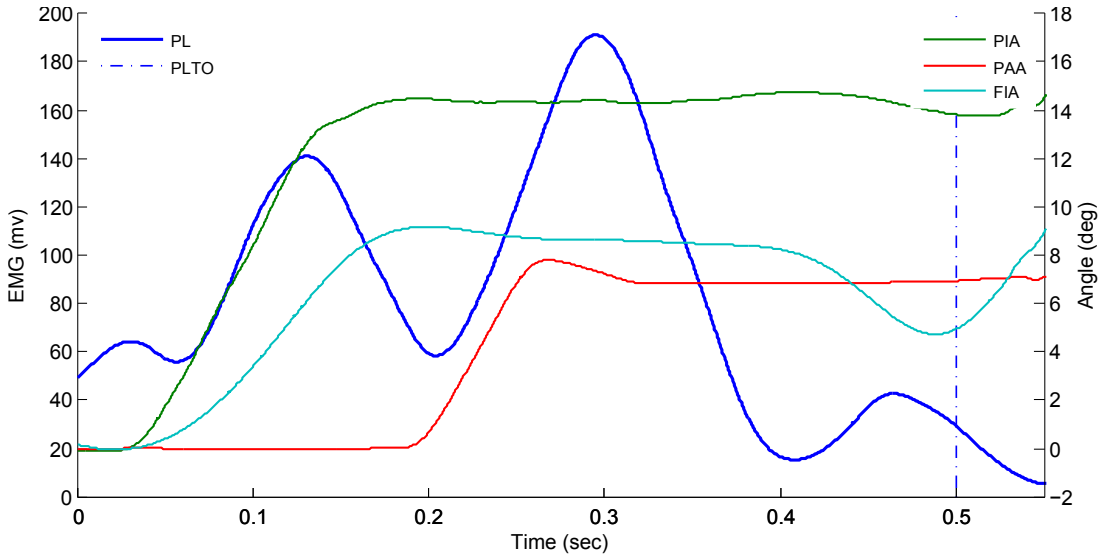

Figure 9.16: Effect of induced foot rotation on peroneus longus muscle activity

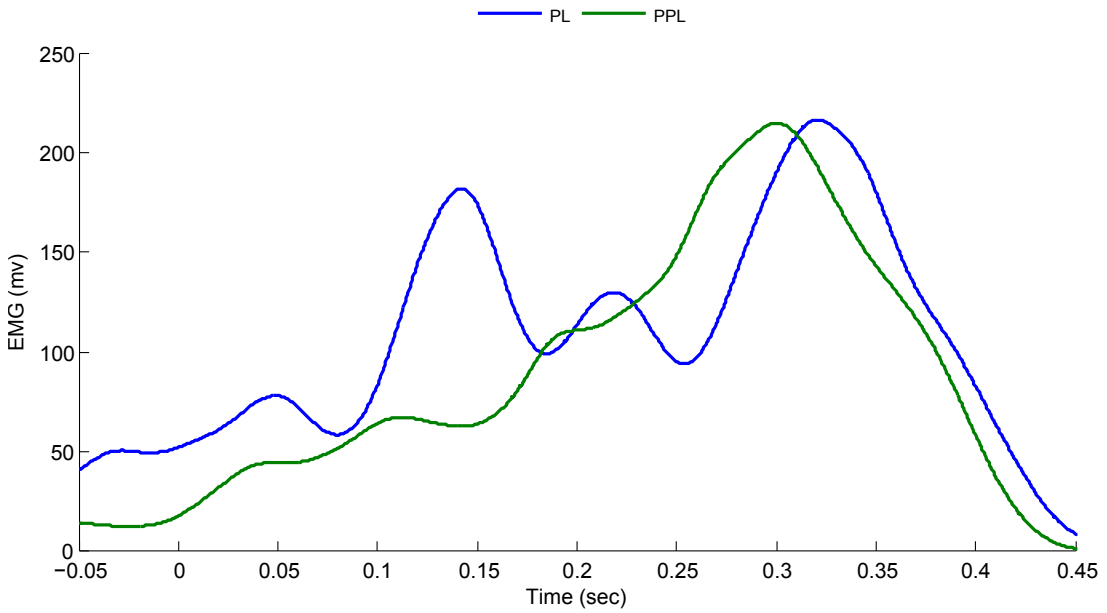

Figure 9.17: EMG activity for the platform stride compared to the previous stride

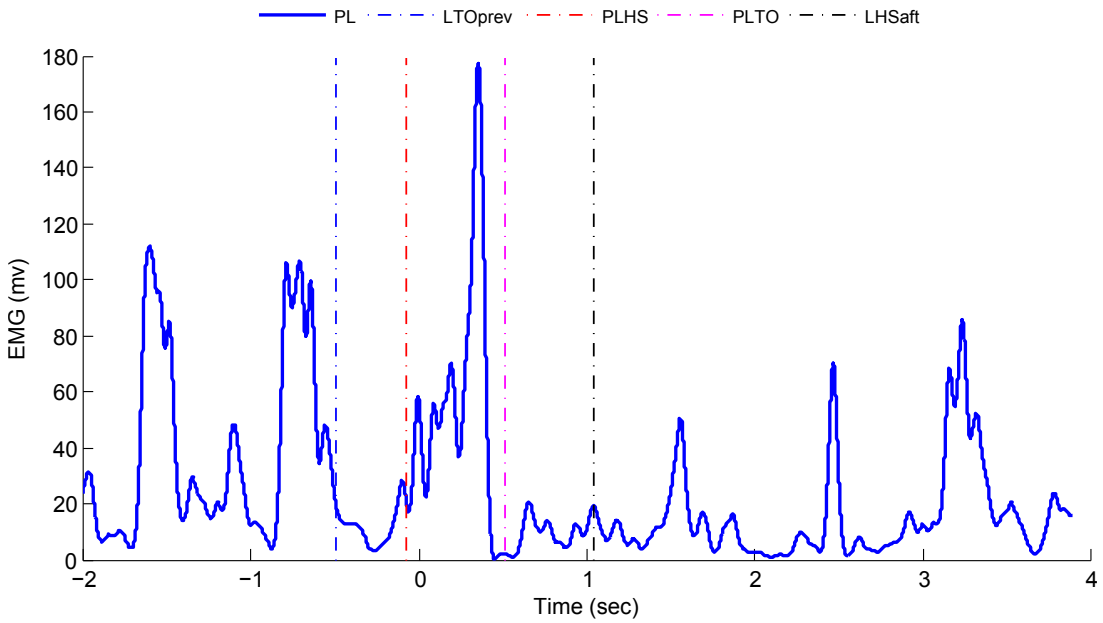

Figure 9.18: EMG activity of the PL muscle highly diminished after induced foot rotation

In Figure 9.18, EMG of the PL muscle through the entire trial is plotted. The first thing that is evident from this figure is the higher maximum value of the EMG signal for the step on the platform, compared to the previous and next steps. Another apparent observation is the highly reduced activity in the steps following foot-strike to the platform.

The EMG of the TA muscle was also plotted against platform flexion and foot plantar-flexion (Figure 9.19). The most interesting observation in this figure is the small parabola in the TA signal that follows the onset of platform flexion and peaks at the end of its rotation.

9.3 Statistical analysis

The secondary objective of this project was to conduct an experimental study to investigate the role of shoes in ankle sprain injury (refer to Section 1.2). The effect of shoes on lower limb muscle activity and body kinematics in response

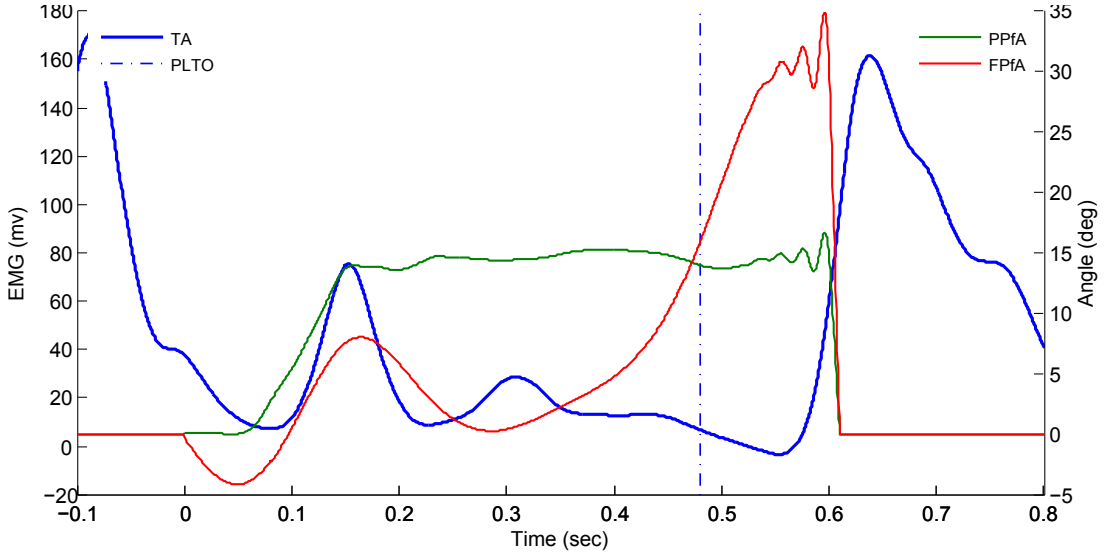

Figure 9.19: Effect of induced foot rotation on TA muscle activity

to sudden supination of the foot of walking subjects was thus investigated; two null-hypothesis are highlighted and tested:

1. Footwear does not affect the lower limb muscle activity of walking subjects when their foot is suddenly supinated.

2. Footwear does not affect body kinematics of walking subjects when their foot is suddenly supinated.

The null-hypothesis were tested using the repeated measures analysis of variance (ANOVA) test. The software package used to perform this test and all other statistical analysis was SPSS®. Within subject factors were defined as the different foot conditions, while the sequence of used shoes in the experiment was considered a between subject factor. This was to account for the fact that the number of subjects in each sequence was no longer the same after applying the exclusion criteria (refer to Section 8.7.3 and 9.1). To give a better understanding of the obtained data, descriptive statistics are also presented in the subsequent tables.

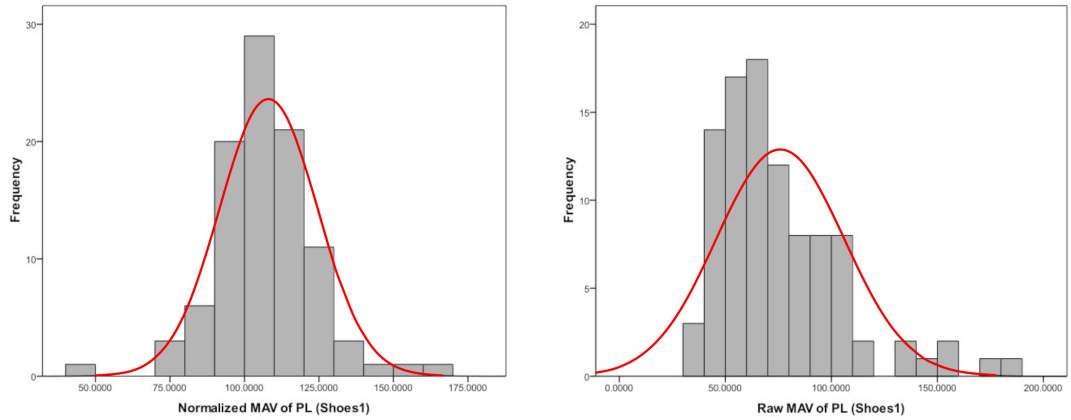

Figure 9.20: Raw versus Normalised data (Normal distribution curve is plotted in red)

One of the requirements for ANOVA is the normality of the data. Testing for normality revealed large deviations in the EMG data (Figure 9.20). This was due to the fact that EMG signals depend on several factors which vary significantly from one subject to another (refer to Section 8.2.5). To account for this, EMG data were normalised, thus, shifting the data into normality (Figure 9.20).

In the tables presented below, statistical significance is assumed when the p-value was less than 0.05. p-values under 0.20 are also reported.

9.3.1 Demographics

Data from the 29 subjects were used to assess the performance of the platform (refer to Section 9.1). The mean weight of these 29 subjects was 70.7 kg (SD 16.2) with a maximum of 113.2 kg and a minimum of 48.4 kg. The mean height of the subjects was 171.7 cm (SD 7.7) with a maximum of 183 cm and a minimum of 156.5 cm.

Of the 29 subjects six were excluded and 23 subjects were included in a study to investigate any contributing role of shoes in causing ankle sprains. This number of subjects remains higher then the 16 subjects required using the power analy-

sis. The six subjects were excluded based on the exclusion criteria presented in sections 8.7.3 and 9.1; mainly because these subjects slowed down their walking when they stepped on the platform causing it to rotate while their right foot was still in contact with the ground.

The average weight of these 23 subjects was 66.9 kg (SD 11.9) with a maximum weight of 97.6 kg and a minimum weight of 48.4 kg. The average height of the subjects was 170.3 cm (SD 8.0) with a maximum height of 183.0 cm and a minimum height of 156.5 cm. The average age of the subjects was 30.6 years (SD 12.1) with a maximum age of 55 years and the minimum age was 19 years. The subjects were divided between 14 females and nine males.

Six of the subjects changed shoes following sequence 1, nine subjects followed sequence 2 and eight subjects followed sequence 3 (refer to Section 7.4.7).

9.3.2 Platform Data

Results of the statistical analysis for the performance of the platform from the 23 subjects are presented in Table 9.1. The variables investigated were the stop and maximum angles as well as the maximum velocity of the platform around each of the three axes of rotation corresponding for each foot condition. The descriptive statistics shown are the mean and standard deviation, while statistics from the multivariate analysis included the estimated mean, the standard error, and the level of significance.

The mean stop angle in inversion and flexion for all foot conditions is no more than 0.2° from the target angle. The mean maximum angle in flexion is slightly higher but is similar between all foot conditions. The performance of the platform in adduction exhibited the highest variability between the different foot conditions; the maximum statistically significant difference was between the stop

angle in barefoot and shoes2 conditions at 0.6°. The velocity of the platform in inversion was closest to target value of $150°/s$. In flexion the velocity exceeded the target value, while in adduction the velocity was lower than the target value.

9.3.3 Kinematic Data

Table 9.2 contains descriptive statistics, as well as ANOVA analysis, of the obtained kinematic data. The included variables are:

- Maximum ankle inversion between FS and TO.
- Maximum ankle flexion during the rotation of the platform.
- X-component of the landing position of the foot on the platform.
- Y-component of the landing position of the foot on the platform.
- Stance time of the right foot at the step just before the platform.
- Stance time of the left foot at the platform step.
- Average gait speed of the subject during the trial.
- Time between RTO and the beginning of the platform rotation.

9.3.4 ARV of EMG data

The ARV of the EMG data was calculated for all three muscles at 11 different intervals within the step on the platform (refer to Section 8.8). The most relevant five are presented here:

Interval 1 Form FS to TO.

Interval 2 From FS until the beginning of platform rotation.

Interval 3 From the beginning of platform rotation until the time it stops rotating completely (i.e. stops rotating in adduction).

Interval 4 From the time the platform stops adducting until TO.

Interval 5 From TO until HS of the next step.

Table 9.3 shows the descriptive statistics of the original and normalised data at these intervals. The lengths of each interval are also recorded in Table 9.4.

ANOVA analysis of the ARV and the maximum value of the normalised data at *interval 1* are presented in Table 9.5. The ARV of the PL and LG was significantly lower in barefoot compared to shoe$s$1, but no significant difference was found with shoes2. The estimated mean, nonetheless, was lower in barefoot compared to shoes2. The length *interval 1* was significantly shorter for barefoot conditions than that for the other two shoes.

Table 9.1: Platform Data (angle data are in degrees and rotational velocity data are in degrees/second)

Measure	FC	Mean	SD	E. Mean	SE	P. comparison
PSIA	BF	14.8	0.5	14.8	0.1	*S1 PS2=0.13
	S1	14.9	0.6	15.0	0.1	*BF
	S2	14.9	0.5	14.9	0.1	PBF=0.13
PMIA	BF	15.3	0.4	15.2	0.0	-
	S1	15.3	0.4	15.3	0.0	-
	S2	15.2	0.5	15.2	0.0	-
PMIV	BF	148.2	10.8	148.3	1.1	**S1 **S2
	S1	142.4	9.4	142.9	1.0	**BF
	S2	143.0	9.4	143.3	1.0	**BF
PSPfA	BF	15.1	0.8	15.1	0.1	-
	S1	15.2	0.7	15.2	0.1	-
	S2	15.2	0.7	15.2	0.1	-
PMPfA	BF	15.8	0.6	15.8	0.1	-
	S1	15.8	0.6	15.8	0.1	-
	S2	15.9	0.5	15.9	0.1	-
PMPfV	BF	177.1	12.9	177.1	1.3	PS2=0.08
	S1	176.7	12.1	175.9	1.2	-
	S2	175.0	11.0	174.6	1.2	PBF=0.08
PSAA	BF	7.8	0.7	7.8	0.1	**S1 **S2
	S1	7.5	1.1	7.4	0.1	**BF PS2=0.14
	S2	7.2	0.7	7.2	0.1	**BF PS1=1.14
PMAA	BF	7.9	0.6	8.0	0.1	PS1=0.06 **S2
	S1	7.8	0.6	7.8	0.1	PBF=0.06 PS2=0.06
	S2	7.6	0.6	7.6	0.1	**BF PS1=0.06
PMAV	BF	141.3	71.8	142.7	7.6	PS1=0.09 PS2=0.13
	S1	129.0	21.0	129.5	2.2	PBF=0.09
	S2	126.3	47.1	128.4	4.9	PBF=0.13

Table 9.2: Kinematic Data

Measure	FC	Mean	SD	E. Mean	SE	P. comparison
	BF	9.8	1.8	9.8	0.2	**S1 **S2
Ank inv (degrees)	S1	7.3	1.9	7.3	0.2	**BF **S2
	S2	8.8	1.9	8.9	0.2	**BF **S1
	BF	4.9	3.4	4.8	0.4	**S1 **S2
Ank flex (degrees)	S1	7.2	3.4	7.2	0.4	**BF **S2
	S2	5.6	2.9	5.6	0.3	**BF **S1
	BF	152.8	40.5	153.4	4.2	*S1 **S2
X land Pos (mm)	S1	162.9	33.8	163.8	3.5	*BF *S2
	S2	174.0	33.0	173.6	3.4	**BF *S1
	BF	104.6	28.8	104.3	2.9	-
Y land Pos (mm)	S1	101.4	27.4	102.6	2.8	-
	S2	102.4	28.4	102.8	2.8	-
	BF	622	50	620	5	**S1 **S2
R Stance T (ms)	S1	646	51	643	5	**BF
	S2	650	52	647	5	**BF
	BF	595	49	593	6	**S1 **S2
L Stance T (ms)	S1	623	58	620	6	**BF
	S2	629	57	626	6	**BF
	BF	1.38	0.12	1.38	0.01	PS1=0.06 *S2
Gait speed (m/s)	S1	1.39	0.15	1.40	0.02	PBF=0.06
	S2	1.39	0.14	1.40	0.01	*BF
	BF	13	20	13	2	**S1 **S2
RTOtoROT (ms)	S1	27	36	26	4	**BF
	S2	23	28	23	3	**BF

Table 9.3: Descriptive statistics of the ARV of EMG data for intervals 1 to 5

		Normalised		Original (mV)	
Measure	Foot Condition	Mean	Std. Dev	Mean	Std. Dev
	Barefoot	94.41	14.05	65.90	21.55
ARV PL 1	Shoes 1	107.66	16.33	76.05	30.35
	Shoes 2	97.94	17.61	68.73	27.24
	Barefoot	90.19	18.05	42.33	23.39
ARV TA 1	Shoes 1	111.25	17.83	53.32	32.33
	Shoes 2	98.56	15.69	46.63	24.34
	Barefoot	94.60	14.52	63.18	21.04
ARV LG 1	Shoes 1	106.89	14.09	72.22	25.96
	Shoes 2	98.51	17.23	65.96	23.59
	Barefoot	60.33	22.37	40.71	17.20
ARV PL 2	Shoes 1	66.85	23.32	46.42	22.40
	Shoes 2	72.10	30.75	49.30	24.07
	Barefoot	159.62	50.95	70.73	29.61
ARV TA 2	Shoes 1	187.23	69.82	84.61	43.02
	Shoes 2	172.31	60.72	77.04	34.16
	Barefoot	46.15	20.89	28.90	11.85
ARV LG 2	Shoes 1	49.87	19.98	32.17	14.68
	Shoes 2	52.85	24.33	33.26	14.24
	Barefoot	97.92	28.39	68.57	30.24
ARV PL 3	Shoes 1	123.11	29.14	87.10	38.01
	Shoes 2	108.93	30.35	77.32	37.26
	Barefoot	96.31	30.58	45.43	27.27
ARV TA 3	Shoes 1	115.86	33.34	56.74	37.73
	Shoes 2	97.78	28.38	47.51	28.59

Table Continued

		Normalised		Original (mV)	
Measure	Foot Condition	Mean	Std. Dev	Mean	Std. Dev
ARV LG 3	Barefoot	85.22	31.82	57.05	29.33
	Shoes 1	99.65	27.01	66.62	27.65
	Shoes 2	90.39	31.22	59.79	26.65
ARV PL 4	Barefoot	108.43	35.87	75.81	33.18
	Shoes 1	116.07	36.58	82.14	41.39
	Shoes 2	99.65	34.50	69.72	34.55
ARV TA 4	Barefoot	46.34	20.60	23.41	24.47
	Shoes 1	60.81	28.55	30.54	30.56
	Shoes 2	53.59	25.18	26.44	24.51
ARV LG 4	Barefoot	131.01	43.44	88.34	42.22
	Shoes 1	152.32	45.68	104.62	49.56
	Shoes 2	133.76	46.97	91.62	46.31
ARV PL 5	Barefoot	29.20	12.34	19.24	7.84
	Shoes 1	32.07	12.10	21.48	8.98
	Shoes 2	31.79	15.97	20.99	10.13
ARV TA 5	Barefoot	120.67	44.75	57.10	46.20
	Shoes 1	125.21	43.50	57.66	31.95
	Shoes 2	117.12	37.60	52.85	25.72
ARV LG 5	Barefoot	22.42	10.09	14.20	6.64
	Shoes 1	26.74	12.59	16.75	7.33
	Shoes 2	27.25	15.25	17.05	9.21

ANOVA analysis data of the ARV for intervals 2 to 5 are presented in Table 9.7. The ARV of the PL in barefoot condition was significantly lower compared to shoe2, which had the highest estimated mean at that interval. In *interval 5*, spanning the rotation of the platform, the ARV of the PL muscle was significantly lower in barefoot compared to shoes1 and shoes2, with shoes1 having the highest

Table 9.4: Descriptive statistics of Time intervals

Measure	Foot Condition	Normalised		Original (ms)	
		Mean	Std. Dev	Mean	Std. Dev
Time 1	Barefoot	96.72	3.92	595.18	48.80
	Shoes 1	101.19	4.08	623.26	57.86
	Shoes 2	102.08	4.22	628.63	57.32
Time 2	Barefoot	20.53	4.51	125.71	26.76
	Shoes 1	24.71	5.80	151.72	36.35
	Shoes 2	24.59	4.84	150.59	27.57
Time 3	Barefoot	38.70	4.80	236.96	23.51
	Shoes 1	38.94	4.49	238.42	22.10
	Shoes 2	39.00	4.05	238.82	18.20
Time 4	Barefoot	37.65	8.01	233.49	60.96
	Shoes 1	37.70	8.80	234.11	66.62
	Shoes 2	38.65	7.77	240.19	62.65
Time 5	Barefoot	83.62	6.33	513.38	40.42
	Shoes 1	86.02	10.08	528.86	69.22
	Shoes 2	87.92	8.62	540.28	58.52

estimated mean. The length of *interval 5* was similar across all foot conditions.

Comparisons of the ARV of the normalised EMG data for the PL, TA, and LG muscles for the steps before and after the platform are recorded in Table 9.7. This analysis revealed no significant difference for the PL and LG between the different foot conditions in both steps.

Table 9.5: Anova analysis of normalised ARV and normalised maximum EMG data for interval 1

Measure	Foot Condition	Mean	95% CI		Pairwise Comparison
			LB	UB	
ARV PL 1	Barefoot	94.41	91.46	97.36	**S1 PS2=0.16
	Shoes 1	107.41	104.00	110.82	**BF **S2
	Shoes 2	98.18	94.50	101.87	PBF=0.16 **S1
ARV TA 1	Barefoot	90.57	86.79	94.34	**S1 **S2
	Shoes 1	110.83	107.10	114.55	**BF **S2
	Shoes 2	98.61	95.31	101.90	**BF **S1
ARV LG 1	Barefoot	94.63	91.60	97.67	**S1 PS2=0.06
	Shoes 1	106.88	103.93	109.83	**BF **S2
	Shoes 2	98.49	94.87	102.10	PBF=0.06 **S1
Max PL 1	Barefoot	98.22	93.60	102.84	**S1 PS2=0.12
	Shoes 1	108.95	103.99	113.90	**BF **S2
	Shoes 2	92.83	88.50	97.16	PBF=0.12 **S1
Max TA 1	Barefoot	91.97	87.55	96.39	**S1 PS2=0.17
	Shoes 1	111.09	106.61	115.57	**BF **S2
	Shoes 2	96.94	92.45	101.42	PBF=0.17 **S1
Max LG 1	Barefoot	100.21	95.06	105.36	PS1=0.10 *S2
	Shoes 1	106.69	102.12	111.26	PS1=0.10 **S2
	Shoes 2	93.10	89.24	96.96	*BF **S1
Time	Barefoot	96.82	96.01	97.64	**S1 **S2
	Shoes 1	101.13	100.28	101.98	**BF
	Shoes 2	102.05	101.16	102.93	**BF

Table 9.6: Anova analysis of the normalised ARV of EMG data for intervals 2 to 5

Measure	Foot Condition	Mean	95% CI		Pairwise Comparison
			LB	UB	
ARV PL 2	Barefoot	61.88	57.38	66.39	PS1=0.08 **S2
	Shoes 1	67.28	62.44	72.12	PBF=0.08 *PS2
	Shoes 2	73.17	66.78	79.55	**BF *S1
ARV TA 2	Barefoot	162.17	151.78	172.55	**S1
	Shoes 1	187.45	172.93	201.97	**BF *S2
	Shoes 2	170.92	158.37	183.47	*S1
ARV LG 2	Barefoot	47.34	43.08	51.59	PS1=0.07 **S2
	Shoes 1	50.88	46.78	54.98	PBF=0.07 PS2=0.18
	Shoes 2	54.31	49.36	59.26	**BF PS1=0.18
Time 2	Barefoot	20.55	19.61	21.49	**S1 **S2
	Shoes 1	24.49	23.29	25.69	**BF
	Shoes 2	24.47	23.46	25.48	**BF
ARV PL 3	Barefoot	97.07	91.24	102.90	**S1 **S2
	Shoes 1	122.56	116.52	128.60	**BF **S2
	Shoes 2	109.30	102.95	115.65	**BF **S1
ARV TA 3	Barefoot	96.68	90.28	103.07	**S1
	Shoes 1	116.03	109.07	123.00	**BF **S2
	Shoes 2	99.01	93.20	104.82	**S1
ARV LG 3	Barefoot	84.29	77.76	90.83	**S1 PS2=0.09
	Shoes 1	99.87	94.35	105.39	**BF **S2
	Shoes 2	90.86	84.50	97.22	PBF=0.09 **S1
Time 3	Barefoot	38.71	37.72	39.71	-
	Shoes 1	38.93	37.99	39.87	-
	Shoes 2	39.07	38.22	39.91	-

Table Continued

Measure	Foot Condition	Mean	LB	UB	Comparison
ARV PL 4	Barefoot	108.97	101.55	116.40	*S2
	Shoes 1	115.45	107.82	123.08	**S2
	Shoes 2	99.42	92.24	106.60	**S1
ARV TA 4	Barefoot	45.54	41.29	49.80	**S1 **S2
	Shoes 1	59.82	53.92	65.72	**BF *S2
	Shoes 2	53.06	47.80	58.32	**BF *S1
ARV LG 4	Barefoot	131.72	122.86	140.57	*S1
	Shoes 1	150.92	141.48	160.36	**BF **S2
	Shoes 2	132.50	122.77	142.22	**S1
Time 4	Barefoot	37.72	36.05	39.39	-
	Shoes 1	37.86	36.02	39.70	-
	Shoes 2	38.67	37.04	40.30	-
ARV PL 5	Barefoot	29.72	27.17	32.27	**S1 *S2
	Shoes 1	33.05	30.66	35.44	**BF
	Shoes 2	32.45	29.15	35.76	*BF
ARV TA 5	Barefoot	118.09	108.96	127.21	-
	Shoes 1	123.47	114.58	132.37	*S2
	Shoes 2	114.56	107.17	121.95	*S1
ARV LG 5	Barefoot	22.55	20.44	24.66	**S1 **S2
	Shoes 1	27.36	24.90	29.82	**BF
	Shoes 2	27.76	24.59	30.92	**BF
Time 5	Barefoot	83.72	82.44	85.00	*S1 **S2
	Shoes 1	86.55	84.49	88.62	*BF PS2=0.16
	Shoes 2	88.22	86.46	89.98	**BF PS1=0.16

Table 9.7: Anova analysis of the normalised ARV of EMG data for the steps before and after the platform

Measure	Foot Condition	Mean	95% CI		Pairwise Comparison
			LB	UB	
ARV PL prev	Barefoot	64.45	60.12	68.79	PS1=0.17
	Shoes 1	67.78	63.37	72.19	PBF=0.17 PS2=0.15
	Shoes 2	64.11	60.08	68.13	PS1=0.15
ARV TA prev	Barefoot	71.50	64.76	78.25	*S1 **S2
	Shoes 1	78.85	70.95	86.75	*BF
	Shoes 2	81.75	74.11	89.39	**BF
ARV LG prev	Barefoot	63.34	60.06	66.62	-
	Shoes 1	65.53	62.10	68.95	-
	Shoes 2	64.66	60.57	68.75	-
Time prev	Barefoot	96.82	96.01	97.64	**S1 **S2
	Shoes 1	101.13	100.28	101.98	**BF PS2 = 0.14
	Shoes 2	102.05	101.16	102.93	**BF PS1 = 0.14
ARV PL aft	Barefoot	41.35	37.39	45.30	PS1=0.17
	Shoes 1	44.57	39.90	49.23	PBF=0.17
	Shoes 2	42.60	38.50	46.70	-
ARV TA aft	Barefoot	46.36	40.57	52.14	PS1=0.17
	Shoes 1	50.21	45.12	55.30	PBF=0.17
	Shoes 2	48.15	43.43	52.88	-
ARV LG aft	Barefoot	46.95	43.20	50.71	-
	Shoes 1	48.42	44.39	52.45	-
	Shoes 2	48.23	43.60	52.86	-
Time aft	Barefoot	96.82	96.01	97.64	**S1 **S2
	Shoes 1	101.13	100.28	101.98	**BF PS2 = 0.14
	Shoes 2	102.05	101.16	102.93	**BF PS1 = 0.14

9.3.5 Within Trial analysis of EMG data

Within trial analysis for the ARV and maximum value of the EMG signal was performed to compare between the step on the platform, and the steps before and after the platform. Table 9.8 reveals that the ARV of the EMG for all muscles was significantly higher then the other two steps. Also apparent, is the significantly higher ARV of the previous step compared to the one after, in all foot conditions. The maximum value of the EMG signal displayed similar results as that of the ARV, with the only exception being for that of the TA when using shoes2 (Table 9.9).

9.3.6 Spectral analysis of EMG data

Spectral analysis of the EMG signal was performed using the *PEMG* Matlab® module, to obtain the mean and mode frequency for the PL and LG muscles (refer to Section 8.8). In Table 9.10, the mean and SD of the mean frequency of both normalised and original data for each foot condition are presented. Data corresponding to the platform step, and both the step before and after it are shown in the table. The mode frequency shows a similar pattern and is thus not presented as it offers no extra information. It is worth noting the effect normalisation has in reducing the spread of the data around the mean.

To check for significant differences between the different foot conditions, ANOVA analysis of the normalised mean frequency was performed. Table 9.11 shows that the mean frequency for both the PL and LG muscles for the platform step, was significantly lower in barefoot condition compared to shoes1 and shoes2. No significant difference between the three different foot conditions was found in the previous step for the PL muscle, while significant difference was evident when studying the LG muscle. The differences between the estimated means of the

three foot conditions, however, was less than that at the platform step.

9.3.7 Correlation analysis

Table 9.12 summarises the correlation analysis used to investigate the factors affecting the platform performance. Correlation analysis was also performed to investigate if the variations in the platform performance had a significant effect upon muscle activity data (Table 9.13). Gait speed and the time between right toe-off and the beginning of platform rotation were also considered in this analysis.

Table 9.8: Anova analysis of the normalised ARV of the EMG data for the platform step and the steps before and after the platform

Measure	Step	Mean	95% Confidence Interval		Pairwise Comparison
			Lower Bound	Upper Bound	
ARV PL BF	plat	94.408	91.458	97.357	**PRE **AFT
	prev	64.454	60.117	68.791	**PLA **AFT
	aft	41.349	37.394	45.304	**PLA **PRE
ARV PL S1	plat	107.410	103.997	110.823	**PRE **AFT
	prev	67.782	63.370	72.193	**PLA **AFT
	aft	44.565	39.897	49.233	**PLA **PRE
ARV PL S2	plat	98.183	94.496	101.870	**PRE **AFT
	prev	64.106	60.078	68.134	**PLA **AFT
	aft	42.596	38.496	46.696	**PLA **PRE
ARV TA BF	plat	90.566	86.791	94.341	**PRE **AFT
	prev	71.504	64.755	78.253	**PLA **AFT
	aft	46.356	40.572	52.139	**PLA **PRE
ARV TA S1	plat	110.828	107.103	114.554	**PRE **AFT
	prev	78.851	70.951	86.751	**PLA **AFT
	aft	50.214	45.124	55.304	**PLA **PRE
ARV TA S2	plat	98.605	95.314	101.897	**PRE **AFT
	prev	81.749	74.106	89.392	**PLA **AFT
	aft	48.155	43.425	52.884	**PLA **PRE
ARV LG BF	plat	94.634	91.601	97.666	**PRE **AFT
	prev	63.340	60.064	66.616	**PLA **AFT
	aft	46.953	43.199	50.708	**PLA **PRE
ARV LG S1	plat	106.878	103.926	109.830	**PRE **AFT
	prev	65.527	62.105	68.949	**PLA **AFT
	aft	48.423	44.395	52.451	**PLA **PRE
ARV LG S2	plat	98.488	94.872	102.105	**PRE **AFT
	prev	64.662	60.571	68.753	**PLA **AFT
	aft	48.232	43.603	52.862	**PLA **PRE

Table 9.9: Anova analysis of normalised maximum EMG data for the platform step and the steps before and after the platform

Measure	Step	Mean	95% Confidence Interval		Pairwise Comparison
			Lower Bound	Upper Bound	
Max PL BF	plat	98.225	93.605	102.844	**PRE **AFT
	prev	67.702	62.052	73.352	**PLA **AFT
	aft	37.240	32.623	41.857	**PLA **PRE
Max PL S1	plat	108.946	103.990	113.901	**PRE **AFT
	prev	72.807	67.392	78.221	**PLA **AFT
	aft	39.986	35.168	44.805	**PLA **PRE
Max PL S2	plat	92.829	88.501	97.158	**PRE **AFT
	prev	68.778	63.520	74.035	**PLA **AFT
	aft	36.229	32.645	39.813	**PLA **PRE
Max TA BF	plat	91.971	87.547	96.394	*PRE **AFT
	prev	82.883	77.473	88.293	*PLA *AFT
	aft	67.216	55.747	78.685	**PLA *PRE
Max TA S1	plat	111.093	106.614	115.572	**PRE **AFT
	prev	97.072	90.127	104.018	**PLA **AFT
	aft	80.223	73.022	87.423	**PLA **PRE
Max TA S2	plat	96.936	92.449	101.423	**AFT
	prev	97.119	90.455	103.783	**AFT
	aft	75.722	69.664	81.780	**PLA **PRE
Max LG BF	plat	100.214	95.065	105.363	**PRE **AFT
	prev	74.496	70.102	78.891	**PLA **AFT
	aft	41.400	37.253	45.547	**PLA **PRE
Max LG S1	plat	106.689	102.117	111.262	**PRE **AFT
	prev	77.591	72.631	82.550	**PLA **AFT
	aft	42.343	37.112	47.574	**PLA **PRE
Max LG S2	plat	93.097	89.237	96.956	**PRE **AFT
	prev	76.089	70.960	81.217	**PLA **AFT
	aft	40.713	36.544	44.882	**PLA **PRE

Table 9.10: Descriptive statistics for the mean frequency of EMG data

		Original		Normalised	
Measure	Foot Condition	Mean	Std. Dev	Mean	Std. Dev
Mean	Barefoot	114.51	30.94	96.34	9.61
freq PL	Shoes 1	119.77	38.03	99.58	10.02
plat step	Shoes 2	124.32	36.22	104.07	11.05
Mean	Barefoot	116.47	29.16	101.01	12.34
freq PL	Shoes 1	114.69	30.23	98.92	10.12
prev step	Shoes 2	116.46	32.49	100.07	10.79
Mean	Barefoot	112.37	26.80	97.40	11.06
freq PL	Shoes 1	114.91	29.68	99.12	11.57
next step	Shoes 2	119.91	29.68	103.48	10.49
Mean	Barefoot	98.08	22.78	96.69	9.99
freq LG	Shoes 1	101.08	23.57	99.46	8.89
plat step	Shoes 2	105.44	23.49	103.86	8.06
Mean	Barefoot	94.67	15.29	98.55	8.22
freq LG	Shoes 1	96.36	16.96	100.10	8.97
prev step	Shoes 2	97.82	18.07	101.35	8.49
Mean	Barefoot	99.74	17.08	96.57	7.08
freq LG	Shoes 1	103.69	20.30	100.07	8.15
next step	Shoes 2	106.74	18.88	103.36	8.99

Table 9.11: Anova analysis for the normalised mean frequency of EMG data

			95% CI		Pairwise
Measure	Foot Condition	Mean	LB	UB	Comparison
PL Mean	Barefoot	96.057	94.061	98.053	*S1 **S2
Frequency at	Shoes 1	99.677	97.575	101.780	*BF *S2
Platform step	Shoes 2	104.266	101.961	106.570	**BF *S1
Mean	Barefoot	100.920	98.335	103.506	-
Freq PL	Shoes 1	99.088	96.969	101.206	-
Prev step	Shoes 2	99.993	97.729	102.256	-
Mean	Barefoot	97.629	95.325	99.933	**S2
Freq PL	Shoes 1	99.194	96.786	101.602	*S2
next step	Shoes 2	103.177	101.054	105.300	**BF *S1
Mean	Barefoot	96.470	94.380	98.560	**S1 **S2
Freq LG	Shoes 1	100.010	98.203	101.817	**BF **S2
Plat step	Shoes 2	103.520	101.852	105.188	**BF **S1
Mean	Barefoot	98.114	96.433	99.795	PS1=0.08 *S2
Freq LG	Shoes 1	100.493	98.642	102.343	PS1=0.08
Prev step	Shoes 2	101.392	99.612	103.173	*BF
Mean	Barefoot	96.972	95.525	98.419	*S1 **S2
Freq LG	Shoes 1	99.977	98.269	101.685	*BF *S2
next step	Shoes 2	103.050	101.182	104.919	**BF *S1

Table 9.12: Factors affecting platform rotation

	PMIA	PMPfA	PMAA	PSIA	PSPfA	PSAA
X land pos	-.03	0.57**	-0.43**	0.21**	0.73**	-0.47**
Y land pos	0.34**	-.03	-.01	0.58**	-0.13*	0.14*
LAnk drop	0.27**	0.49**	-0.27**	0.62**	0.53**	-0.29**
COM drop	.02	0.47**	-0.17**	.11	0.48**	-0.35**
Avg Gspeed	.03	.09	-.07	.07	0.16**	-0.12*
RTOtoROT	-0.19**	.05	-0.16**	-0.22**	0.17**	-0.22**
PMIA	1.00	-.01	.10	0.65**	-.11	.11
PMPfA	-.01	1.00	-0.14*	0.21**	0.74**	-0.32**
PMAA	.10	-0.14*	1.00	-.07	-0.31**	0.54**
PSIA	0.65**	0.21**	-.07	1.00	0.17**	-.02
PSPfA	-.11	0.74**	-0.31**	0.17**	1.00	-0.42**
PSAA	.11	-0.32**	0.54**	-.02	-0.42**	1.00
PMIV	.10	-0.33**	0.34**	.06	-0.40**	0.28**
PMPfA	.06	0.38**	-0.28**	0.18**	0.49**	-0.22**
PMAA	.087	-.196**	.182**	.043	-.316**	.063

Table 9.13: Correlation analysis (Pearson)

	mean Freq PL	mean Freq G	ARV PL	ARV TA	ARV G
mean Freq PL	1.00	0.46**	-.06	-0.14*	-0.14*
mean Freq G	0.46**	1.00	.00	-.06	-0.23**
ARV PL	-.06	.00	1.00	0.30**	0.76**
ARV TA	-0.14*	-.06	0.30**	1.00	0.30**
ARV G	-0.14*	-0.23**	0.76**	0.30**	1.00
ank inv	.06	.00	-.04	-0.14*	-.05
ank flex	.06	.05	.05	.01	.02
land rot	.03	.01	-0.27**	-.03	-0.27**
X land pos	-.06	.01	.08	0.29**	0.15*
Y land pos	.08	0.12*	.10	0.13*	.10
Gait speed	-.05	-.02	0.29**	0.23**	0.17**
RTOtoROT	-0.14*	-0.18**	-.01	-.06	.00
PMIA	-.08	-.07	-.04	0.18**	.02
PMPfA	-.09	-.05	-.01	0.13*	.01
PMAA	.02	-.05	-.03	-.03	-.07
PMIV	.01	.05	-0.13*	-0.19**	-0.16**
PMPfV	-.02	-.01	-.07	-.08	-.03
PMAV	.06	.01	-.05	-.05	-.09
PSIA	-.06	.07	-.01	0.21**	.09
PSPfA	-0.17**	-.08	.02	.08	.08
PSAA	.01	-.07	.03	-0.15*	-.03

10 Discussion

10.1 Platform performance

The robotic manipulator designed and described previously in this thesis is the first to allow sudden induced supination, or inversion of the foot of a dynamic subject. The platform was fully tested and optimised before utilising it in this research (refer to Section 5.4). After ensuring proper function, the platform was used in a study to assess the role of shoes in ankle sprains. This study was the first real challenge for the platform, as it had to act on more subjects than during testing, covering a wide range of body weights and walking patterns. This was an important opportunity to assess the performance of the platform and to further optimise it.

Data from the 29 processed subjects with all 600 successful trials were first analysed (refer to Section 9.1). The performance of the platform was found to be very good. The majority of the maximum rotation angles around each of the three rotation axes, were clustered within a range of 2° of the target angle. In inversion and flexion, most of the values were larger than the target angle of 15°. The stop angle data for all three axes were more scattered, but they were still clustered within 2° of the target angle. The stop angle data, on the other hand, were clustered around the target angle. The stop angle around a given axis is defined as the angle of the platform when its rotational velocity around

that axis first drops to zero (refer to Section 8.6). The stop angle as such relates to the primary movement of the platform. Further movement of the platform due to the dynamic load generated by the walking subject, as well as the fact that the actuators are powered by compressible air (refer to Section 4.2.5), are represented by the maximum angle. It is then desirable to have a stop angle as close as possible to the target angle and maximum angle that does not exceed the target angle by a significant amount. Since this is the first study involving the newly designed platform, and because the effect of the degree of rotation have not yet been investigated, it was decided to exclude trials with outlier rotation values (refer to Section 9.1).

Statistical analysis of the platform data for the included trials is shown in Table 9.1. The analysis showed some statistical significance in the rotation angles between different foot conditions. The maximum observed difference of 0.6° was seen at the adduction stop angle of the platform between the barefoot condition and shoes2 condition. This difference was lower than the standard deviation of the adduction angle data. The correlation analysis (Table 9.13) revealed that the observed variations in the platform degree of rotation were not responsible for the changes in the studied EMG and kinematic statistics. As such, the observed statistical difference between the three foot conditions was shown to have no effect on the studied statistics.

In order to further improve the performance of the platform, it was necessary to identify the factors affecting its performance, hence the correlation analysis in Table 9.12. This table contains normalised data for each subject and foot condition, thus the effect of subject weight is reflected. The main factor affecting the rotation of the platform was shown to be the landing position on the platform (XLP and YLP). This was an expected result, where the farther away the subject lands from the axis of rotation, the higher the resulting moment load the platform

has to counteract. Indeed, there was a positive correlation between the landing position of the foot in the Y and X axes, and the platform rotation in inversion and flexion respectively. The rotation of the platform in adduction, on the other hand, had a negative correlation with the landing position in the X axis. This was due to the fact that in adduction, and unlike flexion and inversion, the platform was rotating against the direction of the body load.

10.2 Kinematic data implications

While kinematics of normal gait are well documented, this was the first such study to investigate the effect of sudden foot supination of walking subjects on body kinematics. The rotation of the platform was observed to affect the body kinematics of subjects. It is important to understand which changes can be attributed as an injury-defence mechanism and which are a direct consequence of platform rotation. At this stage it would be difficult to interpret all observed results without undergoing further in depth research which is beyond the scope of this project. The analysis presented here is designed to serve as the foundation and basis for further studies accordingly.

10.2.1 Acceleration

The speed and acceleration of the platform were important factors to consider when rotating the foot of moving subjects. This is depicted in Figures 9.4 and 9.8. As the platform accelerated downwards in inversion and flexion, the load on the footplate, and ultimately the foot and ankle, represented by the SG value dropped down. When the platform started decelerating, on the other hand, the load of the foot increased (refer to Section 9.2.2). As such, controlling the acceleration and deceleration of the platform allows altering the load on the foot. One use of this

can be to suddenly decelerate the platform during rotation and then accelerate it again. This could be used, for example, when studying the reaction time of the lower limb muscles. Another use could be in the randomisation of the platform rotation to counteract the effect of 'learning'.

The reason for this relation between acceleration of the footplate and the load on the foot can be explained by Newton's 2nd law:

$$\sum F_{\vec{y}} = Ma_{\vec{y}}$$

Assuming the second foot of the subject is off the ground, the subject will be only supported by the footplate. Hence, the acceleration of the subject will be similar to the point of the footplate where the subject's foot lies. Since the platform is rotating rather then translating, the linear downward deceleration of a point on the foot plate is dependent on the distance from the axis of rotation, the further away from the axis the larger the linear acceleration given a constant angular acceleration. This translates to larger changes of the forces acting on the foot.

The foot of the subject was not attached to the foot-plate; when the platform rotates, the subject translated downwards due to gravity alone. As such, if the point where the subject's foot lies accelerates with a value higher then the gravitational acceleration, the foot-plate will no longer be in contact with the subject's foot. This is what happened in the case relating to Figure 9.8. Apparent in this figure, is the delayed inversion of the subject's foot since before the platform came to a stop, the foot was no longer in contact with the foot-plate.

10.2.2 Foot inversion

The relation between platform rotation and foot inversion was described in Section 9.2.2. As expected, foot inversion was mainly induced by the rotation of

the platform around the x-axis. Rotation of the platform around its z-axis was also seen to influence the inversion of the foot. This was due to the fact that the platform rotated around its own axes of rotation, as opposed to the foot axes. When a subject stepped on the footplate with their foot abducted, the x-axis of the foot was oblique to that of the platform. In that case, platform inversion resulted in reduced inversion of the foot and some plantar-flexion. When the platform adducted, however, the x-axis of the foot became more aligned with that of the platform, thus increasing the degree of foot inversion. It is worth noting that subjects landed on the footplate with an average abduction angle of 12.8°.

It can also be seen from the figures in Section 9.2.2 that foot inversion was always less than the platform inversion. This can be attributed to the orientation of the tibia relative to the level ground, as foot inversion is the x-axis rotation of the foot relative to the tibia. This effect is highlighted in Figures 10.1a and 10.1b.The orientation of the tibia (or tibia progression) was calculated by our custom body model relative to the lab's reference frame (refer to Section 8.5). As the orientation of the tibia relative to x-axis of the lab increased, the value of foot inversion decreased, and vice versa. In Figure 9.6, foot inversion seems to stop and slightly evert during the adduction of the platform, opposite to what is observed in. This can be attributed to the larger increase in the tibia rotation angle, which counteracts the increase of foot inversion due to platform adduction. After the platform stopped rotating, the foot was seen to continue to invert while the tibia rotation decreased. While positive rotation of the tibia will relieve foot inversion, we postulated that it would also shift the load on the foot to the lateral side; this can be investigated by attaching a pressure mat to the footplate. Having the load shift to the lateral edge of the foot in that way could increase the likelihood of the foot rolling over its lateral edge. The way a

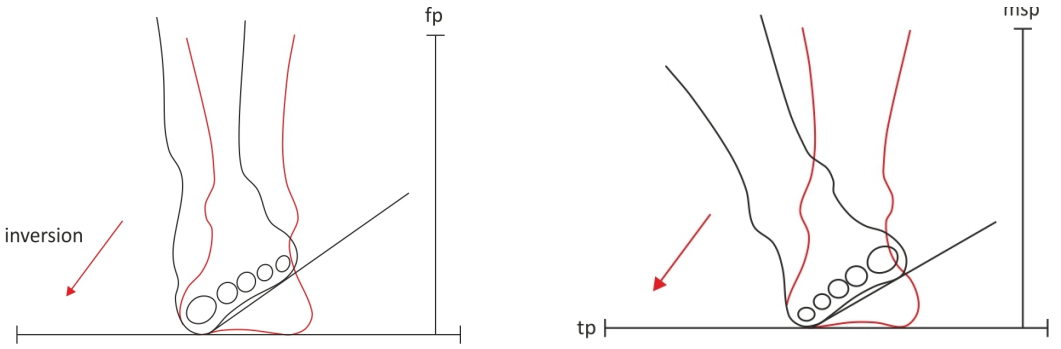

(a) Ankle is inverted when foot rotated and tibia is perpendicular to level ground

(b) Tibia's rotation relative to level ground counteracts ankle inversion when the foot is rotated

Figure 10.1: Effect of tibia orientation on ankle inversion

person positions their body in reaction to a sudden foot inversion and which tibia orientation is better in reducing ankle sprains has to be further investigated.

On average the maximum foot inversion caused by the rotation of the platform was 9.8°, 7.3°, and 8.8° in unshod, shoes1 and shoes2 foot conditions respectively (Table 9.2). While there was a significant difference between the three foot conditions, the fact that the foot markers were moved from barefoot to the shoes reduced the validity of such a direct comparison. It is suggested to devise a method which allows the markers to be directly attached to the foot event when wearing shoes. This could be achieved for example by cutting small holes in the shoes corresponding to where the markers would attach to the foot.

10.2.3 Foot plantar-flexion

Induced foot plantar-flexion was caused mainly by the rotation of the foot-plate around the y-axis. The mean induced plantar-flexion of the foot was 4.9°, 7.2°, and 5.6° in barefoot, shoes1, and shoes2 conditions respectively (Table 9.2). This was much lower than the platform plantar-flexion angle of 15°. Also noted in Table 9.2, is the great variability in the results. The reason behind this variability was the dynamic nature of the conducted experiments, where subjects

were walking naturally in the laboratory. After HS, a subject's foot started rotating into dorsi-flexion. When the platform starts rotating, it counteracts the normal dorsi-flexing of the foot, and caused a plantar-flexing motion (Figures 9.9 and 9.15). The maximum plantar-flexion angle of the foot, thus, depends on when the platform starts rotating in the GC and the extent of foot dorsi-flexion at that moment.

10.2.4 Left and right body kinematics

In the current research, the platform was used to suddenly supinate the left foot of a walking subject. To investigate how this affected the subject's body kinematics, data from the stride when the foot was supinated was compared to that from a normal stride. Ideally, the reference stride would be that of the left foot just before the platform step. Due to a limitation in the number of Vicon® cameras available, the data for the stride before the platform could not be captured (refer to Section 7.4.3). Kinematic data corresponding to the right stride just before platform rotation were, thus, used instead. It is important to note that the platform started rotating just after RTO, and as such, the kinematic data corresponding to the final phase of the right stride (RTO to RHS) were influenced by the platform rotation.

The effect of foot supination on the y-axis component of the COM relative to the subject's ankle is demonstrated in Figure 9.11. The rotation of the platform caused the COM of the subject to shift away from the left foot. Since at that stage of the GC, the left foot was the only part supporting the body, such positioning of the COM was likely to shift the load on the foot to its medial side.

Platform rotation affects hip kinematics in both flexion/extension and adduction/abduction (refer to Section 9.2.4). As the platform tilted, the left side of the pelvis dropped down which caused the observed decrease in hip adduction.

The reasons behind this decrease in left hip extension and increased right hip flexion were more difficult to interpret. Whether they were due to an injury prevention mechanism or just as a direct result of the dropping of the platform must be further investigated. It was also interesting to note the changes in hip flexion/extension kinematics with the decrease in left stance time.

Knee flexion/extension movement was similar between the two sides, with the left knee flexing slightly just after the platform stopped tilting downwards. This can be compared to knee flexion due to landing from a jump, where the dropping of the platform shifts the ground downwards simulating a small drop. The drop of the platform also causes the knee to extend earlier than normal.

The main purpose of the platform is to supinate the foot of a walking subject and as such differences were expected to be seen between left and right foot plantar-flexion. In normal gait, and as shown by the green curve of Figure 9.15, the foot rotates towards dorsi-flexion slightly after foot strike. The planter-flexion of the platform acts to counteract such movement, hence that second small parabola in the blue curve representing the left foot plantar-flexion. Since the platform stays plantar-flexed during the entire left stance, the left foot does not reach the same dorsi-flexion angle as that of the right. The increased plantar-flexion angle at TO can be similarly explained.

10.3 EMG data analysis

10.3.1 Effect of platform rotation on muscle activity

A platform was designed to invert or supinate the foot of dynamic subjects in order to understand more about the risk factors of ankle injury and how to reduce such injuries. For it to be of any use, the platform must have an observable effect

on the reaction of the studied muscles. This is demonstrated in Figures 9.16, 9.17, and 9.19 where the effect of the platform rotation on the PL and TA muscles is illustrated. It is apparent from Figure 9.17 that the greatest observable difference occurs during the rotation of the platform. When investigating muscle activity, this interval is of the greatest importance.

Figure 9.18 compares the PL muscle activity for the platform step and the step before. It is obvious to the eye the increased muscle activity at the platform step. The statistical analysis presented in Tables 9.8 and 9.9, to compare the activity of the three studied muscles between the platform step and those before and after it, also reveals significant difference. This observable difference between the different steps is present in all studied foot conditions. The analysis reveals that the induced foot supination generated significantly higher muscle activity compared to the normal steps.

An intriguing result is also observed where the muscle activity of the step following the foot supination is significantly lower than that of the step previous to the platform. This is also demonstrated in Figure 9.18, where the diminished muscle activity of the PL muscle for the step, and even several steps, following foot supination is observed. This is such an important observation as it demonstrates that an initial non-injury causing foot supination may predispose the ankle for injury. It is worth noting, however, that this is an intriguing finding and this study was not specifically designed to investigate this effect. It is as such highly recommended that further studies be conducted to investigate this effect.

10.3.2 Average rectified value

ARV analysis of the filtered and enveloped EMG data for five intervals in the platform step are presented in Tables 9.5 and 9.6. When comparing between different foot conditions, the ARV of the EMG signal for the interval spanning

the duration of platform rotation is significantly lower than that of both shod conditions. This is consistent with previous studies conducted at IMAR (Kerr *et al.* 2009; Ramanathan *et al.* 2011a; Ramanathan *et al.* 2011b).

When looking at interval 2 spanning from HS until just before the platform begins rotating, the ARV of the PL muscle is significantly higher in S2 compared to BF, and in S1 it is significantly higher than the BF condition at P=0.08. One possible explanation for this could be that subjects are pre-tensing their muscles more in shoe conditions in preparation for the platform rotation, especially since subjects already know that the platform will supinate. Pre-activated muscles have been suggested in the literature to be an important protective factor against ankle sprains (refer to Section 2.2.5). The fact that the PL muscle is more active in shod conditions may be to compensate for the reduced proprioception of the foot introduced by the use of shoes (refer to Section 2.2.6). It is important to note, however, that such comparison is not available in the current research for the step before at a similar interval, since the timing of HS for that step was not captured. It is also possible that such differences are present in the step before where the platform was not present. It is recommended that such behaviour is further investigated in future studies.

When investigating the interval spanning the entire stance phase, however, the ARV in barefoot condition is significantly lower than the S1 condition only. The mean of the ARV in the BF condition remains lower than that in S2 condition but this is not statistically significant. During the last part of the stance phase (interval 4), however, the ARV of the PL EMG signal is significantly lower in S2 condition compared to BF condition. This and the fact that the current experiment was designed to detect a true difference that is higher than 20% (refer to Section 7.2), may be responsible to the lack of statistical significance between the BF and S2 conditions when looking at the whole stance phase interval. It

is not clear why the PL muscle was less active in S2 condition compared to BF condition for interval 4, where in intervals 2, 3, and 5 it was higher. Notice also that the mean Maximum PL muscle activity for S2 condition, and while no statistical significance is present, is lower than that for BF condition. This is in contrast to the statistically higher Maximum PL activity in S1 condition when compared to BF condition. While this study does not seek to compare the performance between different shoe types in relation to how they may contribute to ankle sprain injuries, the different results obtained from the two shoes used demonstrate that the newly designed system is suitable for such studies.

When looking at interval 3 spanning the entire duration of platform rotation, the ARV for the PL muscle is significantly higher in both shoes conditions compared to the BF condition. This supports the findings of the previous SSIR studies conducted at IMAR and demonstrates their validity for DSIR conditions. This study thus offers further support for the theory first suggested by Kerr *et al.* (2009) that the use of shoes may predispose the wearer to ankle sprain injury.

To investigate whether such differences between the three foot conditions were revealed by the sudden supination of the foot, or if they were always present irrespective of the platform rotation, the ARV of the EMG signal for the different foot conditions were also compared for the steps before and after the platform (Table 9.7). Indeed for both the PL and LG, the means of the ARV were much closer together with no statistical significance between them. This implies that different shoes affect the foot differently and may possess different protective functions. Indeed McKay *et al.* (2001) highlighted that shoes containing air-cells seem to increase the risk of ankle sprains.

10.4 Applications of the newly developed system

The newly designed robotic platform allows safe and controlled supination and inversion of the foot and ankle of dynamic subjects, so as to mimic real life ankle spraining conditions (refer to Section 2.2.2). The fact that the platform was synchronised and integrated to work with motion and EMG capture systems means that researchers can safely test and measure the reactions of the musculoskeletal system in ankle injury-like conditions. Below is a list of the possible applications of the newly developed system which is by no means exhaustive.

10.4.1 Investigating the risk factors for ankle sprain injury

Ankle sprain injury occurs when the foot is being loaded in an inverted or supinated position (Safran *et al.* 1999; Puffer 2001). The designed robotic platform presented in this thesis allows safe simulation of ankle sprain injury by inducing controlled foot and ankle inversion/supination of dynamic subjects. The platform was also synchronised with a bilateral four-channel EMG system and a Vicon® motion capture system. This allows researchers to assess the effect of induced inversion/supination on the musculoskeletal system and ultimately reveal more information about the risk factors of this injury.

10.4.2 Testing and improving footwear design

As stated earlier, footwear can play a negative role in ankle sprain injury and this was further validated by the experimental study presented in this thesis. Footwear however protects the foot from cuts and abrasion and as such it is not recommended that people stop wearing footwear. A better solution would be to advance and improve the design of footwear allowing protection of the foot against ankle sprain injury rather than contributing towards it. This can be

achieved if there was an effective method to safely test the performance of footwear in conditions that usually cause ankle sprain injury. The already available platforms which can safely rotate the foot and ankle to mimic real life ankle sprain conditions were shown to be limited (refer to Section 2.3). The newly developed system presented in this thesis has targeted many of those limitations and would allow effective testing of different footwear, revealing their effect on the musculoskeletal system during foot supination and inversion of dynamic subjects. This is hoped to help identify better footwear that is less likely to contribute towards ankle sprain injury or which can better protect against such injury. The new system can also be used by companies that design, manufacture and sell footwear allowing them to test and improve their products before releasing them on to the market. Similarly the developed system can be used to assess and improve the performance of different taping methods and ankle braces in protecting the foot against ankle sprain injury.

10.4.3 Assessing the effectiveness of the different ankle injury rehabilitation techniques

Proper rehabilitation and training of the ankle after injury is important to reduce the risk of re-injury. The new system can be used to compare the reaction of the musculoskeletal system due to sudden foot and ankle supination or inversion before and after the rehabilitation and training programs. This is hoped to assess the effectiveness of such programs and to identify those which provide better outcomes.

10.4.4 Identifying subjects who are vulnerable to ankle sprain injury

Bahr *et al.* (2007) has demonstrated how a special training program helped reduce the frequency of ankle sprains in subjects with a history of such injury. The developed system presented in this thesis is hoped to help identify subjects who are more vulnerable to ankle sprain injury regardless of whether they had or had not suffered a previous injury. This would allow such individuals to undergo special training and ultimately reduce the risk of sustaining an injury. Professional athletes for example would greatly benefit from this where injuries can be quite costly.

10.4.5 Other uses

While the robotic platform was designed to allow safe simulation of an ankle sprain injury it can also be utilised for other applications. The system can be used to investigate the reaction of subjects with diminished foot proprioception to induced foot rotation such as subjects with diabetic neuropathy. Ultimately the system could help advance methods that would improve the proprioception of such individuals. Priplata *et al.* (2006) for example found that vibrating insoles could reduce postural sway in subjects with diabetic neuropathy and those who suffered unilateral stroke. Our new system could help further assess the benefits of such devices by investigating any improvements in the reaction of such subjects to induced foot rotation.

11 Conclusion and Recommendations

11.1 Summary

A new system was developed that allows assessing the effect of sudden foot and ankle inversion/supination on the musculoskeletal system of dynamic subjects (e.g. walking, running, jumping, etc...). The system consists of a newly designed robotic platform (which is the main component of the system), a Vicon® motion capture system, a bilateral four-channel EMG system, and a software that was specifically written to automatically extract, manage and process all the generated data. The system is designed to be modular where more systems (like the Pedar® in-shoe pressure measurement system or Oxycon® for oxygen consumption) can be added to expand its functionality.

A 3-DOF rotating robotic platform was designed,built and embedded in the IMAR Sports Laboratory floor. The robotic platform is powered by three pneumatic actuators and can rotate independently around three different axes and as such can induce supination or inversion of the foot of dynamic subjects. Electronic and pneumatic circuits, along with the control software and interface, were also designed and built to allow the required function from the platform. A strain gauge was attached to the platform to allow detection of foot strike to the plat-

form. To protect the foot and ankle of possible injury resulting from platform rotation when the foot was partially on the platform, four laser emitter/receivers were utilised that could detect the occurrence of such cases and signal the platform to stay levelled. To monitor the platform's rotation around the three axes of rotation three optical encoders were utilised. The angle output data of the platform were validated using an analogue and a digital angle finders and a tractograph. Testing and optimisation of the platform were then conducted to ensure the robotic platform satisfied all the requirements.

The platform was then synchronised to work with a bilateral electromyographic system, and a Vicon® MX motion capture system. The robotic platform can also synchronise with other systems (like the Pedar® in-shoe pressure measurement system) thus adding more functionality.

In order to facilitate and automate the processing of the captured data, and to extract the required statistics, a set of Matlab® modules were written. The modules were written so they can be used in future work involving the newly developed system. The coded software includes modules for indexing the data, processing of the platform, EMG, and Vicon® data, for generating various useful plots, and for exporting the resultant data in an output suitable for use with statistical analysis software. A module that detects various events of the gait cycle was also written and validated. A biomechanical model of the foot and ankle was written to allow measurement of foot inversion, plantar-flexion and tibia progression angles, since the supplied Vicon® PiG® model has limited foot modelling capabilities.

Thirty-six volunteers were recruited to participate in an experimental study to validate the new system and investigate the role of shoes in ankle sprains. Seven of the 36 recruited volunteers had to be excluded from the study due to technical difficulties. Data from the remaining 29 subjects were used to assess the perfor-

mance of the platform, while data from 23 subjects were used to investigate the role that shoes has upon ankle sprains.

Statistical analysis was conducted using SPSS® software and the obtained results demonstrated the validity of the newly developed system. The achieved rotations (STOP ANGLE) by the platform were centred around the target angles, and the small variations among the achieved rotations did not correlate to the observed changes in the studied EMG and body kinematics. The results of the EMG analysis revealed that the use of shoes causes increased muscle activity compared to the barefoot condition. The experiment showed that this increased muscle activity when shoes were worn is not seen during normal gait, but rather only when the foot was being supinated. While the study was not designed to compare the risks and benefits of different shoes, the obtained results demonstrate the ability and suitability of the new system for use in such future studies. Another intriguing finding was the observed reduction in the activity of the tested muscles after sudden supination of the foot. Due to the significance of such a finding, a future study to further investigate this matter is highly recommended.

The conducted analysis of the kinematic data, while still in its early stages, revealed significant changes in body kinematics caused by the rotation of the platform. Many of those changes are as a direct consequence of the platform rotation rather than an injury protective reaction by the body. More research is required to understand which body reactions can help protect against injury.

The newly developed system is hoped to help provide a better understanding of the risk factors of ankle sprain injury and how to prevent this injury. The system can be used to help improve the design of current footwear and identify which footwear provides better protection against ankle sprain injury. The system can also be used to assess the effectiveness of different ankle injury rehabilitation schemes and different training programs that aim to reduce ankle sprain inju-

ries. The new system can be utilised to identify individuals who are at risk of sustaining an ankle sprain injury. The system can also be utilised in studies outside the scope of ankle sprain injuries.

It is worth noting that with the exception of off-the-shelf components, all platform components and electronic and pneumatic circuitry were designed specifically for this project. The same is true for robot control PIC® code, the biomechanical model of the foot and ankle, and the data management and processing software.

11.2 Limitations

Ankle sprain injuries usually occur when subjects are unsuspecting. When subjects volunteer to experiments utilising the robotic platform they are fully informed that the platform will rotate their foot (due to ethical reasons). This takes away the element of surprise and could possibly affect the reaction of subjects to the induced foot rotation. To address this issue researchers could randomise the rotation of the platform by having it rotate in some trials and keeping it stationary in others. This would not necessarily guarantee that the subject will be unsuspecting every time the platform rotated and a method for identifying trials where the subject was unsuspecting from those where the subject was prepared for the platform rotation must be realised. Another method that researchers could utilise would be to have the subject focus and engage in an external activity like dribbling a basket ball and trying to score the ball in a basketball ring. Such external activities could also be designed to simulate different sports activities where ankle injury is known to be common thus allowing a more realistic and targeted simulation of an ankle sprain injury.

11.3 Future recommendations and suggestions

11.3.1 System recommendations and improvements

- Add a pressure mat to the foot-plate which would provide important data regarding pressure distribution under the foot (refer to Section 6.6). This pressure mat can also be used to provide the landing position of the subject on the foot-plate to the control algorithm, thus allowing for better rotational accuracy and repeatability. The landing position was indeed shown to be the most significant factor affecting the accuracy of the platform rotation (refer to Section 9.1)
- Implement different rotation profiles, mainly those simulating loading and unloading the foot during rotation. This is important since ankle sprains have been suggested to occur during loading of the foot (refer to Section 2.2.2).
- The power of this study was limited by the number of available cameras, which prevented the capturing of the stride before and after the platform. It is highly suggested to increase the number of Vicon® cameras (this has since been addressed and new cameras were added to the system).
- The platform was designed such that it can accommodate foot-plates with different surface geometry (refer to Section 4.2.1). Foot-plates with uneven surface can be used to investigate the effect of different surface terrain on ankle sprains.

11.3.2 Suggested future studies and possible applications for the new system

The experimental study presented in this thesis is the first such study that attempts to investigate the effect of shoes on both, lower limb muscle activity and body kinematics, due to induced supination of the foot of walking subjects. It also sets the foundation for further studies to be conducted using the newly developed system. Below is a list of suggested research topics that can be conducted to help understand more about ankle sprains and ultimately aid in the prevention of such injuries.

- This study revealed statistically significant changes in lower limb muscle activity and body kinematics due to sudden supination of the foot. The role (if any) these changes play in the protection or causing of ankle sprains, however, is not fully understood. For this reason it is recommended to undertake a future prospective study where the feet of active individuals are supinated. Such study will then identify those individuals who later on sustain an ankle sprain and compare their data with that from uninjured individuals.
- The current study showed differences in the lower limb muscle activity between the two used shoes. After understanding how such changes in lower limb muscle activity relate to ankle sprain injuries (previous point) the new system can be used to identify which shoes performs better in terms of reducing the chances of having ankle sprains.
- The current study revealed a significant reduction in activity of the lower limb muscles for the step following induced supination of the foot. This study, however, was not designed for that purpose which limits the strength of such findings. We suggest undertaking further research to investigate this

topic. It is important to be able to capture the EMG and gait parameters data for the step before the platform and at least one step after. It is also important to ask subjects to continue walking straight forward for several steps after they strike the platform. To remove the possibility that such effect is caused by the EMG acquisition device, it is recommended to conduct this research with two different EMG hardware set ups.

- Ankle sprains occur mostly when the foot is in a supinated or inverted position. The platform provides the ability to either supinate or invert the foot, thus allowing comparison of the effects due to those two different modes of rotation.
- The platform allows controlling the delay before the platform starts rotating after foot contact. We suggest a study to investigate the effect of varying the delay time. This can help to understand in which instances the foot is most susceptible to ankle sprains.
- A study to investigate the effect of varying the degree of rotation and possibly identifying the optimum safe rotation angle that will reveal the most details.
- Muscle fatigue is shown to affect the output of the measured EMG signal. We suggest a study to investigate the minimum number of trials before the onset of muscle fatigue. Note that such a number will obviously vary between different individuals, and as such, it important to document the physical activity of participating subjects.
- Individual with a history of ankle sprain have been shown to be more likely to suffer from further ankle sprains. It is important to conduct a study with such subjects and to investigate the differences obtained from subjects with no ankle sprain history. This research would help in the understanding of which factors play a role in the protection against ankle sprains.

- Proper rehabilitation of the ankle after injury is essential to reduce the risk of re-injury. There are several different rehabilitation techniques that can be employed and the new system can help identify which are the most effective. Such research would benefit from a database containing data from healthy subjects and those with a history of ankle sprains.

This list is by no means exhaustive and only aims to present a few of the many different studies that can be undertaken with the newly developed system. It is also worth noting that the system can also be adapted to rotate the foot of running subjects.

Bibliography

Abboud RJ (2002). Relevant foot biomechanics. Current Orthopaedics, 16(3): 165–179.

ALLAIR (2008). TRD manufacturing. [Online image], available at: http://www.allair.com/products_pneumotion.htm (Accesed 27 july 2011).

Anandacoomarasamy A and **Barnsley L** (2005). Long term outcomes of inversion ankle injuries. British Journal of Sports Medicine, 39:: e14.

Armitage P, **Berry G**, and **Matthews JN** (2002). Statistical methods in medical research (Chapter 4). Blackwell Science, 4 edition.

Ashton-Miller JA, **Ottaviani RA**, **Hutchinson C**, and **Wojtys EM** (1996). What best protects the inverted weightbearing ankle against further inversion? The American Journal of Sports Medicine, 24(6): 800–809.

Attarian DE, **Mccrackin HJ**, **Devit DP**, **Mcelhaney JH**, and **Garrett WE** (1985). A biomechanical study of human lateral ankle ligaments and autogenous reconstructive grafts. The American Journal of Sports Medicine, 13(6): 377.

Bahr R and **Bahr IA** (2007). Incidence of acute volleyball injuries: a prospective cohort study of injury mechanisms and risk factors. Scandinavian Journal of Medicine & Science in Sports, 7(3): 166–171.

Bahr R, **Lian**, and **Bahr IA** (2007). A twofold reduction in the incidence of acute ankle sprains in volleyball after the introduction of an injury prevention program: a prospective cohort study. Scandinavian Journal of Medicine & Science in Sports, 7(3): 172–177.

Bamberg E (2002). Constraints . [Online image], available at: http://www.mech.utah.edu/~me4000/tutorials/introProMechanica/constraints.html (Accesed 27 july 2011).

Basmajian JV and **De Luca CJ** (1985). Muscles alive: their functions revealed by electromyography, ch3. Williams & Wilkins.

Baumhauer JF, **Alosa DM**, **Renström PAFH**, **Trevino S**, and **Beynnon B** (1995). A prospective study of ankle injury risk factors. The American Journal of Sports Medicine, 23(5): 564–570.

Benesch S, **Pütz W**, **Rosenbaum D**, and **Becker H** (2000). Reliability of peroneal reaction time measurements. Clinical Biomechanics, 15(1): 21–28.

Beynnon BD, **Murphy DF**, and **Alosa DM** (2002). Predictive factors for lateral ankle sprains: A literature review. Journal of Athletic Training, 37(4): 376–380. PMID: 12937558 PMCID: 164368.

Callaghan MJ (1997). Role of ankle taping and bracing in the athlete. British Journal of Sports Medicine, 31(2): 102 –108.

Chan YY, **Fong DT**, **Yung PS**, **Fung KY**, and **Chan KM** (2008). A mechanical supination sprain simulator for studying ankle supination sprain kinematics. Journal of Biomechanics, 41(11): 2571–2574.

Chopra P (2007). Kinematics of a robotic arm. [Online image], available at: http://openrobotics.blogspot.com/ (Accesed 27 july 2011).

Clinghan R, **Arnold GP**, **Drew TS**, **Cochrane LA**, and **Abboud RJ** (2008). Do you get value for money when you buy an expensive pair of running shoes? British Journal of Sports Medicine, 42(3): 189 –193.

D'souza A (2011). Products . [Online image], available at: http://www.indiamart.com/dynamicengineers/aboutus.html (Accesed 27 july 2011).

Ebbutt, **Wood**, and **King** (2005). The vicon manual.

Eechaute C, **Vaes P**, **Duquet W**, and **Van Gheluwe B** (2007). Test-Retest reliability of sudden ankle inversion measurements in subjects with healthy ankle joints. Journal of Athletic Training, 42(1): 60–65.

Ferrari A, **Benedetti MG**, **Pavan E**, **Frigo C**, **Bettinelli D**, **Rabuffetti M**, **Crenna P**, and **Leardini A** (2008). Quantitative comparison of five current protocols in gait analysis. Gait & Posture, 28(2): 207–216.

Frankeny JR, **Jewett DL**, **Hanks GA**, and **Sebastianelli WJ** (1993). A comparison of ankle-taping methods. Clinical Journal of Sport Medicine, 3(1): 20–25.

Garrick JG and **Requa RK** (1988). The epidemiology of foot and ankle injuries in sports. Clinics in sports medicine, 7(1): 29–36.

Grüneberg C, **Nieuwenhuijzen PHJA**, and **Duysens J** (2003). Reflex responses in the lower leg following landing impact on an inverting and Non-Inverting platform. The Journal of Physiology, 550(3): 985–993.

Gutierrez-Farewik EM, **Bartonek A**, and **Saraste H** (2006). Comparison and evaluation of two common methods to measure center of mass displacement in three dimensions during gait. Human Movement Science, 25(2): 238–256.

Hawkins RD, **Hulse MA**, **Wilkinson C**, **Hodson A**, and **Gibson M** (2001). The association football medical research programme: an audit of injuries in professional football. British Journal of Sports Medicine, 35(1): 43 –47.

Hopkins JT, **McLoda T**, and **McCaw S** (2007). Muscle activation following sudden ankle inversion during standing and walking. European Journal of Applied Physiology, 99(4): 371–378.

Isakov E, **Mizrahi J**, **Solzi P**, **Susak Z**, and **Lotem M** (1986). Response of the peroneal muscles to sudden inversion of the ankle during standing. Int J Sport Biomech, 2(2): 100–109.

Kadaba MP, **Ramakrishnan HK**, and **Wootten ME** (1990). Measurement of lower extremity kinematics during level walking. Journal of Orthopaedic Research, 8(3): 383–392.

Kernozek T, **Durall CJ**, **Friske A**, and **Mussallem M** (2008). Ankle bracing, Plantar-Flexion angle, and ankle muscle latencies during inversion stress in healthy participants. Journal of Athletic Training, 43(1): 37–43.

Kerr R, **Arnold GP**, **Drew TS**, **Cochrane LA**, and **Abboud RJ** (2009). Shoes influence lower limb muscle activity and may predispose the wearer to lateral ankle ligament injury. Journal of Orthopaedic Research, 27(3): 318–324.

Konradsen L, **Peura G**, **Beynnon B**, and **Renström P** (2005). Ankle eversion torque response to sudden ankle inversion torque response in unbraced, braced, and pre-activated situations. Journal of Orthopaedic Research, 23(2): 315–321.

Lake MJ (2000). Determining the protective function of sports footwear. Ergonomics, 43: 1610–1621.

Linford CW, **Hopkins JT**, **Schulthies SS**, **Freland B**, **Draper DO**, and **Hunter I** (2006). Effects of neuromuscular training on the reaction time and electromechanical delay of the peroneus longus muscle. Archives of Physical Medicine and Rehabilitation, 87(3): 395–401.

Lynch SA, **Eklund U**, **Gottlieb D**, **Renstrom PA**, and **Beynnon B** (1996). Electromyographic latency changes in the ankle musculature during inversion moments. The American Journal of Sports Medicine, 24(3): 362.

McKay GD, **Goldie PA**, **Payne WR**, and **Oakes BW** (2001). Ankle injuries in basketball: injury rate and risk factors. British Journal of Sports Medicine, 35(2): 103 –108.

Milgrom C, **Shlamkovitch N**, **Finestone A**, **Eldad A**, **Laor A**, **Danon YL**, **Lavie O**, **Wosk J**, and **Simkin A** (1991). Risk factors for lateral ankle sprain: a prospective study among military recruits. Foot & Ankle, 12(1): 26–30.

Murphy DF, **Connolly DAJ**, and **Beynnon BD** (2003). Risk factors for lower extremity injury: a review of the literature. British Journal of Sports Medicine, 37:: 13 –29.

Nieuwenhuijzen PHJA, **Grüneberg C**, and **Duysens J** (2002). Mechanically induced ankle inversion during human walking and jumping. Journal of Neuroscience Methods, 117(2): 133–140.

Nordin M and **Frankel VH** (2001a). Basic biomechanics of the musculoskeletal system (Chapter 6). Lippincott Williams & Wilkins, 3rd edition.

Nordin M and **Frankel VH** (2001b). Basic biomechanics of the musculoskeletal system (Chapter 9). Lippincott Williams & Wilkins, 3rd edition.

Perry J and **Burnfield JM** (2010). Gait analysis: normal and pathological function (chapter 1). SLACK incorporated, 2 edition.

Priplata A, **Patritti B**, **Niemi J**, **Hughes R**, **Gravelle D**, **Lipsitz L**, **Veves A**, **Stein J**, **Bonato P**, and **Collins J** (2006). Noise-enhanced balance control in patients with diabetes and patients with stroke. Annals of Neurology, 59(1): 4–12.

Puffer JC (2001). The sprained ankle. Clinical Cornerstone, 3(5): 38–49.

Ramanathan AK, **Parish EJ**, **Arnold GP**, **Drew TS**, **Wang W**, and **Abboud RJ** (2011a). The influence of shoe sole's varying thickness on lower limb muscle activity. Foot and Ankle Surgery, 17(4): 218–223.

Ramanathan AK, **Wallace DT**, **Arnold GP**, **Drew TS**, **Wang W**, and **Abboud RJ** (2011b). The effect of varying footwear configurations on the peroneus longus muscle function following inversion. The Foot, 21(1): 31–36.

Ramot Y (1990). The dynamics of the subtalar joint in sudden inversion of the foot. Journal of Biomechanics, 112: 9–14.

Ricard MD, **Schulties SS**, and **Saret JJ** (2000). Effects of High-Top and Low-Top shoes on ankle inversion. Journal of Athletic Training, 35(1): 38–43. PMID: 16558606 PMCID: 1323436.

Riegger CL (1988). Anatomy of the ankle and foot. Physical therapy, 68(12): 1802–1814.

Robbins S and **Waked E** (1997). Hazard of deceptive advertising of athletic footwear. British Journal of Sports Medicine, 31(4): 299 –303.

Robbins S, **Waked E**, and **Mcclaran J** (1995). Proprioception and stability: Foot position awareness as a function of age and footware. Age and Ageing, 24(1): 67 –72.

Safran MR, **Benedetti RO**, **Bartolozzi III AR**, and **Mandelbaum BR** (1999). Lateral ankle sprains: a comprehensive review part 1: etiology, pathoanatomy, histopathogenesis, and diagnosis. Medicine & Science in Sports & Exercise, 31(7): S429.

Sekizawa K, **Sandrey MA**, **Ingersoll CD**, and **Cordova ML** (2001). Effects of shoe sole thickness on joint position sense. Gait & Posture, 13(3): 221–228.

Taghirad HD (2007). SGP schematic. [Online image], available at: http://saba.kntu.ac.ir/eecd/ecourses/roboticsII.htm (Accesed 27 july 2011).

Thacker SB, **Stroup DF**, **Branche CM**, **Gilchrist J**, **Goodman RA**, and **Weitman EA** (1999). The prevention of ankle sprains in sports. The American Journal of Sports Medicine, 27(6): 753 –760.

Ubell ML, **Boylan JP**, **Ashton-Miller JA**, and **Wojtys EM** (2003). The effect of ankle braces on the prevention of dynamic forced ankle inversion*. The American Journal of Sports Medicine, 31(6): 935 –940.

Vaes P, **Duquet W**, and **Van Gheluwe B** (2002). Peroneal reaction times and eversion motor response in healthy and unstable ankles. Journal of Athletic Training, 37(4): 475–480. PMID: 12937570 PMCID: 164380.

Waddington G and **Adams R** (2000). Textured insole effects on ankle movement discrimination while wearing athletic shoes. Physical Therapy in Sport, 1(4): 119–128.

Willems TM, **Witvrouw E**, **Delbaere K**, **Mahieu N**, **De Bourdeaudhuij I**, and **De Clercq D** (2005a). Intrinsic risk factors for inversion ankle sprains in male subjects: a prospective study. The American Journal of Sports Medicine, 33(3): 415.

Willems TM, **Witvrouw E**, **Delbaere K**, **Philippaerts R**, **De Bourdeaudhuij I**, and **De Clercq D** (2005b). Intrinsic risk factors for inversion ankle sprains in females–a prospective study. Scandinavian Journal of Medicine & Science in Sports, 15(5): 336–345.

Wilson EL and **Madigan ML** (2007). Effects of fatigue and gender on peroneal reflexes elicited by sudden ankle inversion. Journal of Electromyography and Kinesiology, 17(2): 160–166.

Wright IC, **Neptune RR**, **Van den Bogert AJ**, and **Nigg BM** (2000). The influence of foot positioning on ankle sprains. Journal of Biomechanics, 33(5): 513–519.

Yeung MS, **Chan KM**, **So CH**, and **Yuan WY** (1994). An epidemiological survey on ankle sprain. British Journal of Sports Medicine, 28:: 112 –116.

A Detailed drawings of the platform design

This appendix can only be provided upon request from Professor Abboud due to sensitive and confidential material related to the design that is property of IMAR.

B Electronic circuit diagram

This appendix can only be provided upon request from Professor Abboud due to sensitive and confidential material related to the design that is property of IMAR.

C Platform's control software

This appendix can only be provided upon request from Professor Abboud due to sensitive and confidential material related to the design that is property of IMAR.

D Foot Bodymodel

```
{*Initialisations*}
{*================*}

OptionalPoints(LASI,RASI,RPSI,LPSI,LKNE,LANK,LMANK,LD1MT,LTOE,LP3MT)
ref = [{0,0,0},{1,0,0},{0,0,1},xyz]


{*KINEMATICS*}
{*===========*}

{* Tibia *}


LAJC2 = ((LANK+LMANK)/2)
LFC = ((LD1MT+LTOE)/2)

SACR = (LPSI+RPSI)/2
PELF = (LASI+RASI)/2

Pelvis = [PELF,LASI-RASI,PELF-SACR,yzx]

If ($LAsisTrocanterDistance + $RAsisTrocanterDistance) <> 0 Then
    LATD = $LAsisTrocanterDistance
Else
    LATD = 0.1288*$LLegLength-48.56
EndIf

C = $LLegLength*0.115-15.3
InterASISDist=DIST(LASI,RASI)
aa = InterASISDist/2
mm = $MarkerDiameter/2
COSBETA = 0.951
SINBETA = 0.309
COSTHETA = 0.880
SINTHETA = 0.476
COSTHETASINBETA = COSTHETA*SINBETA
COSTHETACOSBETA = COSTHETA*COSBETA

```

```
LHJC = {C*COSTHETASINBETA − (LATD + mm) * COSBETA,
       −C*SINTHETA + aa,
        −C*COSTHETACOSBETA − (LATD + mm) * SINBETA}*Pelvis


LKneeOS = ($MarkerDiameter+$LKneeWidth)/2
LKJC=CHORD(LKneeOS,LKNE,LHJC,LTHI)


LTIBIAf1 = [LAJC2,LANK−LMANK,LAJC2−LKJC,yxz]
LTIBIAf2 = [LAJC2,LANK−LMANK,LANK−LKNE,yxz]

LTIBIAi1 = [LAJC2,LP3MT−LAJC2,LMANK−LANK,xzy]

{*dont use these 2 as they involve p3mt which change
position with foot condition*}
LTIBIAp3 = [LAJC2,LKJC−LAJC2,LAJC2−LP3MT,zyx]
LTIBIAp4 = [LAJC2,LKNE−LANK,LAJC2−LP3MT,zyx]

{* foot *}

FOOTf1 = [LFC,LANK−LMANK,LFC−LAJC2,yzx]
FOOTf2 = [LFC,LANK−LMANK,LP3MT−LAJC2,yzx]

FOOTi1 = [LAJC2,LP3MT−LAJC2,LD1MT−LTOE,xzy]

{* angles *}


LFLEX1 = <FOOTF1,LTIBIAF1,yxz>
{* these 2 give slightly bigger angles when barefoot at platform
rotation *}
LFLEX2 = <FOOTF1,LTIBIAF2,yxz>
LFLEX3 = <FOOTF2,LTIBIAF1,yxz>

{* This gives more accurate results *}
LFLEX4 = <FOOTF2,LTIBIAF2,yxz>

LINV1 = <FOOTi1,LTIBIAi1,yxz>


{* using footf1 will not give good inversion progression as it looks on the
lmal and mmal markers as such it will under state inversion progression. *}
LFootprog1 = <ref,FOOTf1,yxz>(−1)

{* this will give better inversion progression, i.e. more
reprisentative of foot *}
LFOOTprog2 = <ref,FOOTi1,yxz>


LFOOTprog2 = <−180−LFOOTprog2(1),−LFOOTprog2(2),−180−LFOOTprog2(3)>

LTIBIAprog1= <ref,LTIBIAf1,yxz>

LTIBIAprog2= <ref,LTIBIAf2,yxz>
```

```
94
95 LTIBIAprog3= <ref,LTIBIAp3,yxz>
96 LTIBIAprog4= <ref,LTIBIAp4,yxz>
97
98
99 OUTPUT (LAJC2)
100 OUTPUT (LFLEX1,LFLEX2,LFLEX3,LFLEX4,LINV1,LFootprog1,LFootprog2,
101      LTIBIAprog1,LTIBIAprog2,LTIBIAprog3,LTIBIAprog4)
```

E Ethical approval form

Presented in the two following pages is a copy of the ethical approval form that was submitted to the University of Dundee ethical committee.

UNIVERSITY OF DUNDEE UNIVERSITY RESEARCH ETHICS COMMITTEE APPROVAL FORM

Title of project: The effect of shoes on foot proprioception and its role in ankle sprains.

Name of lead Investigator, Department (or equivalent), Status (e.g. staff, student): Ahmad Dahrouj, Institute of Motion Analysis & Research(IMAR), Division of Surgery & Oncology, Ninewells Hospital & Medical School, Postgraduate Student.

Other Academic Staff involved (e.g. supervisor, co-researchers): Prof. R J Abboud and Dr. Tim Drew.

E-mail address:a.dahrouj@dundee.ac.uk

Date:25/10/06 UREC Ref no. (LEAVE BLANK):

			YES	NO	N/A
1	Will you describe the main procedures to participants in advance so that they are informed about what to expect in your study?		✓		
2	Will you tell participants that their participation is voluntary?		✓		
3	Will your participants be able to read and understand the participant information sheet?		✓		
4	Will you obtain written informed consent for participation?		✓		
5	If the research is observational, will you ask participants for their consent to being observed?				✓
6	Will you tell participants that they may withdraw from the research at any time without penalty and for any reason?		✓		
7	With questionnaires, will you give participants the option of omitting questions they do not want to answer?				✓
8	Will you tell participants that their data will be treated with full confidentiality and that, if published, it will not be identifiable as theirs?		✓		
9	Will you give participants a brief explanation of the purpose of the study at the end of their participation in it, and answer any questions?		✓		
10	Will your project involved deliberately misleading participants in any way?			✓	
11	Is there any realistic risk of any participants experiencing either physical or psychological distress or discomfort? If Yes, give details on a separate sheet and state what you will tell them to do if they should experience any problems (e.g. who they can contact for help).			✓	
12	Do participants fall into any of the following special groups? Note that you may also need to obtain satisfactory Disclosure Scotland (or equivalent) clearance.	Children (under 18 years of age)		✓	
		Children under 5 years of age			
		Pregnant women			
		Participants studied with respect to contraception or conception		✓	
		People with learning or communication difficulties		✓	
		People in custody			
		People engaged in illegal activities (e.g. drug-taking)		✓	
		Non-human animals		✓	
		Patients		✓	
		More than 5000 participants		✓	
				✓	
				✓	

Please tick either Box A or Box B below and provide any details required in support of your application. If you ticked NO to any of Q1-9 or YES to any of Q10-12 then you must tick Box B.

A. I consider that this project has **no** significant ethical implications to be brought before the University Research Ethics Committee. (✓)	

It has bee suggested that the shoes we wear play a negative role in ankle sprains. This project builds on previous research and will help us understand more about the role of shoes in ankle injury. For this purpose a rotating platform has been embedded in the IMAR sports lab. Participants in this research will walk on the platform, barefoot and with shoes. As they step on it, the platform will rotate, in three directions and to a safe angle, along with the participant's foot. Muscle activity data, EMG, of the leg and motion data, captured using Vicon, of the participant will be recorded. Data from shod, wearing shoes, and unshod, barefoot, trials will be compared and will help us understand more the role of shoes in ankle injury. Ultimately, data from this study and other associated projects will be utilized to design better footwear and reduce the possibility of injury.

B. I consider that this project may have ethical implications that should be brought before the Ethics Committee.	

Please provide all the further information listed below in a separate attachment. Note that this description will be read by non-specialists and must be readily comprehensible by a lay person.

1. Title of project.
2. Purpose of project and its academic rationale.
3. Brief description of methods and measurements and how data will be stored.
4. Participants: recruitment methods, number, age, gender, exclusion/inclusion criteria.
5. Consent and participant information arrangements, debriefing.
6. A clear statement of the ethical considerations raised by the project and how you intend to deal with them.
7. Estimated start date and duration of project.

I am familiar with the University of Dundee *Code of Practice for Research on Human Participants*, and have discussed them with the other researchers involved in the project. I confirm that my research abides by these guidelines.

Signed Ahmad Dahrouj Name Ahmad Dahrouj Date 22/04/2009
(Lead Investigator)

There is an obligation on the lead researcher to bring to the attention of the Ethics Committee any issues with ethical implications not covered by the above checklist.

UREC v. 1.6, 20 April 2006

F Recruitment poster

Presented in the next page is the recruitment poster that was used to advertise for the conducted study. This poster was posted throughout the University of Dundee campus and in Ninewells hospital.

UNIVERSITY OF DUNDEE
HELP US
prevent ankle injuries
We are looking for volunteers to participate in the final stages of a three-year research project investigating the role of shoes in ankle sprains.
Participation in this research will benefit wearers of sports shoes.
Certificates of volunteer participation will be given on request.
If you are in general good health, have not suffered an ankle injury in the last six months and can spend some time helping, please contact us via the tear-off slips below
We appreciate your time
This study has been reviewed and approved by the University Committee on Research Ethics
ANKLE INJURY RESEARCH
a.dahrouj@dundee.ac.uk
01382 496332

G Participant information sheet

Subjects who showed interest in taking part of the study discussed in this thesis were sent a an information sheet that explained the nature of the study and what they were excepted to do. A copy of this sheet is presented in the following two pages.

The effect of shoes on foot proprioception and its role in ankle sprains

INVITATION TO TAKE PART IN A RESEARCH STUDY
You are being asked to take part in a research study, which will help understand the role shoes we wear play in ankle sprains. This Project is supervised by Prof. Rami Abboud and Dr. Tim Drew. Ahmad Dahrouj, a PhD student, will be conducting the research.

PURPOSE OF THE RESEARCH STUDY
This study will help us understand more about the role of shoes in ankle sprains. Ultimately, data from this study and other associated projects will be utilized to design better footwear and reduce the possibility of injury. Participation in this research would benefit all people who use shoes especially while participating in sports activities, which is when most ankle sprains occur.

COMMITMENT
The study will require about an hour and a half to be completed with 1 visit/session. During the session you will be asked to walk, barefoot and with shoes, in the IMAR sport's lab. This lab has been fitted with a rotating platform which will safely rotate your foot when you step on it. Motion capture markers and EMG electrodes will be attached to your body; they will provide us with the data we need to better understand the role of shoes in ankle sprains.

TERMINATION OF PARTICIPATION
You may decide to stop being a part of the research study at any time without explanation.

RISKS
There are no known risks for you in this study.

COST, REIMBURSEMENT AND COMPENSATION
Your participation in this study is voluntary. You will not receive any payment after completion of the testing.

CONFIDENTIALITY/ANONYMITY
The data we collect do not contain any personal information about you except your physical activity ands sports that you participate in.
No one will link the data you provided to your identity and name.
The results of this research might be published in academic journals and in the researchers PhD thesis.
No one will able link any of the published materials to you.

FOR FURTHER INFORMATION ABOUT THIS RESEARCH STUDY
Ahmad Dahrouj will be glad to answer your questions about this study at any time.

You may contact him at a.dahrouj@dundee.ac.uk

Ahmad Dahrouj, Teaching and Research Suite, TORT Centre, Ninewells hospital,

Dundee

The University Non-Clinical Research Ethics Committee of the University of Dundee has reviewed and approved this research study.

H Consent form

All subjects who participated in the conducted study were asked to sign a consent form, a copy of which is presented in the following page.

The effect of shoes on foot proprioception and its role in ankle sprains

It has been suggested that the shoes we wear play a negative role in ankle sprains. This project builds on previous research and will help us understand more about the role of shoes in ankle injury. For this purpose a rotating platform has been embedded in the IMAR sports lab. Participants in this research will walk on the platform, barefoot and with shoes. As they step on it, the platform will rotate along with the participant's foot on it. Muscle activity data of the leg and motion data of the participant will be recorded. Data from shod (wearing shoes) and unshod (barefoot) trials will be compared and will help us understand more the role of shoes in ankle injury.

By signing below you are agreeing that you have read and understood the Information Sheet and that you agree to take part in this research study.

_____ _____

Participant's Name Signature

_____ _____

Signature of person obtaining Date

I Data processing modules

This appendix can only be provided upon request from Professor Abboud due to sensitive and confidential material related to the design that is property of IMAR.